16

LAND SURFACE RESPONSE TO CLIMATE CHANGE FORCING OVER SOUTHERN AFRICA

Debbie Anne Shannon

Thesis Presented for the Degree of

DOCTOR OF PHILOSOPHY

in the Department of Environmental and Geographical Science

UNIVERSITY OF CAPE TOWN

November 2000

PREFACE

The land surface is important to the climate system for the exchanges of moisture, momentum and heat. Momentum, radiation, and sensible and latent heat fluxes between the atmosphere and the surface will likely affect atmospheric dynamics, temperature, precipitation and humidity fields (Sato *et al.*, 1989). These may subsequently feed back into the land surface processes as part of a cyclical system. Therefore it is evident that our livelihood is largely dependent on interactions and exchanges between the land surface and climate system (Henderson-Sellers *et al.*, 1993) and it is thus essential that we gain a better understanding of the interactive sensitivity. This is of particular relevance in the context of the portended future global climate change.

In the present study the interactions between the land surface and the atmosphere are considered over the southern African region. This region has a climate showing a high degree of spatial and temporal variability, most notably with rainfall. Regional climates are characterised by summer, winter and all-year-round rainfall. There are steep vegetation gradients and a wide range of vegetation types adapted to suit the variable climate. These factors, combined with the societal implications of changes in the climate and land surface systems, make southern Africa a challenging and important study domain for examining the sensitivity between the different elements of the atmosphere and biosphere.

This research makes use of a biosphere model driven by climate change data derived from a general circulation model (GCM). Regions susceptible and sensitive to changes on an annual and seasonal basis are identified and examined. The thesis comprises 8 chapters. The first chapter, **Chapter 1**, provides some background information on climate change, biosphere-atmosphere interactions, GCMs and transient simulations, vegetation models and vegetation representation over southern Africa. This chapter also sets out the research objectives. The following chapter, **Chapter 2**, introduces the atmospheric GCM model data from the Hadley Centre Model (HadCM2) used in the analysis. The chapter additionally provides a detailed description of the biosphere model, the Integrated Biosphere Simulator (IBIS). **Chapter 3** examines the Hadley Centre HadCM2 GCM input data used in driving the biosphere model, while **Chapter 4** presents the input forcing data and configuration of the IBIS model. In **Chapter 5** the results of the IBIS model simulation are examined on the annual scale and in **Chapter 6** the results are examined on the seasonal scale. Some of the implications of climate

change are considered in **Chapter 7**. This chapter also places the HadCM2 GCM model data used in driving IBIS into the context of the latest emissions scenarios. In the final chapter, **Chapter 8**, an overview summary is provided and conclusions are drawn.

I owe thanks to a number of people for their help in various stages of my thesis. Firstly, I would like to thank **Jon Foley** from the University of Wisconsin-Madison in the United States of America for allowing me to use the biosphere model (IBIS) he and his group have developed. **Veronica Fisher**, formerly from the University of Wisconsin-Madison, is also acknowledged for her advice and help with the initial stages involved with setting up the model to run on the SGI in the Department of Environmental and Geographical Science at the University of Cape Town. Both Veronica Fisher and Jon Foley have been invaluable in clarifying and answering a number of queries I have had, particularly during the early stages of using the model.

I would also like to thank my colleagues in the **Department of Environmental and Geographical Science** at the University of Cape Town. In particular, I wish to thank **Debbie Hudson** for her useful thesis tips and for her advice along the way, and **Jeremy Main** and **Christopher Jack** for their help with systems administration related queries. **Gillian Drew** (who assisted me with drawing the GIS vegetation category map), **Anne Mulock-Houwer** and **Christopher Lennard**, and my other fellow peers in the **Climate System Analysis Group** are gratefully acknowledged for their friendship and for their assistance in various aspects of my thesis.

I am grateful to the **National Research Foundation** (formerly the Foundation for Research and Development) for the financial assistance they have provided in the form of scholarships for my honours, masters and doctoral theses.

I am indebted to my **parents** for their encouragement, love and support during the course of my studies, and for their guidance through my life. I wish to thank my sister, **Lynne Shannon**, for her encouragement and advice, and for keeping me company by doing her doctorate at the same time as me! I would also like to thank my fiancé, **Justin Sparks**, for his endless love, patience, and encouragement. I am grateful for the support provided by all my family and friends over the years.

Finally, I would like to thank my supervisor, **Bruce Hewitson**, for the numerous opportunities he has provided me with during my post-graduate studies, and for the many useful and insightful suggestions and discussions along the way.

CONTENTS

Abstract ii

Preface iii

Chapter 1 Background 2

1.1 Climate, climate change and the climate system 2

1.2 Biosphere-atmosphere interactions 3

1.3 General Circulation Models 5

1.4 Transient climate change GCM runs 7

1.5 Vegetation models 7

1.6 Vegetation types represented over southern Africa 8

1.6.1 Biome response to climate change 9

1.7 Research objectives 11

Chapter 2 Data and model descriptions 13

2.1 Introduction 13

2.2 The Hadley Centre Model 14

2.2.1 The IS92 emission scenarios 15

2.3 The IBIS Model 16

Chapter 3 Hadley Centre transient run simulation 22

3.1 Evaluation of the Hadley Centre transient simulation 22

3.2 Broad scale changes in the Hadley Centre transient simulation 25

3.3 The southern African region 26

3.3 .1 Surface temperature 26

3.3.2 Sea level pressure 30

3.3.3 Relative humidity 30

3.3.4 Precipitation 31

3.3.5 Wind speed 35

Chapter 4 IBIS model simulation 38

4.1 Data and model configuration 38

4.2 Base vegetation input fields 43

Chapter 5 IBIS model simulation annual results 47

5.1 Differences between the early and late 21st century 47

5.1.1 Annual Net Primary Productivity 49

5.1.2 Annual average evapotranspiration 52

5.1.3 Sensible heat fluxes 55

5.1.4 Soil temperatures 58

5.1.5 Soil moisture 61

5.1.6 Response regions 64

5.2 Trends in the HadCM2 input data 64

5.2.1 Region 1 65

5.2.2 Region 2 65

5.2.3 Region 3 65

5.2.4 Region 4 66

5.2.5 Region 5 66

5.3 Vegetation and annual trends in IBIS response 68

5.3.1 Region 1 77

5.3.2 Region 2 79

5.3.3 Region 3 80

5.3.4 Region 4 81

5.3.5 Region 5 82

5.3.6 Synthesis 84

Chapter 6 IBIS model simulation seasonal results 91

6.1 Dominant seasonal response 91

6.2 Summer seasonal differences between the early and late 21st century 94

6.2.1 Net Primary Productivity 94

6.2.2 Average evapotranspiration 95

6.2.3 Sensible heat fluxes 96

6.2.4 Soil temperatures 97

6.2.5 Soil moisture 98

6.2.6 Latent heat fluxes 98
6.2.7 Leaf area index (upper and lower canopies) 99
6.3 Winter seasonal differences between the early and late 21st century 101
6.3.1 Net Primary Productivity 101
6.3.2 Average evapotranspiration 102
6.3.3 Sensible heat fluxes 103
6.3.4 Soil temperatures 104
6.3.5 Soil moisture 104
6.3.6 Latent heat fluxes 105
6.3.7 Leaf area index (upper and lower canopies) 106
6.4 Seasonal and monthly scale trends in IBIS output data 108
6.4.1 Introduction 108
6.4.2 Principal Components Analysis Methods 109
6.4.3 Principal component loading results 111
6.4.4 Principal component scores results 117
6.4.4.1 Ibisdyn 118
6.4.4.2 P1 121
6.4.4.3 P4 124
6.4.5 Synthesis 126
6.5 A case study of vegetation change and process links 128

Chapter 7 Implications of land surface sensitivity in the context of global climate change scenarios 133

7.1 Consequences and impacts 133
7.1.1 A global context 133
7.1.2 Land surface sensitivity and impacts over southern Africa 135
7.2 The latest emission scenarios 138
7.2.1 Background 138
7.2.2 The SRES scenarios of current models 140
7.2.2.1 Precipitation 141
7.2.2.2 Temperature 143
7.2.2.3 The HadCM2 model in the context of current SRES scenarios 144

Chapter 8 Summary and conclusions 147

8.1 Overview 147

8.2 Summary of results 148

8.2.1 The Hadley Centre transient run simulation 149

8.2.2 Mean annual IBIS results 149

8.2.3 Seasonal and intra-seasonal results 150

8.2.4 Implications of land surface sensitivity in a climate change context 151

8.3 Caveats 152

8.4 Conclusions 153

References 156

Appendices

Appendix A Acronyms A1

Appendix B Trend graphs B1

Appendix C Special report on emissions scenarios A2 and B2 storylines for the different general circulation models C1

Appendix D Summer seasonal differences between the early and late 21st century D1

Appendix E Winter seasonal differences between the early and late 21st century E1

CHAPTER 1

BACKGROUND

CHAPTER 1

BACKGROUND

1.1 Climate, climate change and the climate system

Changes in atmospheric phenomena can be categorised loosely into those constituting "weather" and those constituting "climate". The weather represents large hourly to daily fluctuations, which occur with the development and movement of weather systems over time, through non-linear "chaotic" dynamics (IPCC, 1996). This makes such systems unpredictable beyond much more than a few weeks. Climate (the focus of this thesis) is the average characteristic of weather, usually taken as being over a period of 30 years. The climate involves variations in which the atmosphere interacts with the other components of the climate system, in addition to "external" forcing (e.g. the sun) (IPCC, 1996). The components interacting in the climate system (figure 1.1) include the atmosphere, oceans, sea ice, land (vegetation, albedo, biomass, ecosystems etc.), snow cover, land ice and hydrology.

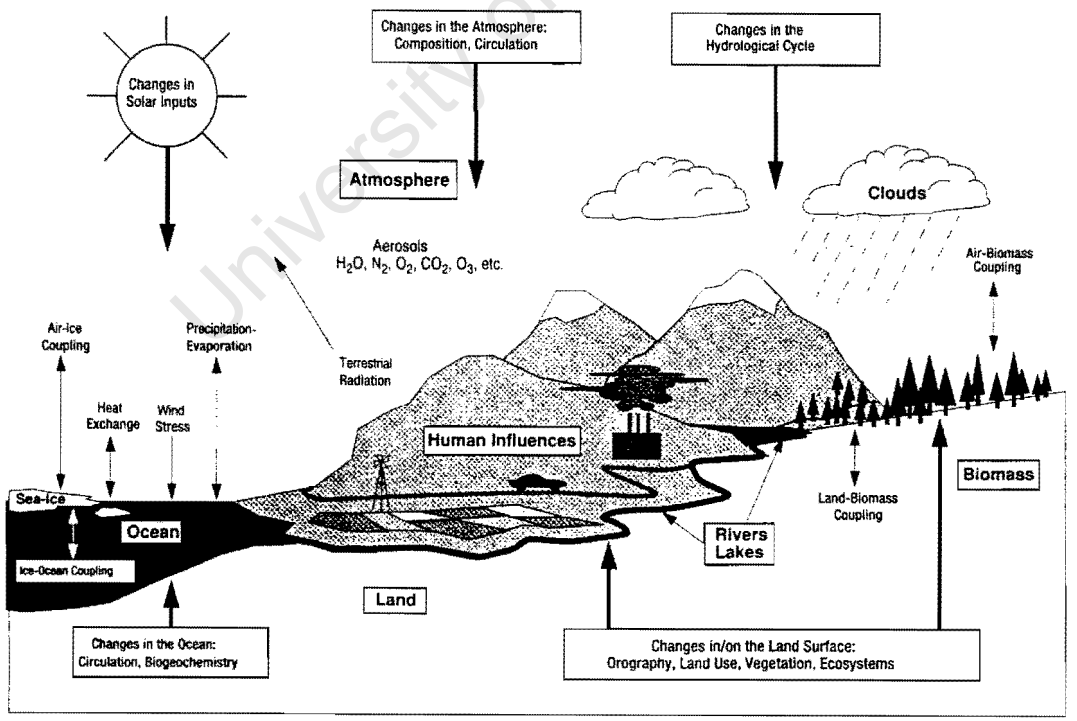

Figure 1.1 Schematic diagram of the components interacting in the climate system (IPCC, 1996). Note: Bold typeface indicates the different components, thin arrows are interactive processes and bold arrows show aspects which might change.

Year-to-year variations in weather at a particular location can be sizeable. However, if one considers large areas over an extended period of time, there is evidence to suggest that there have been some important systematic changes, e.g. increases in global mean surface air temperature (recent years have been the warmest on the instrumental record) and a rise in sea level.

A global issue that has become a concern on government agendas over the last decade, is the significant impacts humans have had on the global environment over the last century. This is primarily a response to industrial expansion, land use changes, agriculture and the burning of fossil fuels (Parry and Carter, 1998). The enhancement of the greenhouse effect is largely attributed to the aforementioned, through the emission of greenhouse gases such as Carbon Dioxide (CO_2), Methane (CH_4) and Nitrous Oxide (N_2O). Atmospheric CO_2 values in pre-industrial times were of the order of 280-300 ppm, but by the early 1980s the values were in the range of 335-340 ppm, representing a substantial increase. For the most part the increase can be ascribed to the burning of fossil fuels (Hansen *et al.*, 1981). Should this trend continue at present levels, there would be an almost steady increase in concentrations for a minimum of two centuries, with estimates in the order of 500 ppm by the end of the 21st century (IPCC, 1996).

The climate is expected to continue changing in the future, and therefore it is important to examine some of the key areas of interaction and response e.g. sea level rise, terrestrial biota (biosphere-atmosphere interactions), sea ice reduction and marine biota. In this way an improved understanding of the interactions and responses between key variables within the climate system can be obtained.

1.2 Biosphere-atmosphere interactions

The land surface is important to the climate system for the exchanges of moisture, momentum and heat. A large percentage of water fluxes from the land surface to the atmosphere move through vegetation (Dickinson, 1992). The interactive effect between the climate and the biosphere initiates feedback loops, with a change in either the climate or biosphere impacting on both systems. The biosphere interacts with the climate system by altering and governing land surface properties (e.g. roughness, evapotranspiration and albedo) introducing a feedback (figure 1.2). In addition, trace gases such as carbon dioxide, methane and nitrous oxide are controlled, and this impacts on the earth's radiative balance (Heimann, 1998). Very little is known about the climate controls on such feedbacks and how they might function in a changed climate system.

The identification of climate thresholds for plant species is important, since these thresholds are crucial in terms of predicting climate change impacts (Schulze, 1997). In terms of vegetation development, light, temperature and moisture are the primary climatic determinants (Schulze, 1997).

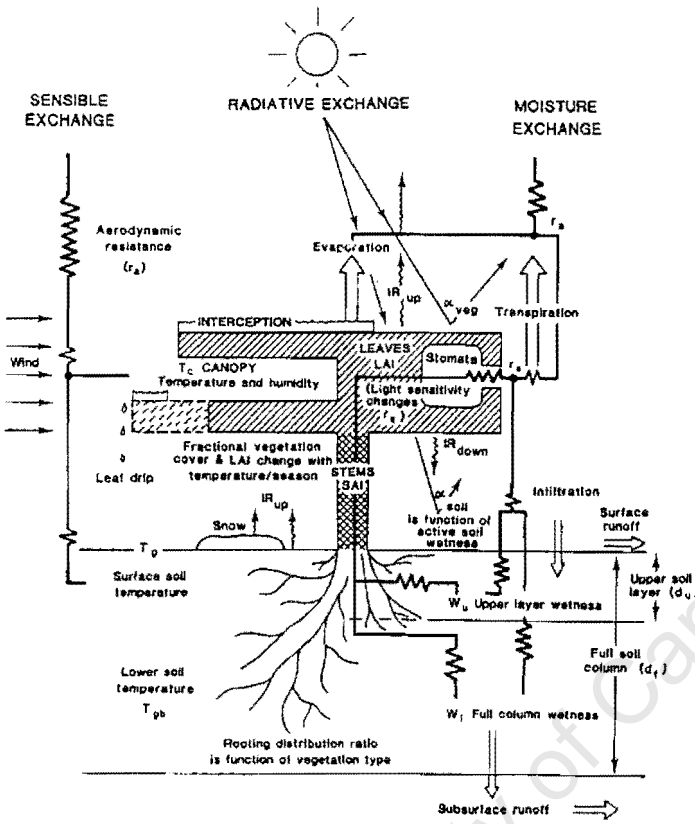

Figure 1.2 Schematic diagram showing some of the interactions between the biosphere and atmosphere (McGuffie and Henderson-Sellers, 1999).

Biosphere-climate exchanges are strongly coupled and recent modelling studies have shown that an atmospheric CO_2 increase could directly impact vegetation physiology such that photosynthesis could be enhanced and evapotranspiration reduced during the growing season (Sellers, 1998). It is recognised that it is necessary to monitor and predict global water, energy and CO_2 cycles; this requires observations (using satellites, field experiments, in situ measurements and monitoring of vital indicators), along with modelling analyses aimed at a synthesis and possible future projection of climate (Sellers, 1998). A useful review on modelling energy, water and carbon exchanges between the land surface and atmosphere is provided in Sellers *et al.* (1997).

The response of the land surface to changes in the climate system is two-fold. Physiological processes are responsible for the *short-term* response of vegetation or ecosystems to climate.

Rates of photosynthesis and respiration are modified by CO_2 concentrations, climate, nutrient and water availability, as well as ecosystem properties (Leemans, 1998). Ecosystem characteristics (e.g. C3 versus C4 plants) are also significant determinants (see Chapter 7). Ecological processes determine the *longer-term* response. Each species has a distinct threshold and will react differently from other species in response to environmental changes, and species adaptability to changing conditions is variable.

Biomes have varied notably in the past (see for example Foley (1994a), Foley *et al.* (1994), de Noblet *et al.* (1996), Harrison *et al.* (1995), Kutzbach *et al.* (1996), TEMPO (1996)), which would suggest that they should continue to do so in the future. Therefore, in modelling studies examining climate change in the future it is necessary to include biosphere models, thereby incorporating the potential biome shifts in scenarios and predictions. However, integrating climate and terrestrial ecosystem models does raise a number of difficulties, since their spatial and temporal scales are vastly different (Aber, 1992). The atmosphere is a well-mixed system, while the terrestrial ecosystem is not. Thus the latter needs to be examined over longer time scales and shorter spatial scales (Aber, 1992). General circulation models tend to operate at time steps of minutes to hours and at scales of hundreds of kilometres. Terrestrial ecosystem models, on the other hand, often operate at monthly to annual time steps at scales of tens of metres.

1.3 General circulation models

General circulation models (GCMs) have been used and designed historically for short-term weather prediction (Henderson-Sellers and McGuffie, 1987). The atmospheric GCMs were developed in the 1950s and 1960s, when ideas for longer period integrations of numerical weather prediction schemes were formulated. Numerical prediction thus extended to hemispheric and global scales (Henderson-Sellers and McGuffie, 1987). The term GCM could refer to weather forecast models and therefore in a climate change context, the term GCM is understood to mean general circulation *climate* model (Henderson-Sellers and McGuffie, 1987). The first atmospheric general circulation model was developed by Phillips (1956) and was a quasi-geostrophic two-layer hemispheric model, which could capture zonal flow and midlatitude eddies. Smagorinsky (1963) made important contributions in the further advancement of GCMs in the early 1960s. He developed a two-layer model that solved primitive equations for a 60-day period, and considered the region between the equator and the 64° latitude. His model included planetary waves and the kinematics of a sphere. Since this time, models have grown

substantially and this has been aided to a large extent by improvements in computational facilities and capabilities over the last few decades (Peixoto and Oort, 1992).

A general circulation model consists of a series of equations describing atmospheric dynamics with prescribed initial and boundary conditions as well as physical constants. In addition, sub-grid scale processes are parameterised. Parameterisation implies the minimum scale at which a process can be resolved. Features such as clouds, for example, are very important, but are sub-grid scale and therefore difficult to represent realistically. Clouds, along with the hydrological balance over the land surface and the surface oceanic heat flux have been identified as the primary uncertainties in GCMs (IPCC, 1996).

A better understanding of the climate system has been gained using GCMs, suitable to reproduce climate fields through the conservation of energy, over the years and validation and improvement of parameterisations has been a major focus (Henderson-Sellers and McGuffie, 1987). GCMs have been used particularly over the last decade or so for projections of a possible future climate. In fact, they are the only quantitative tools available for predicting future climates (Trenberth, 1996). Climate GCMs are used in studies such as these to ascertain whether or not a perturbation of certain model parameters has a significant effect on the climate (Henderson-Sellers and McGuffie, 1987).

Current GCMs tend to have at least 18 layers in the vertical and operate at a resolution of 2.5° for short runs, but at a lower resolution for lengthier runs (more than 30 years). More recently, there has been a rapid increase in coupled ocean-atmosphere models. Representation of the ocean in coupled models is in one of the following forms: a swamp ocean with no heat storage or ocean currents, a slab mixed-layer ocean with no ocean currents but some heat storage, or a dynamical ocean GCM where there is heat storage, upwelling and ocean currents (Meehl, 1992). The last of these three is computationally intensive, yet potentially the most powerful tool for studying the global climate (Meehl, 1992).

Evaluating GCMs presents a challenging task. Atmospheric, oceanic, land surface and sea ice models and their interactions are being evaluated and notable advances are being made. There have been problems such as flux adjustments and spin up in coupled models, which affect the representation of sea ice, thermohaline circulation and temperature at the surface. The flux adjustments requirements are nonetheless declining with the improvement of the atmospheric,

sea ice, oceanic and land surface models (IPCC, 1996), and many recent models do not necessitate flux adjustments. Model spin-up problems arise from the different time scales existing within the different components of the GCM. The atmosphere operates at a time scale of the order of weeks, the ocean surface and land surface at a seasonal scale, while the deeper ocean operates at a scale of thousands of years. Because of this, the atmosphere and ocean are usually spun up separately and then coupled for a further spin up period.

In evaluating GCMs, the key considerations are their representation of the current and recent climate, and physical processes important to the climate system. The development of more accurate coupled models has been a primary focus for some time, since it is more generally accepted that it is through these models that we can get a scientific understanding of climate and climate change (IPCC, 1996). There is therefore the need for improved parameterizations and a higher resolution than they currently possess.

1.4 Transient climate change GCM runs

It has been recognised that anthropogenic global warming should be considered as a transient problem, using coupled ocean-atmosphere GCMs (Hasselmann, 1993). It was not however until the 1990s that ocean models became suitably realistic and computational resources sufficient for such endeavours. Computational requirements have meant that very often an experiment has not been able to cover the full build-up period of greenhouse gases from the early 1800s (Hasselmann, 1993). Therefore there are two types of simulation "starts" that have resulted. There is the "cold start" simulation, where the initial state of greenhouse gas build-up is taken as the present or near present, and there is the "warm start" simulation where the simulation is initiated at the start of the greenhouse gas build-up in the early 19th century. "Cold start" simulations tend to underestimate climate change and "warm starts" are therefore perhaps more plausible. A "cold start" could be anticipated to experience a temporal lagging in response to an increase in CO_2, such that the initially slow increase followed by a faster increase in temperature anomalies could merely be an artefact of the "cold start" (Meehl *et al.*, 1993).

1.5 Vegetation models

Biosphere models tend to be categorized into three types, namely, land surface models, equilibrium vegetation models and terrestrial biogeochemical models (Foley *et al.*, 1996). The first of these is used primarily by atmospheric GCMs in order to represent biophysical

interactions between the atmosphere and the land surface. Examples of such models are the Biosphere-Atmosphere Transfer Scheme (BATS) of Dickinson (1984) and Dickinson *et al.* (1986), the Simple Biosphere Model (SiB) of Sellers *et al.* (1986) and SiB2 of Sellers *et al.* (1996a and 1996b), the Canadian Land Surface Scheme (CLASS) as described in Verseghy (1991, 1993), the Interactions between Soil Biosphere Atmosphere (ISBA) as described by Noilhan and Planton (1989) and the Land Surface Transfer Scheme (LSX) (Pollard and Thompson (1995a, 1995b) which is used in the GENESIS GCM. In essence, such models simulate water, momentum and energy balance, operate globally, and have prescribed soil and vegetation. While serving a useful and necessary function, there is a notable shortcoming since these models do not account for changes in vegetation cover, which could consequentially alter the climate. The second type, equilibrium vegetation models, has been used to simulate vegetation patterns and how they might differ under alternative climate regimes. Examples of such models include BIOME of Prentice *et al.* (1992) and the Equilibrium Vegetation Ecology Model (EVE) of Bergengren *et al.* (2000). The third type, terrestrial biogeochemistry models, simulates the carbon and mineral nutrient flow in vegetation, detritus and soil organic matter pools. Vegetation and soil are usually prescribed and the models are concerned with net primary production, carbon storage and nutrient cycling. Examples of such models are DOLY of Woodward *et al.* (1995) and DEMETER of Foley (1994b).

These 3 model types tend to have developed separately in an unconnected manner, which has made it awkward to examine the biosphere and its interactions with the climate system as a whole. Furthermore, models often neglect or ignore vital relationships existing within the land surface, and lack consideration of time-dependent ecosystem relationships (resulting in an inability to capture vegetation dynamics). Foley *et al.* (1996) point out the need for a more integrated, dynamic approach to modelling the biosphere. With this in mind, they developed the Integrated Biosphere Simulator (IBIS), in an attempt to solve some of the inherent problems.

1.6 Vegetation types represented over southern Africa

Southern Africa has a range of vegetation types adapted to suit the variable climate, from those which can withstand drought for long periods of time, to those tolerant of plentiful rainfall. The classification of vegetation is unenviable and will be dependent on both the needs of the classifier and the resolution to be considered. It is a means of summarising a vastly more complicated system into a manner that can be handled with more ease. Rutherford and Westfall (1986) have classified southern African vegetation broadly into biomes. A biome is described as

recognisable on a continental or sub-continental scale. Rutherford and Westfall (1986) distinguished 7 biomes (figure 1.3), namely, Desert, Forest, Fynbos, Grassland, Nama-Karoo, Savanna and Succulent Karoo.

Figure 1.3 Biomes map of southern Africa (Rutherford, 1997).

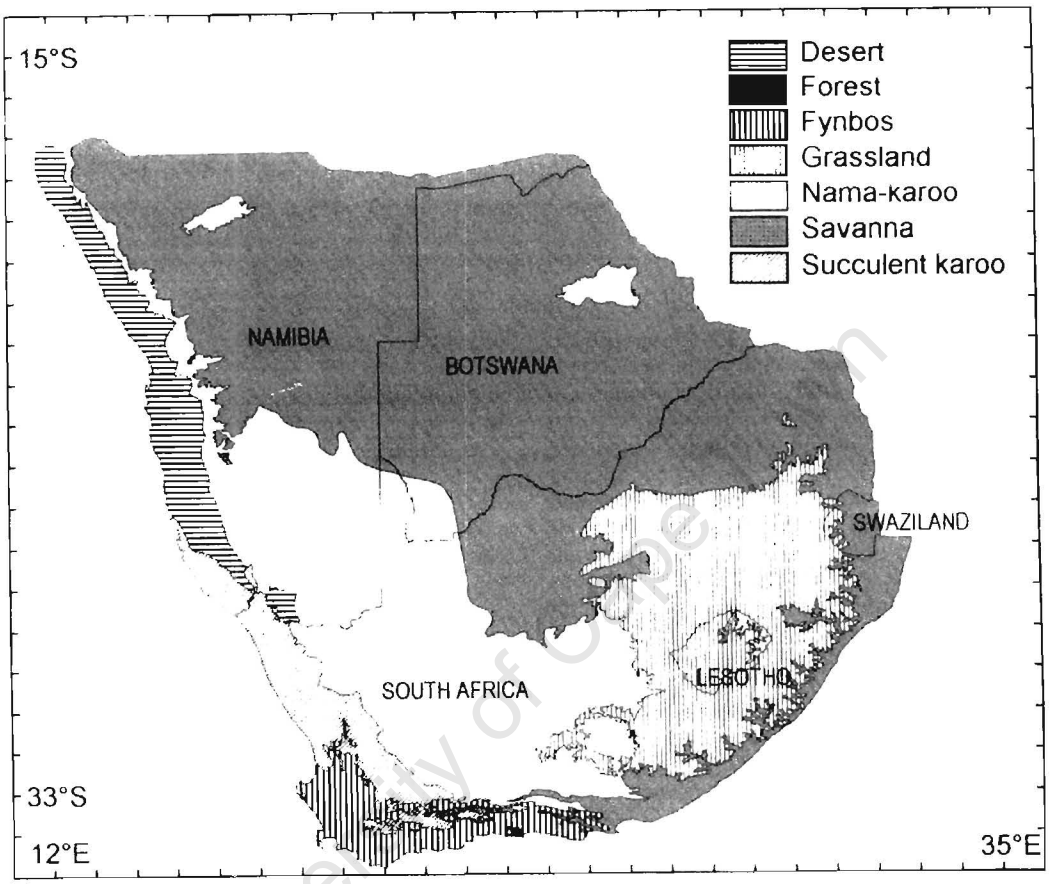

1.6.1 Biome response to climate change

Although studies have considered the effect of global climate change on biomes, and often individual species, little attention has been paid to considerations of those factors affecting the atmospheric response to vegetation change over southern Africa. Some of the potential changes, which could be anticipated with respect to biomes, have been discussed in Midgley and O'Callaghan (1993) and relate to climate change assumptions made by the formerly operational Interdepartmental Co-ordinating Committee for Global Climate Change (unpublished). Midgley and O'Callaghan's (1993) approach is therefore based on a number of broad assumptions in terms of the climate response. Table 1.1 presents a summary of the primary threats and vegetation responses as identified by Midgley and O'Callaghan (1993). There is the need for an approach considering interactions between the land surface and the atmosphere with a stronger

physical foundation (particularly with respect to more recent climate change scenarios), which is presented in this thesis.

Biome	Primary threats	Vegetation response
Desert *Summer rainfall from 13mm to 85mm, arid, minimum temperatures above zero, low species diversity*	▪ Atmospheric vapour pressure deficit increase ▪ Increasing plant thermal stress	▪ Possible extinction of some specialised species
Nama-Karoo *Summer and all-year rainfall areas, with, rainfall between 100mm and 520mm, sub-zero winter temperatures, drought tolerant plants*	▪ Atmospheric vapour pressure deficit increase ▪ Increasing thermal stress ▪ Shrubs favoured above grasses due to CO_2 increase ▪ Soil aridification	▪ Vegetation composition change (C_3 shrubs favoured above C_4 grasses)
Savanna *Grasses interspersed with woody vegetation, summer rainfall areas predominantly, great variability of minimum temperatures*	▪ Increasing vapour pressure deficit ▪ Increasing thermal stress ▪ Soil aridification ▪ Trees favoured above grasses due to CO_2 increase	▪ Woody vegetation will replace grasses
Grassland *Summer rainfall of between 400mm and 2000mm, hail common, frost tolerant, minimum temperatures below 1°C*	▪ Soil aridification ▪ Increasing vapour pressure deficit ▪ Increasing thermal stress ▪ Reduced competitively of dominant C_4 plants against C_3 plants	▪ Invasion of shrubs and trees from Nama-Karoo and Savanna Biomes ▪ Reduced fire frequency
Succulent Karoo *Winter rainfall regime, characterized by strong summer aridity*	▪ Primary changes in southern parts ▪ Convective rainfall increase inducing increased erosive force and destructive hailstorms ▪ Increasing thermal stress	▪ Major loss of leaf-succulent species ▪ C_4 grasses have competitive advantage (due to increased summer rainfall); increased CO_2 will favour C_3 grass and non-succulent shrubs ▪ Increased risk of fire
Fynbos *Mediterranean vegetation, winter or even rainfall regimes, variable rainfall amounts, low height vegetation, very high diversity, relies on fires every 10-15 years for seed dispersal*	▪ Changing seasonality of rainfall and predictability; changed fire regime ▪ Increased thermal stress ▪ Increased vapour pressure deficit ▪ Nutrient cycling disruptions ▪ Threat of invasive alien woody plants increased	▪ Loss of specialist species ▪ Grasses will experience greater success in lowland areas
Forest *Woody type vegetation, usually evergreen and multi-layered*	▪ Fragmentation overshadows effects of climate change ▪ Soil desiccation	▪ Greater forest fragmentation ▪ Slow-growing species will become extinct

Table 1.1 Vegetation changes predicted for each biome (Midgley and O'Callaghan, 1993).

1.7 Research Objectives

The primary aim of this research is to examine the sensitivity (in terms of fluxes and other land surface features) between the biosphere and atmosphere over the southern African region within a modelling context. Knowledge is improved in terms of our understanding of the sensitivity of the biosphere over southern Africa to atmospheric changes introduced over an extended period of time. This study represents the first such study of a transient nature considering the southern African region. It also identifies key areas of sensitivity within southern Africa.

The broad research objectives are as follows:

- To apply a biosphere model over the southern African domain.
- To introduce changes in the biosphere model atmospheric input data, such that a potential future climate state impact scenario is initiated.
- To examine the general circulation model atmospheric input variables in terms of the changes they reflect over the region.
- To examine the sensitivity of the land surface, as represented by the biosphere model, to atmospheric changes over southern Africa, as simulated by a general circulation model.
- To identify and examine regions over southern Africa that are most susceptible and sensitive to change.
- To examine the annual as well as seasonal response in various biosphere model output variables (such as vegetation type, net primary productivity, sensible heat fluxes, evapotranspiration, soil moisture and soil temperature).
- To examine the consequences and impacts of changes in key variables and to place these changes in the context of the latest emission scenarios.

CHAPTER 2

DATA AND MODEL DESCRIPTIONS

CHAPTER 2

DATA AND MODEL DESCRIPTION

2.1 Introduction

Many climate change experiments using GCMs have been done in more recent times. These have been in both a transient and equilibrium mode, and include greenhouse gas integrations with or without aerosol forcing. Experiments with Regional Climate Models (RCMs) have also been undertaken. A range of experiments has therefore been used in impact assessments. Nonetheless, it is not always clear how the results relate to other GCM climate change experiments[1]. With this in mind, the Intergovernmental Panel on Climate Change (IPCC) scenarios for Climate Impacts Assessments Task Group defined criteria for experiments concerned with impact assessments from 1998 and beyond, the results of which could be deposited at the IPCC Data Distribution Centre[2].

Some of the criteria defined were the following:

- An IS92a type scenario forcing (middle-of-the-range with modest assumptions) should be used (described in more detail in 2.2.1).
- Integrations must be historically forced.
- Greenhouse gas integrations may be with or without aerosol forcing.
- Results need to be currently available and in the public domain.
- Models must be documented.
- Models need to have formed part of the Atmospheric Model Intercomparison Project (AMIP) described in Gates (1992) or the Coupled Model Intercomparison Project (CMIP) (Lambert and Boer, 2000).

The following modelling centres were selected by IPCC scenarios for Climate Impacts Assessments Task Group on the basis of the above: the United Kingdom Hadley Centre for Climate Prediction and Research (HadCM2 and later HadCM3), the German Climate Research Centre (ECHAM4), the Canadian Centre for Climate Modelling and Analysis (CGCM1), the US Geophysical Fluid Dynamics Laboratory (GFDL-R15), the Australian Commonwealth Scientific

[1] http://ipcc-ddc.cru.uea.ac.uk/

[2] http://ipcc-ddc.cru.uea.ac.uk/

and Industrial Research Organisation (CSIRO-Mk2), the National Centre for Atmospheric Research (NCAR-DOE) and the Japanese Centre for Climate System Research (CCSR).

In this study, input data from transient experiments performed using the HadCM2 are employed to drive a biosphere model. This chapter presents a description of the Hadley Centre Model (which is used in the HadCM2 experiments) and places the simulation used in this thesis in the context of the IS92 IPCC emission scenarios. Following this, the specifics of the biosphere model (the Integrated Biosphere Simulator or IBIS) used in this study are presented.

2.2 The Hadley Centre Model

The Hadley Centre's new Unified Model (Cullen, 1993) is used in the HadCM2 experiments[3] performed at the Hadley Centre. These experiments include a control simulation (multi-century) and historically forced climate change experiments. There are four experiments that use high and low anthropogenic forcing scenarios (historic CO_2 for 1860-1989, and a 0.5% or 1% compound increase from 1990-2099), with and without the effects of sulphate aerosols. This research uses experiment 1, which is a non-sulphate greenhouse gas integration with historic CO_2 from 1860-1989 and a 1% compound increase in CO_2. The non-sulphate aerosol forcing simulation is used, since the HadCM2 sulphate aerosol forcing is represented in a rather simplistic manner. There is also not a high degree of confidence as to how realistic the sulphate aerosol forcing projected into the future is.

Four ensemble simulations of each experiment have been performed and are readily available for download on the Internet[4]. In an ensemble simulation, the historic and future greenhouse gas changes are identical, but the time point at which increasing greenhouse gas concentrations are initiated in the ocean-atmosphere system varies. Differences between ensemble simulation results are an indication of the degree of unpredictability of the climate system. The underlying climate change predicted is not dissimilar, but there may be significant interannual or interdecadal variations (as a result of natural model climate variability). Results from different ensembles may be averaged. However, this could obscure the climate change signal, and it is therefore not recommended, particularly in studies considering impacts[5]. Thus, in this research,

[3] Subsequently experiments using the more recent HadCM3 model have become available, but this was not anticipated in the near future at the time when data were obtained from the Data Distribution Centre.

[4] http://ipcc-ddc.cru.uea.ac.uk/

[5] http://ipcc-ddc.cru.uea.ac.uk/

a single ensemble simulation is used. In terms of choosing an ensemble, this was done by selecting one from the suite of equally probably ensemble members and therefore represents a scenario response. It is therefore recognized that different scenarios may produce somewhat different responses.

The HadCM2 model is a coupled ocean-atmosphere model that has a spatial resolution of 2.5° latitude by 3.75° longitude, which translates to a grid resolution of 278km north-south by 417km east-west at the equator, and 295km at 45° north and south (Johns *et al.*, 1997). The model has 19 levels in the atmosphere and 20 in the ocean. There are 4 soil layers in the land surface scheme. The hydrology scheme has a single moist layer, and allows soil drainage and surface run-off. The cloud scheme is a penetrative convective scheme (Gregory and Rowntree, 1990), but additionally allows downdraughts explicitly. Layer clouds and their water content for precipitation are formulated following Smith (1990). Slingo and Wilderspin's (1986) radiative flux calculations are used. Flux adjustments are made to water and heat fluxes to minimise errors in current day climate (see Murphy (1995)). The global mean temperature increase in response to a doubling of CO_2 is 2.5°C, which is in the range of more recent experiments (e.g. Boer *et al.* (2000), Roeckner *et al.* (1999), Stouffer and Manabe (1999)).

2.2.1 The IS92 emission scenarios

Future climate change projections depend, in part, on the assumptions with respect to future greenhouse gas emissions and aerosol precursors and the percentage of emissions remaining in the atmosphere. The IPCC 1992 Supplementary Report to the IPCC (1990) Scientific Assessment (IPCC, 1992) included six alternative IPCC scenarios, IS92a to IS92f. These scenarios reflect worlds of vastly different economic, social and environmental conditions that may evolve with future greenhouse gas emissions. Some of the emissions included in the scenarios are Carbon Dioxide (CO_2), Methane (CH_4), Nitrous Oxide (N_2O), halocarbons, precursors of tropospheric ozone and sulphate aerosols, and aerosols from biomass burning. Figures 2.1a) and b) show CO_2 concentrations for the different scenarios.

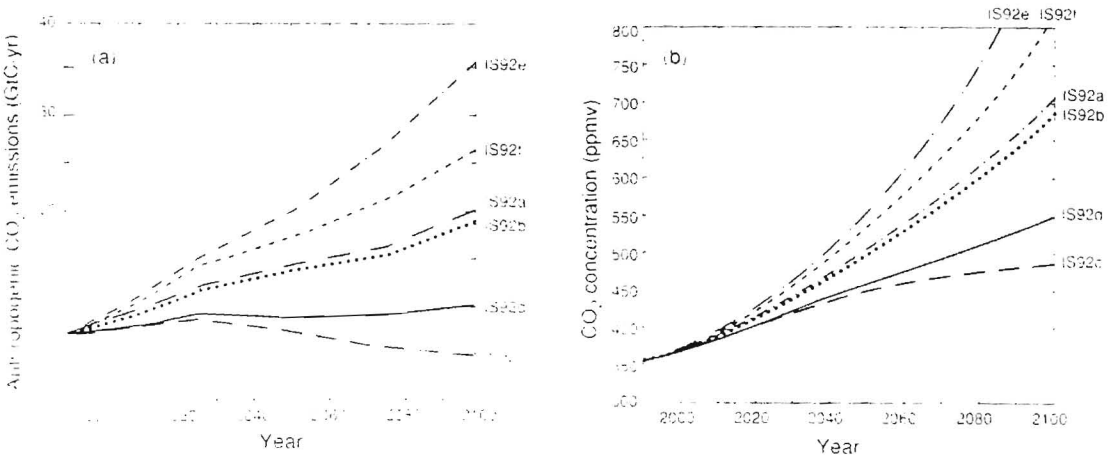

Figure 2.1 a) Anthropogenic CO_2 emissions under the IS92 scenarios and b) Resulting atmospheric CO_2 concentrations (IPCC, 1996)

The Hadley Centre HadCM2 transient run data employed in this study use the IS92a scenario. This is a middle-of-the-range scenario with modest assumptions tending to offset one another. Some of these assumptions are an economic growth of approximately 2.3% per annum between 1990 and 2100, a population of 11.3 billion by 2100 and use of both conventional and renewable energy sources (IPCC, 1992). The two extreme scenarios are IS92c and IS92e. IS92c is an extreme scenario of CO_2 emissions dropping below 1990. IS92e is the scenario of the highest greenhouse gas emissions.

2.3 The IBIS Model

This research makes use of a terrestrial biosphere model, IBIS, developed by J.A. Foley and others at the University of Wisconsin-Madison. The following section will provide an overview description of the workings and operation of the model (based on Foley *et al.* (1996) to which the reader is referred for more detail). IBIS includes within a single model, representations of all three biosphere models described in chapter 1 (viz. land surface models, equilibrium vegetation models and terrestrial biogeochemical models), and is designed in such a manner so as to be incorporated directly within atmospheric GCMs. There are several components within IBIS, operating at different time steps (see Figure 2.2 for a detailed flow chart showing the various components). These include land surface and physiological processes, phenological behaviour and leaf display, as well as transient changes in carbon balance and vegetation structure.

The land surface module simulates energy, water, carbon and momentum balance between the soil, vegetation and atmosphere. This module is based on LSX in GENESIS and operates on a

short time step (30 minutes). In this way, the model has the advantage of being able to be incorporated directly in atmospheric GCMs more readily. Woody and herbaceous plants are represented, and the module has six soil layers (simulating soil water, temperature and ice content, and capturing seasonal and diurnal cycles of heat and moisture in the upper metres). In the vertical, liquid water transport, heat diffusion, uptake of water by roots, and soil freezing and thawing are represented. The model assumes that plant functional types can take up water differentially. In essence, woody plants can draw water from deeper soil layers than herbaceous plants. Transpiration rates are calculated separately for each plant functional type.

Water and CO_2 exchanges are heavily dependent on physiological processes controlling photosynthesis and stomatal conductance. Physiological processes are light sensitive and therefore the model divides the vegetation canopy into sunlit and shaded portions. Separate calculations for photosynthesis and stomatal conductance are performed for each fraction.

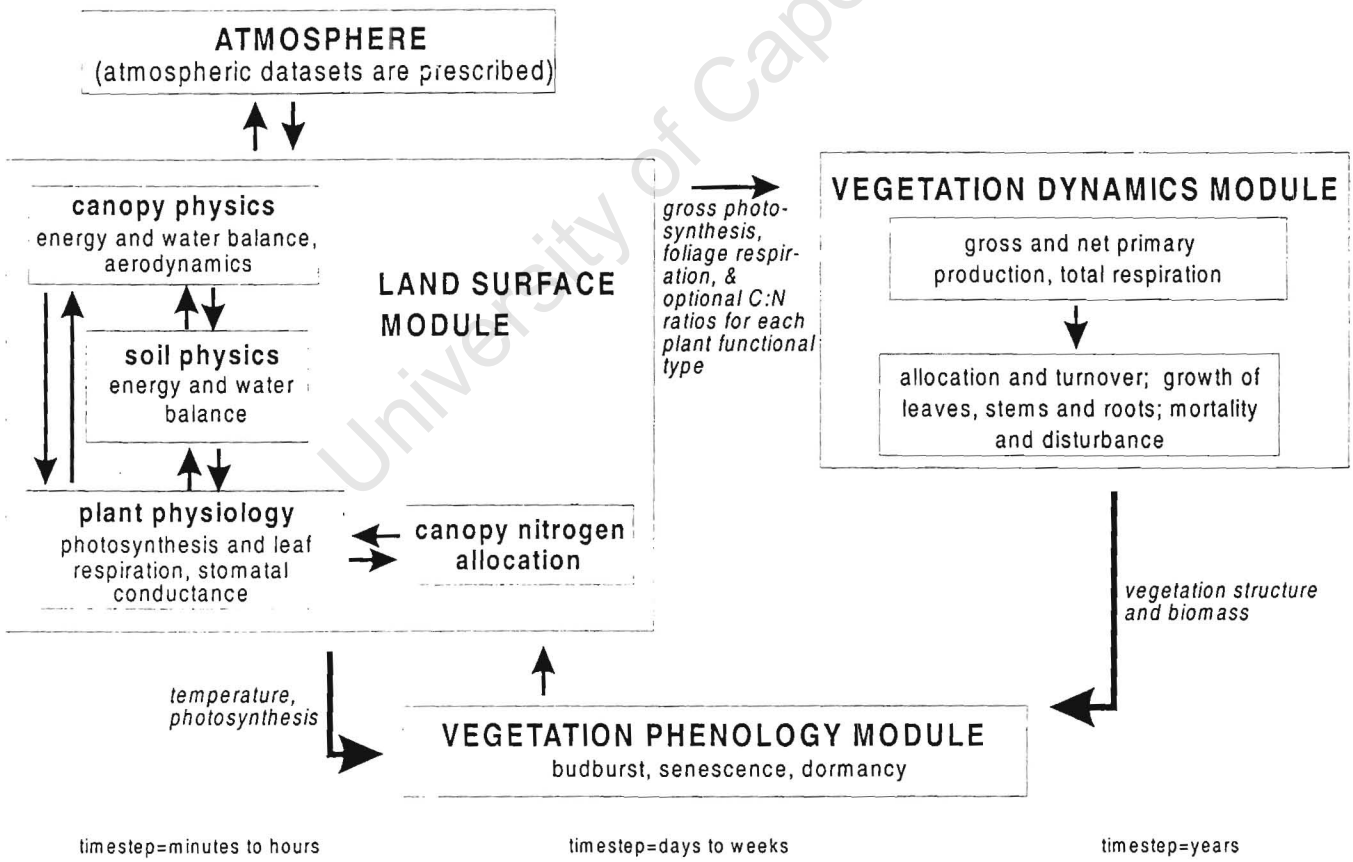

Figure 2.2 The various components of the IBIS model (modified from Foley *et al.* (1998))

Vegetation cover in the *model code* is represented in the form of *plant functional types*, of which there are twelve in the current model (Figure 2.3). The fifteen *vegetation categories* or classes (Figure 2.4) which are *inputs* into the model (i.e. converted into plant functional types by the model code) are represented as a combination of plant functional types (Woodward and Cramer, 1996), modified from Prentice *et al.* (1992) and Haxeltine and Prentice (1996). Plant functional types possibly existing in each grid cell are resolved using climatic constraints such as winter temperature limits, minimum chilling requirements and growing degree days. Winter deciduous plants, for example, shed their leaves when average daily temperature falls below 5°C in the case of deciduous trees and warm grasses, and below 0°C in the case of cool grasses. Drought-deciduous plants are made to shed their leaves during the two least productive months of the year. The model is limited at present by the lack of fire as a disturbance mechanism (this applies particularly to savanna ecosystems).

Carbon balance and vegetation dynamics are represented in a simple manner. Plant growth and competition are distinguished by the plant's ability to capture light and water from a mutual resource pool and competition between trees and grasses is simulated. For example, vegetation in the upper canopy captures light first, effectively shading vegetation in the lower canopy. The lower canopy, however, uptakes soil moisture first. Competition is also present within the same layer vegetation, as a result of annual carbon balance differences. These differences result from differences in leaf form (needle leaf or broadleaf), phenology (deciduous or evergreen), and photosynthetic pathway (C_3 or C_4). Leaf area index is calculated by dividing leaf carbon storage by specific leaf area for each plant functional type.

Studies using the IBIS model include those of Foley *et al.* (1996), Foley *et al.* (1998) and Levis *et al.* (1999). Model performance studies over southern Africa have not been done, but it is noted that the model has been validated over other domains. Given the good performance over these domains, coupled with the model being run (in the context of this thesis) at a resolution not endeavouring to capture microscale flora (such as the Western Cape Fynbos), validation in other regions is considered adequate.

1. Tropical broadleaf evergreen tree
2. Tropical broadleaf drought-deciduous tree
3. Warm-temperate broadleaf evergreen tree
4. Temperate conifer evergreen tree.
5. Temperate broadleaf cold-deciduous tree
6. Boreal conifer evergreen tree
7. Boreal broadleaf cold-deciduous tree
8. Boreal conifer cold-deciduous tree
9. Evergreen shrub
10. Deciduous shrub
11. Warm (C_4) grass
12. Cool (C_3) grass

Figure 2.3 Plant functional types represented in IBIS

1. Tropical evergreen forest/woodland
2. Tropical deciduous forest/woodland
3. Temperate evergreen broadleaf forest/woodland
4. Temperate evergreen conifer forest/woodland
5. Temperate deciduous forest/woodland
6. Boreal evergreen forest/woodland
7. Boreal deciduous forest/woodland
8. Mixed forest/woodland
9. Savanna
10. Grassland/Steppe
11. Dense shrubland
12. Open shrubland
13. Tundra
14. Desert
15. Polar desert/rock/ice

Figure 2.4 Vegetation categories/classes represented in IBIS

In Foley *et al.* (1996) the IBIS model is described and a simulation is performed in order to determine the model agreement with reality. The simulation conducted is a 50-year integration, using climatological and soil boundary conditions. The 50-year period is not sufficient to reach equilibrium in terms of vegetation biomass, but gives a clear indication of the model's

behaviour. Water balance results show that surface flux components as well as evapotranspiration and runoff patterns are realistic regionally and on a global scale. In terms of the carbon balance, adequate simulations of net primary productivity, biomass and leaf area are produced, despite the complexity of the processes considered. Global vegetation cover is fairly represented, as indicated by the kappa statistic (Monserud, 1990) calculations of 0.47. On a category level there is a wider range of agreement.

Foley *et al.* (1998) directly couple the GENESIS GCM and the IBIS model, through a common treatment of land surface and ecophysiological processes (which determine water, carbon, energy and momentum fluxes between soils, vegetation and the atmosphere). The GENESIS GCM simulates the general circulation and atmospheric physics, while IBIS predicts transient change in vegetation structure. A 30-year simulation is performed (using present day CO_2 concentrations and observed sea surface temperatures) at a coarse GCM horizontal resolution (4.5° latitude by 7.5° longitude) and a moderate biosphere model resolution (2° latitude by 2° longitude). The simulation does not reach equilibrium in this period, but the study does indicate some important behavioural features. Zonal temperature and precipitation distributions are correctly simulated, but there are some regional biases, e.g. the high northern latitudes are too warm, while the Himalayas, central South America and north-central Africa are cooler than observed. With respect to precipitation, South America, equatorial Africa and Indonesia appear to be too dry and northern Africa and China are wetter than observed. The model realistically captures forests and grasslands, but there are regional misrepresentations, such as in central Canada and southern South America (forest cover is not simulated) and northern Africa (grasslands extend too far into this region). However, these results are likely to improve with increased resolution, and the study demonstrates the feasibility of climate-vegetation model coupling experiments, particularly in the context of global climate change and vegetation feedbacks.

In Levis *et al.* (1999), the premise that the Earth's vegetation and climate may have more than one state is investigated. The GENESIS atmospheric GCM is used in conjunction with IBIS, in a transient interaction, using a common land surface interface. In this paper, two climate simulations of the present day, using different initial conditions, are examined. In the one instance observed vegetation is used to initialise the model. In the other, high-latitude tundra is replaced with evergreen boreal forests. The results are encouraging since they show the climate-vegetation system to converge at the same equilibrium state.

CHAPTER 3

HADLEY CENTRE TRANSIENT RUN SIMULATION

CHAPTER 3

HADLEY CENTRE TRANSIENT RUN SIMULATION

3.1 Evaluation of the Hadley Centre transient simulation

Data from the Hadley Centre HadCM2 transient simulation described in Chapter 2 (*viz.* a non-sulphate greenhouse gas integration with historic CO_2 from 1860-1989 and thereafter a 1% compound increase in CO_2) are examined here over the southern African domain south of 20°S. The HadCM2 simulation has been extensively studied globally (Murphy, 1995; Murphy and Mitchell, 1997; Johns *et al.*, 1997) and regionally (Joubert, 1997) and in this section the focus is on a simple evaluation of the basic related features over southern Africa. This is merely to confirm the findings of other studies and to demonstrate the viability of the simulation. To be consistent with time periods considered in the chapters to follow, two three-decade comparative periods, the early (2000-2030) and late (2050-2080) 21st century are considered in the HadCM2 data presented in the sections to follow.

The reliability of a sensitivity study will depend to a large degree on the appropriate representation of spatial and dynamic patterns of the baseline climatology. As a means of broadly evaluating the climatology of the HadCM2 model, these data are compared with the NCEP/NCAR reanalysis data[1]. Daily NCEP/NCAR reanalysis data from 1970-1999 have been averaged into a 30-year climatology of seasonal averages for the conventional summer (December, January, February) and winter (June, July, August) months for mean temperature (at 2 metres) and sea level pressure. These are compared with data from the HadCM2 simulation, which are available for the period 2000-2030. Since these two periods do not match temporally, comparisons and evaluations are not made in terms of absolutes, but rather in terms of the HadCM2 model's basic representation of dynamics and spatial patterns.

It is evident that the NCEP/NCAR reanalysis data mean temperature patterns (figure 3.1) for summer are not notably different in spatial pattern from those of the HadCM2 data (figure 3.2), with both showing higher temperatures over the western central interior and lower temperatures over the eastern escarpment regions. These data compare favourably for winter as well, with

[1] These data are available from the NOAA Climate Diagnostics Center (http://www.cdc.noaa.gov/). Documentation relating to these data may found in Kalnay *et al.* (1996).

both the NCEP/NCAR reanalysis data and HadCM2 data showing temperature minimums over the south-eastern interior and higher temperatures to the north.

In terms of circulation, the NCEP/NCAR reanalysis sea level pressure data (figure 3.3) show a more defined low pressure trough over the west, when compared to the HadCM2 data (figure 3.4) for both summer and winter. The general patterns elsewhere over the sub-continent are not dissimilar between the two, and the South Atlantic and South Indian High Pressures in the HadCM2 data closely resemble those of the reanalysis data.

Therefore, it is clear from the above, that the basic surface pattern in the HadCM2 realistically captures the temperature gradients represented in the NCEP/NCAR reanalysis data as well as the primary circulation features. On the basis of this and the other studies noted, the HadCM2 model is deemed suitable for the sensitivity study presented in this research.

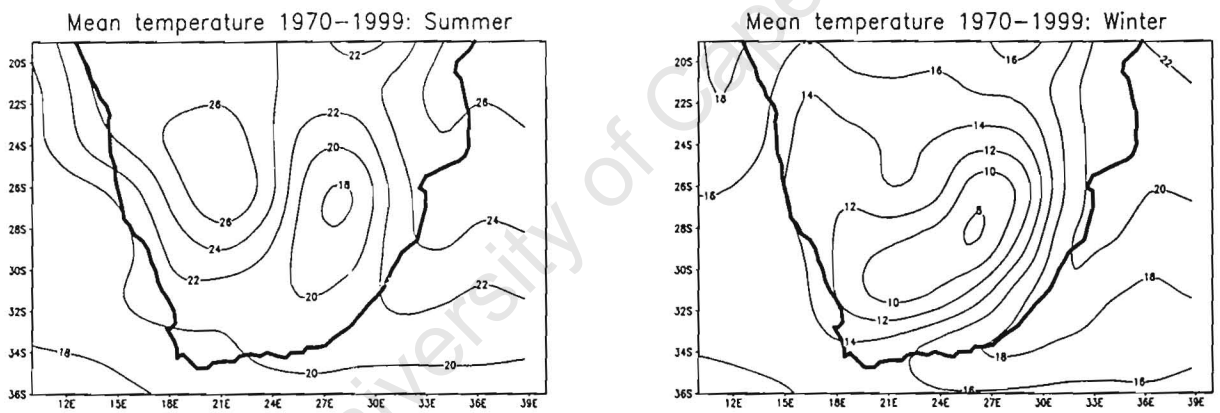

Figure 3.1 NCEP mean temperature (°C) at 2m for 1970-1999

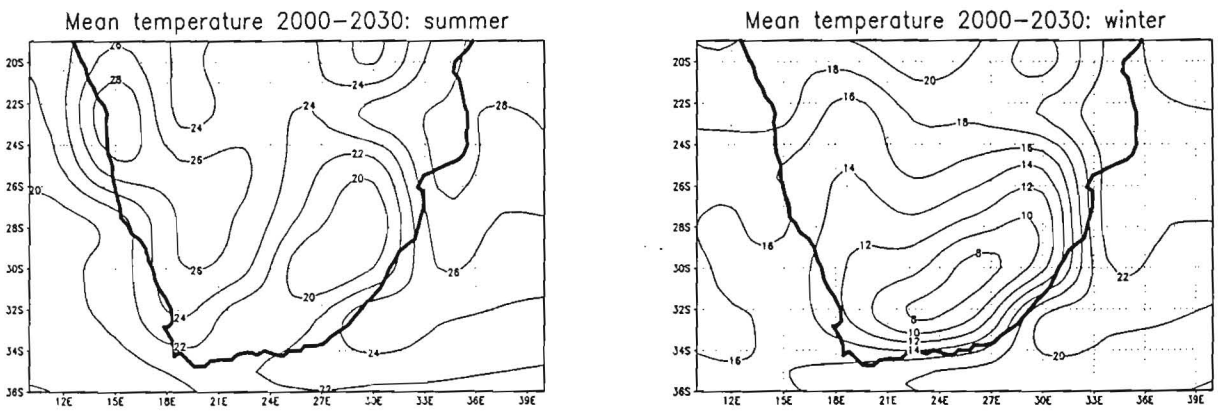

Figure 3.2 HadCM2 mean temperature (°C) at 2m for 2000-2030

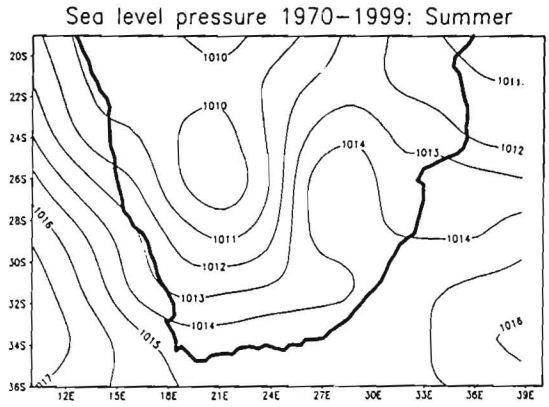

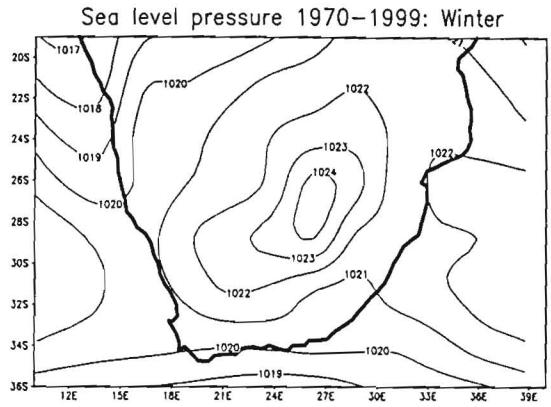

Figure 3.3 NCEP mean sea level pressure (hPa) for 1970-1999

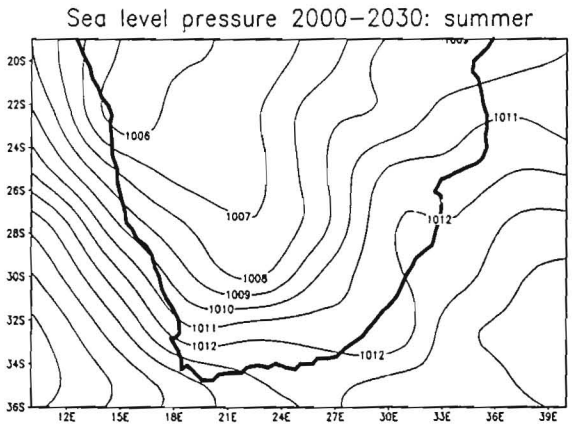

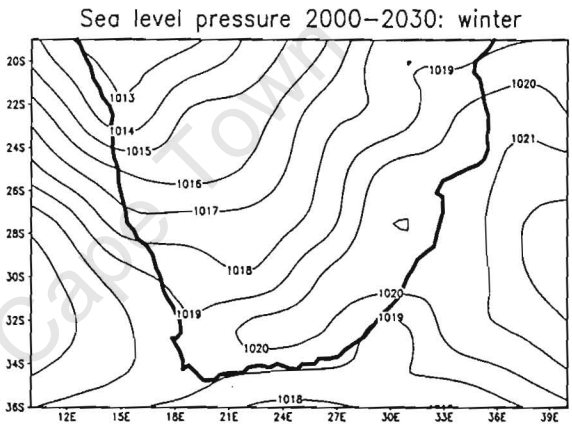

Figure 3.4 HadCM2 mean sea level pressure (hPa) for 2000-2030

3.2 Broad scale changes in the Hadley Centre transient simulation

In general, on sub-continental scale, the HadCM2 transient simulation suggests a southwards extension of the subsidence region of the southern Hadley Cell over the Southern Hemisphere, through the 21st century. This is supported by a zonal sea level pressure increase to the south of the existing hemispheric high pressure belt. The global mean temperature response to an effective doubling of carbon dioxide (CO_2) is approximately a 2.5°C increase.

Regionally, mean temperatures over southern Africa have increased, with a greater magnitude of increase in winter than summer. There is a greater increase in maximum temperatures in summer and a greater increase in minimum temperatures in winter, with the land surface warming to a greater extent than the surrounding oceanic environment. Increases in temperature have implications for the land surface, since temperature increase are likely to promote continental drying.

Wind speed responses are seasonally dependent, with increases to the west of southern Africa in summer, with implications for coastal upwelling, and decreases to the south in winter, representing a decrease in mid-latitude westerly flow, and hence a likely decrease in intensity of midlatitude cyclones. There is an increase in wind speeds to the south of the sub-continent in summer, related to the southwards extension of the southern Hadley Cell.

Relative humidity and precipitation over the region indicate a summer continental drying. However, in both summer and winter there is an increase of almost 10% in moisture availability in the atmospheric column over the southern Africa domain, as indicated by the derived area-averaged specific humidity. This may be significant for plant growth, since increases in specific humidity may counter to some degree the soil drying effect of temperature increases and precipitation decreases during the summer months. In winter there is a significant (up to 40%) increase in precipitation over the eastern interior, with implications for the extension of the growing season. The sections to follow present a more detailed account of these findings over the southern African region.

3.3 The southern African region

In the section to follow, the early 21st century (2000-2030) is referred to as period 1 and the late 21st century (2050-2080) is referred to as period 2.

3.3.1 Surface Temperature

Temperature anomalies are examined in terms of the mean, maximum and minimum for the summer and winter seasons (figures 3.5, 3.6 and 3.7). There is a warming in both summer and winter months, in line with the global mean temperature increase.

a) Summer

The mean temperatures and temperature anomaly maps for periods 1 and 2 are presented in figure 3.5. The mean temperature anomaly map indicates an increase in temperature with a maximum increase over the central interior of 2.7°C. This decreases to a 0.9°C increase over the southern coastal regions and 1.5°C over the east coast. The maximum temperature anomaly (figure 3.6) from period 1 to 2 shows an increase of 2.7°C over the central interior, decreasing over the south coast to 0.9°C, and 1.5°C over the east coast. It is evident from the minimum temperature and temperature anomaly maps (figure 3.7), that minimum temperatures have increased by up to 2.7°C over the western interior, and 0.9°C to 1.4°C over the south and eastern coastal regions, between periods 1 and 2. These increases in mean, maximum and minimum temperatures will promote a summer continental drying.

b) Winter

Figure 3.5 displays the mean temperature and temperature anomalies over the southern African domain. The mean temperature anomaly map indicates an increase from period 1 to 2 of up to 2.8°C over the western interior, moderating to a 1.4°C increase over the southern coastal region. Maximum temperature anomalies (figure 3.6) between periods 1 and 2 exhibit an increase of 2.2°C over the western interior, 1.2°C to 1.4°C over the south, and up to 1.6°C over portions of the east coast. Figure 3.7, displaying the minimum temperatures and temperature anomalies, shows that between periods 1 and 2 the minimum temperature has increased by approximately 3.3°C over the interior regions. Minimum temperature increases over the southern coast are about 1.5°C. Winter temperature increases, like summer, are also indicative of a drying of the land surface.

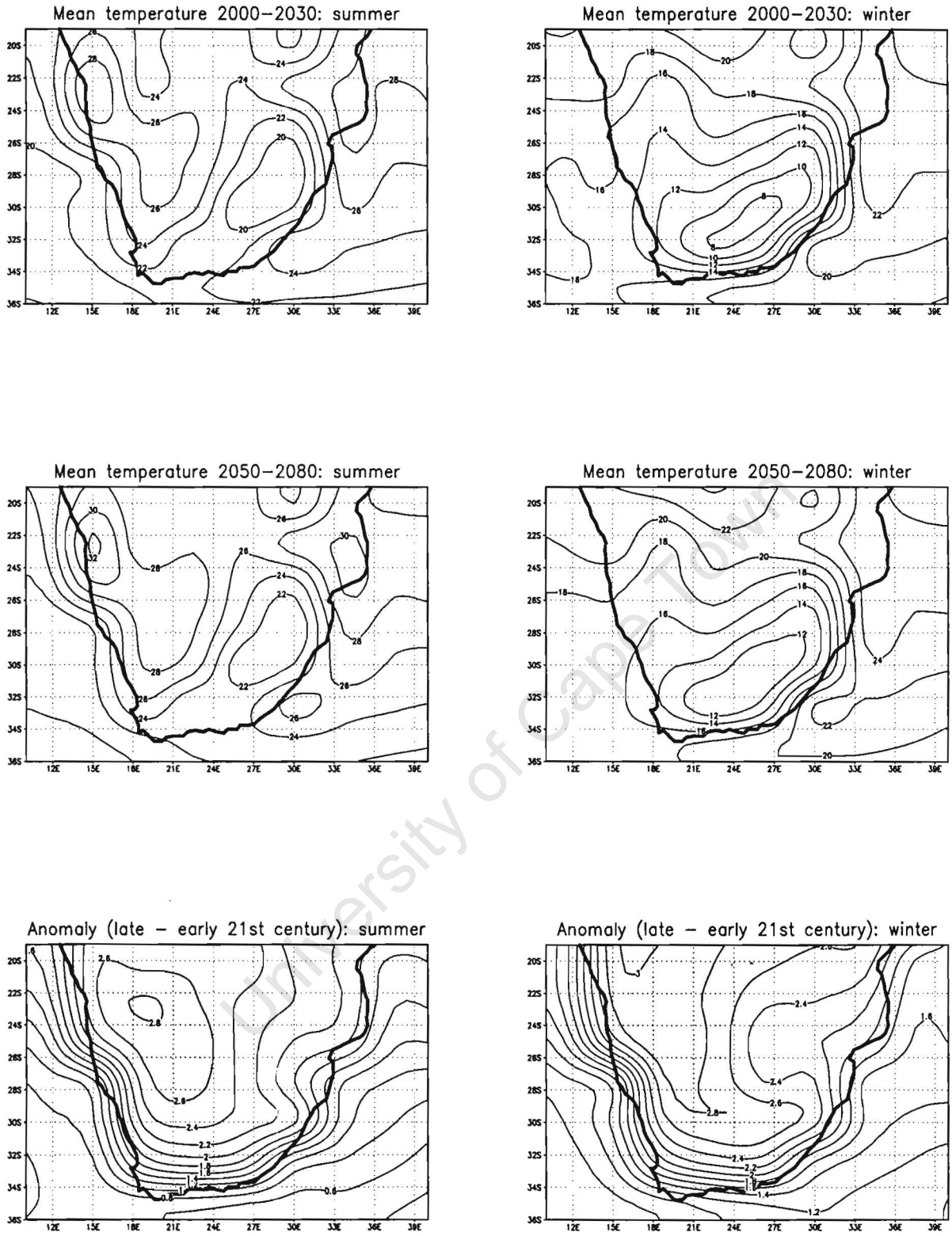

Figure 3.5 HadCM2 mean temperature (°C) and temperature anomalies for summer and winter

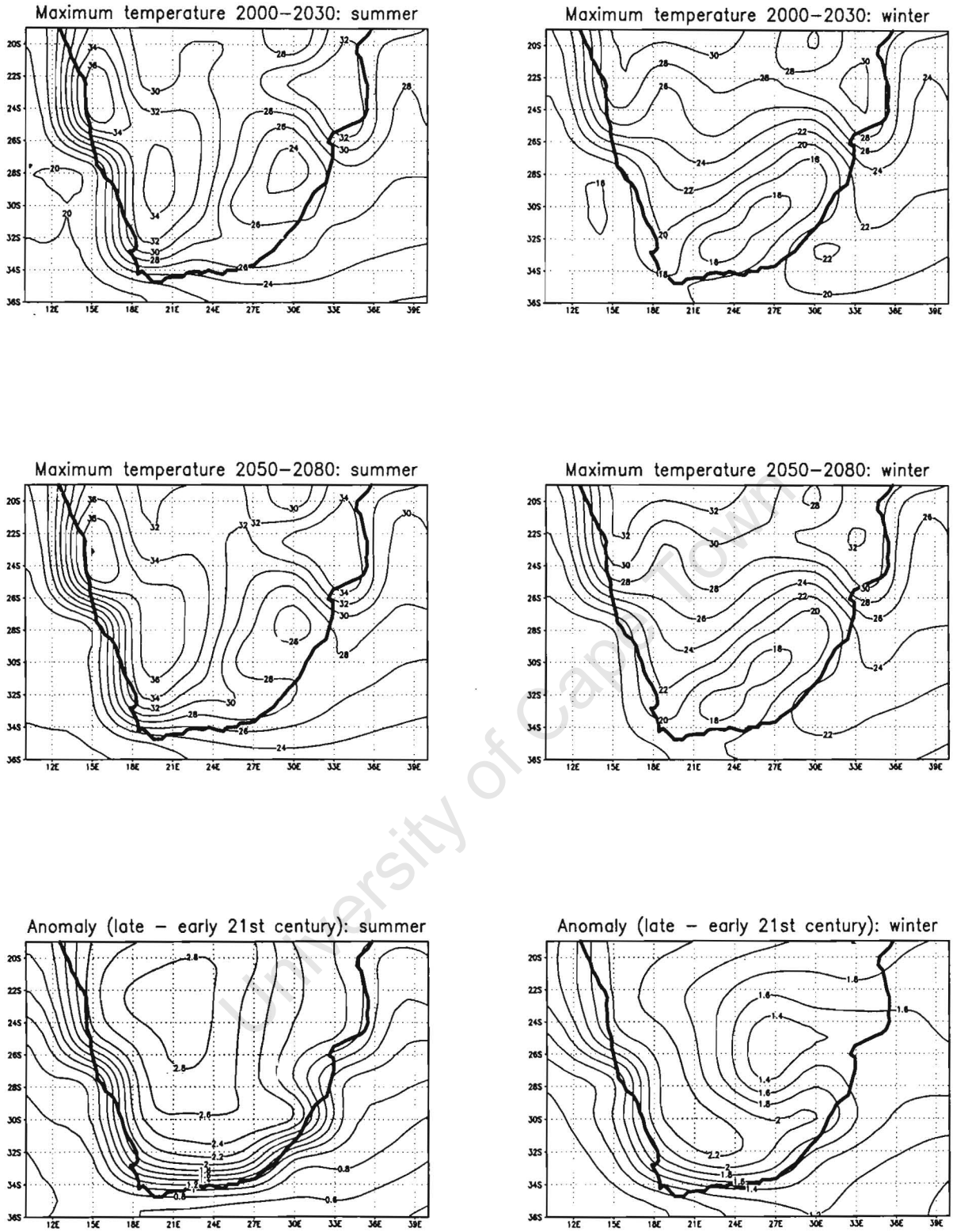

Figure 3.6 HadCM2 maximum temperature (°C) and temperature anomalies for summer and winter

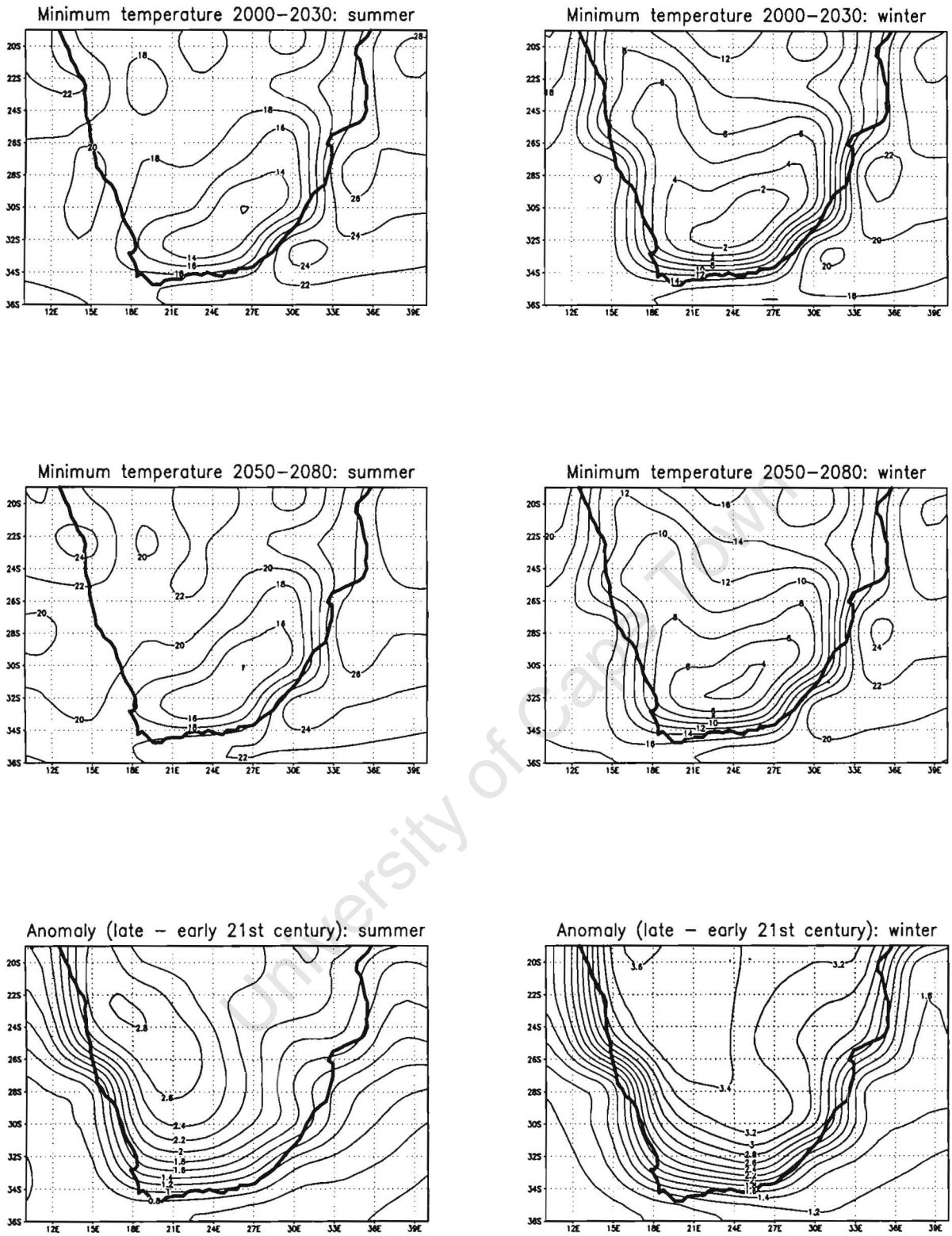

Figure 3.7 HadCM2 minimum temperature (°C) and temperature anomalies for summer and winter

3.3.2 Sea level pressure

a) Summer

The sea level pressure anomaly (figure 3.8) from period 1 to 2 indicates a weakening of the low pressure in the west and western interior (0.6 hPa). There is a slight strengthening of pressure over the south (0.2 hPa). There is a zonal increase in sea level pressure to the south of the existing high pressure belt, indicating a southwards extension of the subsidence region of the southern Hadley Cell.

b) Winter

It is evident from figure 3.8, that between periods 1 and 2 there is a decrease in pressure over the entire sub-continent. Decreases over the west and western interior are up to 1 hPa, declining to a decrease of 0.2 hPa over the coastal regions. A southwards extension of the southern Hadley Cell is suggested by the increases in zonal sea level pressure to the south of the southern African domain.

3.3.3 Relative humidity

a) Summer

From period 1 to 2 there is a general decrease in relative humidity over most of the region (figure 3.9), with the greatest decrease over the northern interior (4.5%) and little change over the coastal regions (increases and decreases of 0.5%). The changes over the north represent an absolute decrease of up to 10%, while over the coastal regions the absolute increase is insignificant.

Specific humidity changes are more useful indicators of moisture in the atmospheric column. Using basic moisture equations relating temperature, pressure and relative humidity, specific humidity may be determined[2]. The area-averaged specific humidity for the southern African grid window considered in the analyses has been calculated for periods 1 and 2. Indications are for an increase in specific humidity from approximately 13.7 g kg^{-1} to 14.7 g kg^{-1}, which represents an absolute increase of almost 10%. This is particularly significant in the context of the potential available moisture for plant growth over the sub-continent. Therefore, although mean temperatures have increased, which would promote a summer drying, increases in specific humidity may counter the drying effect on vegetation.

[2] See http://www.faqs.org/faqs/meteorology/temp-dewpoint/

b) Winter

There is a relative humidity increase (figure 3.9) over a large portion of the country (up to 5.5% over the south central interior and 1% over the south coast) between periods 1 and 2. There is a decrease over the west coast (2%). In terms of absolute increases, the changes over the south central interior represent increases in excess of 10%, while the changes over the remainder of the region are less significant. Area-averaged specific humidity has also been calculated for the winter season and shows an increase from about 8.25 g kg^{-1} to 9.4 g kg^{-1} between periods 1 and 2 respectively. This represents an increase of almost 9%, which is again significant in terms of available moisture within the atmospheric column over the domain. As is the case for summer, the increase in specific humidity may potentially counter to some degree the likely soil drying effect on vegetation as a result of the temperature increase.

3.3.4 Precipitation

a) Summer

It is evident from figure 3.10, that between periods 1 and 2 there is a decrease in precipitation over the east (of between 0.2 and 0.6 mm day^{-1}), over the Botswana/Namibia border (0.4 mm day^{-1}) and Northern Zimbabwe (0.4 mm day^{-1}). There is a precipitation increase over the north-east (0.2 mm day^{-1}). The precipitation decreases represent a change of up to 15%, while increases over the north-east are of the order of 5%. There is a therefore a general drying out in terms of precipitation and relative humidity over most of the region, although specific humidity has increased over the region by up to 10%. The increase in specific humidity implies an increase in potential moisture available for plant growth, subject to a rainfall mechanism being present.

b) Winter

Figure 3.10 indicates that from period 1 to 2 there is a decrease in precipitation over the Western Cape and south coast (0.1 mm day^{-1}), but an increase further inland and further east (up to 0.6 mm day^{-1} in places). This represents an absolute decrease of 15% over the coast, and an absolute increase of 40% over the inland eastern regions. The increase over the inland eastern regions is significant in terms of plant growth, since this region generally receives most rainfall during the summer season. This may therefore be important in terms of vegetation productivity, since this may represent an extension of the growing season, with the increase in moisture in the atmospheric column being further supported by increases in specific humidity over the region.

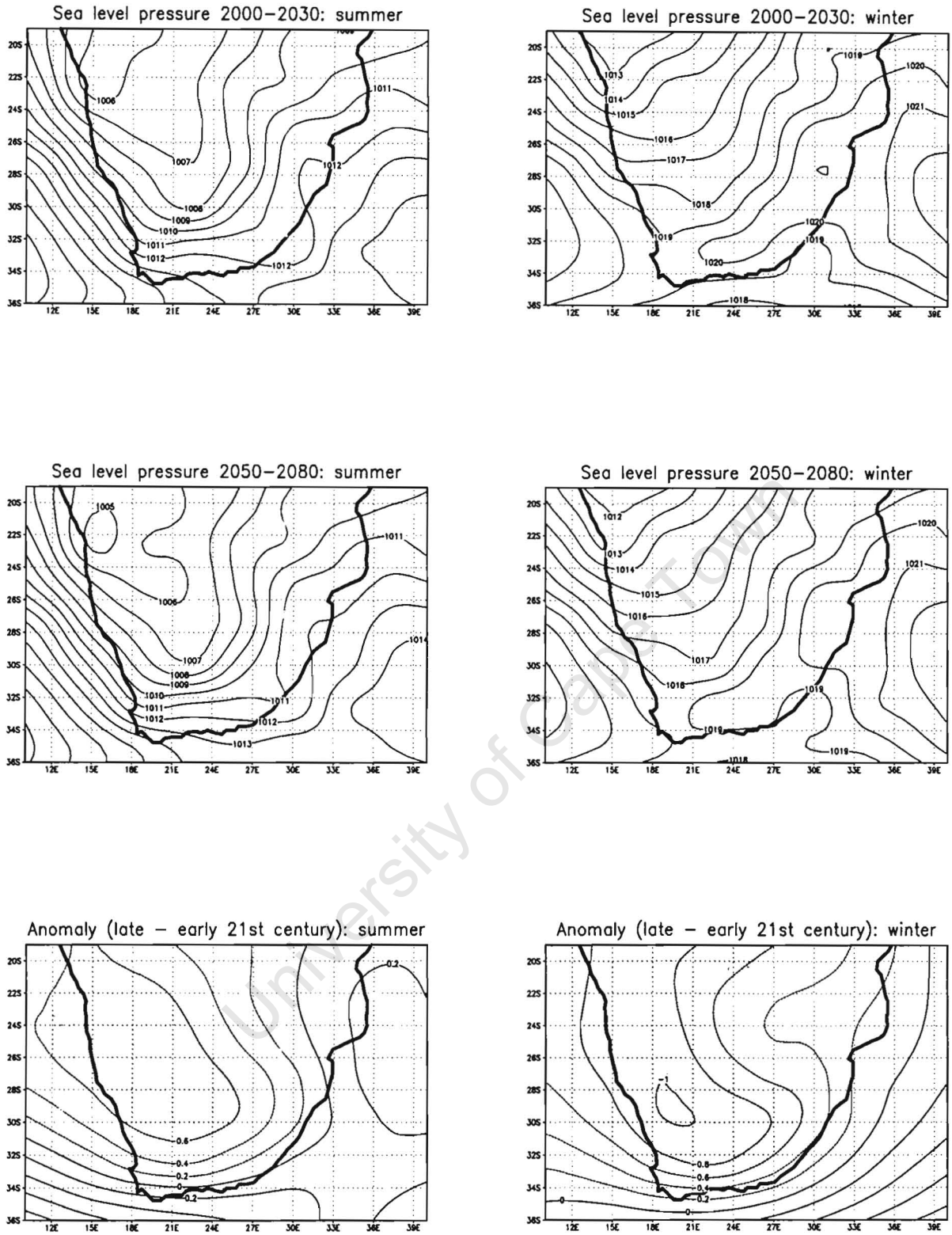

Figure 3.8 HadCM2 sea level pressure (hPa) and sea level pressure anomalies for summer and winter

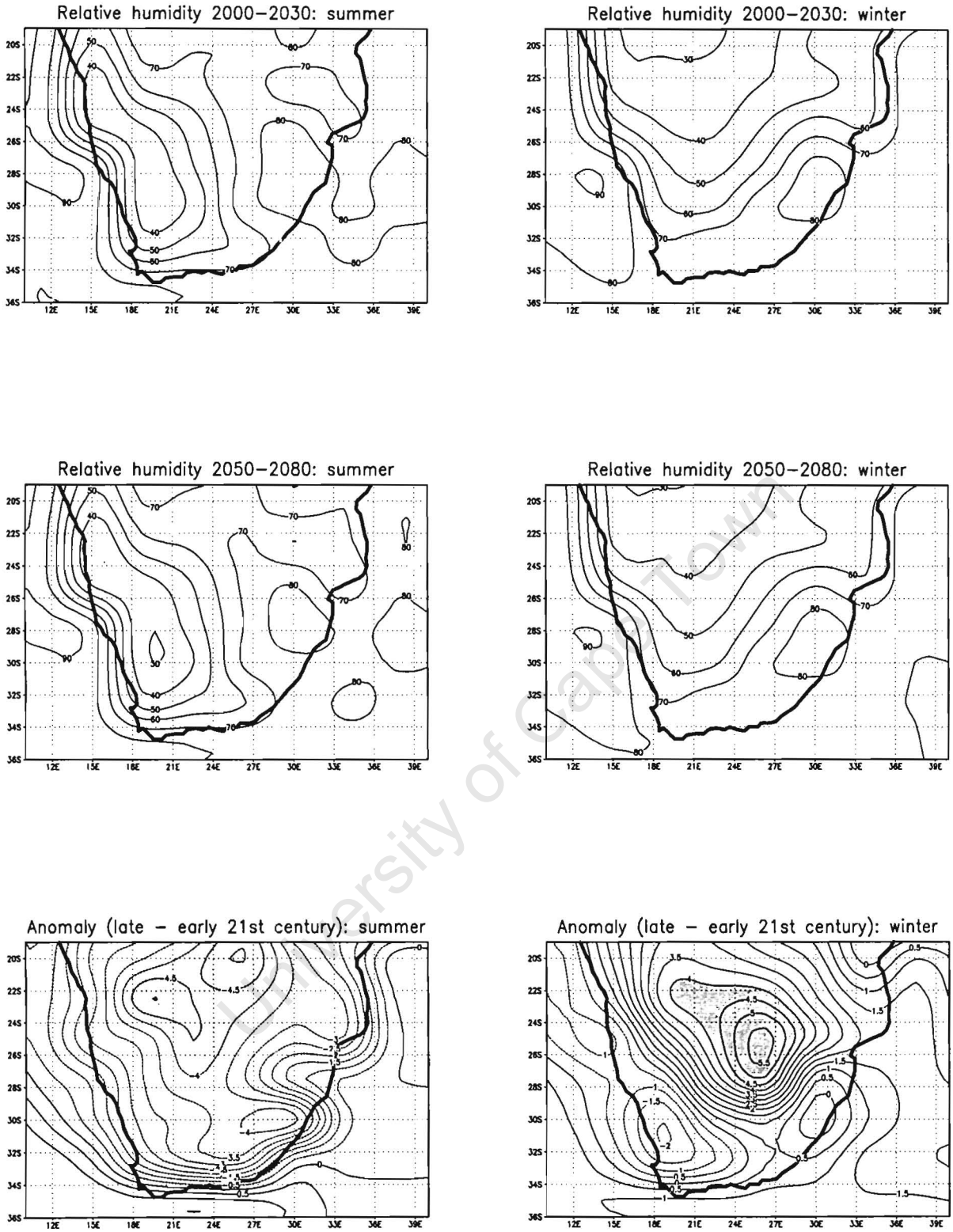

Figure 3.9 HadCM2 relative humidity (%) and relative humidity anomalies for summer and winter

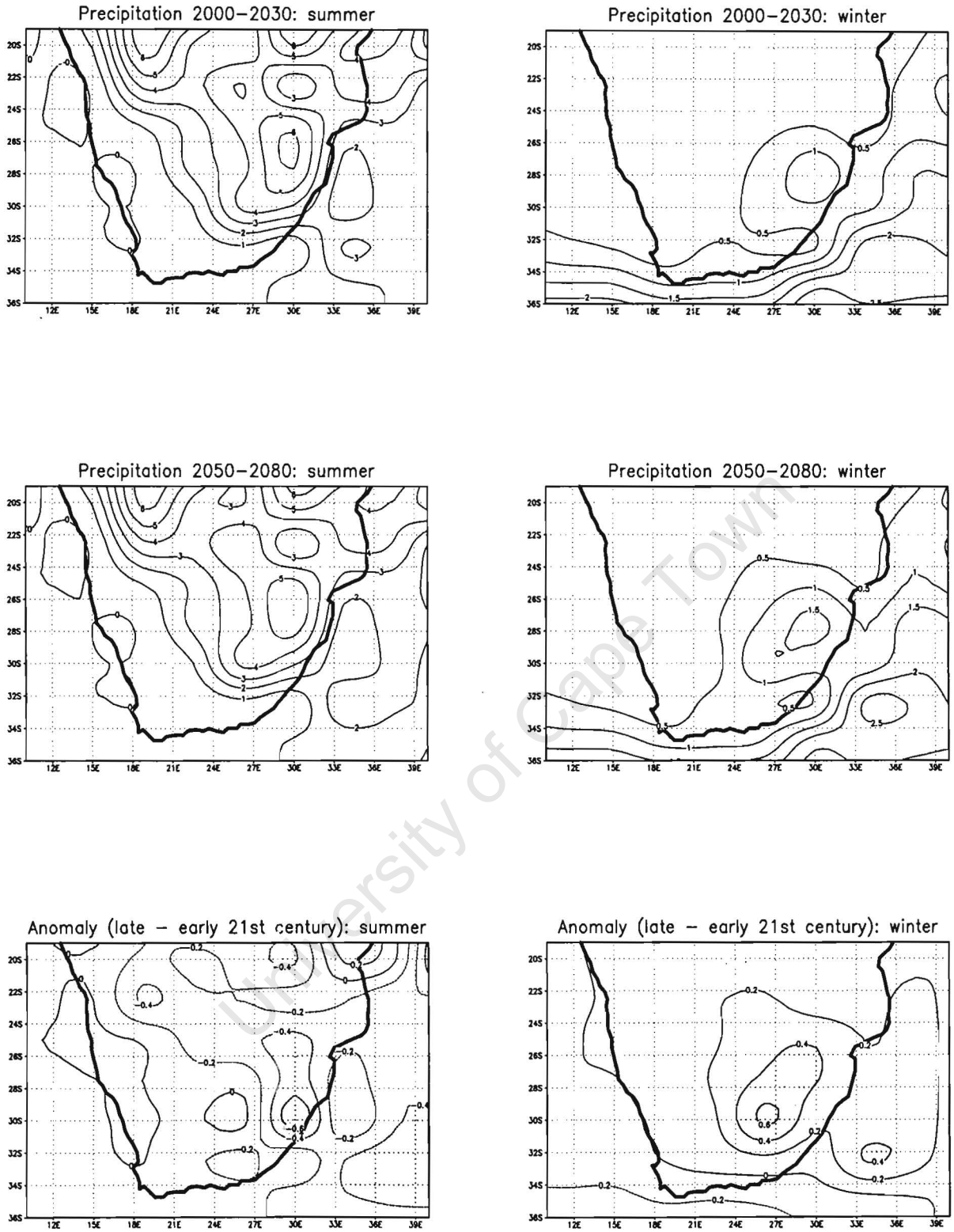

Figure 3.10 HadCM2 precipitation (mm day^{-1}) and precipitation anomalies for summer and winter

3.3.5 Wind speed

a) Summer

Wind speeds from period 1 to period 2 (figure 3.11) indicate that there is an increase over the sub-continent (the maximum increases are 0.2 to 0.3 m s^{-1}), which represents an absolute wind speed increase of 5%. There are wind speed increases to the west of the country in addition (0.5 m s^{-1}); an absolute increase of 6%. This may be important in terms of coastal upwelling, since upwelling may be promoted with an increase in wind speed. Therefore, heat transfer from the sub-continent to the surrounding oceanic environment may be promoted via the associated offshore airflow, and hence continental drying may be enhanced. There are also increases in wind speed to the south of the sub-continent, related to the southwards extension of the southern Hadley Cell.

b) Winter

Figure 3.11 shows that from period 1 to 2 there is a decrease in wind speed over the southern interior (0.2 m s^{-1}) and south (0.35 m s^{-1}), and an increase over the western central interior, north-west (0.15 m s^{-1}) and over the Indian Ocean to the east of the sub-continent (0.2 m s^{-1}). The increases are of the order of 5% and the decreases are of the order of 3%. The decreases to the south of southern Africa may be placed in the context of the subtropical jet stream, with the decrease suggesting either a polewards shift or a decreased intensity of the jet stream. This has implications for midlatitude cyclones, which may be expected to perhaps decrease in intensity (this is further supported by the 15% decrease in precipitation over the SW Cape). However, it is not possible to draw conclusions as to the frequency changes of midlatitude cyclones.

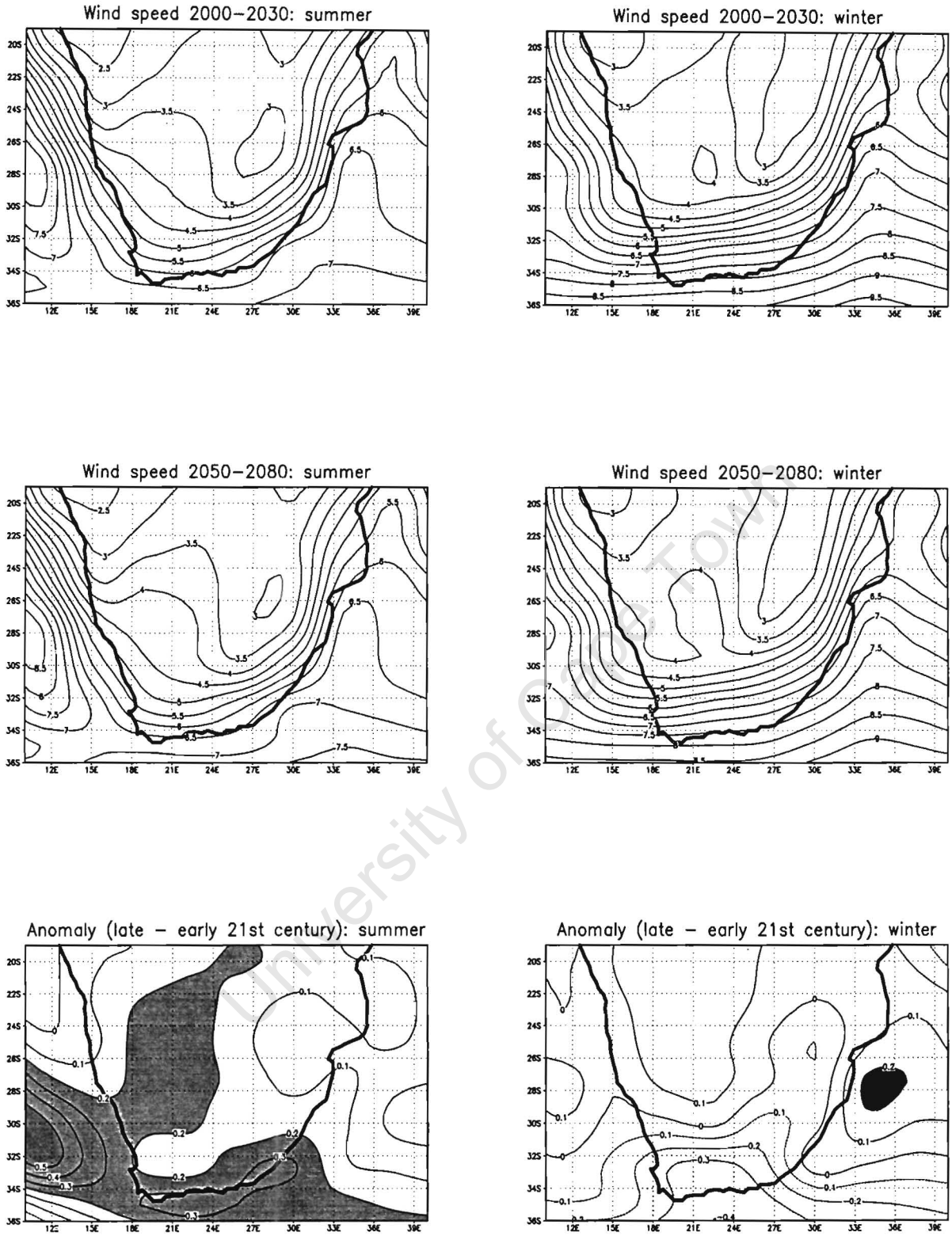

Figure 3.11 HadCM2 wind speed (m s^{-1}) and wind speed anomalies for summer and winter

CHAPTER 4

IBIS MODEL SIMULATION

CHAPTER 4

IBIS MODEL SIMULATION

4.1 Data and model configuration

The base climate input fields (provided by the model developers) for the IBIS model are indicated in table 4.1. Monthly mean cloudiness, monthly mean precipitation rate, mean "wet" days per month and monthly mean temperature are derived from the CLIMATE[1] data set (version 2.1), which is a significant update of Leemans and Cramer's (1991) 0.5°x0.5° analysis of station data for 1931-1960. Monthly mean relative humidity is adapted from World Weather Disc data. Monthly mean relative humidity at sigma level 0.995 and monthly mean wind speed at sigma level 0.995, are determined from NCEP/NCAR reanalyses[2] (long-term mean for 1958-1997). Wind speed is calculated from daily data, and averaged over the month and therefore does not capture sub-daily variances. This leads to wind speeds of about 0.5 m s^{-1} lower than they would be if they had been calculated on a finer temporal scale. Soil texture is taken from Webb *et al.* (1993). The ETOPO5 (Earth Topography – 5 minutes) gridded elevation data, available from the National Geophysics Data Center[3] are used to determine the continental/oceanic boundaries and topography.

HadCM2 data from the Hadley Centre model are used to initiate a series of anomaly simulations. In an IBIS anomaly simulation the climatology monthly mean temperature, precipitation, relative humidity, cloudiness, wind speed and mean "wet" days per month are altered by the addition of an anomaly field to reflect a different climate state. In this research cloudiness and the number of "wet" days in a month are left unchanged. "Wet" days per month are not possible to determine, since only monthly precipitation data are available. However, since "wet" days per month are only used to generate stochastic precipitation events within IBIS and don't generally affect total rainfall per month, this is not considered a problem (Foley, *pers. comm.*). Wind speed in IBIS is calculated at sigma level 0.995, and since sigma level data are not available for the HadCM2 data, 10 metre wind speeds are used as an approximation. Wind speeds are often a rough calculation, and since one does not always have sigma level data one often does not have a choice but to use an alternative (Foley, *pers. comm.*). The variables which

[1] http://www.pik-potsdam.de/~cramer/climate.htm
[2] http://www.cdc.noaa.gov/
[3] http://www.ngdc.noaa.gov/

are therefore changed in the anomaly are as follows: monthly mean temperature, monthly mean precipitation rate, monthly mean relative humidity and monthly mean wind speed.

Variable	Units
Monthly mean cloudiness	%
Minimum temperature minus average temperature of coldest month	°C
Monthly mean precipitation rate	mm day^{-1}
Monthly mean relative humidity	%
Monthly mean relative humidity at sig=0.995	%
Soil texture	Represented by a 4-digit number indicating the relative proportions of the soil which are clay, silt and sand
Surface type	Land versus ocean
Monthly mean temperature	°C
Topography	m
Monthly mean temperature range	°C
Monthly mean wind speed at sig=0.991	m s^{-1}
Mean "wet" days per month	Days
Vegetation	Categories
Monthly mean wind speed at sig=0.995	m s^{-1}

Table 4.1 Base climate input fields for the IBIS model

The Unified Model HadCM2 data used to create the anomaly for IBIS are monthly data at a spatial resolution of 2.5°x 3.75°, and are from a non-sulphate aerosol greenhouse gas climate change simulation performed using a 1% compound increase in CO_2 from 1990 to 2099 (and historic CO_2 from 1860 to 1999). Each month of the year is smoothed with a 10-year running mean, in order to reduce the influences of large inter-annual variabilities.

Carbon dioxide (CO_2) is taken as fixed, which is appropriate since in the anomaly an increase in CO_2 is in some way implied by the climate forcing, although the effect of CO_2 fertilization is not represented in the IBIS model. CO_2 is initialised as 0.000350 mol/mol (real) and Oxygen (O_2) as

0.209 mol/mol (real). The model is run hourly over the entire global domain and an accelerated soil spin up procedure is used, such that equilibrium is reached over a shorter period of time. Vegetation can be set to static, dynamic or dynamic from a cold-start. Static vegetation implies that the model vegetation is fixed and hence is unable to vary on an annual basis with the changed input data. Dynamic vegetation fluctuates on an annual basis, being determined by the model input variables. Dynamic vegetation evolving over time without a base vegetation data set is referred to as dynamic from a cold-start, while dynamic vegetation varying from some baseline input vegetation data set is referred to as dynamic (not from a cold-start). In this research the dynamic (not from a cold-start) and static vegetation options are used to initiate two mean climate change runs.

The positive and negative standard deviations from the mean monthly smoothed precipitation, temperature and relative humidity data are determined. These are then used to initiate 5 further plausible climate change scenarios (P1-P5), which are used as a mechanism for placing some degree of confidence in the response to climate change and climate thresholds. In real terms the positive and negative standard deviations from the mean monthly smoothed data translate into a temperature deviation of approximately 0.7°C from the mean, a precipitation deviation of approximately 0.4 mm month^{-1} and a relative humidity deviation of about 3.5%. Table 4.2 shows the resultant seven anomaly simulations performed using IBIS and figure 4.1 shows a snapshot view of each scenario's input parameters. Note that wind speed data were not subjected to the same process as precipitation, temperature and relative humidity data (i.e. positive and negative standard deviations from the mean response), since increases as opposed to decreases could not be justified plausibly for each particular scenario.

In essence each of scenarios P1-P5 is representing a different environment from the mean vegetation response, by means of standard deviation variations from the mean response. Scenario P1 represents an environment with more extreme positive precipitation and temperature changes and a lower relative humidity input than the mean dynamic vegetation model run. This represents an upper extreme scenario. P2 places greater emphasis on temperature increases, while precipitation and relative humidity changes are at the negative standard deviation extreme from the mean. P3 is a scenario of greater than mean precipitation and relative humidity changes and less notable change (increase) in temperature. P4 is a lower scenario extreme with the least change in temperature or precipitation, and a related higher relative humidity change. P5, like P1, represents an upper extreme scenario, but with a greater

change in relative humidity than in P1. Scenarios P1-P5 therefore represent a reasonable range of scenario responses, but are clearly by no means exhaustive.

IBIS model simulation	Model simulation description	Parameters used			
		Temperature	Precipitation	Relative humidity	Wind speed
Ibissta	Static vegetation mean run	Mean	Mean	Mean	Mean
Ibisdyn	Dynamic vegetation mean run	Mean	Mean	Mean	Mean
P1	Dynamic vegetation run with standard deviation scenario 1	Positive standard deviation from mean	Positive standard deviation from mean	Negative standard deviation from mean	Mean
P2	Dynamic vegetation run with standard deviation scenario 2	Positive standard deviation from mean	Negative standard deviation from mean	Negative standard deviation from mean	Mean
P3	Dynamic vegetation with standard deviation scenario 3	Negative standard deviation from mean	Positive standard deviation from mean	Positive standard deviation from mean	Mean
P4	Dynamic vegetation run with standard deviation scenario 4	Negative standard deviation from mean	Negative standard deviation from mean	Positive standard deviation from mean	Mean
P5	Dynamic vegetation run with standard deviation scenario 5	Positive standard deviation from mean	Positive standard deviation from mean	Mean	Mean

Table 4.2 Anomaly perturbations performed using IBIS

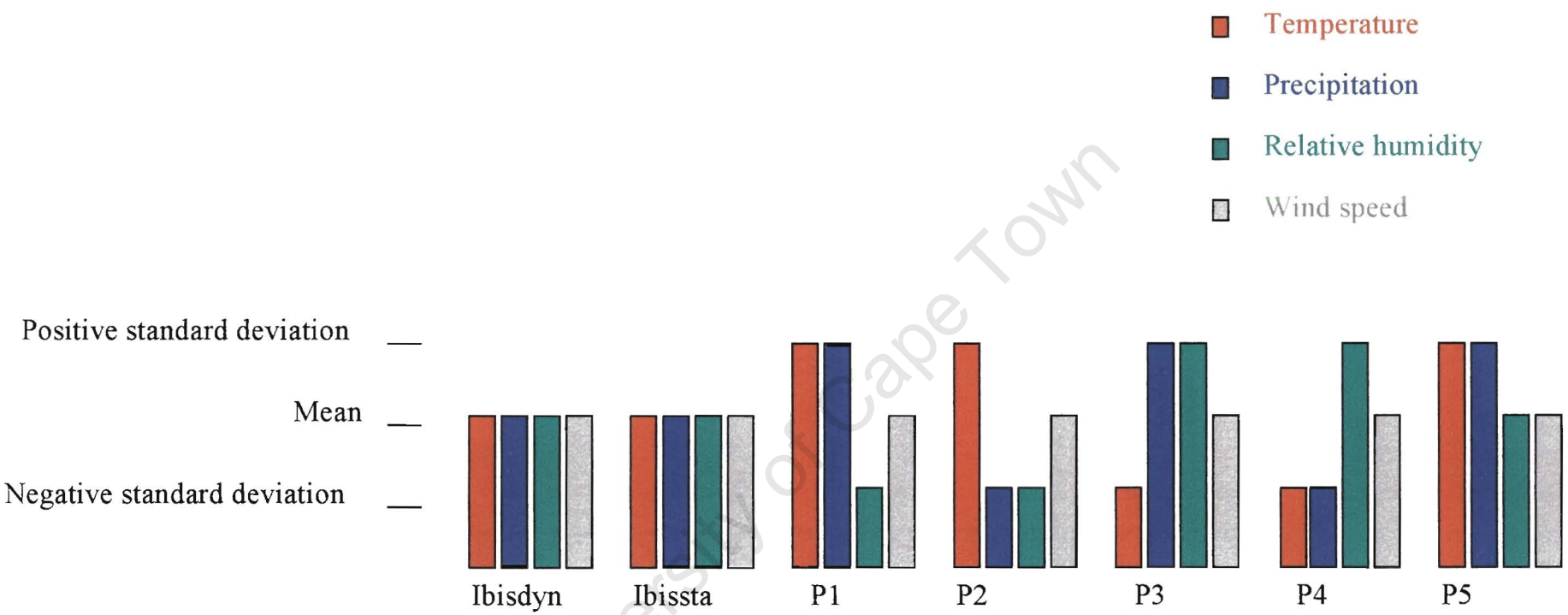

Figure 4.1 Snapshot of the 7 different model simulation scenarios with respect to their input temperature, precipitation, relative humidity and wind speed parameters

Foley *et al.* (1996) conclude that the IBIS model simulation after 50 years has not reached complete equilibrium in terms of vegetation biomass. Foley *et al.* (1998) state that leaf area index reaches equilibrium within approximately 40 years and biomass after a couple more decades in the tropics. Biomass will persistently change in the slower-growing forests in cold climates for a century or more. Based on this and considering the region under examination here is in the subtropics, the IBIS model is run for approximately 65 years with the climatological mean data sets in order to sufficiently stabilise for the purposed of this study. The model is then run for a further 85 years (1995-2080) with anomalies of smoothed annual monthly data sets of precipitation, temperature, relative humidity and wind speed from the HadCM2 transient model run (note that other input variables do not deviate from their mean climate state). Seven IBIS model simulations are initiated in total (one for each of the seven scenarios indicated in table 4.2). Therefore, model sensitivity simulations of a potential future climate state, as represented by changed precipitation, temperature, relative humidity and wind speed are performed, with model output being written on a monthly and annual basis.

It should be noted at this point, that since large-scale GCM simulated features are used to drive the IBIS simulation, the examination of sub-grid scale features is to some extent hindered. Future improvements in a climate change context may be achieved by nesting a regional climate model into a GCM (Giorgi *et al.*, 1994) using IBIS simulations.

4.2 Base vegetation input fields

Figure 4.2 shows the detailed input model vegetation categories (for the dynamic (not from a cold-start) and static model simulations) represented by IBIS at a 0.5° resolution over the southern African domain. In a comparison of figure 4.2 with figure 1.3, it is evident that IBIS fairly reasonably represents the observed vegetation biome distribution. Broadly, the spatial representation of Savanna in IBIS is similar to the observed distribution of Savanna, although it extends too far to the west in South Africa. The Grassland is similarly too far to the west in IBIS and much of the Western Cape is represented as Grassland (since Fynbos is not resolved by the IBIS model). Desert is reasonably realistically represented, while Open shrubland is comparable to the Nama-Karoo and Succulent Karoo biomes. In essence the IBIS vegetation classes are a fair representation of the observed biome distribution in South Africa.

Figure 4.3 shows vegetation categories, at the Hadley Centre model resolution, which is the scale level considered in the present study. Obviously a large amount of spatial detail is lost at this resolution, but the distribution of vegetation types is still realistic and therefore is suitable within the context of the current research, especially given the authenticity of GCM grid cell data. Furthermore, one must bear in mind that there is a diversity of land use. For example, in South Africa approximately 12-13% of the land is under cultivation (Macdonald, 1991), suitably larger proportions are devoted to natural pasture and an urban population inhabits sizeable areas (e.g. Gauteng). Therefore any vegetation representation is not going to be a true representation of the land use within the area. A vegetated surface is assumed in this research, since the primary objective is to examine the sensitivity (of fluxes and other land surface features) between the atmosphere and the biosphere.

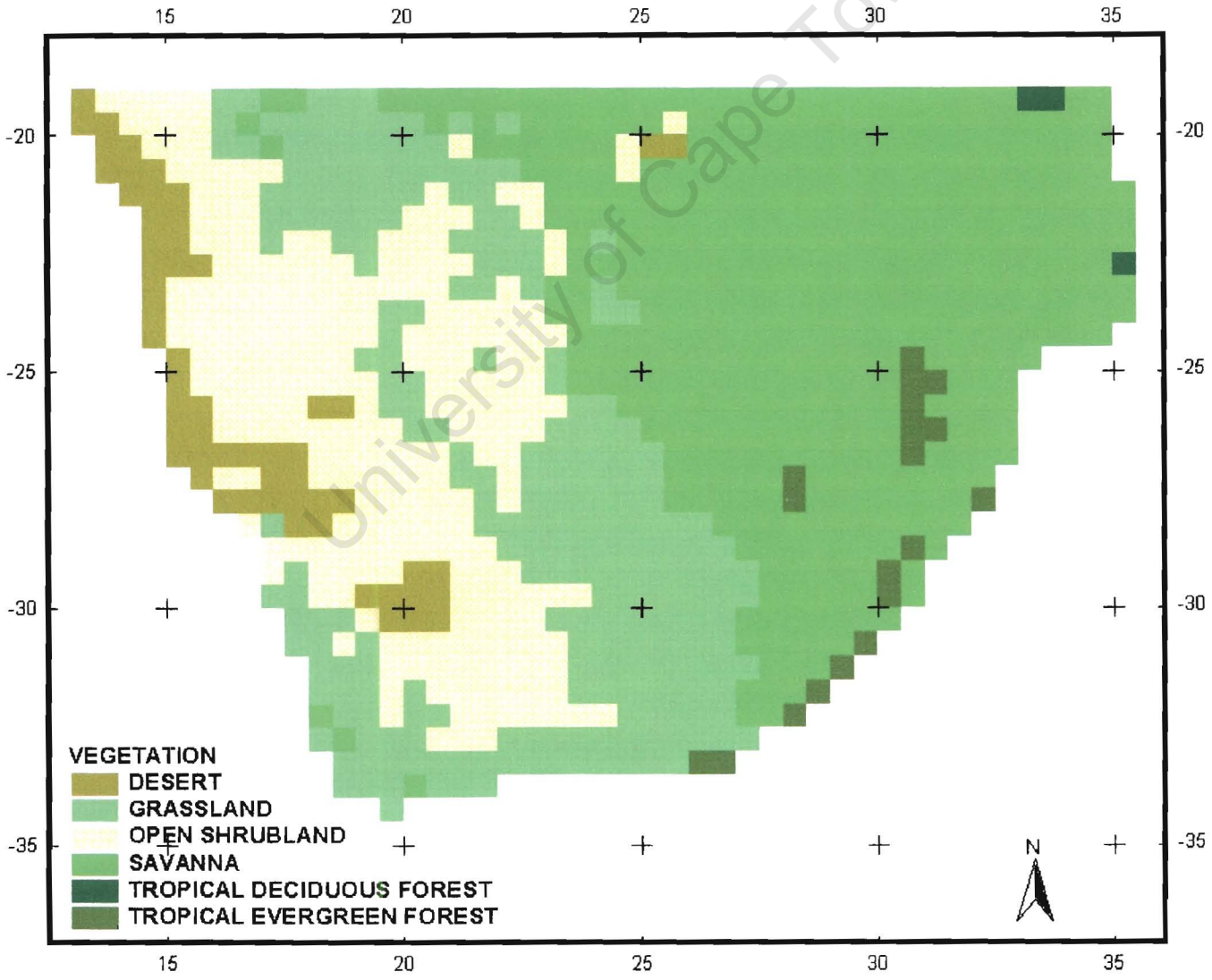

Figure 4.2 0.5° resolution map of vegetation categories produced by the IBIS model over southern Africa

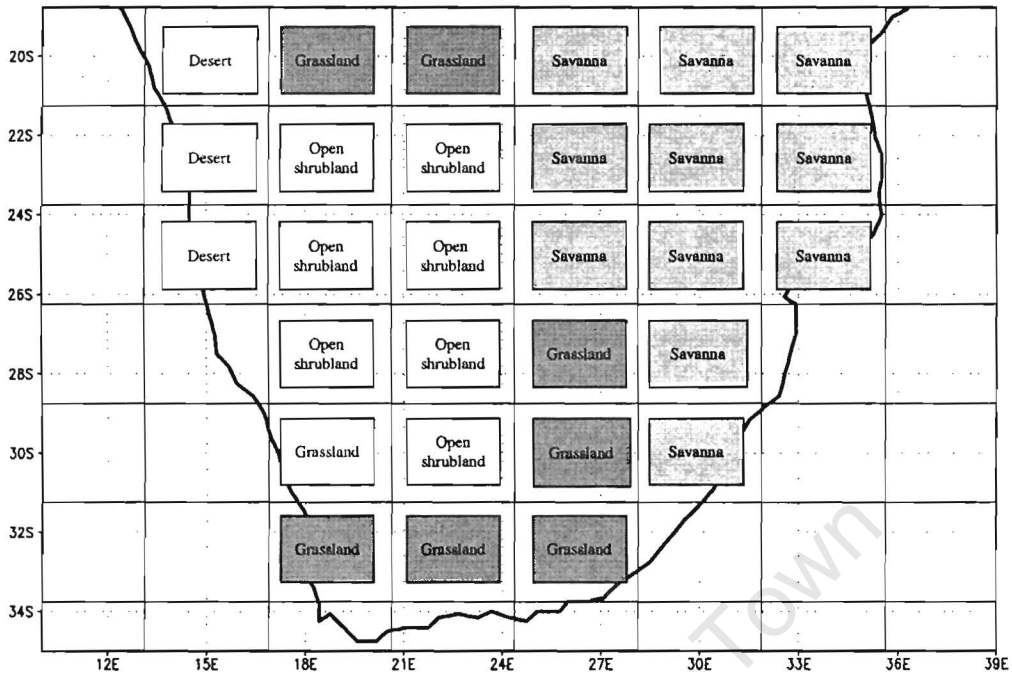

Figure 4.3 Hadley Centre Model resolution depictions of vegetation categories

CHAPTER 5

IBIS MODEL SIMULATION ANNUAL RESULTS

CHAPTER 5

IBIS MODEL SIMULATION ANNUAL RESULTS

The IBIS model simulation reaches close equilibrium after approximately 50-60 simulation years (see Foley *et al.* (1996) and Foley *et al.* (1998)). It is at about this point (1995) that the climate change anomalies from the HadCM2 Hadley Centre Model are initiated in each model simulation. With the above in mind, two three-decade climatology periods were defined and are considered in the sections to follow, *viz.*, the early 21st century (defined as 2000-2030, and referred to as period 1) and late 21st century (defined as 2050-2080, and referred to as period 2).

Results from the IBIS model simulations are presented here in terms of annual changes in some of the model output variables from the 7 model simulations (refer to figure 4.1 in Chapter 4), *viz.* the dynamic vegetation mean run (Ibisdyn), the static vegetation mean run (Ibissta) and the 5 anomaly perturbations (P1-P5). A logical first step is to examine period 1 and the anomaly map differences between period 1 and period 2, in order to obtain an idea of the early 21st century response and the changing response over time, and to establish which areas over southern Africa are showing the greatest response. Since the sample size used is notably small, it would be misleading to conduct Monte-Carlo and other such statistical tests. Thus, the shading representation is not statistically significant scaling, but rather a visual representation of positive and negative values, to aid figure interpretation.

5.1 Differences between the early and late 21st century

Annual net primary productivity (NPP)[1], annual average evapotranspiration, sensible heat fluxes, soil temperature and soil moisture are considered in the analyses in this section. Some central results that emerge from an examination of the anomaly maps follow and a more detailed examination is presented thereafter. In terms of most variables, there are five notable response regions, *viz.*, northern Namibia, the southern Kalahari, the Mozambiquan plains and the SE South African escarpment regions (referred to as the northern and southern escarpment regions). The positioning of these regions is indicated in figure 5.1.

NPP largely shows an increase in most regions for the 7 different scenarios (Ibisdyn, Ibissta, and P1-P5), with scenarios P1, P3 and P5 being most akin to Ibisdyn. Similarly, annual average

[1] The plant energy storage rate of organic matter, in excess of that used for respiration (Whittow, 1984).

evapotranspiration generally increases over the 5 regions, but with some decreases in P1, P3 and P5 over the southern Kalahari and the northern escarpment. Changes in sensible heat fluxes in Ibisdyn and P1-P5 from periods 1 to 2 display increases over some regions (e.g. Northern Namibia and the southern escarpment) and decreases over others (e.g. the Mozambiquan plains and the northern escarpment) while the anomalies in Ibissta are notably dissimilar. Soil temperatures for the different scenarios indicate a general decrease, particularly over northern Namibia and the escarpment regions. Soil moisture anomalies are more complex and variable between the different scenarios.

It is of value to compare the differences between the two mean vegetation runs (*viz.* Ibisdyn and Ibissta), in order to examine the importance of model simulations using the dynamic as opposed to static vegetation option. It is apparent that there is general concordance between the two in terms of annual average evapotranspiration, NPP, soil temperature and soil moisture. However, there is a marked difference in the anomaly for sensible heat fluxes, with flux anomalies of opposite sign over northern Namibia and some dissimilar regions of change. Thus, in terms of model output, sensible heat fluxes are notably dependent on the vegetation being set as dynamic or static, since static vegetation will differ from dynamic vegetation in terms of soil moisture and albedo (both of which affect sensible heat fluxes).

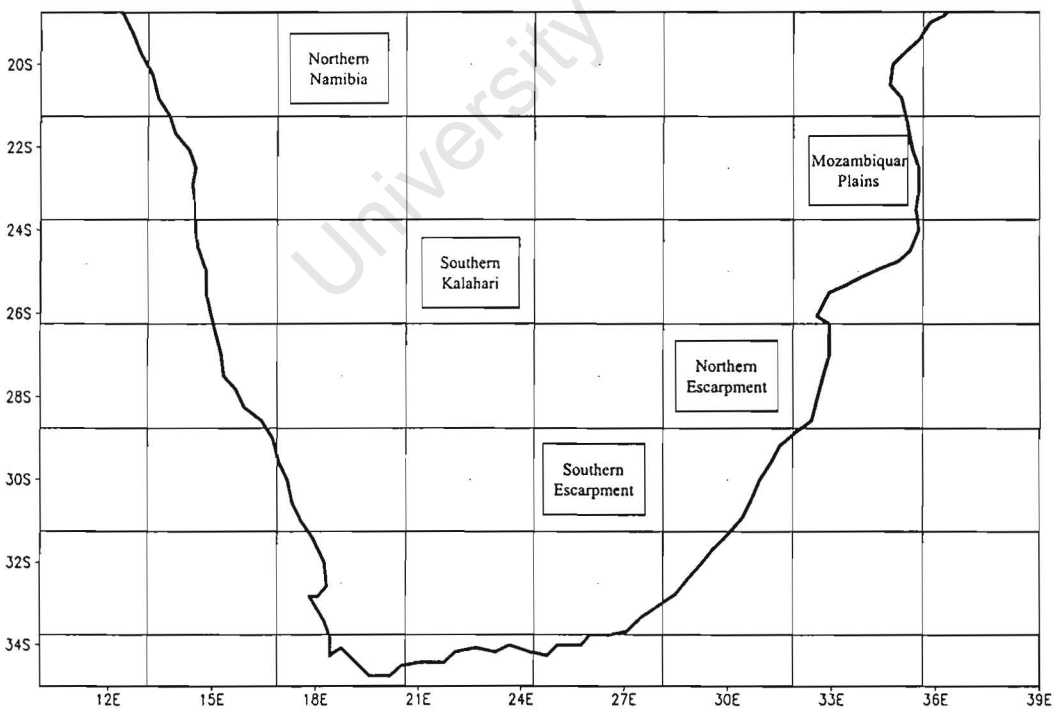

Figure 5.1 The 5 regions showing a notable net primary productivity response

In the sections to follow, figures are presented with contours and contoured changes (which are shaded for regions with notable change). However, since the IBIS model has a land-sea mask, contours will be truncated at oceanic boundaries. Figure 5.2 shows the HadCM2 grid cells superimposed by the contours in order to reinforce the true boundaries for interpretive purposes.

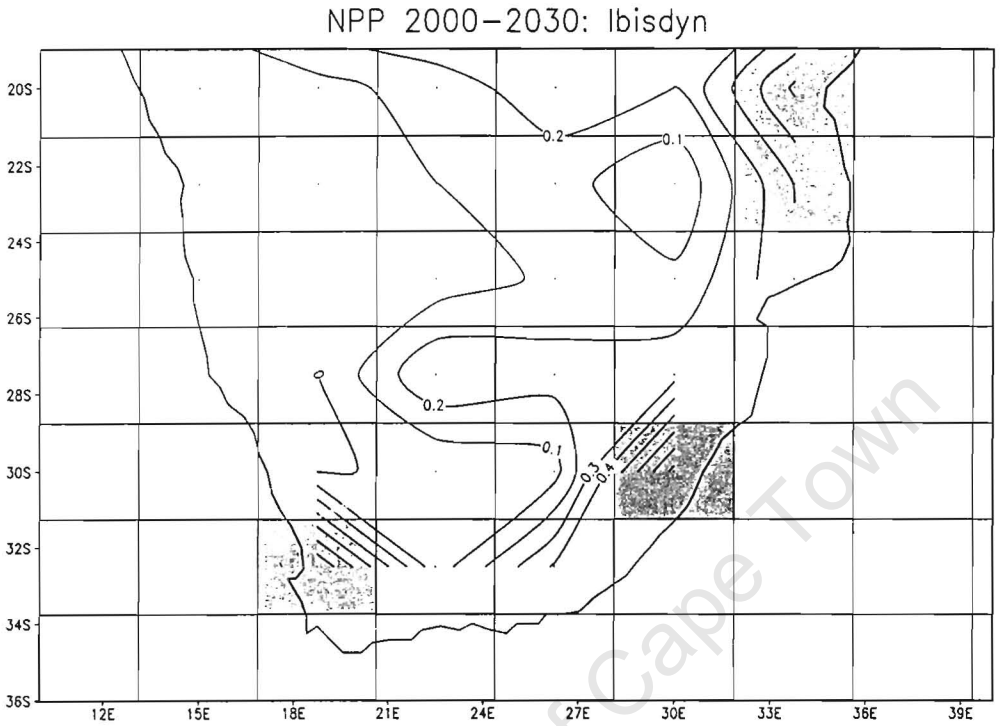

Figure 5.2 True HadCM2 grid cell boundaries without truncation at oceanic boundaries

5.1.1 Annual Net Primary Productivity

(NPP results are displayed on figures 5.3a) - 5.3g). In the early 21st century (period 1), NPP is highest over the east, south and western coastal regions (0.5 - 0.7 kg m^{-2} $year^{-1}$) and lowest over the interior (0 – 0.1 kg m^{-2} $year^{-1}$) in Ibisdyn and P1-P5. Ibissta shows a similar tendency over the coast, but with very low values (-0.3 kg m^{-2} $year^{-1}$) over the South Africa/Zimbabwe border.

In the dynamic vegetation mean run (Ibisdyn), net primary productivity has increased from the early to late 21st century. It is evident that there are a number of key response regions, with sizeable absolute increases in NPP. Notable increases are apparent in northern Namibia (0.06 kg m^{-2} $year^{-1}$), over the southern Kalahari (0.02 kg.$m^{-2}$$year^{-1}$), the Mozambiquan plains (0.04 kg m^{-2} $year^{-1}$), and two regions in the SE of South Africa on the escarpment (0.06 – 0.08 kg m^{-2} $year^{-1}$). These increases translate into absolute increases of 60% (Northern Namibia), 20% (southern Kalahari), 10% (Mozambiquan plains) and 20-25% (escarpment regions). NPP changes for P1-P5 are similar to those in Ibisdyn, but with some differences apparent in some areas.

The anomaly responses fall into two distinct groups in terms of similarity, *viz.*, (P1, P3 and P5) and (P2 and P4), related to commonalities in input precipitation forcing (refer to figure 4.1 in Chapter 4). In P1, P3 and P5, NPP has generally increased, but with notable decreases over the southern Kalahari and a region in South Africa to the SE of this region. NPP over the Mozambiquan plains has also decreased. Increases are evident over two regions in the SE of South Africa on the escarpment, which correspond with the increases observed in the dynamic vegetation mean run. P2 and P4 both display NPP increases over the larger part of the domain, but with a decrease over eastern Botswana. There is not a notable trend in NPP over northern Namibia and the southern Kalahari. There are increases over the SE of South Africa. In the static vegetation mean run (Ibissta), NPP is similar to Ibisdyn, but with greater increases in Northern Namibia. Increases over the escarpment regions are not as large as for Ibisdyn, but are similar to increases observed in the other scenarios.

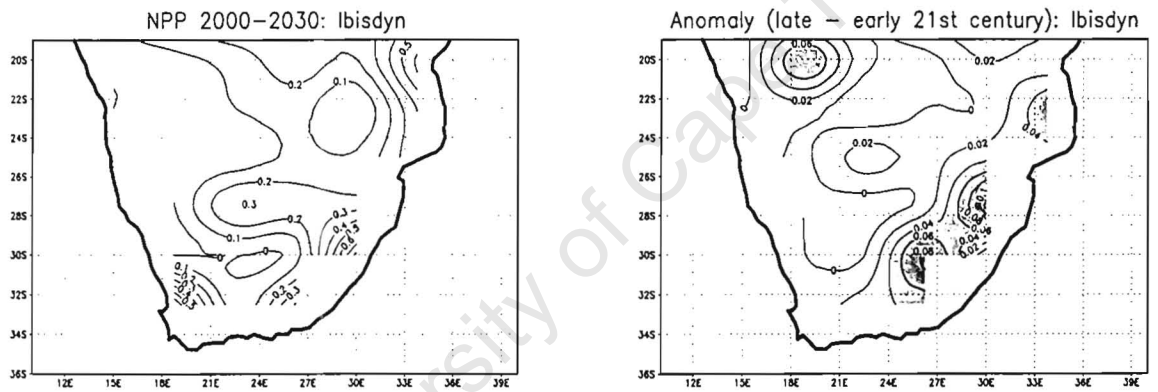

Figure 5.3a) Annual net primary productivity (kg m^{-2} year) for period 1 and the anomaly for Ibisdyn

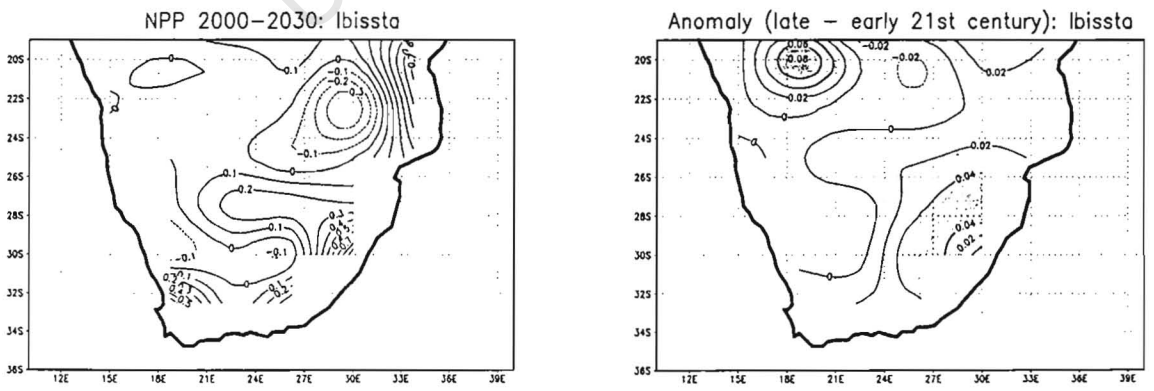

Figure 5.3b) Annual net primary productivity for period 1 and the anomaly for Ibissta

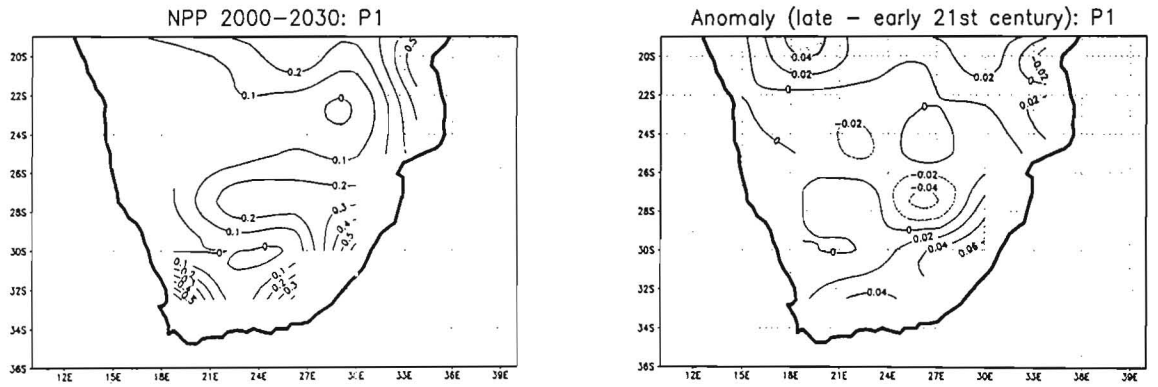

Figure 5.3c) Annual net primary productivity for period 1 and the anomaly for P1

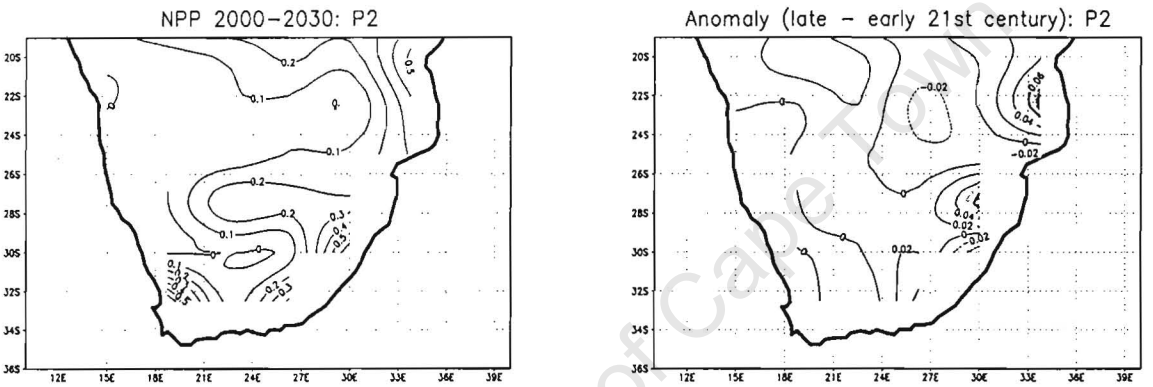

Figure 5.3d) Annual net primary productivity for period 1 and the anomaly for P2

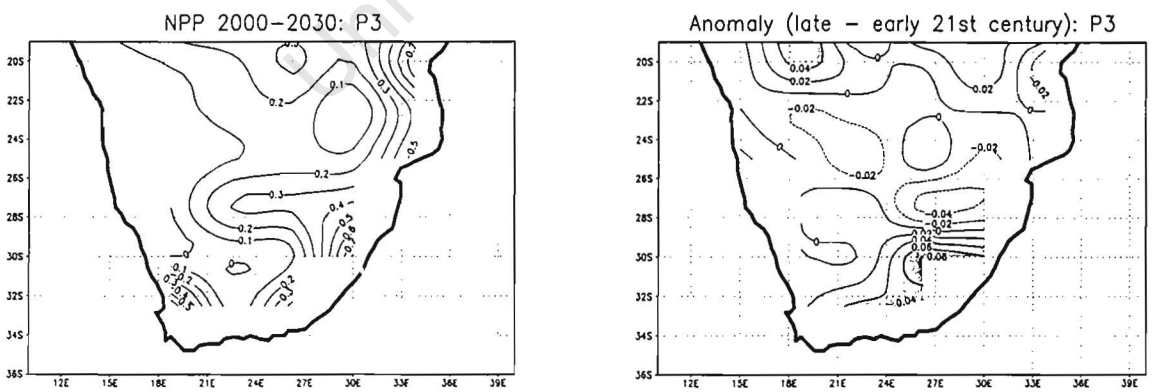

Figure 5.3e) Annual net primary productivity for period 1 and the anomaly for P3

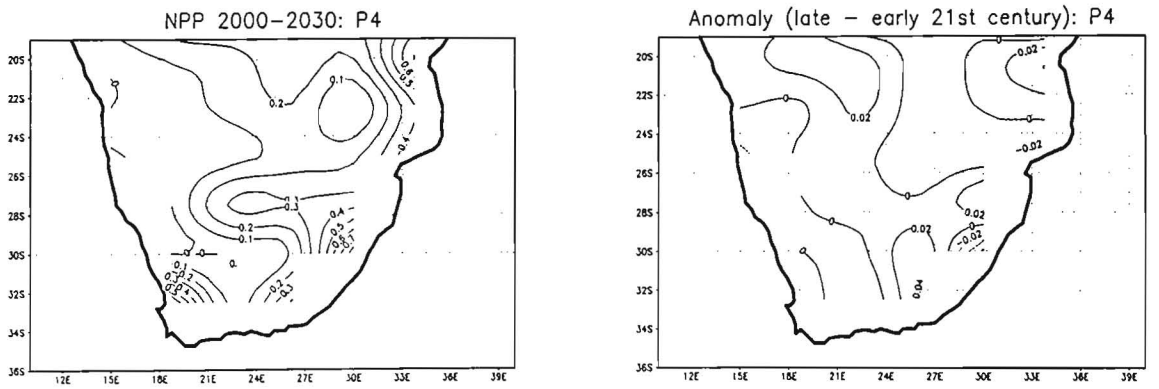

Figure 5.3f) Annual net primary productivity for period 1 and the anomaly for P4

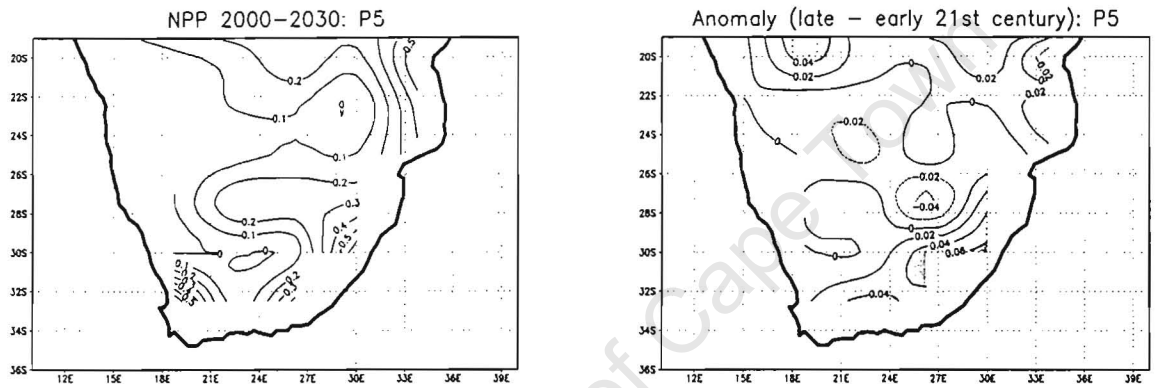

Figure 5.3g) Annual net primary productivity for period 1 and the anomaly for P5

5.1.2 Annual average evapotranspiration

The annual average evapotranspiration (figures 5.4a) – 5.4g)) pattern for period 1 is similar for all scenarios. Highest values are found over the east coast (700 – 800 mm year^{-1}), decreasing to 100 mm year^{-1} or less over the west.

Annual average evapotranspiration has increased through the 21st century in Ibisdyn, most likely as a consequence of the increase in temperature. The regions of increase in period 2 correspond closely with the response regions for NPP, except for the Mozambiquan plains, where there is no discernible increase. Increases in northern Namibia are highest (60 mm year^{-1} – an increase of 15%) and increases over the escarpment and the southern Kalahari are of the order of 20 – 40 mm year^{-1} (an increase of 8%). Annual average evapotranspiration changes for P1-P5 generally correspond with those of Ibisdyn, displaying an increase over most of the domain. There are regions where there are evapotranspiration decreases in P1, P3 and P5 over the southern Kalahari, and the northern portion of SE South Africa on the escarpment. P2 and P4 reflect

decreases over the southern portion of SE South Africa. In Ibissta the responses are almost identical to those of Ibisdyn, implying that dynamic vegetation has little effect on altering annual average evapotranspiration, and that evapotranspiration changes are linked to input temperature changes.

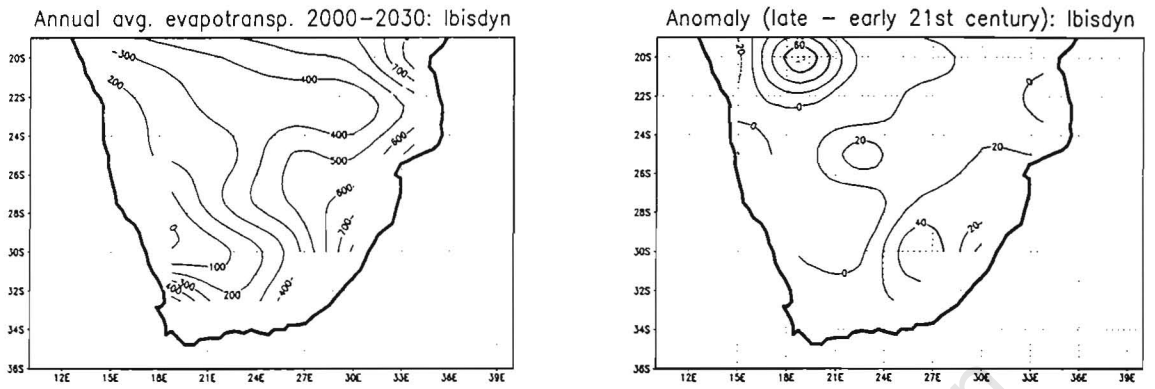

Figure 5.4a) Annual average evapotranspiration (mm year^{-1}) for period 1 and the anomaly for Ibisdyn

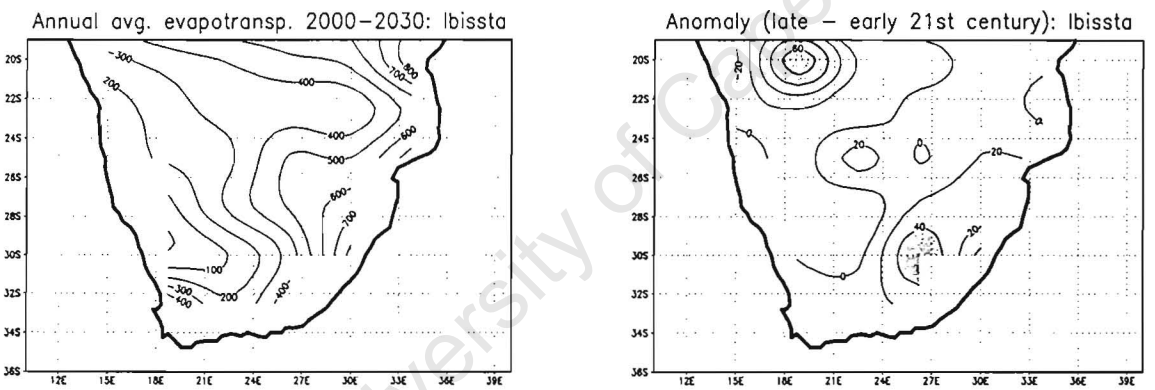

Figure 5.4b) Annual average evapotranspiration for period 1 and the anomaly for Ibissta

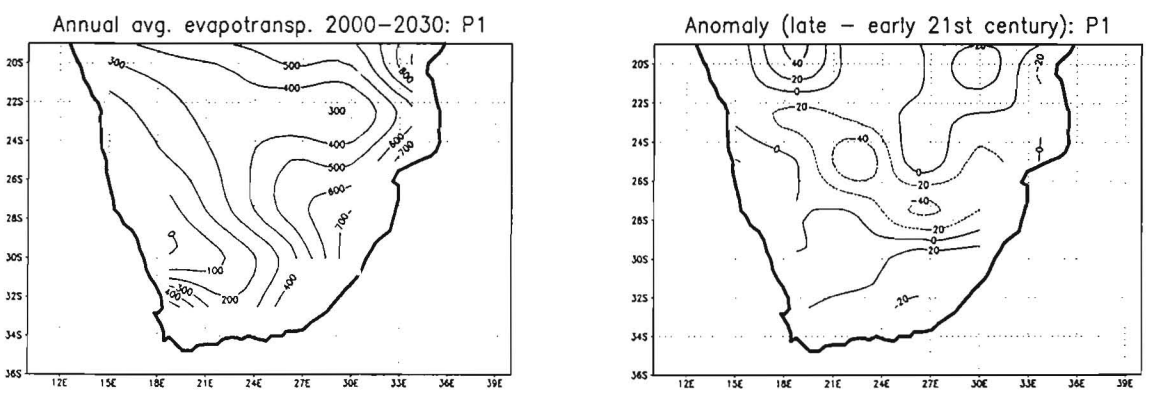

Figure 5.4c) Annual average evapotranspiration for period 1 and the anomaly for P1

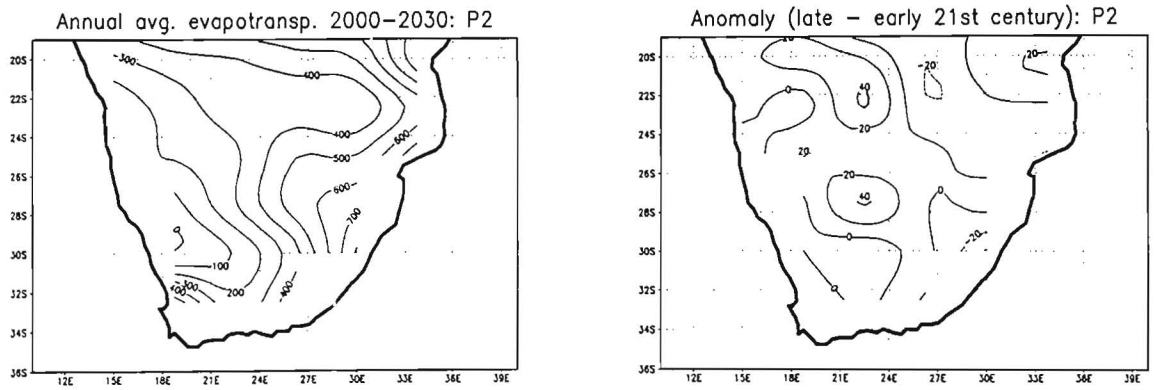

Figure 5.4d) Annual average evapotranspiration for period 1 and the anomaly for P2

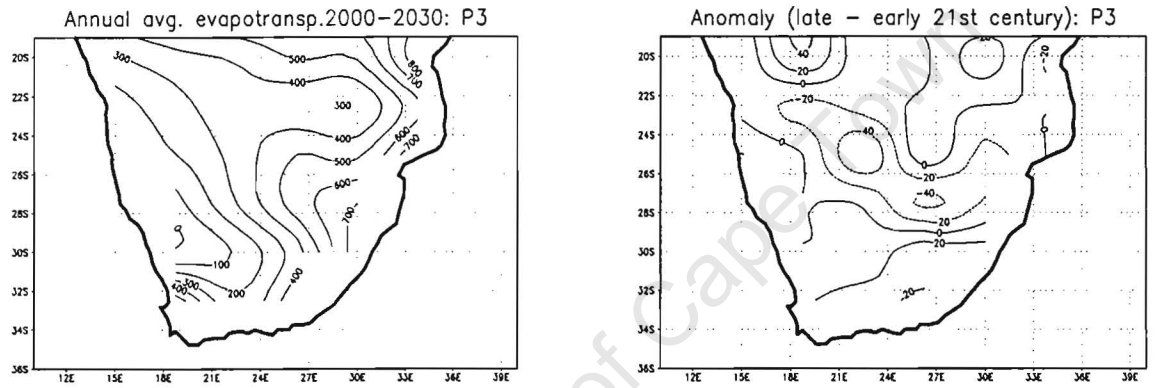

Figure 5.4e) Annual average evapotranspiration for period 1 and the anomaly for P3

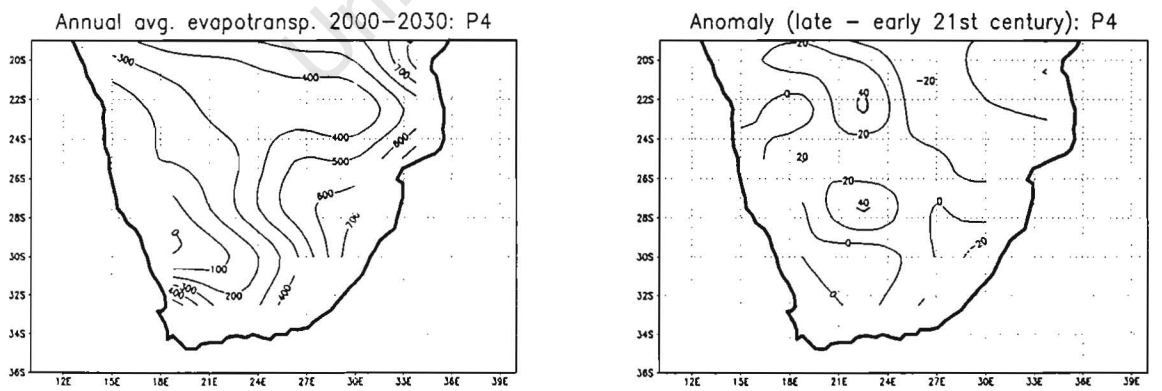

Figure 5.4f) Annual average evapotranspiration for period 1 and the anomaly for P4

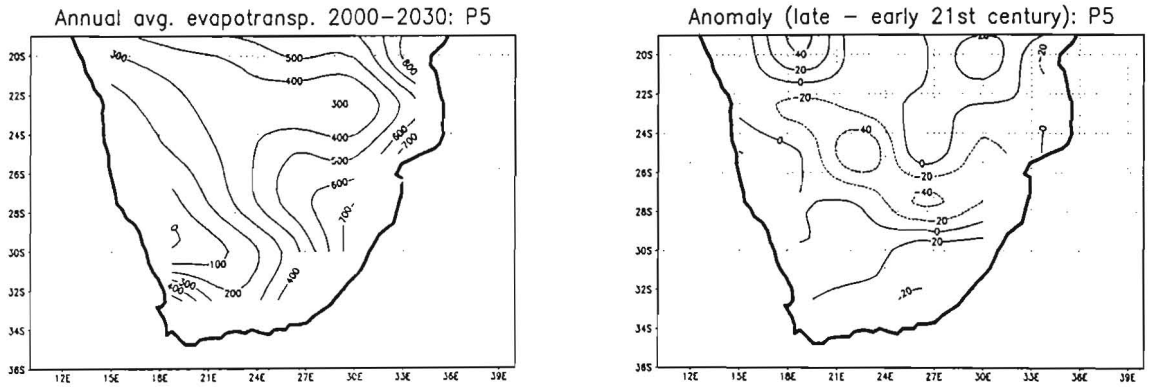

Figure 5.4g) Annual average evapotranspiration for period 1 and the anomaly for P5

5.1.3 Sensible heat fluxes

Sensible heat fluxes (figures 5.5a) – 5.5g)) in Ibisdyn during period 1 are greatest over the east, south and west coastal regions (70 – 85 W m^{-2}) and over the Southern Kalahari (65 – 70 W m^{-2}). Elsewhere values range between approximately 50 and 60 W m^{-2}. P1-P5 are similar, with values within a few W m^{-2} of those in Ibisdyn. Ibissta, however, differs in terms of pattern and flux amounts, which are generally substantially higher (95 W m^{-2} up the west coast of South Africa and 90 W m^{-2} over the South Africa/Zimbabwe border).

Sensible heat fluxes for the dynamic vegetation mean run indicate increases from period 1 to 2 over northern Namibia (3 W m^{-2}) and decreases over the Mozambiquan plains (3 W m^{-2}). There are decreases (6 W m^{-2}) to the north over the South African escarpment region, with increases in the region just south (3 W m^{-2}). Absolute changes in these regions are approximately 5%, except for the northern escarpment, which shows a 10% change. There is a region of change still further south where there is a decrease (6 W m^{-2}). The southern Kalahari reflects no noticeable change. Sensible heat flux anomalies for P1-P5 are similar to those for Ibisdyn in most regions. Differences are apparent in Northern Namibia in P1-P5, where little change is evident.

Sensible heat flux anomalies for Ibissta are not notable over a number of the regions showing a response in Ibisdyn. Anomalies are evident over the southern escarpment region (4% decrease) and northern Namibia (4% decrease), where the response is opposite in sign to the dynamic vegetation scenarios. With respect to model output, sensible heat fluxes are most dependent on dynamic as opposed to static vegetation, related to the fact that static vegetation differs from dynamic vegetation in terms of soil moisture and albedo (both these affect sensible heat fluxes).

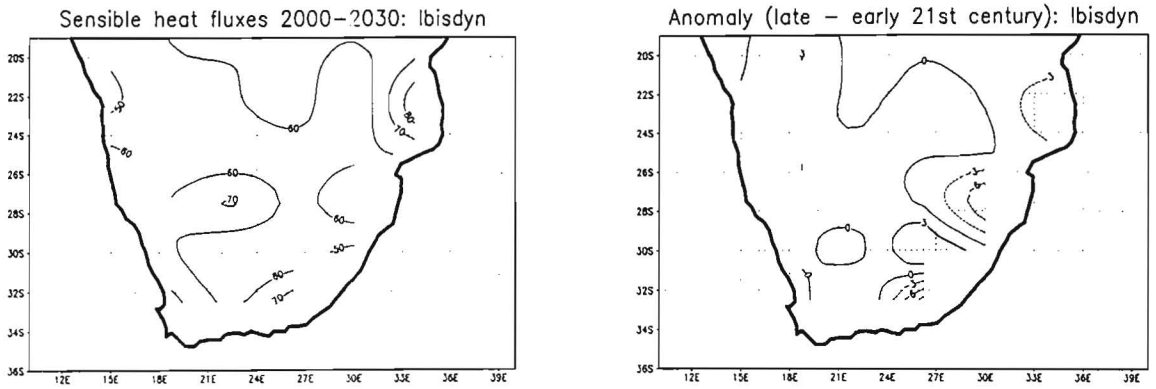

Figure 5.5a) Sensible heat fluxes (W m^{-2}) for period 1 and the anomaly for Ibisdyn

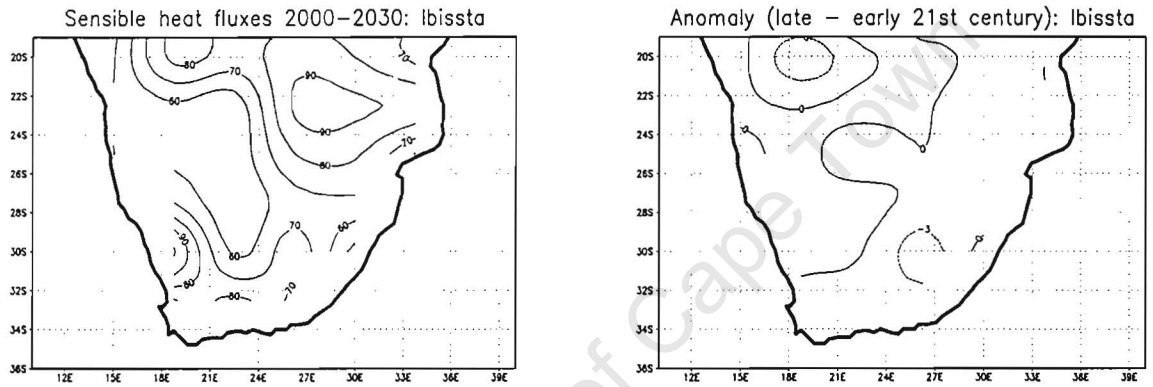

Figure 5.5b) Sensible heat fluxes for period 1 and the anomaly for Ibissta

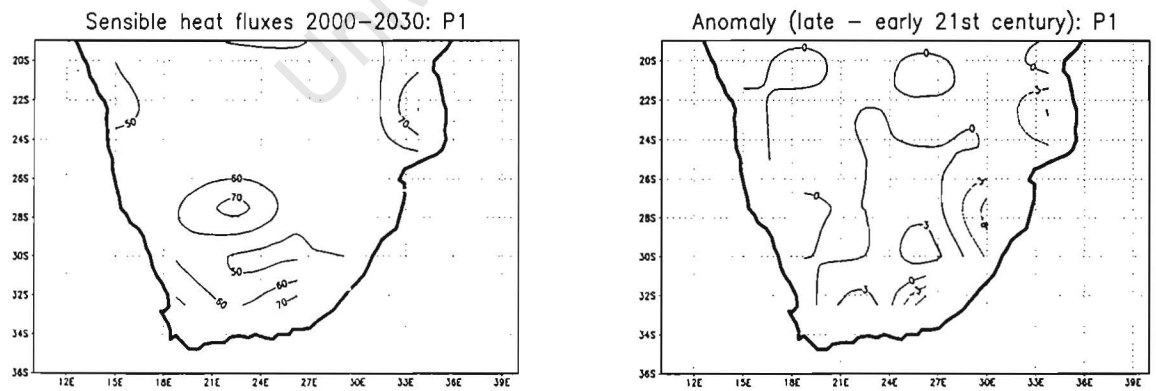

Figure 5.5c) Sensible heat fluxes for period 1 and the anomaly for P1

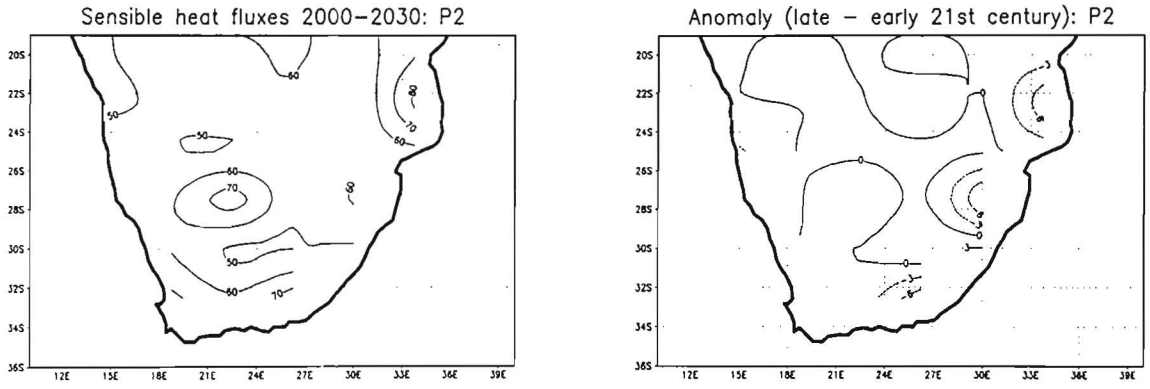

Figure 5.5d) Sensible heat fluxes for period 1 and the anomaly for P2

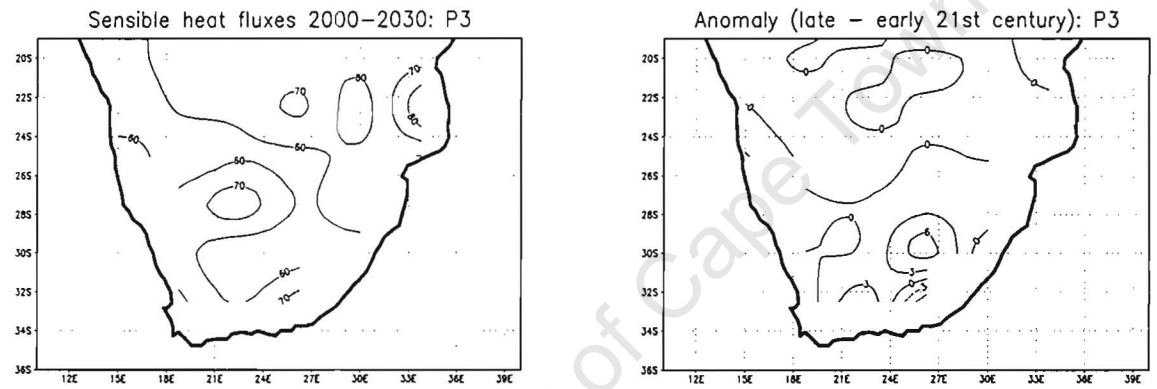

Figure 5.5e) Sensible heat fluxes for period 1 and the anomaly for P3

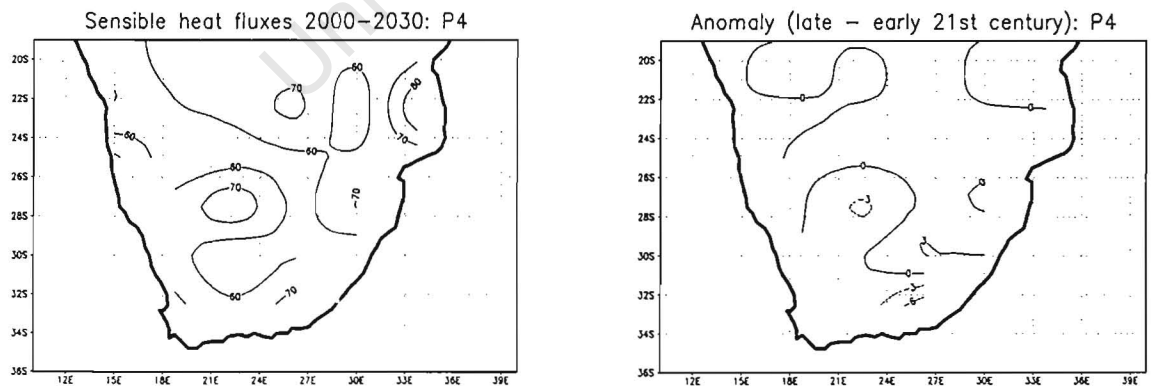

Figure 5.5f) Sensible heat fluxes for period 1 and the anomaly for P4

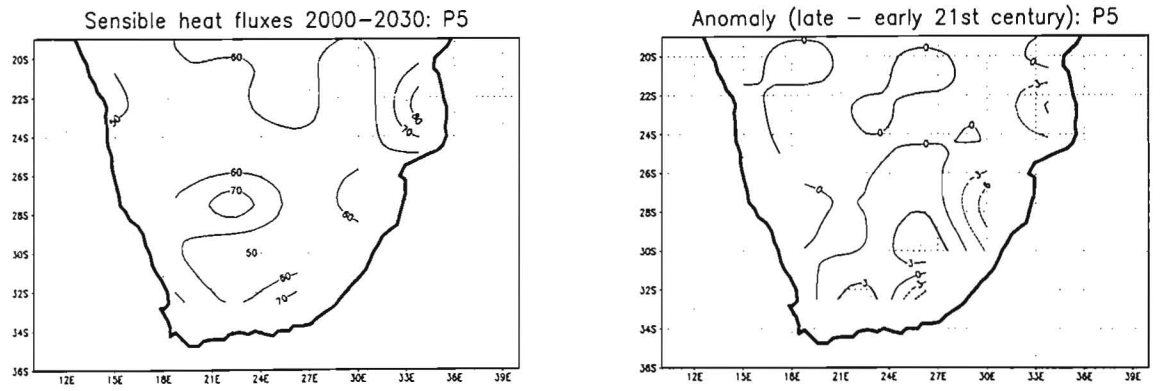

Figure 5.5g) Sensible heat fluxes for period 1 and the anomaly for P5

5.1.4 Soil temperatures

Soil temperatures (figures 5.6a) – 5.6g)) in Ibisdyn and P1-P5 in period 1, are highest over the South Africa/Zimbabwe border (32°C) and southern Namibia (32°C), and lowest to the south (20°C). Ibissta is similar, but with a tendency towards lower values over the east.

Soil temperature in Ibisdyn has decreased over northern Namibia and the South African escarpment region. This is what would be anticipated with the increases in evapotranspiration and NPP evident over the same regions. Soil temperature decreases are generally between 2-4%. Soil temperature anomalies for P1-P5 are consistent with those of Ibisdyn, reflecting a decrease in areas corresponding to a decrease in Ibisdyn. In P2 and P4 there is little change over SE South Africa on the escarpment, whereas P1, P3 and P5 and Ibisdyn indicate notable soil temperature decreases. Soil temperatures for Ibissta show a similar pattern in the anomalies, but the temperature decreases are less than in Ibisdyn (and correspond more closely to the decreases in P1, P3 and P5), being of the order of 1-2%.

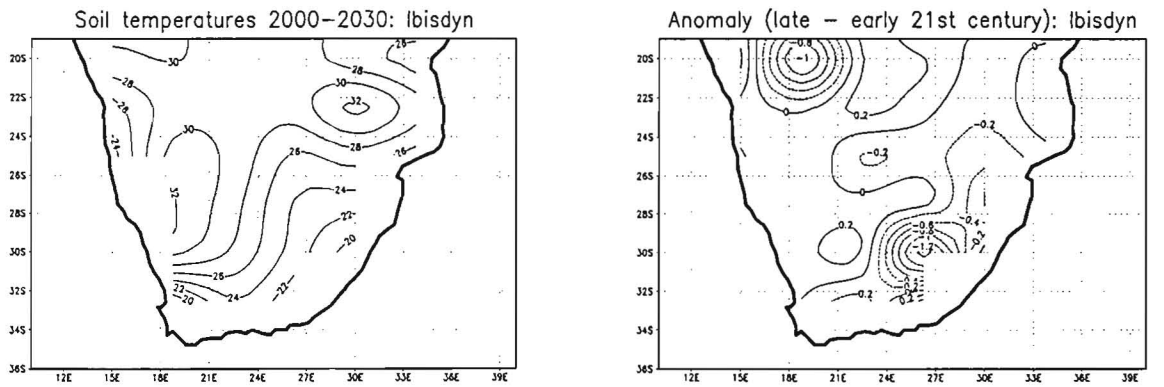

Figure 5.6a) Soil temperatures (°C) for period 1 and the anomaly for Ibisdyn

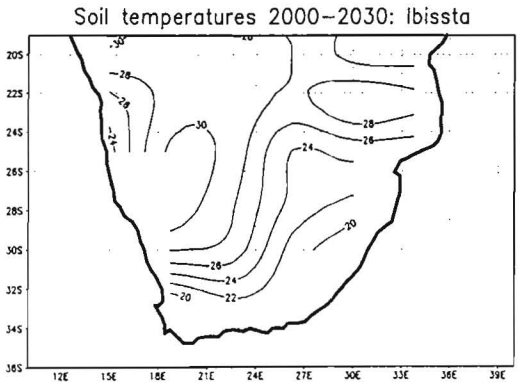

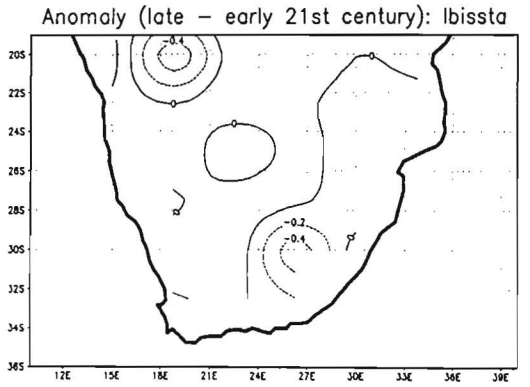

Figure 5.6b) Soil temperatures for period 1 and the anomaly for Ibissta

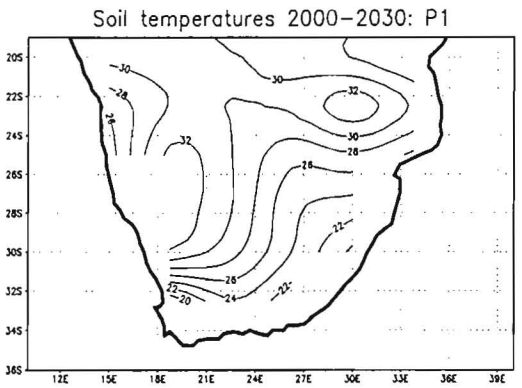

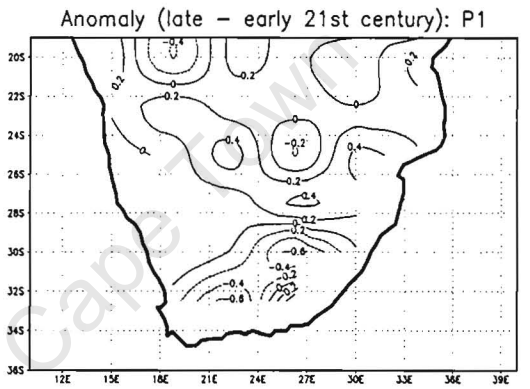

Figure 5.6c) Soil temperatures for period 1 and the anomaly for P1

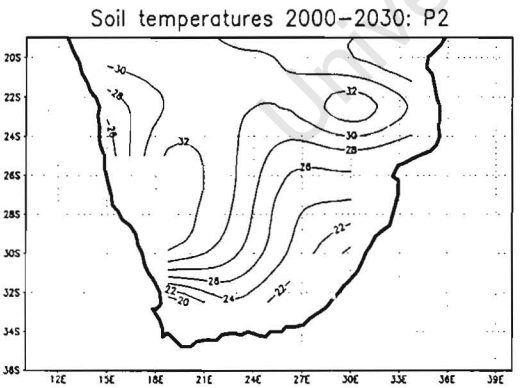

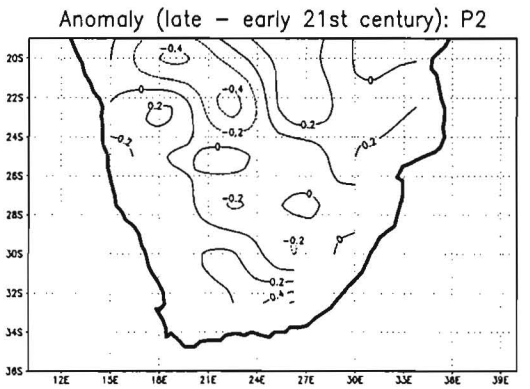

Figure 5.6d) Soil temperatures for period 1 and the anomaly for P2

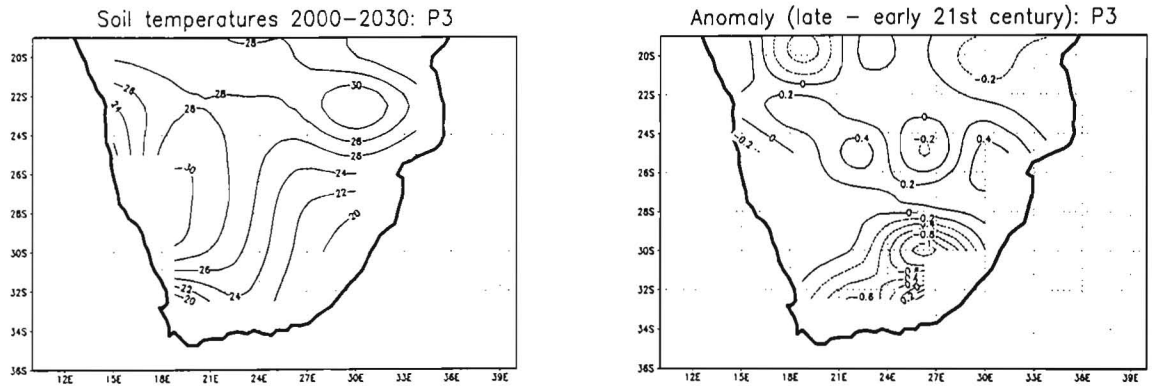

Figure 5.6e) Soil temperatures for period 1 and the anomaly for P3

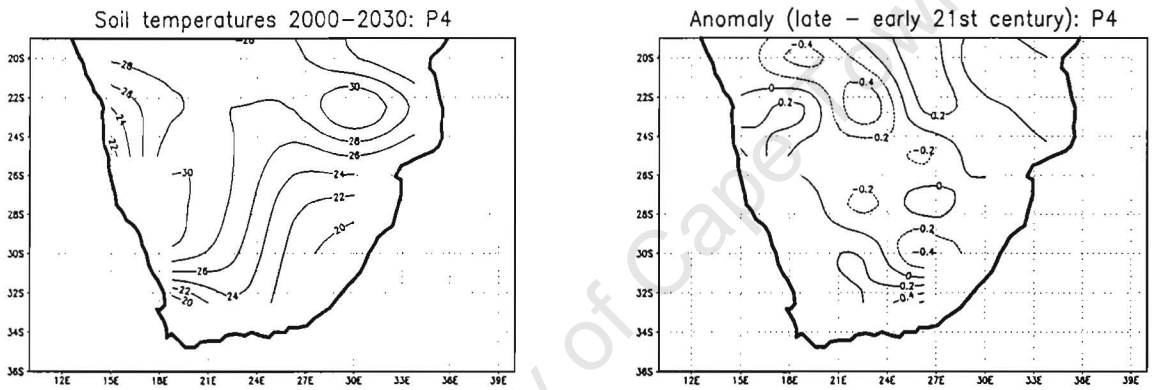

Figure 5.6f) Soil temperatures for period 1 and the anomaly for P4

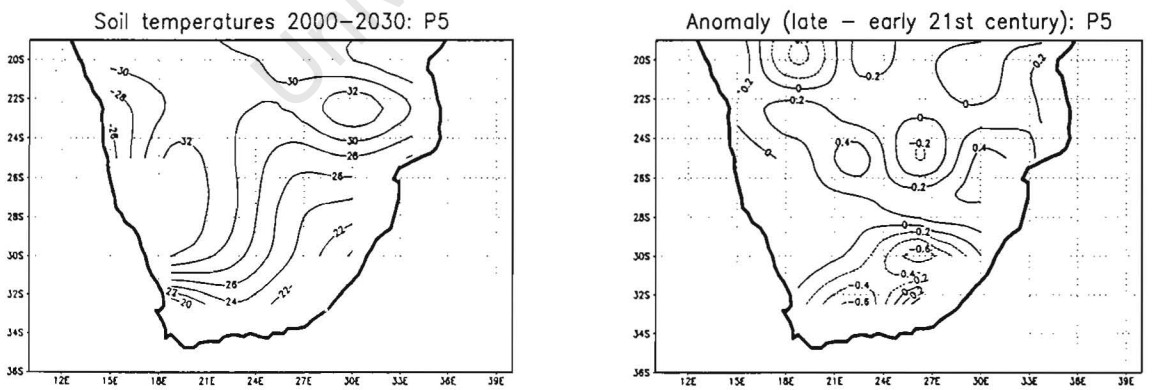

Figure 5.6g) Soil temperatures for period 1 and the anomaly for P5

5.1.5 Soil moisture

The soil moisture fraction (figures 5.7a) – 5.7g)) in the early 2000s (period 1) is highest over the east coast (0.5) and lowest over the southern Kalahari (0.15) in all scenarios.

Soil moisture changes from period 1 to 2 in Ibisdyn, are evident over slightly different regions from those represented in the anomalies described above, except for the Mozambiquan plains where there are soil moisture fractional decreases (0.004). Soil moisture fractional decreases are also evident over NW Namibia (0.012 – the largest absolute change of 4%) and central Botswana (0.004). There are soil moisture increases over the northern central South Africa (0.004) and central Namibia (0.004). Soil moisture decreases in P1-P5 are more pronounced than in Ibisdyn over the SE South African region, corresponding with changes evident for the other variables in this region. Soil moisture anomalies are generally consistent over the remainder of the region. The decrease in soil moisture over NW Namibia is not clearly evident in P2 and P4. P1, P3 and P5 reflect little change over the Mozambiquan plains. In Ibissta the soil moisture anomalies are similar to P1-P5, but increases and decreases are more pronounced over northern Namibia and the escarpment regions. There is no notable response over the Mozambiquan plains.

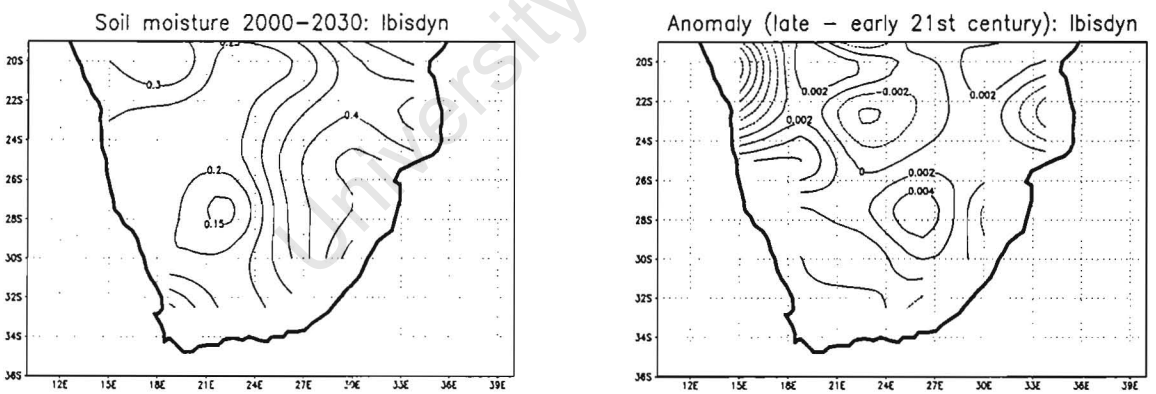

Figure 5.7a) Soil moisture (fraction) for period 1 and the anomaly for Ibisdyn

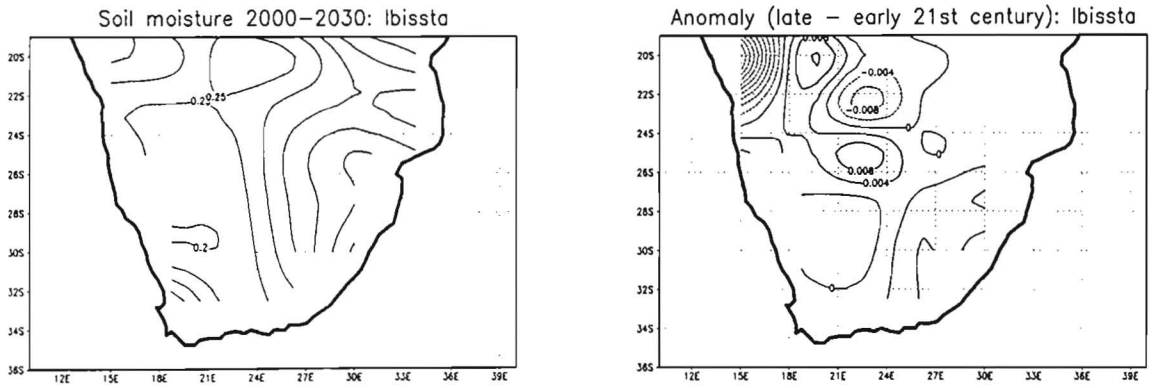

Figure 5.7b) Soil moisture for period 1 and the anomaly for Ibissta

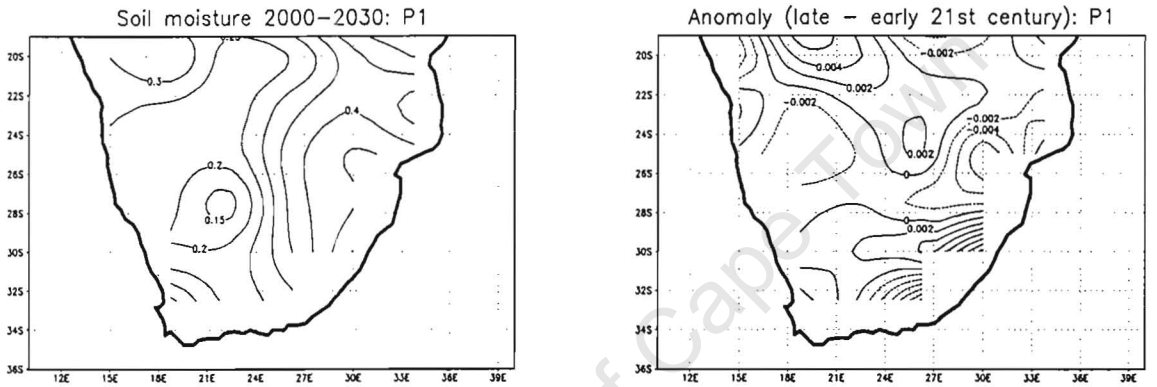

Figure 5.7c) Soil moisture for period 1 and the anomaly for P1

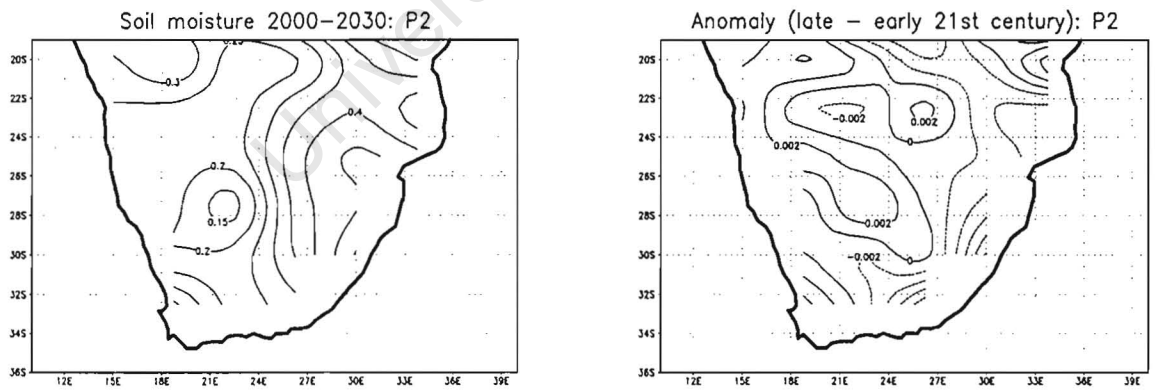

Figure 5.7d) Soil moisture for period 1 and the anomaly for P2

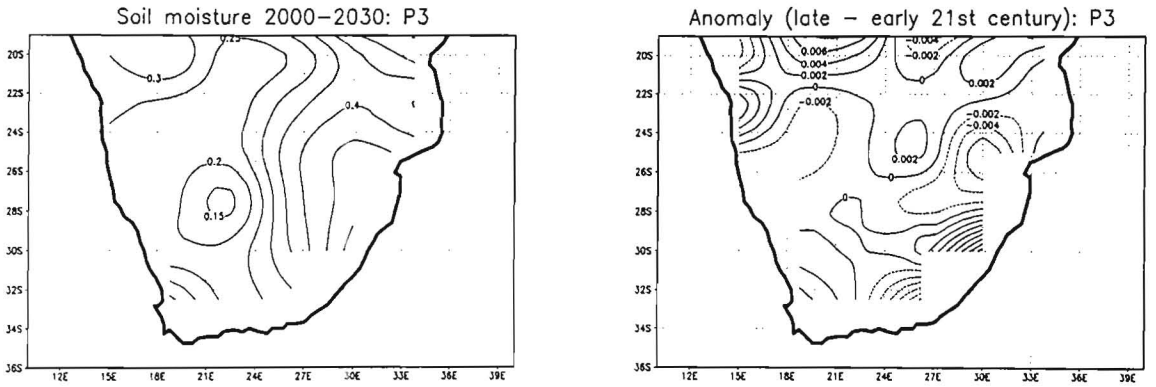

Figure 5.7e) Soil moisture for period 1 and the anomaly for P3

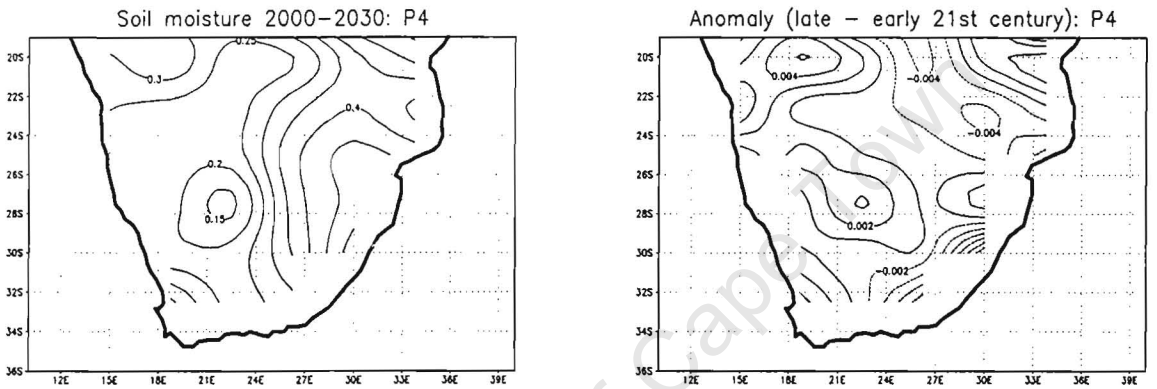

Figure 5.7f) Soil moisture for period 1 and the anomaly for P4

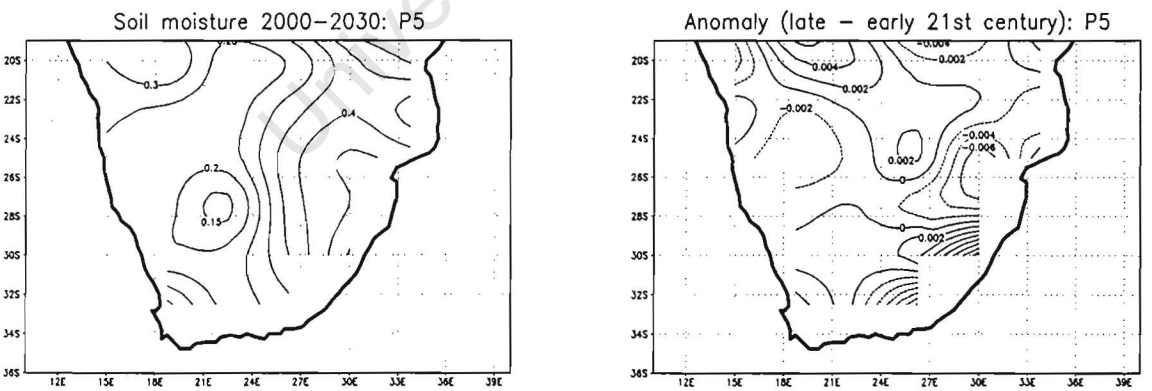

Figure 5.7g) Soil moisture for period 1 and the anomaly for P5

5.1.6 Response regions

There are 5 primary regions where there is a notable response in most variables. These 5 regions (figure 5.8) are examined in more detail in the sections to follow.

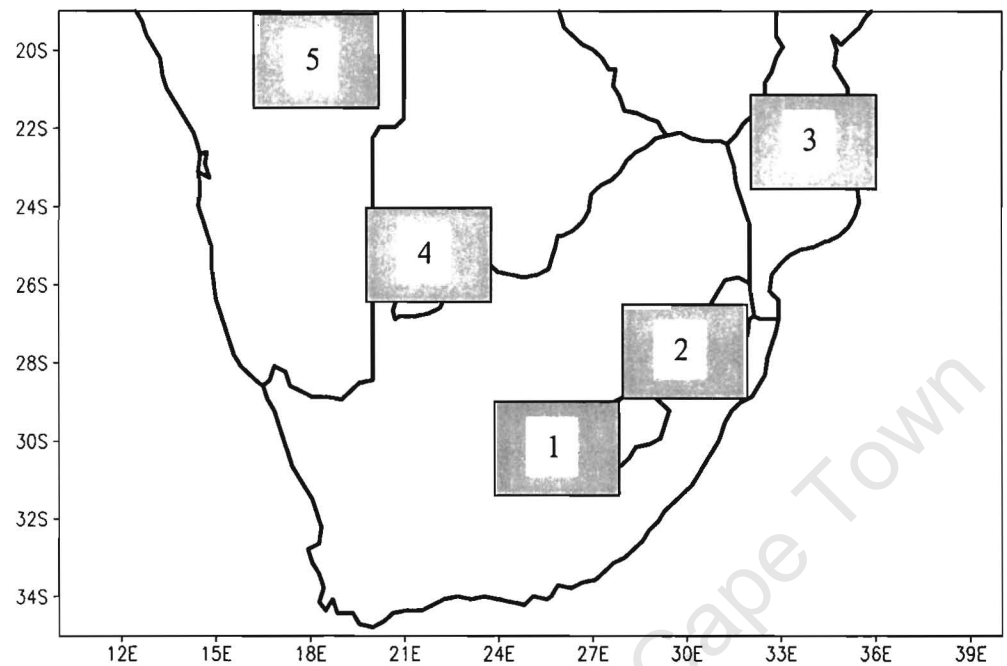

Figure 5.8 Response regions considered

5.2 Trends in the HadCM2 input data

The HadCM2 monthly temperature, precipitation, relative humidity and wind speed data are deseasonalised for the 5 regions (figure 5.8) in order to determine trends. These data are smoothed and deseasonalised using a 13-point (i.e. 13 month) unweighted low pass filter (in the form of a moving average) to remove or dampen high frequencies. Deseasonalisation is performed, since the most obvious source of variance in these data is the seasonal cycle (high frequency), which will distort the long-term annual trend.

In general the trend is for an increase in temperature and decrease in relative humidity, in all regions, through the 21st century. The increase in temperature is consistent with the HadCM2 model's increasing trend (which is approximately 2.5°C with a doubling of CO_2). Precipitation trends are more variable, with increases in some regions, and decreases in others. However, there is an increase in precipitation in the winter months in the summer rainfall regime (all regions fall in this regime) as evidenced in Chapter 3, implying more moisture available for plant growth during the typically drier months of the year. Wind speed changes in the HadCM2

data do not show a clear increasing or decreasing trend and there is not a notable difference between the 5 regions. Most wind speed changes are observed to the west (summer) and south (winter) of the country. Wind speeds vary from 1 m s^{-1} to 13 m s^{-1}. Figures 5.9, 5.10 and 5.11 show the trends for temperature, precipitation and relative humidity respectively. A region-by-region discussion of these trends follows in 5.2.1-5.2.5.

It is of value to note that relative humidity can only decrease if temperature has increased (which is the case). However, while relative humidity may have declined, specific humidity (as evidenced in chapter 3) shows a general increase over the entire domain. Hence, there is a general increase in overall available moisture within the atmospheric column. Precipitation trends are variable, and therefore the increased available moisture in the atmosphere, has not necessarily translated into an increase in rainfall. Regions of increase in precipitation, in fact correspond to regions with the least decrease in relative humidity through the 21st century.

5.2.1 Region 1

Region 1 displays an upward trend in temperature. The total temperature increase is 4°C, with a high annual temperature range of 12°C, related to the fact that the region is inland (on the escarpment) and sub-tropical. Precipitation also shows a discernible increasing trend. Relative humidity has decreased by 2-3% through the 21st century.

5.2.2 Region 2

There is an upward trend in temperature in region 2, with a total temperature increase of 3.5°C and an annual temperature range of 9°C. Precipitation in region 2 shows a slight increase, which is less marked than in region 1. This region displays the highest overall precipitation. Relative humidity values in this region are highest (over 90% at times), with decreases of 2-3% between 2000-2080.

5.2.3 Region 3

Region 3 displays the highest temperatures, but lowest temperature increase (3°C) and smallest temperature range (6°C). This is attributed to the region being in a coastal environment and therefore experiencing moderated temperatures. Precipitation trends are not determinable and precipitation received is low in comparison to other regions. Relative humidity has decreased by 2-3%.

5.2.4 Region 4

The total temperature increase in region 4 is 5°C, with an annual temperature range of 11°C (since it is inland and sub-tropical). Precipitation shows a slight downward trend. Relative humidity has decreased by as much as 6%.

5.2.5 Region 5

Region 5's total increase in temperature is 5°C with a temperature range of 7°C. This region, together with region 4, displays the greatest temperature increase, with an almost identical trend map. Precipitation has decreased slightly, while decreases in relative humidity are of the order of 5%. The relative humidity range is greatest in this region, being between 25% and 80%.

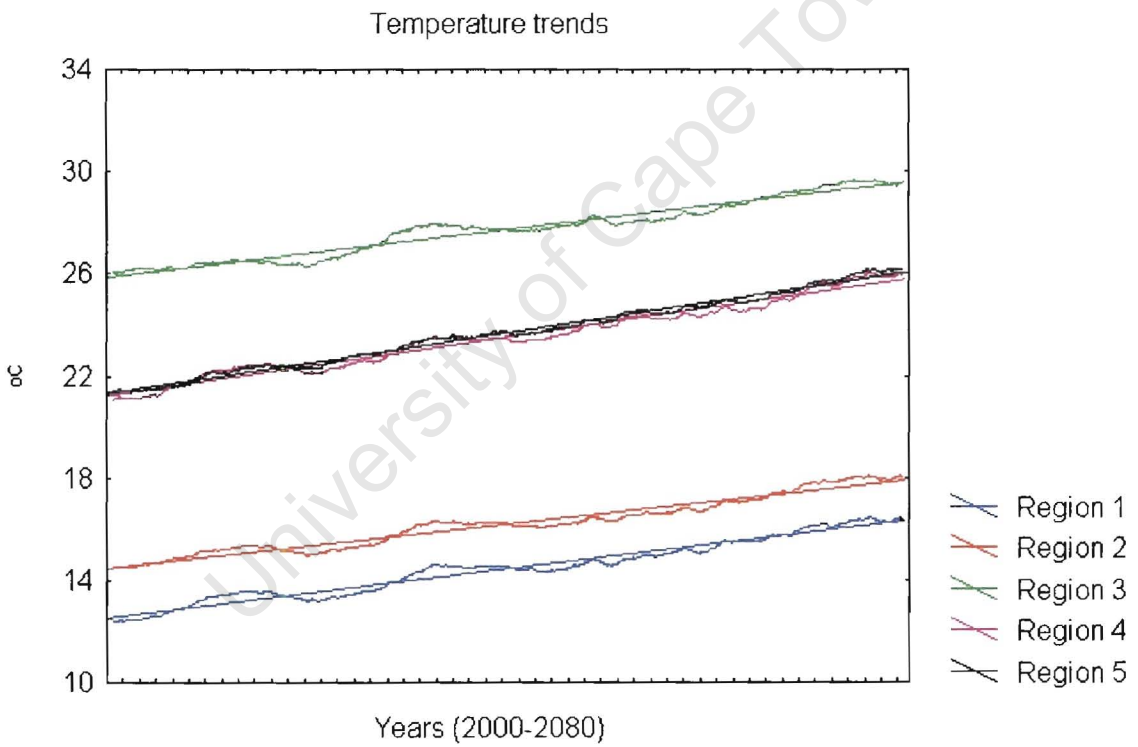

Figure 5.9 Temperature trends (°C) over the 21st century for the 5 different regions

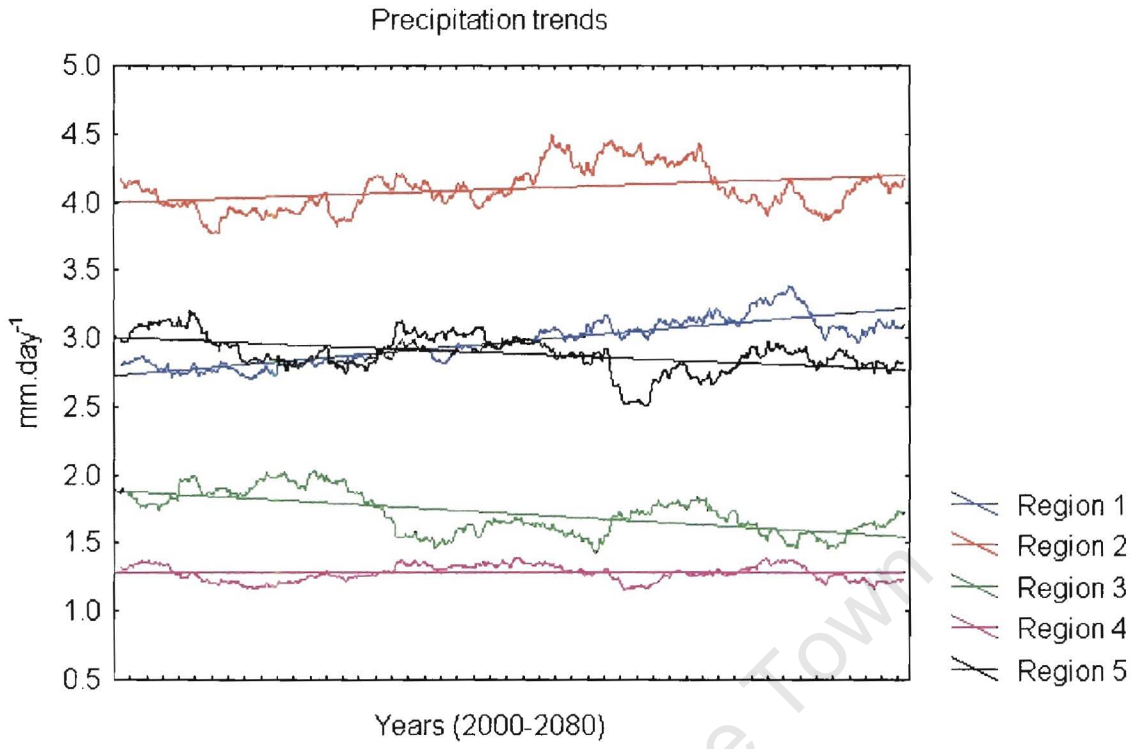

Figure 5.10 Precipitation trends (mm day^{-1}) over the 21st century for the 5 different regions

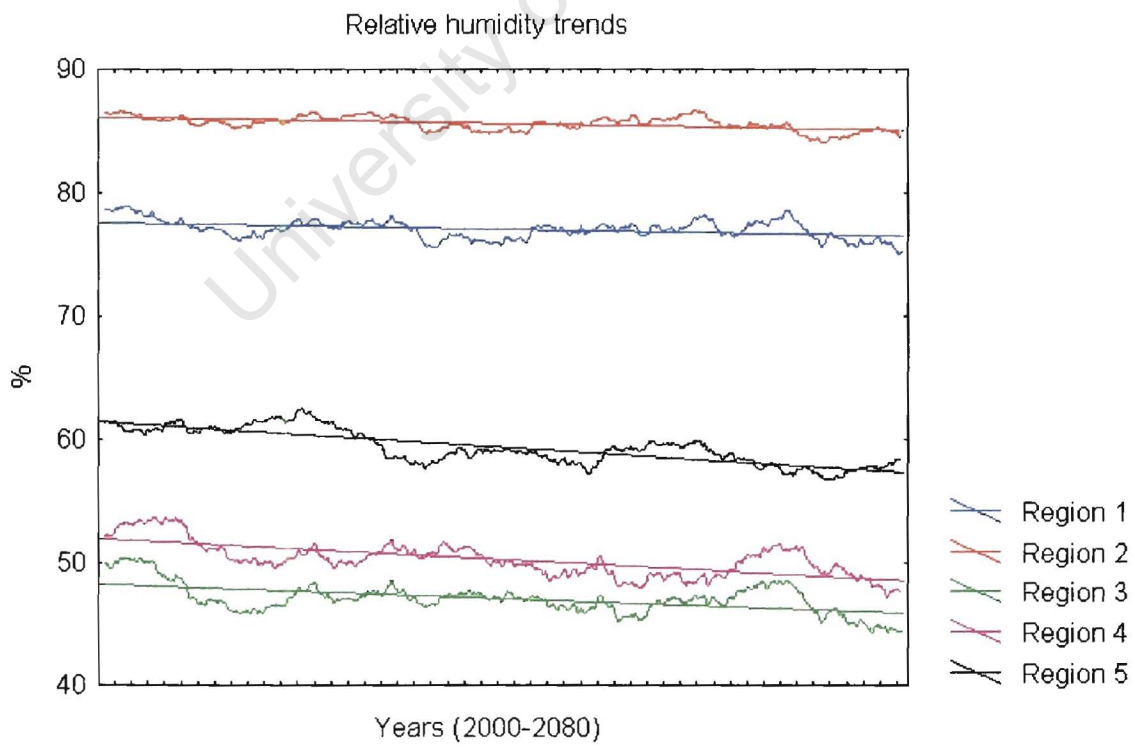

Figure 5.11 Relative humidity trends (%) over the 21st century for the 5 different regions

5.3 Vegetation and annual trends in IBIS response

The vegetation categories in the IBIS model are represented as a combination of plant functional types (Woodward and Cramer, 1996) that are modified from Prentice *et al.* (1992) and Haxeltine and Prentice (1996). (Refer to Chapters 2 and 4 for further details and for a graphic representation of the vegetation categories, respectively.) The functional types represented in the 5 regions over the two time periods are examined for the dynamic vegetation mean run (Ibisdyn), and for the simulations with the different standard deviation scenarios (P1-P5). Note that since Ibissta is a simulation with static vegetation, the vegetation plant functional types remain constant over the entire time period.

Results to follow demonstrate that *precipitation* is important in determining the broad scale vegetation response *across* scenarios (i.e. a general movement towards a more productive vegetation environment), but that the vegetation response differences *between* scenarios are largely dependent on differences in *temperature* and *relative humidity*.

Across scenarios, *precipitation* is the dominant driving factor for annual average evapotranspiration, annual net primary productivity, sensible heat fluxes, soil temperature and soil moisture responses. In terms of inter-scenario response, P1, P3 and P5 (negative standard deviation from the mean precipitation) are distinct from P2 and P4 (positive standard deviation from the mean precipitation) in their response trends. P2 and P4 are most similar to Ibisdyn. Scenario similarities or differences are therefore closely linked to subtle changes in precipitation and are not specifically dependent on vegetation types represented. This is what would perhaps be expected, since these 5 annual variables are directly and indirectly associated with precipitation amounts.

The response of Ibissta is similar to Ibisdyn in terms of most annual variables (e.g. annual average evapotranspiration and annual net primary productivity), except sensible heat fluxes. These fluxes will be related to albedo and soil moisture changes, and hence may differ between static and dynamic vegetation scenarios.

The discussion to follow considers the vegetation response and annual trends in IBIS in more detail. Vegetation, annual net primary productivity, average evapotranspiration, sensible heat fluxes, soil temperature and soil moisture trends are examined for the seven scenarios (*viz.*, Ibissta (static vegetation mean run), Ibisdyn (dynamic vegetation mean run) and P1-P5). Each of

the 5 response regions identified earlier is considered separately. Vegetation category maps (figures 5.12-5.18) are presented overleaf for each scenario and trend graphs for Ibisdyn (figures 5.19-5.23) are reproduced after the discussion of regional trends; trend graphs for the other 6 scenarios are included in Appendix B. Note that it is quite plausible that vegetation could "flip-flop" between states, in an attempt to reach some degree of equilibrium. The vegetation has not reached complete equilibrium, but rather indicates vegetation states, which might be anticipated given the climate scenarios introduced. Certain thresholds will result in the representation of certain vegetation categories, which will change with input forcing scenarios. When reference is made to, for example, "stabilisation to grassland", stabilisation is referred to in the sense that there is a dominant tendency towards grassland. It is quite possible that if the model had been simulated beyond 2100, the vegetation may well have been different. The areas identified as susceptible to change may be addressed further in follow-on research, as a result of their demonstrated sensitivity.

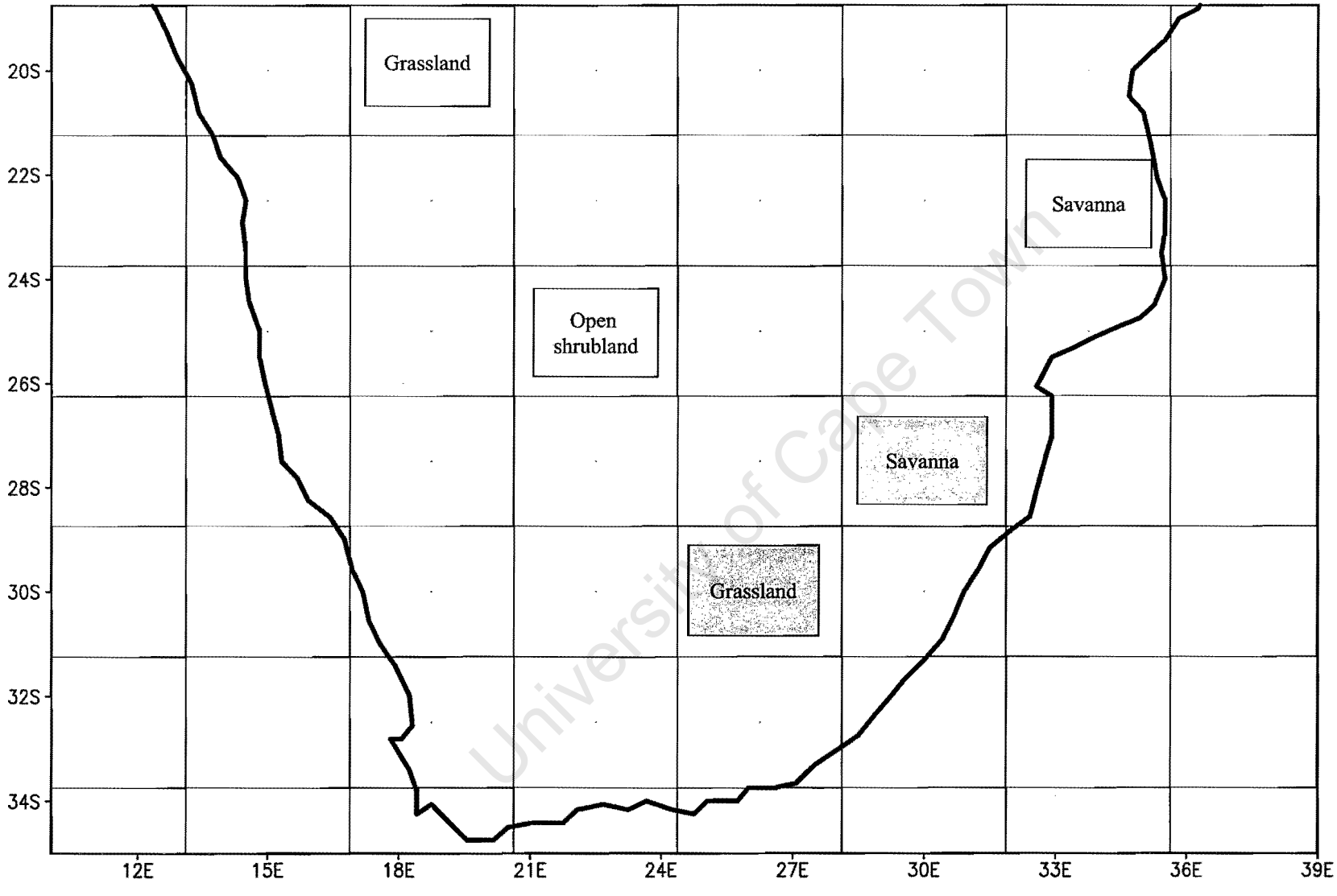

Figure 5.12 Ibissta vegetation for the 5 regions

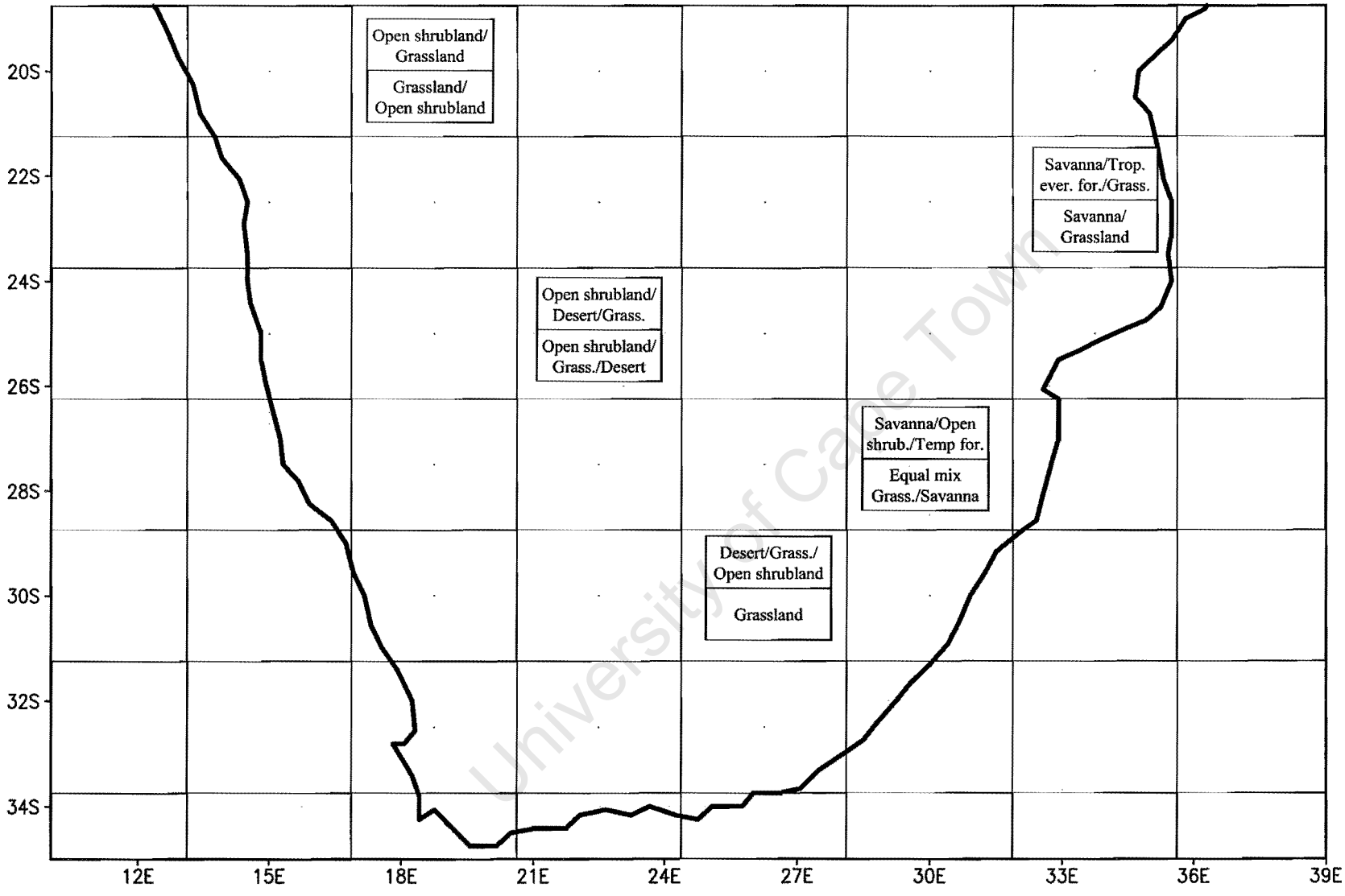

Figure 5.13 Ibisdyn vegetation for the 5 regions for the early (period 1) and late (period 2) 21st century. Note: Lighter shaded boxes are for period 1 and darker shaded boxes, period 2. Vegetation categories are displayed in the order of frequency of representation e.g. "Open shrubland/Grassland" indicates a mix of vegetation with a greater tendency towards Open shrubland than Grassland.

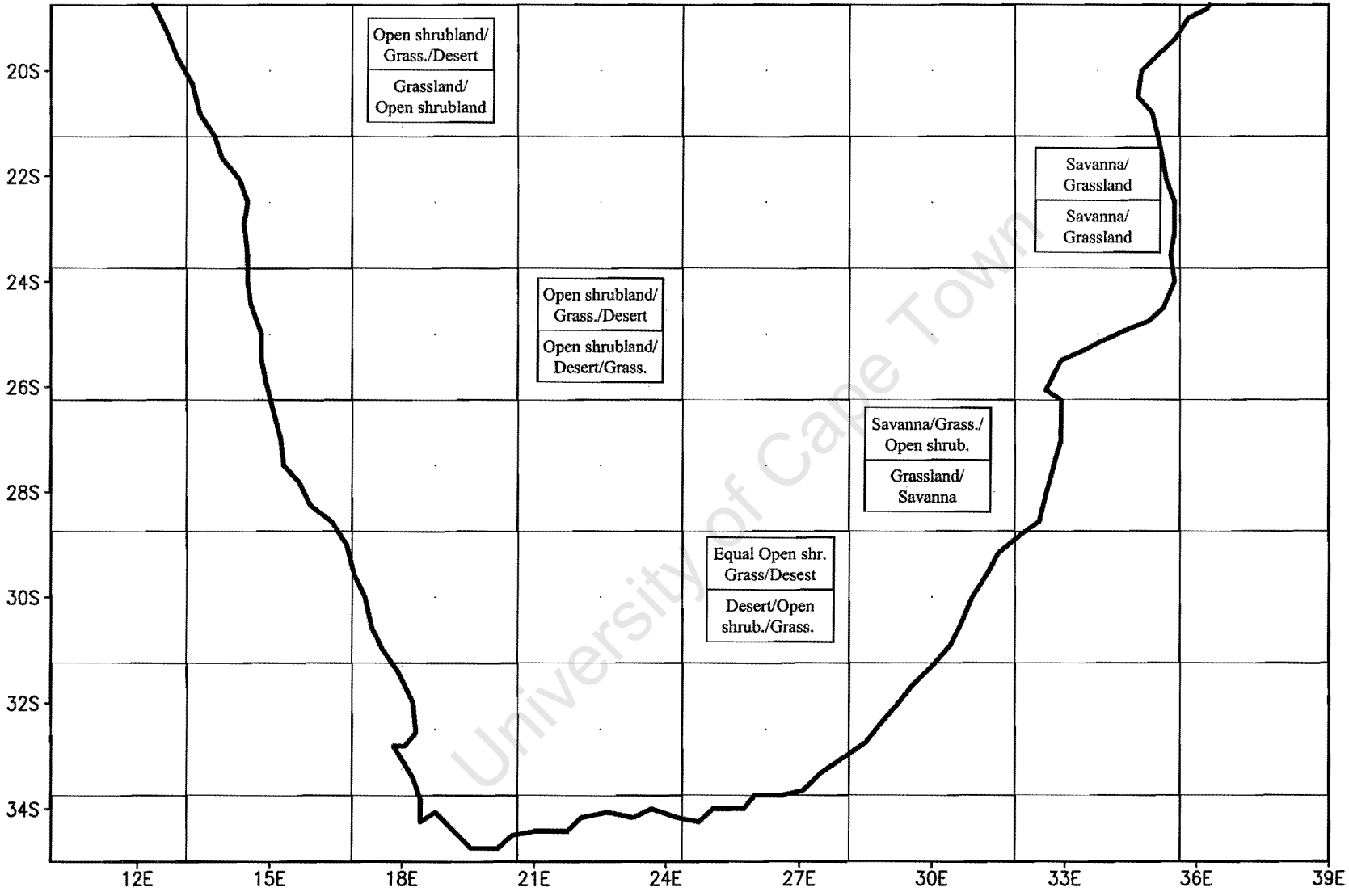

Figure 5.14 P1 vegetation for the 5 regions for period 1 and period 2.

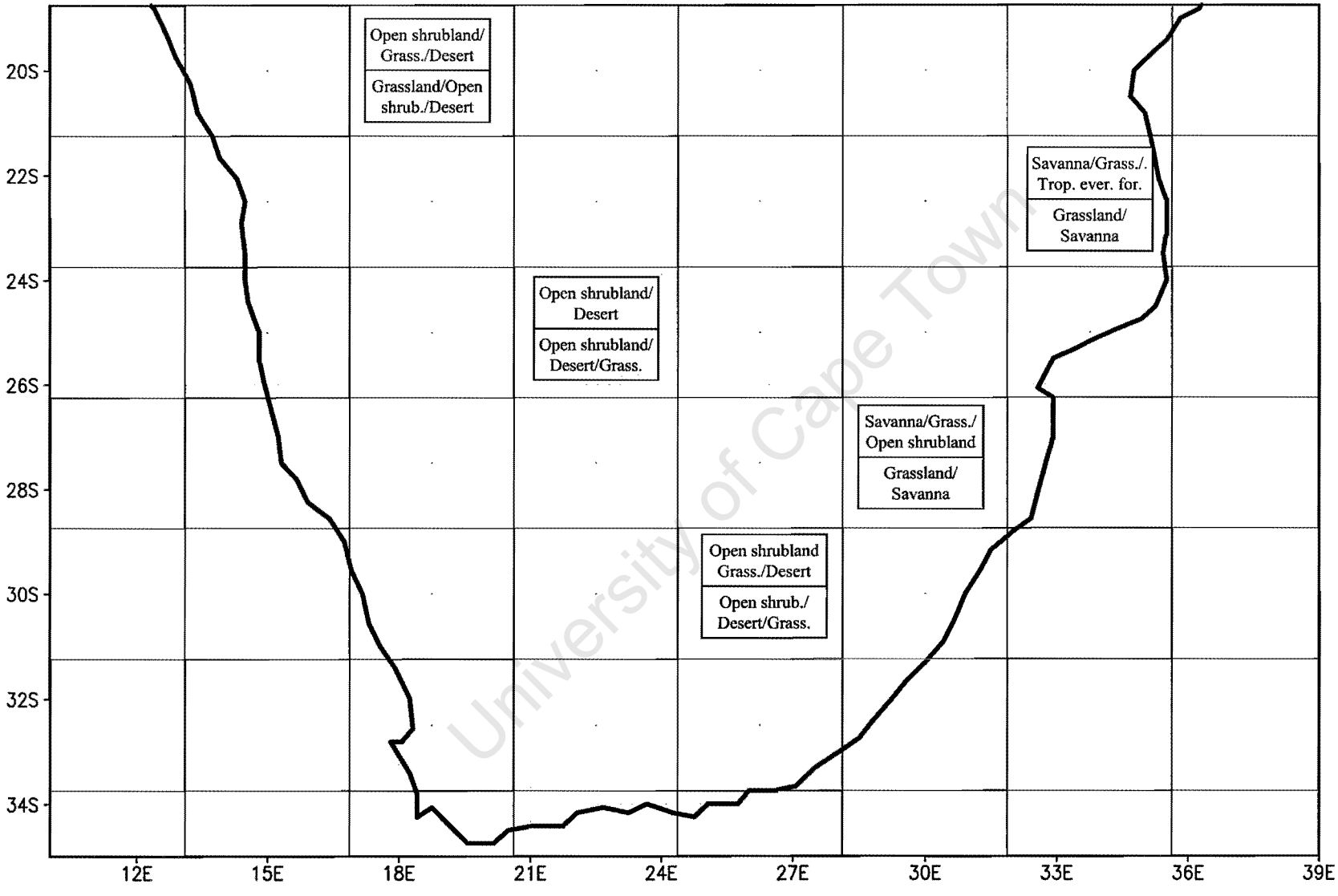

Figure 5.15 P2 vegetation for the 5 regions for period 1 and period 2.

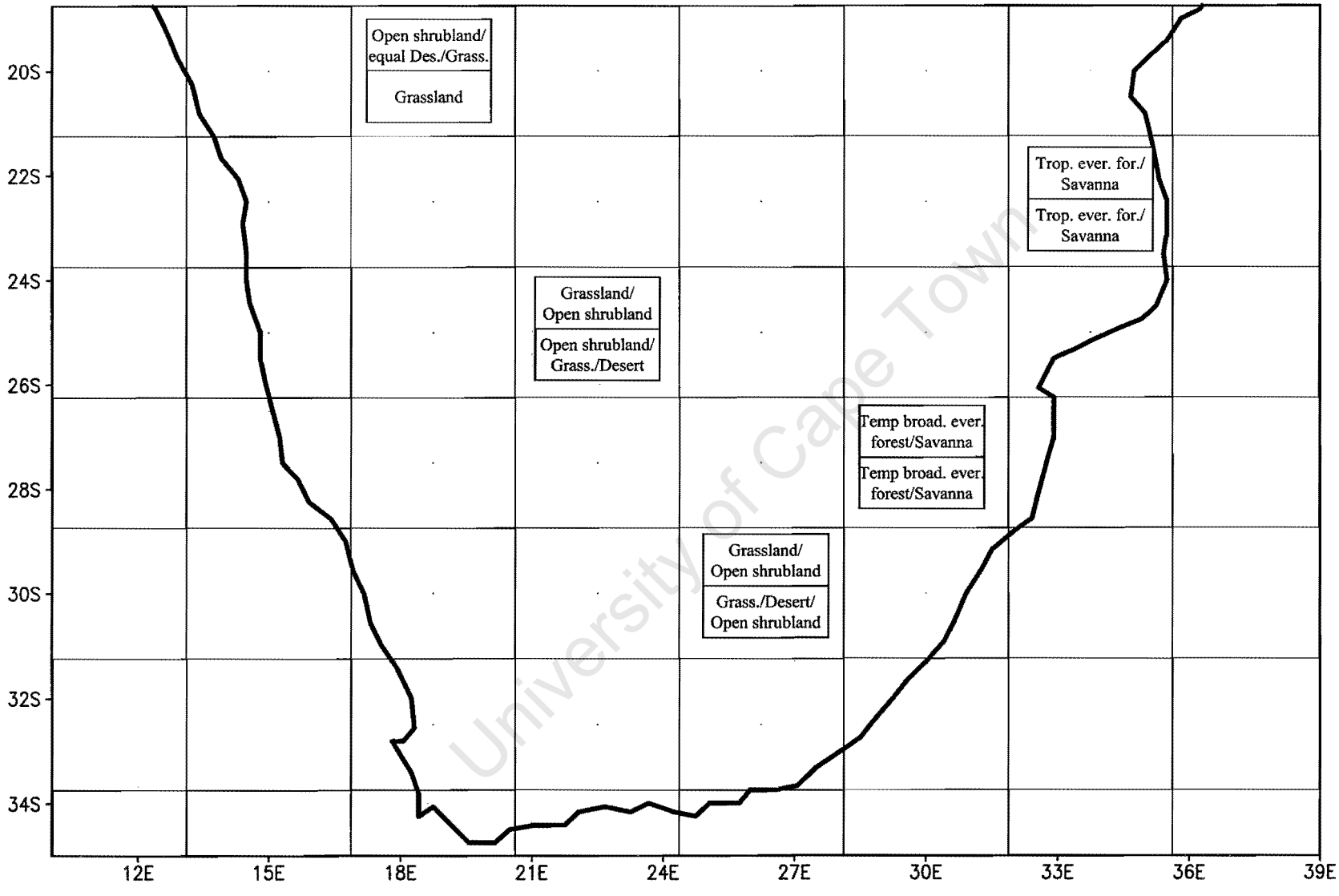

Figure 5.16 P3 vegetation for the 5 regions for period 1 and period 2.

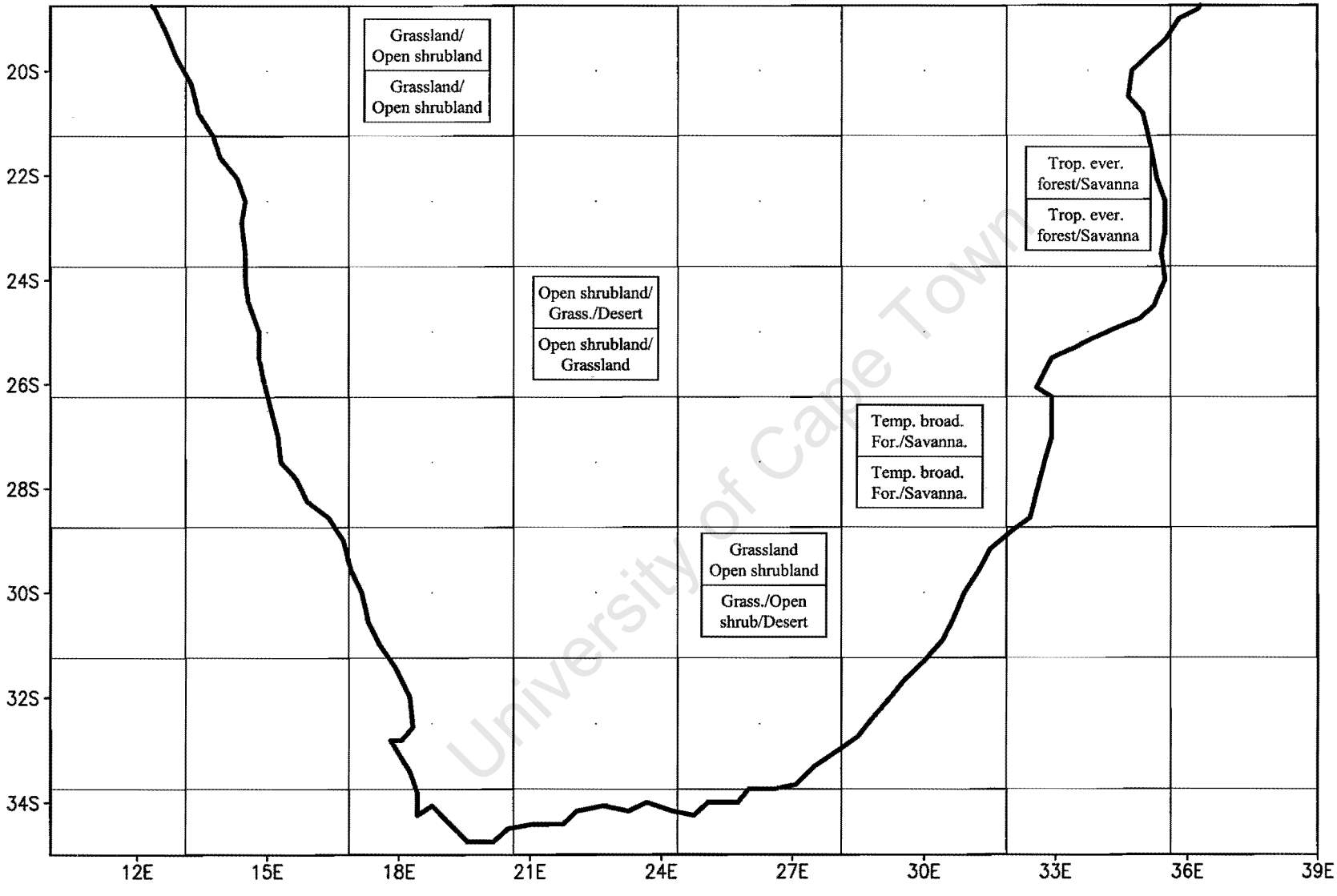

Figure 5.17 P4 vegetation for the 5 regions for period 1 and period 2.

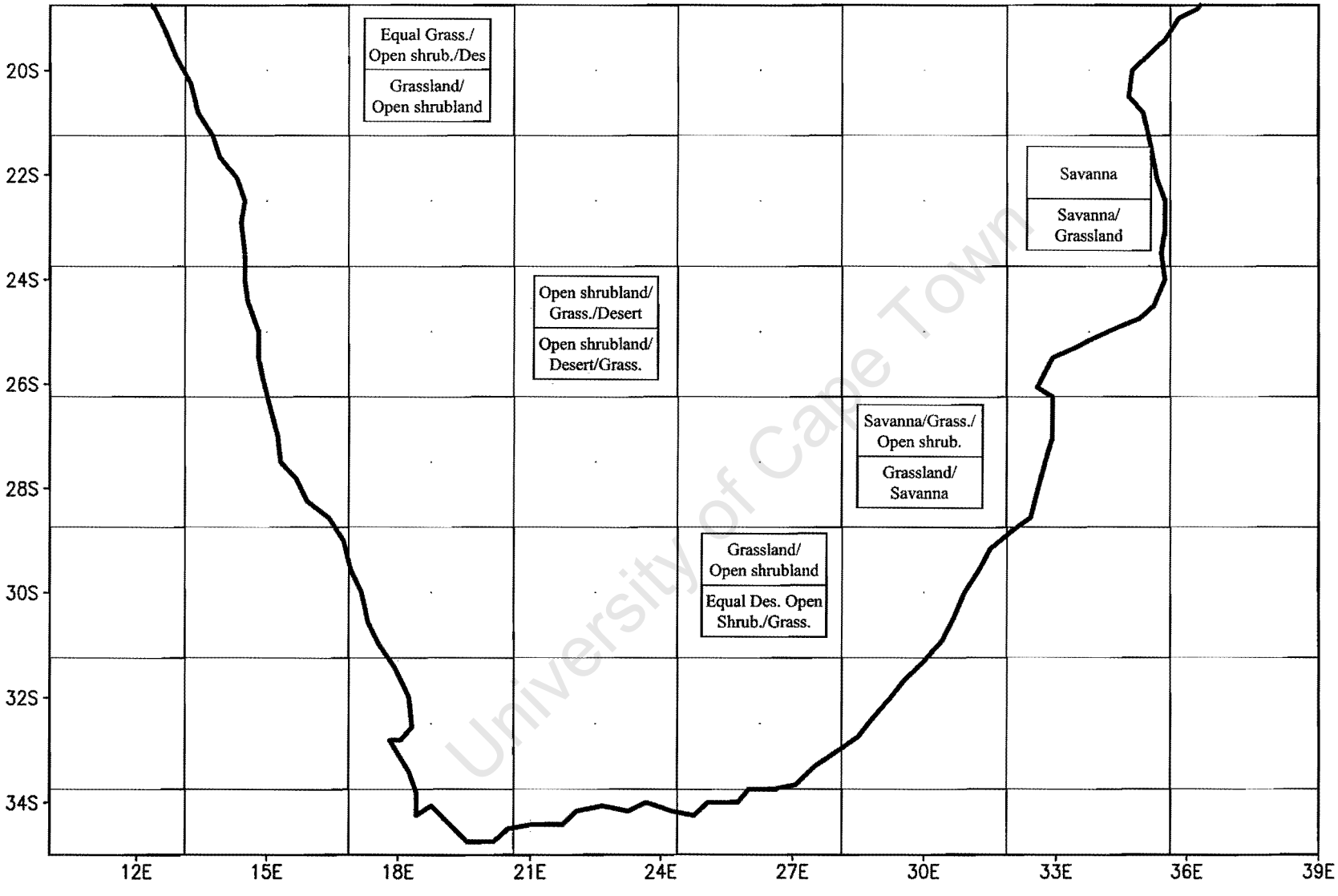

Figure 5.18 P5 vegetation for the 5 regions for period 1 and period 2

5.3.1 Region 1

In Ibisdyn, region 1's (southern escarpment) vegetation in period 1 tends to border between desert, open shrubland and grassland. In period 2 there is stabilisation to grassland. In the simulations with different standard deviation scenarios (P1-P5), the vegetation in region 1 during period 1 has not stabilized, and shows a mix of open shrubland, desert and grassland in all 5 cases. There is more grassland in P3 and P4. In period 2 there is a tendency towards grassland, more so in P3 and P4. There are more cases of desert in P1, P2 and P5 than P3 and P4.

Annual average evapotranspiration in Ibisdyn increases from period 1 to period 2 by, on average, 60 mm $year^{-1}$; there is a decline in evapotranspiration within each period. Annual average evapotranspiration trends for Ibissta are almost identical to those of Ibisdyn and also show an increase of approximately 60 mm $year^{-1}$. The trend responses for P1, P3 and P5 are distinct from those of P2 and P4. In P1, P3 and P5 evapotranspiration in period 1 shows an increasing trend, which is in contrast to Ibisdyn. In P2 and P4 there is no determinable trend. In period 2 there is a decreasing trend in P1, P3 and P5, which corresponds with the decreasing trend in Ibisdyn. P2 and P4 however, indicate an increasing trend. There is a general increase in evapotranspiration from period 1 to period 2 in P1, P3 and P5, yet not as marked as in Ibisdyn.

Evapotranspiration has an important function of returning moisture to the atmosphere (replenishing that lost through precipitation), and is also a vital component in the transfer of energy. Increases in annual average evapotranspiration from period 1 to period 2 may be related to canopy structure, since the retaining capacity of the canopy will have increased with the vegetation shifts away from dryland vegetation e.g. a shift in Ibisdyn from desert/open shrubland/grassland in period 1, to grassland in period 2. Increases in evapotranspiration also may be attributed to the 4°C increase (between 2000-2080) in surface temperatures driving the IBIS model.

Linked to evapotranspiration, are changes in soil moisture. As soil dries out, one would expect soil moisture to decline. Thus, the downward trend in Ibisdyn is what would be expected, since evapotranspiration shows a corresponding downward trend in each period as well. Trends in P1-P5 are also reasonably consistent with trends in Ibisdyn. Ibissta shows a definite increase in fractional soil moisture from period 1 to period 2 (0.1), which is not so clear in the other

scenarios, perhaps as a result of changes in vegetation type altering soil moisture values in the other scenarios.

Soil moisture is in fact a useful indicator of productivity, since soil moisture is a means of relieving stress during periods of drought. Soil moisture is also important in heat transfer, since water conducts heat more easily than air. Therefore, soils with higher soil moisture content will be likely to transmit more heat away from the surface than dry soils.

Annual net primary productivity (NPP) in Ibisdyn has increased by up to 0.1 kg m^{-2} $year^{-1}$, implying a shift away from dryland vegetation types (as evidenced by vegetation changes), perhaps related to the increase in the HadCM2 input precipitation (during the winter months) over the escarpment regions. In Ibissta the NPP between period 1 and 2 has increased less, as a result of the vegetation being static and thus not responding to input changes in the same manner as the dynamic vegetation. There are also general increases in NPP for P1-P5, but they are not as large as those for the mean dynamic run, but still indicate a definite move away from dryland plant functional types. NPP values in P3 tend to be the highest and P2 the lowest.

Increases in NPP will have implications for albedo, since different vegetated surfaces will have different albedos. Decreased albedo (which is probable with the increase in NPP and reduced soil exposure evident in vegetation changes) will result in less incoming radiation being reflected back into space and therefore increased heating of the surface, amplifying the surface temperature increases.

Sensible heat fluxes in Ibisdyn have increased with an increasing trend, on average by approximately 6 W m^{-2}. Perhaps the greatest difference between the static and dynamic simulations, is the sensible heat flux response, which in the case of Ibissta shows the opposite trend response to Ibisdyn. P1, P3, P4 and P5 are consistent with the response in Ibisdyn. Increases in P2 are not so marked.

Soil temperature in Ibisdyn has decreased (on average by 1.2°C), partially as a consequence of increasing vegetation cover and therefore less bare ground for soil exposure. The decrease in soil temperature is also apparent for P1-P5 and Ibissta.

5.3.2 Region 2

In Ibisdyn the vegetation in region 2 (northern escarpment) for period 1 is largely tending towards savanna (with trees), but with cases of open shrubland and forest. In period 2 the vegetation is bordering between savanna and grassland, and is more than likely a mixture of both. Region 2's vegetation in the early 2000s is primarily savanna in P1, P2 and P5. In P3 and P4 there is more of a tendency towards temperate evergreen broadleaf forest with savanna. Period 2 shows a mix of grassland and savanna in P1, P2 and P5, but a mix of savanna and temperate evergreen broadleaf forest in P3 and P4.

Annual average evapotranspiration for Ibisdyn and Ibissta shows no determinable trend between periods 1 and 2. The evapotranspiration response for P1, P3 and P5 indicates an increase during period 1 (approximately 60 mm $year^{-1}$). Period 2 has no determinable trend or a slight decrease in evapotranspiration. In P2 and P4 the response in period 1 shows no marked trend; there is a slight decline in period 2. The evapotranspiration increase for P1, P3 and P5 could be ascribed to the precipitation anomaly inputs (P1, P3 and P5 are inputs with a positive standard deviation from the mean precipitation), resulting in greater moisture available for evapotranspiration. Increases in evapotranspiration may also be in response to the increase in input temperatures (3.5°C by 2080).

Soil moisture changes are linked to evapotranspiration and additionally do not show a well-defined response in Ibisdyn. P3 and P5 show an increase in period 1; changes in period 2 are minimal. Ibissta's soil moisture has increased slightly over the 21st century (by a fraction of 0.01).

Net primary productivity in Ibisdyn has increased from period 1 to 2 (0.1 kg m^{-2} $year^{-1}$) with an increasing trend. NPP in P2 and P4 has also increased over the 21st century. In P1, P3 and P5, NPP is increasing in period 1, but with no determinable trend in period 2. Values of NPP are highest in P3 and lowest in P2. In Ibissta there is a slight increase in NPP from period 1 to period 2. The NPP increased in the different scenarios will have inferences on albedo, which will likely decrease and hence enhance the surface temperature increase.

Sensible heat fluxes in Ibisdyn have a downward trend and have declined through the 2000s. In P1, P3 and P5, sensible heat fluxes are decreasing in period 1. The trend in period 2 is largely level. In P2 and P4, sensible heat fluxes are decreasing during period 1 and level or slightly

decreasing in period 2. Ibissta's sensible heat fluxes have marginally decreased with a declining trend. In all cases sensible heat fluxes have declined through the 21st century.

Soil temperature in Ibisdyn has decreased (up to 1°C) with a declining trend, in response to the increase in surface cover and thus reduced bare soil exposure and therefore soil temperatures. Ibissta shows a similar response. In P1, P3 and P5, soil temperature has decreased during period 1. The trend is not determinable in the period 2. Soil temperatures are lowest in P3. P2 and P4 do not have marked trends.

5.3.3 Region 3

In Ibisdyn the vegetation in region 3 (Mozambiquan plains) largely tends towards savanna, with a few cases of tropical evergreen forest and one of grassland in period 1. Period 2 is primarily savanna with a small mix of grassland. In P1, P2 and P5 in period 1 there is mainly savanna. In P3 and P4 there is primarily tropical evergreen broadleaf forest with some savanna. In period 2 there is a mix of savanna and grassland in P1, P2 and P5. P3 and P4 show a mix of savanna and tropical evergreen forest.

Annual average evapotranspiration shows no determinable trend between the early and late 2000s in all 7 scenarios. This could be, in part, due to region 3 being situated on the coast and therefore being more of a moderated environment showing lower temperature and relative humidity changes than in other regions, and a slightly declining precipitation trend in the HadCM2 model simulation.

Soil moisture in Ibisdyn shows a declining trend in periods 1 and 2, with a decrease of approximately 0.01, and therefore a decline in run-off potential and a decrease in storage capacity during periods of drought. P2 and P4 also show a declining trend in period 1, but an almost level or minimally decreasing trend in period 2. Period 1 soil moisture in P1, P3 and P5 has the opposite trend to Ibisdyn, P2 and P4. Soil moisture for Ibissta is decreasing with a declining trend through the 21st century.

Annual net primary productivity in Ibisdyn increases slightly during period 1, with no determinable trend in period 2. There is a slight increase over the 21st century. NPP trends for P1, P3 and P5 are similar to those of Ibisdyn. P4 shows a slight decline in period 1 and P2 a slight increase. Both show no marked trend in the later 2000s. NPP in Ibissta exhibits a

minimally declining trend in period 1 and no determinable trend in period 2. Thus, region 3 is not displaying a marked change in productivity over the 21st century. This could be attributed to the input precipitation showing no notable trend, and hence there is not a coupled increase in moisture availability for plant growth.

Sensible heat fluxes have decreased with a downward trend in Ibisdyn. In P1, P3 and P5, sensible heat fluxes have also decreased from period 1 to period 2. The trend in period 1 is downward, but largely level in period 2. In P2 there is a decrease in sensible heat fluxes through the 21st century, with a downward trend. P4 is slightly increasing in trend in period 1 but this levels out in period 2. Ibissta's trend is not determinable in the period 1, but slightly increasing in period 2.

Soil temperature exhibits an upward trend in Ibisdyn, with a slight increase through the 21st century. This is likely due to the fact that vegetation exposure has increased (since vegetation in period 1 is savanna with some tropical evergreen forest, while period 2 is savanna with some grassland). In contrast, in P1, P3 and P5, soil temperature has a declining trend in period 1 and a minimally increasing trend in the period 2 (linked to the differences from the mean vegetation response). In P2 and P4, soil temperature increases during period 1, but levels out in period 2. Results for Ibissta also show an upward trend in period 1, but a slight downward trend in period 2.

5.3.4 Region 4

Region 4's (southern Kalahari) vegetation in Ibisdyn in period 1 has a tendency towards open shrubland, with cases of desert and grassland. Period 2 is also predominantly shrubland, with cases of grassland and desert. In P1, P2, P4 and P5 in period 1 there is a dominance of open shrubland. Grassland dominates in P3. In period 2 the vegetation has a tendency towards open shrubland in all 5 scenarios, but with cases of grassland and desert (except for P4).

In Ibisdyn and Ibissta, annual average evapotranspiration shows a slight increase from period 1 to period 2. The trend in period 1 is level and is increasing in period 2. In P1, P3 and P5, evapotranspiration has decreased from period 1 to period 2, probably linked to the lack of a marked vegetation response. P2 and P4 do not exhibit any determinable increases or decreases.

Soil moisture in Ibisdyn, P1, P3 and P5 does not indicate any clear trend. In P2 and P4 there is a slight decrease in periods 1 and 2. Ibissta reflects a stable situation in period 1, and an increasing trend in period 2.

Annual net primary productivity increases slightly from period 1 to period 2 in Ibisdyn and Ibissta. NPP for P1, P3 and P5 indicates a minimal decrease in period 1. NPP in period 2 is slightly lower. These changes are related to the vegetation response. NPP in P2 and P4 is similar in period 1 and period 2.

In Ibisdyn, P2 and P4 sensible heat fluxes exhibit a slight decline in period 1 and a slight increase in the period 2, but without any clear trend. In P1, P3 and P5 sensible heat flux values do not show a marked increase or decrease through the 21st century.

Soil temperature in Ibisdyn has an increasing trend in period 1 and a declining trend in period 2, with a general decrease in soil temperature, in association with the slight increase in net primary productivity. In contrast, P1, P3 and P5 show an increase in soil temperature from period 1 to period 2 (between 0.5° and 1°C) with an increasing trend. These changes are probably associated with the decrease in vegetation productivity for these 3 scenarios. Soil temperature has also marginally increased with an increasing trend in P2 and P4.

5.3.5 Region 5

The vegetation in region 5 (northern Namibia) for Ibisdyn in period 1 has a tendency towards shrubland, but with cases of grassland. The vegetation in period 2 has shifted to predominantly grassland, with cases of open shrubland. Vegetation in period 1 is mainly open shrubland in the case of P1 and P2. P5 has an equal mix of open shrubland and grassland dominating. P3 and P4 show a tendency towards grassland. In period 2, P1 and P2 have a tendency towards a mix of open shrubland and grassland, while in P3, P4 and P5 grassland dominates, but with some open shrubland.

Annual average evapotranspiration in Ibisdyn has increased over the 21st century, but with a slight declining trend in period 2. The mean increase is roughly 70 mm year^{-1}. This increase is higher than in the other 4 regions, probably linked to the greater increase in temperature over the region (5°C) and the notable shifts away from dryland vegetation. P1, P3 and P5 show an overall increase in evapotranspiration through the century, with a declining trend in the period 1 and an

increase through period 2. P2 and P4 indicate an increasing trend with an increase in evapotranspiration over the 21st century (approximately 40 mm year^{-1}). Evapotranspiration for Ibissta is consistent with the increase in evapotranspiration through the 21st century in the other simulations, and has the same trends as Ibisdyn.

Soil moisture in Ibisdyn and Ibissta has an increasing trend in period 1 and a decreasing trend in period 2. In P1 and P5 trends are level or slightly increasing, with an increase in soil moisture over the period. In P3, soil moisture in the early part of the century is declining, but there is an overall increase in soil moisture through the century. In P2 and P4 there is an increase overall with an increase in period 1, but little change in period 2.

Annual net primary productivity has increased from period 1 to period 2 in Ibisdyn and Ibissta, although there is a declining trend in period 2. The mean increase is about 0.05 mm year^{-1}. NPP in period 1 is decreasing in P1, P3 and P5, but minimally increasing in period 2; there is an overall increase. P2 and P4's NPP is increasing with an increasing trend. The surface temperature increase is likely to be exacerbated by the increase in NPP, consequent of the decrease in albedo.

Sensible heat fluxes have increased from period 1 to period 2 in Ibisdyn. In contrast, in Ibissta the fluxes have decreased. In P2 and P4 there is a marginal increase in sensible heat fluxes through the 21st century. In P1 and P5 sensible heat fluxes have declined in period 1 and increased in period 2. P3 shows no determinable trend. Sensible heat fluxes in this region are an important consideration, since they will have implications for the formation of thermal lows. With an increase in sensible heat fluxes at the surface, there is the possibility of enhanced formation of thermal lows.

Soil temperatures in Ibisdyn have decreased by approximately 1°C, corresponding with the increase in productivity of the vegetation and the consequent reduction of bare soil exposure. Soil temperatures in Ibissta have also decreased, but by 0.6°C. In P1, P3 and P5, there is an increasing trend in period 1 and a decreasing trend in period 2, with a general decrease in soil temperatures. P2 and P4 also exhibit a decrease in soil temperatures.

5.3.6 Synthesis

Responses (of annual average evapotranspiration, annual net primary productivity, sensible heat fluxes, soil temperatures and soil moisture) in IBIS to the trends in forcing data highlight some important differences between the mean dynamic vegetation run (Ibisdyn) and scenarios P1-P5. It is evident that responses in the dynamic vegetation runs generally fall into groups of similar response, *viz.* (P1, P3 and P5), (P2 and P4) and Ibisdyn. These response groupings are related to the input *precipitation* driving the IBIS model simulation. In the case of P1, P3 and P5, the input precipitation has a positive standard deviation from the mean response. P2 and P4 have input precipitation values that have a negative standard deviation from the mean response. This categorization of variables into groups of similar response, based on precipitation, is to be expected, since the variables under question are all in some manner linked to precipitation amounts. Ibisdyn and Ibissta are similar in many respects, except for sensible heat fluxes (which will be affected by alteration of albedo, in the case of dynamic vegetation).

Input temperature, precipitation and relative humidity are all playing key roles in determining the plant functional types represented in each region in the early (period 1) and late (period 2) 21st century. There is a *broad scale* tendency for vegetation to move away from dryland categories, which is most likely in response to *precipitation* trends, since temperature increases would not account for such changes. It is evident from section 5.2 that precipitation has not necessarily increased in amount through the 21st century. In fact, it may well have decreased. Thus, what must be important in terms of plant functional types is the slight increase in precipitation in the winter months over the summer rainfall regimes, resulting in greater all-year-round vegetation productivity.

Temperature and *relative humidity* play a significant role in determining the *inter-scenario* vegetation response differences. Categories P1, P2 and P5 all represent scenarios where temperature has a positive standard deviation from the mean. These 3 regions, in conjunction with Ibisdyn, have similar vegetation categories represented in period 1 and period 2. P3 and P4 represent regions of negative standard deviation from the mean temperature and positive standard deviation from the mean relative humidity, and have similar vegetation categories and responses. These 2 regions also tend to represent less dryland vegetation than the other regions, which would be expected, since temperatures are lower and relative humidities are higher in these two scenarios. Change in wind speed would obviously play some role, but in terms of vegetation, it appears that its role is less significant than the other three variables.

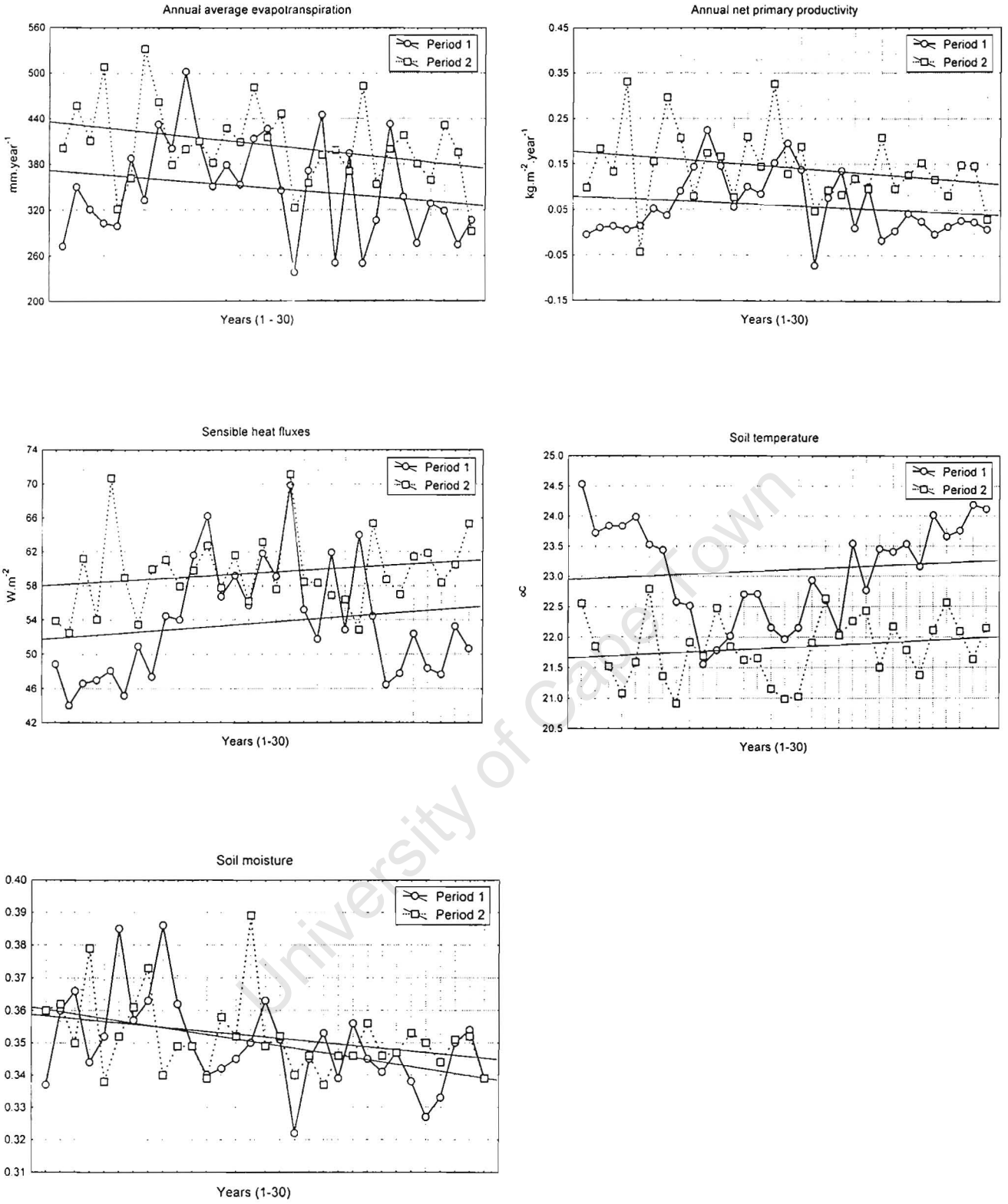

Figure 5.19 Trend graphs for region 1 for Ibisdyn

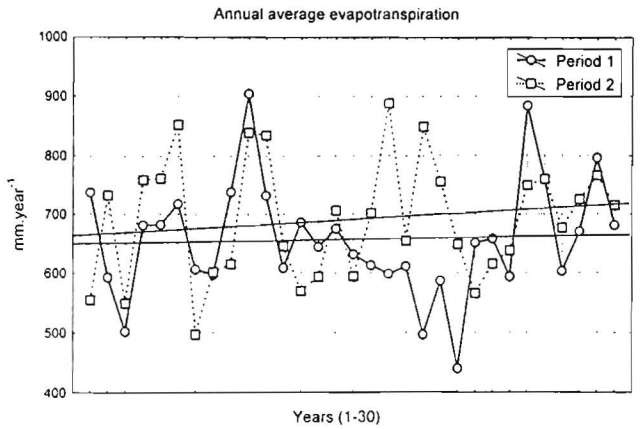

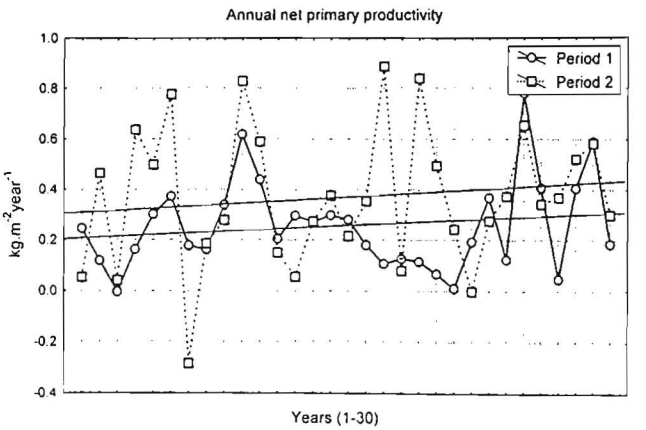

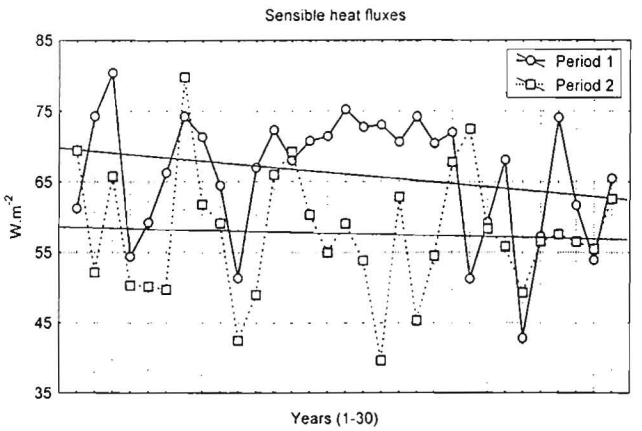

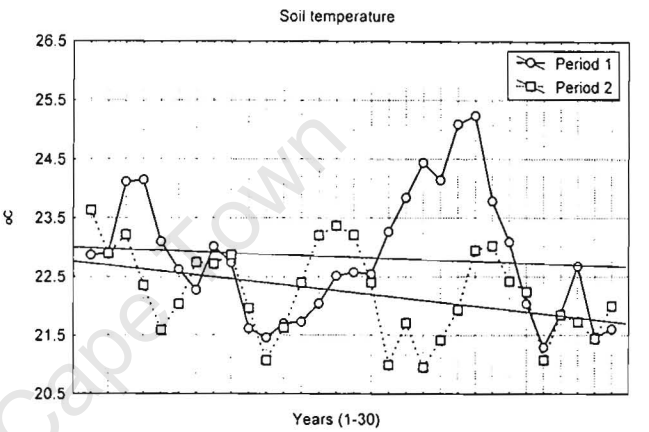

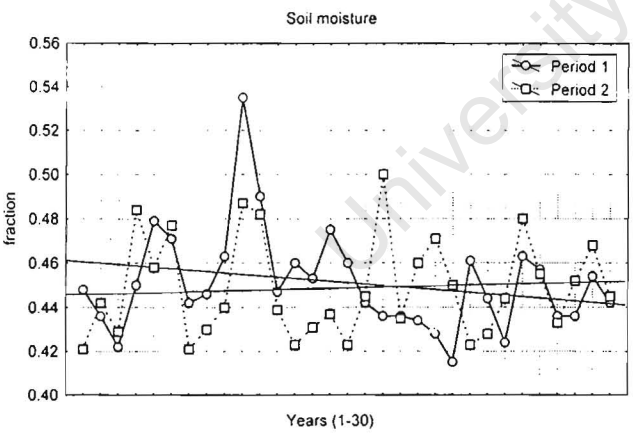

Figure 5.20 Trend graphs for region 2 for Ibisdyn

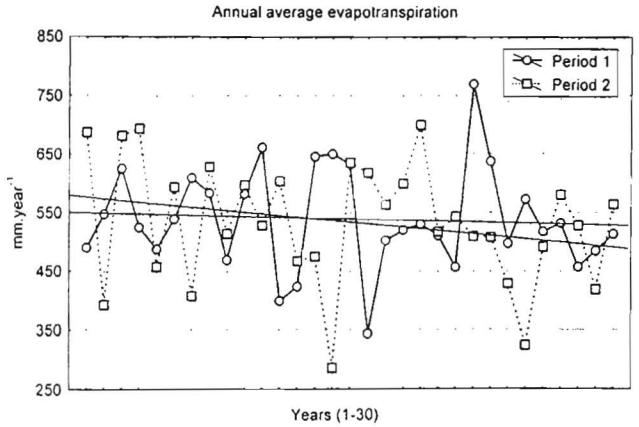

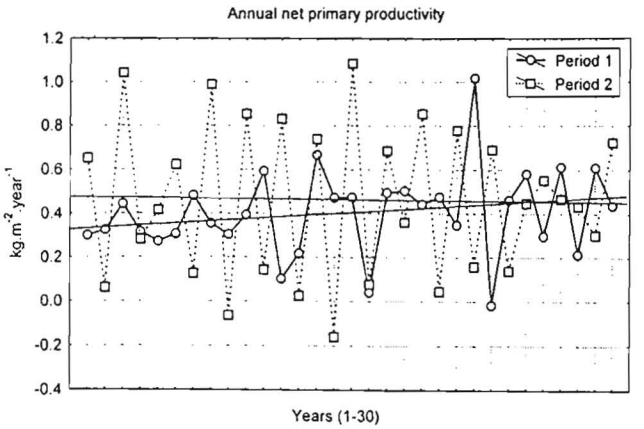

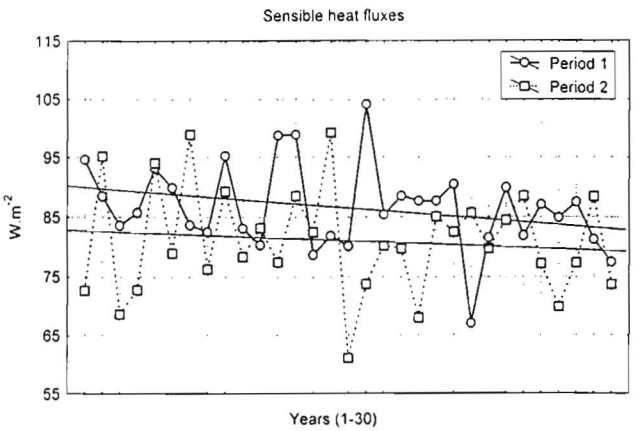

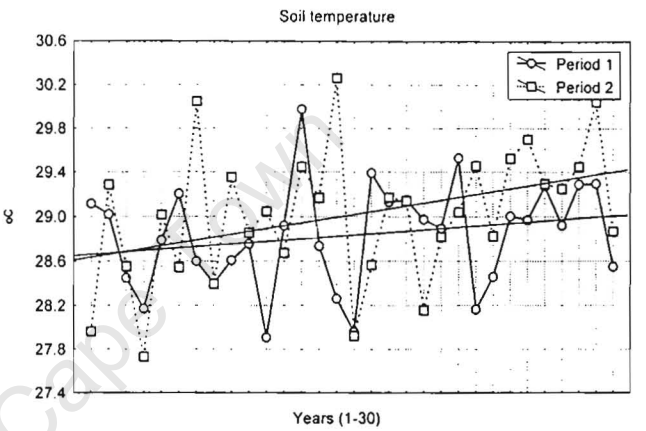

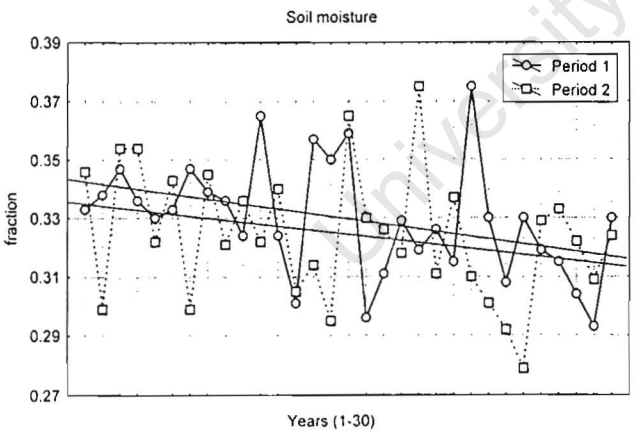

Figure 5.21 Trend graphs for region 3 for Ibisdyn

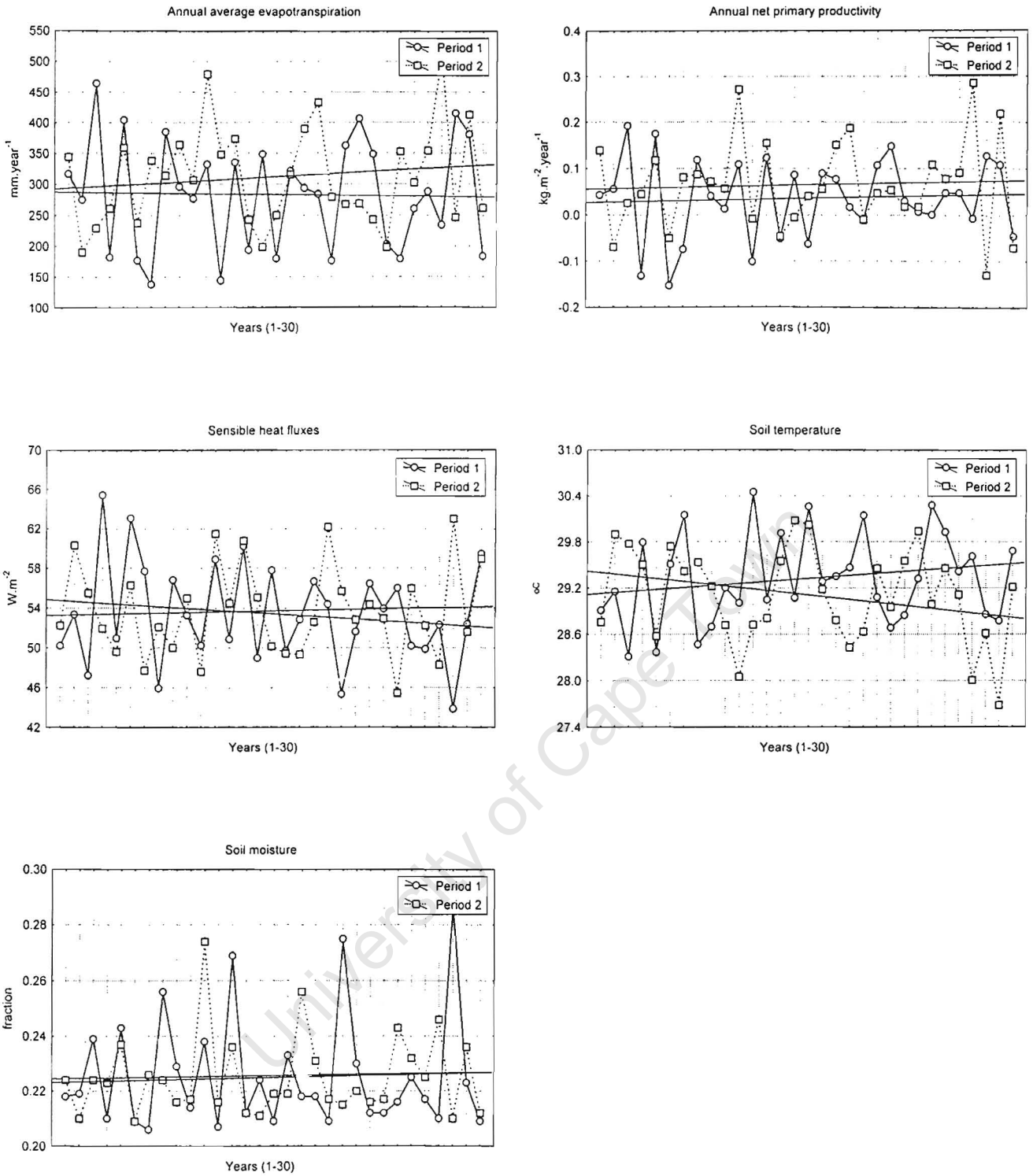

Figure 5.22 Trend graphs for region 4 for Ibisdyn

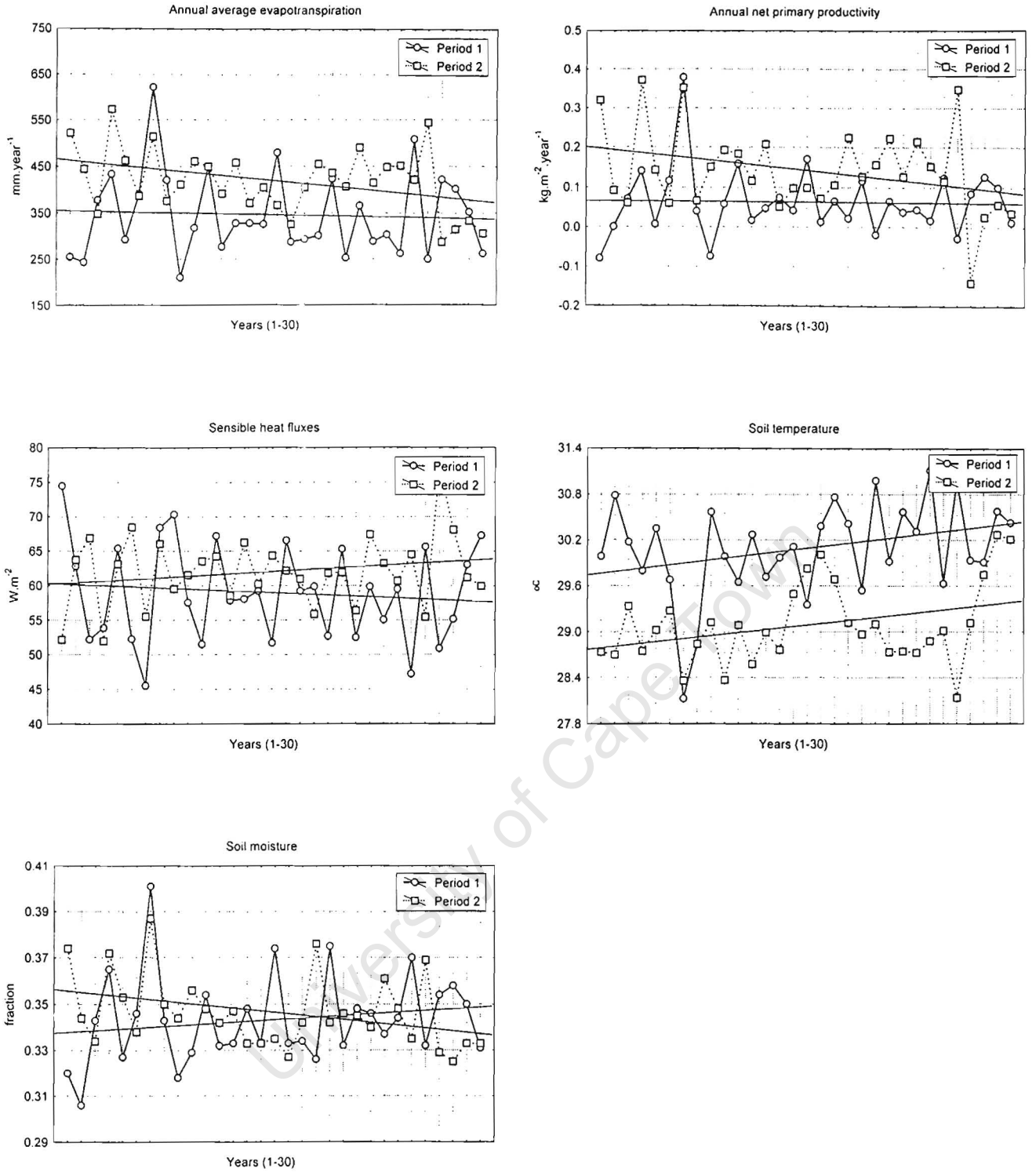

Figure 5.23 Trend graphs for region 5 for Ibisdyn

CHAPTER 6

IBIS MODEL SIMULATION SEASONAL RESULTS

CHAPTER 6

IBIS MODEL SIMULATION SEASONAL RESULTS

Seasonal analyses presented in this chapter are performed for the same 7 scenarios in Chapter 4. The summer (defined as December, January, February) and winter (defined as June, July, August) seasons are determined from monthly output. IBIS simulation monthly output includes a number of variables in addition to those discussed in the preceding chapter, including latent heat fluxes and leaf area index (upper and lower canopies). These variables are considered as well as those examined in Chapter 5 for the annual output. In addition to the summer and winter seasons, a more detailed examination on a monthly basis is undertaken, to consider broader regional aspects of change at this time scale and to better understand the significance of the transition seasons.

6.1 Dominant seasonal response

The sensitivity of the variables considered is generally most pronounced in summer, since summer is the primary growing season (and most of the domain falls within the summer rainfall regime). The dominant response is indicative of a spatial change towards a more productive vegetation environment and an extension of the growing season into the typically less productive winter months is suggested.

The summer and winter seasonal response scenarios may be grouped in relation to IBIS model input precipitation, relative humidity and temperature differences. With respect to leaf area indices (upper and lower canopies) and net primary productivity, there is a grouping of scenarios according to differences in *temperature* and *relative humidity* forcing inputs. In the model simulations, P1, P2 and P5 all represent scenarios of a positive standard deviation from the mean temperature input and a negative (or mean in the case of P5) standard deviation from the mean relative humidity input (refer to figure 4.1 in Chapter 4). These 3 scenarios are most similar to Ibisdyn with respect to NPP and leaf area indices. P3 and P4, which represent scenarios of a negative standard deviation from the mean temperature and a positive standard deviation from the mean relative humidity, show some differences from Ibisdyn, P1, P2 and P5. Ibissta shows little change in either NPP or leaf area indices, by the very nature that the vegetation is not changing.

Scenarios for other variables (e.g. sensible heat fluxes, latent heat fluxes, soil temperatures, soil moisture and average evapotranspiration) may be grouped according to their differences in input *precipitation* forcing. P1, P3 and P5 all represent scenarios of a positive standard deviation from the mean precipitation input, and together with Ibisdyn and Ibissta (except in the case of sensible heat fluxes), show commonality of response. P2 and P4 (both representing scenarios of a negative standard deviation from the mean precipitation) group together in terms of showing a common response.

A number of key response regions emerge for the summer season (figure 6.1). The most notable regions demonstrating consistency in variable and scenario response are Northern Namibia and the escarpment regions (particularly the south-western and southern escarpment). In winter, changes are less pronounced, with the south-western escarpment region displaying the most consistency in response between variables and scenarios. The dominant summer and winter response regions are discussed in more detail below. The sections to follow (6.2 and 6.3) will consider the variable specific response between different scenarios and over the different regions of the southern African domain.

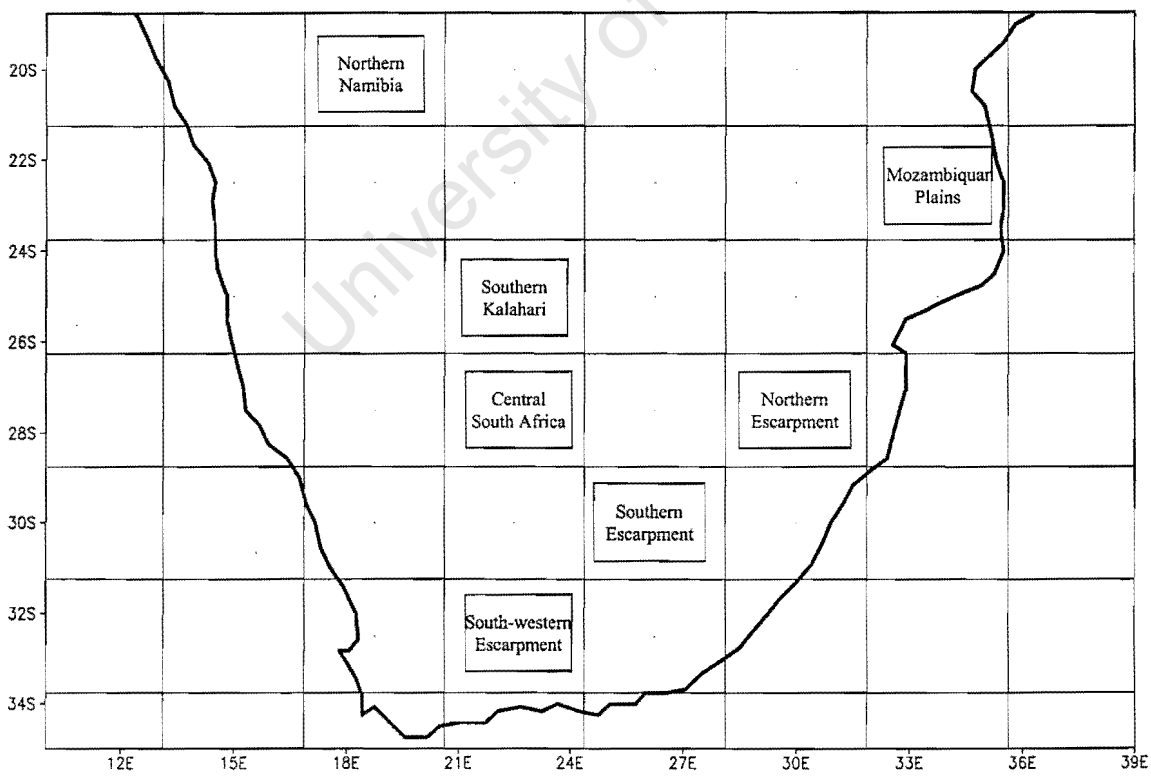

Figure 6.1 Some key response regions in the summer simulation. The darker shaded regions show the most consistent and dominant response in the majority of variables and scenarios.

In the northern Namibian summer, in all scenarios, there is a general increase in net primary productivity, with most vegetation productivity increases between the early (period 1) and late (period 2) 21st century occurring in the lower canopy (there is a decrease in upper canopy leaf area indices and an increase in lower canopy leaf area indices). These increases in productivity correspond well with the general movement of vegetation away from more dryland vegetation categories. Average evapotranspiration has also increased, with the increase in available moisture being obtained from the increase in the moisture retaining capacity as a result of the increase in leaf area index of the lower vegetation canopy. This is important in terms of replenishing atmospheric moisture lost through precipitation. Soil moisture has increased, linked to the increase in NPP and consequent reduced soil exposure. The increase in soil moisture is important in terms of storage capacity, particularly during extended dry spells. Soil temperatures have correspondingly declined. There is an increase in latent heat fluxes. As evidenced in Chapter 3, there is an increase in wind speed over a portion of the sub-continent, which probably accounts for the latent heat flux increases, since wind speed increases will allow for a greater redistribution of heat.

Over the south-western and southern escarpment regions during summer, NPP has increased from period 1 to period 2, partly related to the increase in input precipitation in the IBIS model simulation. Vegetation in these regions therefore has a tendency to move away from more dryland vegetation categories. Most increases in vegetation productivity are in the lower canopy (there is an increase in leaf area indices in the lower canopy). Associated with the increase in NPP and input precipitation, is an increase in average evapotranspiration, resulting in moisture availability for atmospheric replenishment. Increases in average evapotranspiration are not apparent for P2 and P4, probably due to these two scenarios both having a lower than mean (i.e. negative standard deviation from the mean) input precipitation. Soil moisture has increased in the SW escarpment in all scenarios except P2 and P4, but shows little change in the southern escarpment region. Increases in soil moisture are linked to the increase in both NPP and input precipitation. Soil temperatures have declined in both regions as well, related to the NPP increases. Latent heat fluxes have increased, corresponding with the increase in wind speed over the domain.

Over the south-western escarpment in winter, NPP has increased from period 1 to period 2. There is a marked decrease in upper canopy leaf area indices and increase (approximately 100%) in lower canopy leaf area indices. Vegetation productivity has therefore increased in the

winter months, but with a movement away from taller vegetation. The notable increases in productivity are linked to the increase in input precipitation and have important implications for an extension of the growing season. Linked to this are increases in average evapotranspiration. Soil moisture changes are not consistent, since they show little change in Ibisdyn, marginal decreases in P1-P5, and increases in Ibissta. Soil temperatures have increased minimally (0.2°C), which would not perhaps be anticipated, given the increase in NPP over the region.

In terms of the dynamic vegetation mean run (Ibisdyn) as opposed to the static vegetation mean run (Ibissta), there is good agreement in response regions and response direction for most variables, but with two notable exceptions being sensible heat fluxes (as discussed in the annual analysis in Chapter 5) and leaf area index (to be expected, since vegetation in not changing in Ibissta).

In the IBIS simulations using monthly input forcing of, for example, precipitation and relative humidity, the model code makes the necessary conversion to daily and sub-daily scales (in order for the model to make daily and sub-daily calculations of canopy physiology etc.). There is therefore also output of IBIS model simulated monthly precipitation and relative humidity, as derived from daily-determined values. The patterns are therefore not unlike the input forcing, but the amounts may differ (especially with respect to precipitation, which tends to be stochastically generated).

6.2 Summer seasonal differences between the early and late 21st century

A more detailed analysis of the specific changes in summer over the southern African domain follows. Figures for the dynamic vegetation mean simulation are presented in the text below, while figures for the static vegetation mean simulation and P1-P5 are included in Appendix D.

6.2.1 Net Primary Productivity

NPP values in the early 21st century (period 1) in the dynamic vegetation mean run (Ibisdyn - figure 6.2) and P1-P5 are highest over the SE of South Africa on the escarpment (0.1 kg m^{-2} $month^{-1}$) and over the north (0.1 kg m^{-2} $month^{-1}$). There is very low productivity over the South Africa/Zimbabwe border. Patterns in the static vegetation mean run (Ibissta) are similar, but values are lower over the South Africa/Zimbabwe border and higher over the SE of South Africa over the escarpment (0.12 kg m^{-2} $month^{-1}$).

In Ibisdyn, there are notable increases over Northern Namibia (0.025 kg m^{-2} $month^{-1}$), the Mozambiquan plains (0.03 kg m^{-2} $month^{-1}$) and the SE of South Africa on the escarpment (0.025 kg m^{-2} $month^{-1}$) from the early (period 1) to late (period 2) 21st century. These increases translate to a marked percentage change of 60% in Northern Namibia, 30% over the Mozambiquan plains and 40% over the escarpment. The increases in Northern Namibia and over the SE of South Africa on the escarpment are consistent for Ibissta (except there are only increases over the southern portion of the escarpment and not the north) and P1-P5. Increases evident in Ibisdyn over the Mozambiquan plains are consistent in P1, P2 and P5. Increases and decreases in regions other than the 5 regions identified in Chapter 5 are apparent in some scenarios, but with no consistent changes in all scenarios. NPP increases are indicative of a general movement away from dryland vegetation categories.

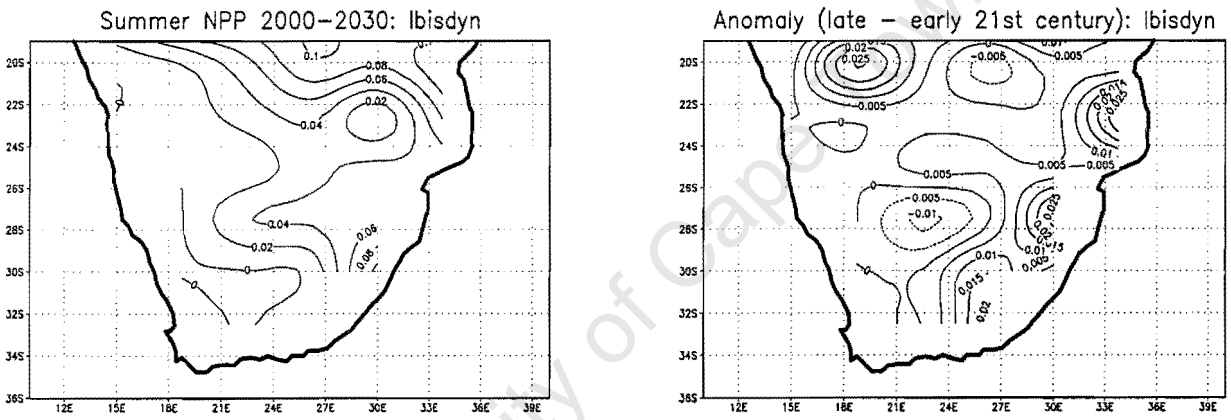

Figure 6.2 Summer net primary productivity or NPP (kg m^{-2} $month^{-1}$) for period 1 and the anomaly for Ibisdyn

6.2.2 Average evapotranspiration

Average evapotranspiration for period 1 increases northwards and eastwards from approximately 0.5 mm day^{-1} in the SW to 4 mm day^{-1} in the NE in all 7 scenarios (see figure 6.3 for Ibisdyn results).

From period 1 to period 2 there is an increase in average evapotranspiration over the SE of South Africa on the southern escarpment region (up to 0.3 mm day^{-1} – approximately 15%) and Northern Namibia (0.4 mm day^{-1} – about 15%) and the southern Kalahari (0.2 mm day^{-1} – approximately 10%). There are also minor changes in other regions. Ibissta shows a similar response to Ibisdyn. The increase in evapotranspiration over the southern portion of the escarpment and northern Namibia is also consistent for P1, P3 and P5, but not for P2 and P4. P1-

P5 indicate some changes in other regions, but with no general consistency between all scenarios. Average evapotranspiration increases are perhaps primarily due to an increase in surface temperature, promoting greater vertical uplift and heat redistribution.

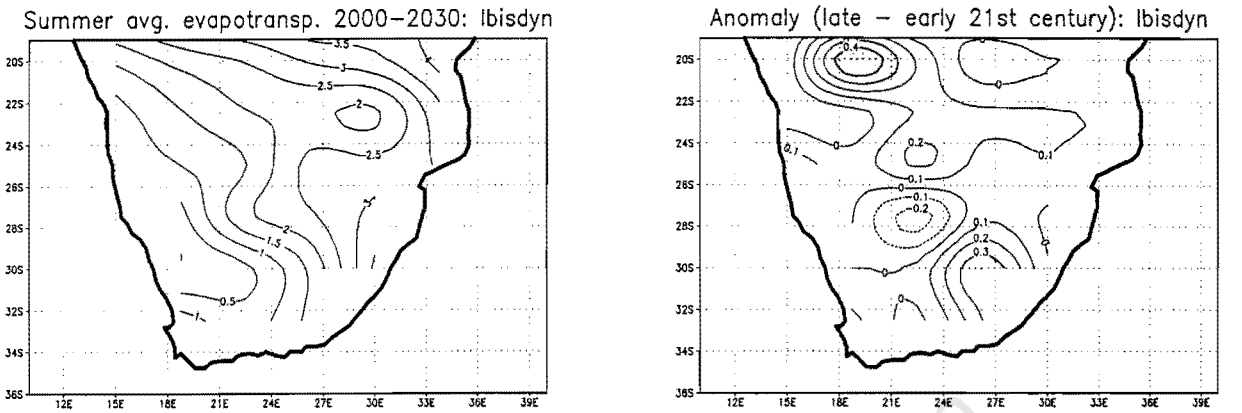

Figure 6.3 Summer average evapotranspiration (mm day^{-1}) for period 1 and the anomaly for Ibisdyn

6.2.3 Sensible heat fluxes

In period 1 in Ibisdyn sensible heat fluxes (figures 6.4) are highest in the southern regions (140 W m^{-2}) and decrease northwards to 50 W m^{-2}. Fluxes for Ibissta and P1-P5 are similar.

In Ibisdyn in period 2 there are increases in sensible heat fluxes over the southern portion of the SE of South Africa on the escarpment (6 W m^{-2} - 7%), and decreases over the northern portion (3 W m^{-2} - 4%) and decreases over the southern Kalahari (9 W m^{-2}, which is 13%). There are also changes in regions other than those identified in Chapter 5, such as decreases over central Botswana (6 W m^{-2}), increases over northern central South Africa (3 W m^{-2}) and decreases to the south of the escarpment regions (-15 W m^{-2}). In P1-P5, the changes in sensible heat fluxes are consistent over the southern portion of the SE of South Africa on the escarpment. Ibissta shows a change direction of opposite sign. The increase over the northern central South African region is consistent for Ibissta, but P1, P4 and P5 indicate a decrease. Other regions of apparent change are not consistent between different scenarios.

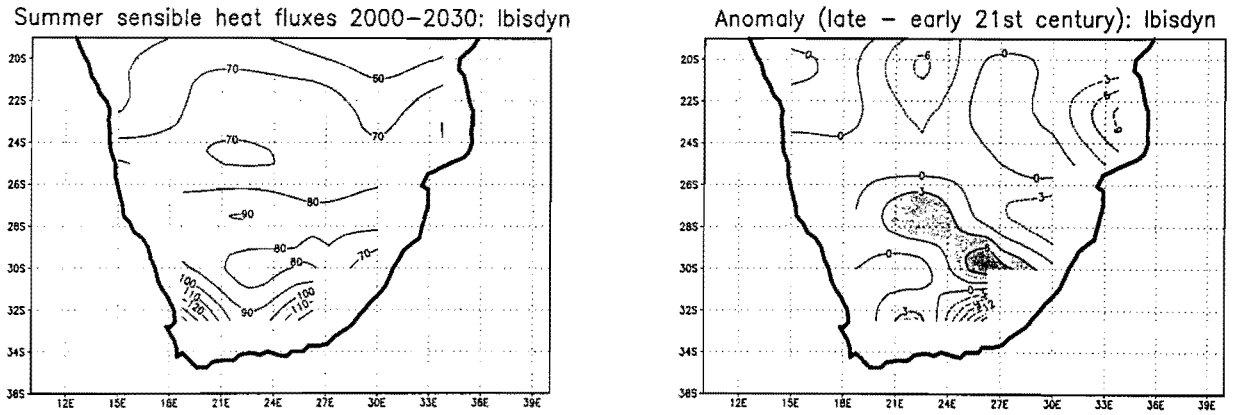

Figure 6.4 Summer sensible heat fluxes (W m^{-2}) for period 1 and the anomaly for Ibisdyn

6.2.4 Soil temperatures

Soil temperatures in period 1 are highest over the west of South Africa (38°C) and the South Africa/Zimbabwe border (36°C), and lowest over the coastal regions to the SW (24°C) and south (22°C) in Ibisdyn (figure 6.5). Temperatures and patterns for the other scenarios are similar, but with higher temperature maximums in P1, P2 and P5 (40°C) over the west of South Africa and higher minimums (24°C) over the coastal regions.

In Ibisdyn in the anomaly there are decreases in soil temperatures over the southern (1.8°C) and northern (0.6°C) portions of SE South Africa on the escarpment, over Northern Namibia (1.2°C) and the Southern Kalahari (0.3°C). These decreases are probably attributed to the decreased soil exposure through an increase in net primary productivity and leaf area index. The decreases over the southern portion of the escarpment and Northern Namibia are consistent for Ibissta and P1-P5. Decreases over the Southern Kalahari are also evident for Ibissta, but P1, P3 and P5 all indicate increases.

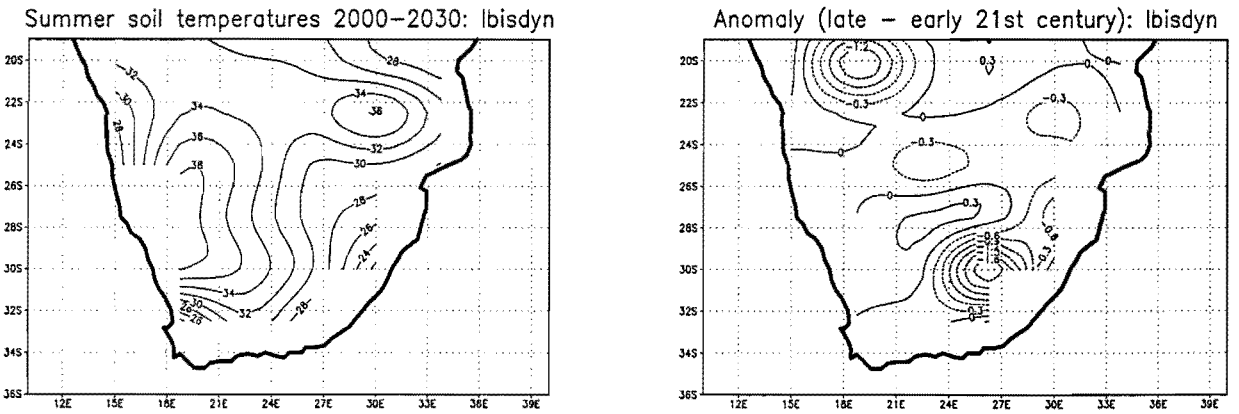

Figure 6.5 Summer soil temperatures (°C) for period 1 and the anomaly for Ibisdyn

6.2.5 Soil moisture

Soil moisture in period 1 is highest to the east (fraction of 0.55) and NE (0.6), and lowest over the central interior of South Africa (0.15) in Ibisdyn (figure 6.6) and P1-P5. Ibissta is similar, but soil moisture is higher over the central interior of South Africa (0.25).

Soil moisture in period 2 for Ibisdyn shows minimal and somewhat indiscernible increases over the southern portion of SE South Africa on the escarpment (0.004) and decreases over the northern portion (0.004), and increases over northern Namibia (0.008). The increases over the southern escarpment are apparent in Ibissta and the increases over northern Namibia are apparent in Ibissta, P1, P3 and P5. P2 and P4 both show slightly more discernible decreases over the Mozambiquan plains (0.016 and 0.012 respectively) and increases over northern Botswana (0.008).

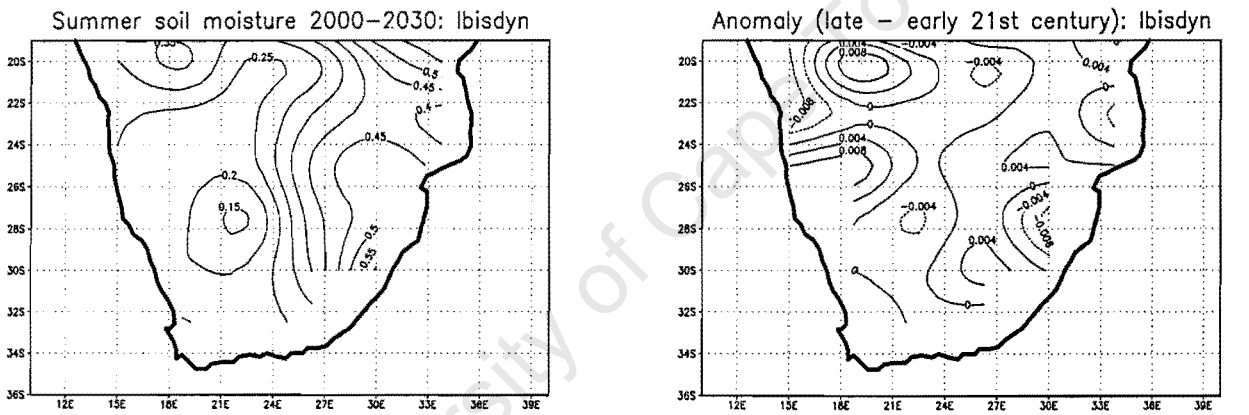

Figure 6.6 Summer soil moisture (fraction) for period 1 and the anomaly for Ibisdyn

6.2.6 Latent heat fluxes

Period 1's latent heat fluxes in Ibisdyn (figure 6.7) are highest to the north (110 W m^{-2}), decreasing southwards and westwards (to 10 W m^{-2}). Fluxes for Ibissta, P3 and P4 are almost identical, while those of P1, P2 and P5 are similar in pattern, but with slightly higher values (120 W m^{-2}) in the NE.

Latent heat flux in period 2 for Ibisdyn shows an increase in latent heat fluxes over Northern Namibia (14 W m^{-2}), the Southern Kalahari (6 W m^{-2}) and the southern and northern portions of SE South Africa on the escarpment (10 W m^{-2} and 2 W m^{-2} respectively). This translates to percentage changes of approximately 10%. These increases in latent heat fluxes are associated

with stronger surface heating and convection (through the increased temperature over the 21st century), promoting evaporation. There are decreases over central northern South Africa (6 W m^{-2}). In Ibissta the anomalies are in largely the same regions. P1, P3 and P5 all indicate an increase in Northern Namibia (4 W m^{-2}), the southern portion of the escarpment (6 W m^{-2}) and central northern South Africa (4 W m^{-2}). There are decreases over the Southern Kalahari (8 W m^{-2}), the northern portion of the escarpment (4 W m^{-2}) and in some other regions. P2 and P4 have responses in regions other than the 5 regions previously considered, except in the case of the Mozambiquan plains (2 W m^{-2} increase), and the responses from period 1 to period 2 are dissimilar to the other scenarios.

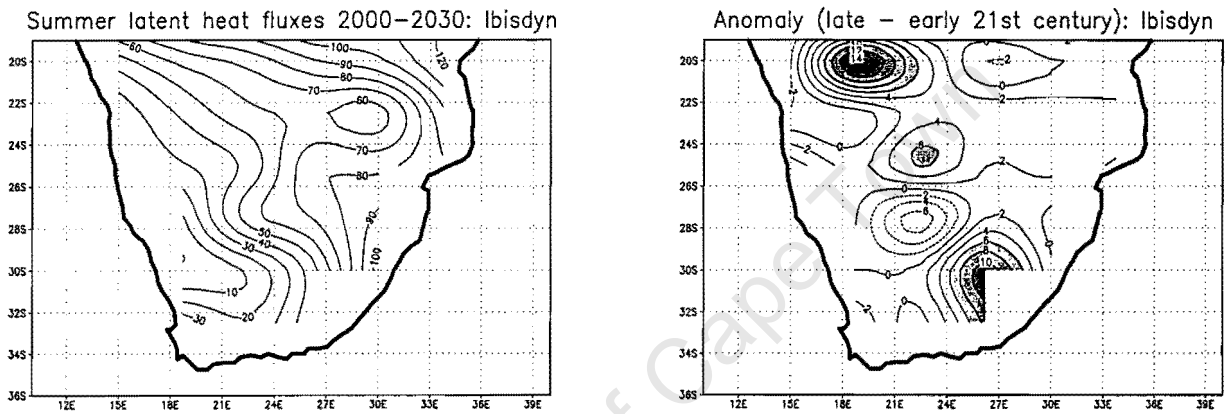

Figure 6.7 Summer latent heat fluxes (W m^{-2}) for period 1 and the anomaly for Ibisdyn

6.2.7 Leaf area index (upper and lower canopies)

Leaf area index of each plant functional type is calculated by dividing leaf carbon by specific leaf area (Foley *et al.*, 1996). In period 1 leaf area indices for the upper canopy in Ibisdyn (figure 6.8) exhibit high values over the SW, east and south coasts (5), and over the north (4). Very low values (less that 0.5) occur over the remainder of the domain. Patterns and indices in P1-P5 are comparable. However, Ibissta has a different pattern and values are much lower (there is a maximum over the east of 1.4) and decrease to the west (0.1).

From period 1 to period 2 in Ibisdyn, leaf area indices for the upper canopy have decreased over the northern portion of SE South Africa on the escarpment (0.7), to the south of the southern portion (1) and over the Mozambiquan plains (0.8). Ibissta shows little change. P1, P2 and P5 are in agreement with the decrease over the northern escarpment (between 0.3 and 0.6), while P3 and P4 both indicate an increase (0.3). The decrease to the south of the southern escarpment is

consistent for P1-P5 (decreases of between 0.4 and 1). The decrease over the Mozambiquan plains in Ibisdyn is reflected for P2 and P5.

Indices for the lower canopy in Ibisdyn (figure 6.9) are high over the north central South Africa (3.3), the escarpment region (2.4), Botswana/Zimbabwe border (2.7) and northern Namibia (3). P1-P5 are similar. However, Ibissta shows a very different pattern, with leaf area indices decreasing to the west (0.3) and highest to the south and east (2.4).

From period 1 to period 2 for Ibisdyn, there is an increase over the southern (0.9) and northern (1.8) portions of the escarpment, Mozambiquan plains (1.8) and Northern Namibia. The response for P1, P2 and P5 is similar. P3, P4 and Ibissta are in agreement with the increase in the southern portion of the escarpment and Northern Namibia. Leaf area indices for the lower canopy indicate an increase, while the upper canopy indices are decreasing.

The decrease in upper canopy leaf area indices and increase in lower canopy leaf area indices suggests a movement towards lower level vegetation cover with fewer trees and reduced amounts of tall vegetation through the 21st century.

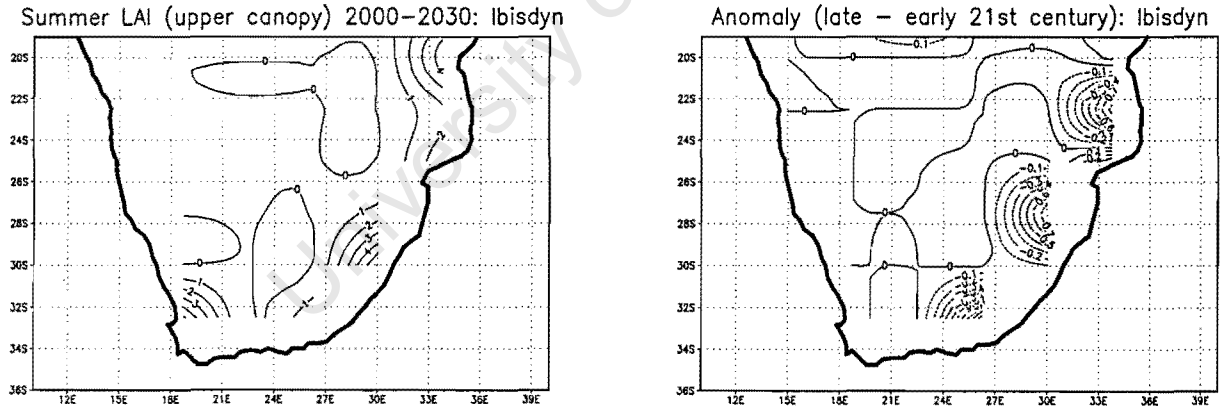

Figure 6.8 Summer LAI (upper canopy) for period 1 and the anomaly for Ibisdyn

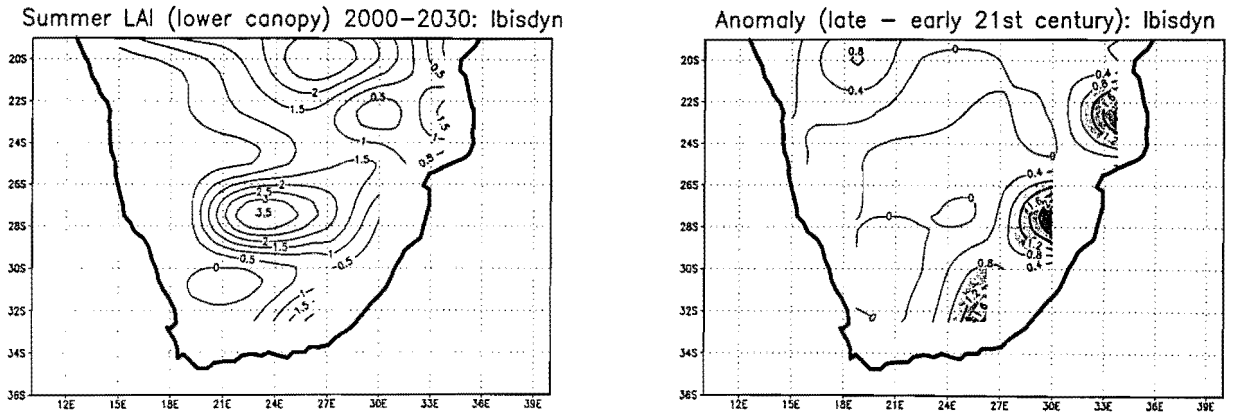

Figure 6.9 Summer LAI (lower canopy) for period 1 and the anomaly for Ibisdyn

6.3 Winter seasonal differences between the early and late 21st century

The winter seasonal differences in key variables are less pronounced than summer, since winter is not the growing season (rainfall is generally at a minimum) over the majority of southern Africa. The change direction (increase or decrease) of the variables considered is generally less marked. Figures for the dynamic vegetation mean simulation are included in the text below, while figures for the static vegetation mean simulation and P1-P5 may be found in Appendix E.

6.3.1 Net primary productivity

In period 1 in Ibisdyn (figure 6.10), Ibissta and P1-P5, NPP indicates the highest productivity over the Western Cape (0.08 kg m^{-2} $month^{-1}$) and the southern coast, both of which fall in the winter rainfall regime, and over the east coast. The remainder of the domain has low or sub-zero productivity since it is not the growing season and rainfall is at its minimum.

In period 2 for all scenarios there is generally little change in winter productivity over the summer rainfall regions, with isolated regions of increase. Over the Western Cape there is a small increase in productivity in Ibisdyn (0.002 kg m^{-2} $month^{-1}$), P1 and P3, but negligible change in P2, P4, P5 and Ibissta.

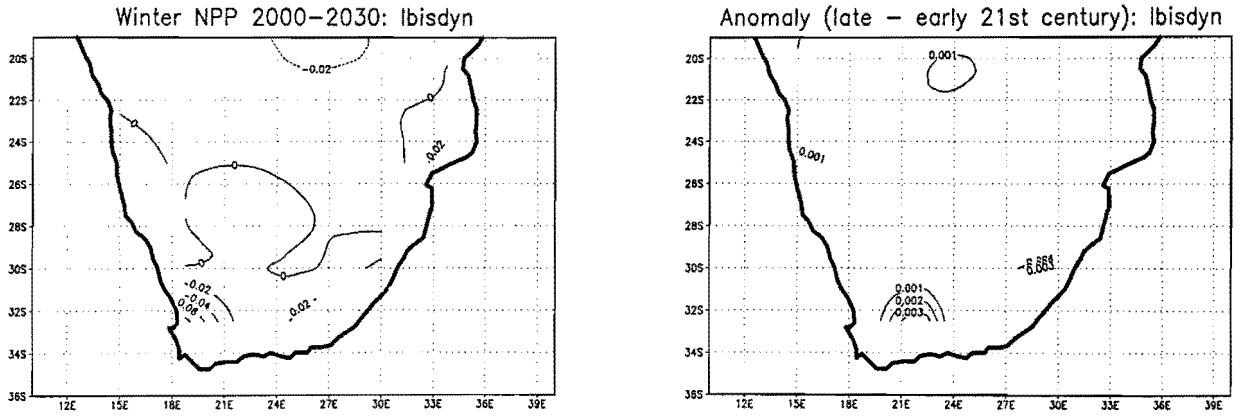

Figure 6.10 Winter net primary productivity (kg m^{-2} $month^{-1}$) for period 1 and the anomaly for Ibisdyn

6.3.2 Average evapotranspiration

In Ibisdyn (figure 6.11), average evapotranspiration in period 1 is highest over the SW (1.2 mm day^{-1}), south (0.8 mm day^{-1}) and east coasts (1.2 mm day^{-1}) and lowest over the interior and west coast regions (between 0 and 0.2 mm day^{-1}). Amounts and patterns are similar for the other scenarios.

From period 1 to period 2 in Ibisdyn, average evapotranspiration has increased over the SE of South Africa on the escarpment (0.04 – 0.06 mm day^{-1}) and Northern Namibia (0.02 mm day^{-1}), but decreased over the southern Kalahari (0.02 mm day^{-1}). Increases over the southern portion of the escarpment are consistent for Ibissta, P1, P3 and P5. P1, P2, P3 and P5 show decreases in the northern portion of the escarpment. Decreases over the southern Kalahari in Ibisdyn are also reflected for P1, P2, P4 and P5. P1, P3 and P5 show decreases over the Mozambiquan plains, while in Ibisdyn and Ibissta there are decreases just south of this region. P2 and P4 both indicate increases in evapotranspiration over northern central South Africa.

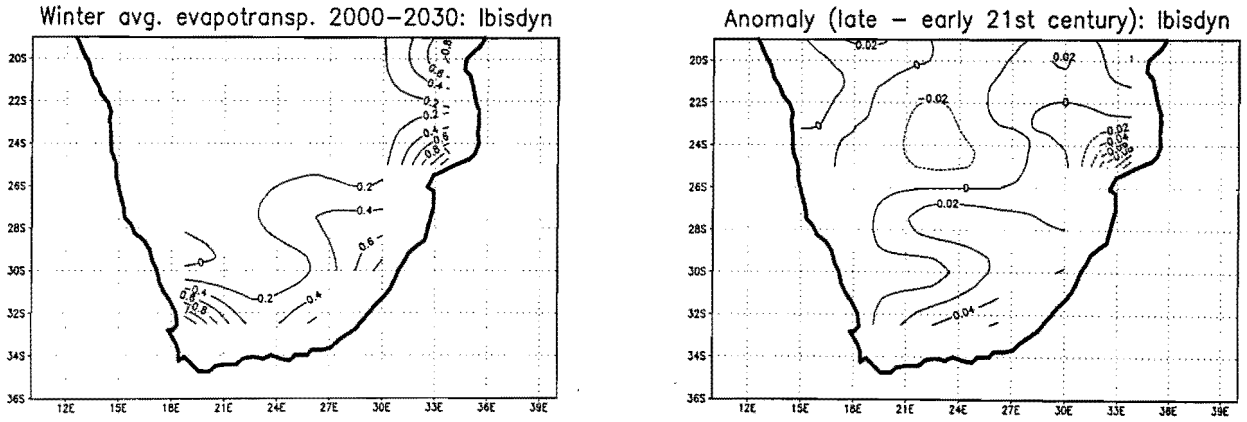

Figure 6.11 Winter average evapotranspiration (mm day^{-1}) for period 1 and the anomaly for Ibisdyn

6.3.3 Sensible heat fluxes

Sensible heat fluxes in Ibisdyn (figure 6.12) during period 1 are lowest in the south (20 W m^{-2}) and increase further northwards (up to approximately 60 W m^{-2}). Fluxes for P1-P5 are similar. The fluxes for Ibissta are similar in the south, but are higher in the north (70 W m^{-2}).

In Ibisdyn, from period 1 to period 2, sensible heat fluxes have increased over the southern portion of SE South Africa on the escarpment (4 W.m^{-2}) and decreased over the northern portion of the escarpment (6 W m^{-2}). There are also increases over Northern Namibia (5 W m^{-2}) and the Southern Kalahari (1 W m^{-2}), and decreased over the Mozambiquan plains (4 W m^{-2}). Increases and decreases are generally of the order of 10%. Increases over the southern portion of the escarpment are also apparent for P1, P3, P4 and P5, while Ibissta shows the opposite response of a decrease. Decreases over the northern portion of the escarpment and increases over the Mozambiquan plains are consistent for P1, P2 and P5. Ibissta, in contrast, shows increases over the Mozambiquan plains. Sensible heat fluxes are consistent over Northern Namibia, where P1-P5 and Ibisdyn show increases. Ibissta shows little change.

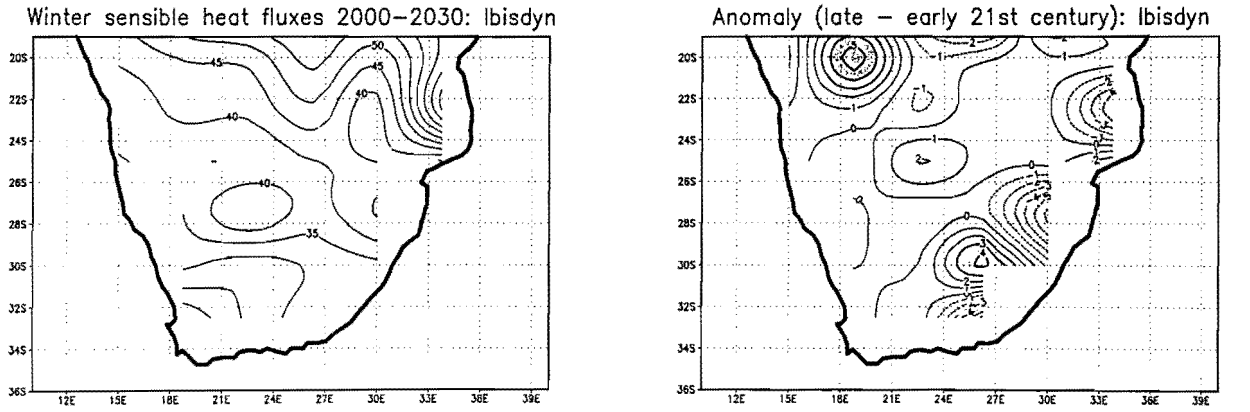

Figure 6.12 Winter sensible heat fluxes (W m^{-2}) for period 1 and the anomaly for Ibisdyn

6.3.4 Soil temperatures

Soil temperatures in all scenarios (see figure 6.13 for Ibisdyn) increase northwards from approximately 14°C to 26°C. Soil temperatures have decreased from period 1 to period 2 over the escarpment regions (0.3 – 0.8°C) and Northern Namibia (0.8°C), with responses in other regions as well. The decrease over the southern portion of the escarpment and over Northern Namibia is apparent in all scenarios.

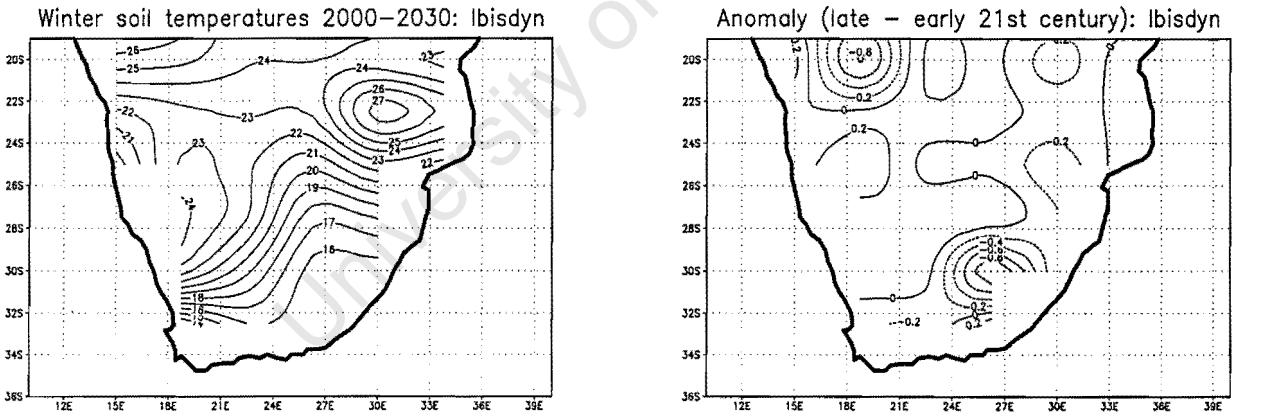

Figure 6.13 Winter soil temperatures (°C) for period 1 and the anomaly for Ibisdyn

6.3.5 Soil moisture

Soil moisture is highest over the SW Cape (fraction of 0.45) and the east coast (0.4 - 0.45), and lowest over the central interior of South Africa (0.15) in Ibisdyn (figure 6.14) and P1-P5. Soil moisture in Ibissta is not as low over the central interior (0.24).

From period 1 to period 2 in Ibisdyn, there is no notable change over the 5 regions identified in Chapter 5, but a slight increase over the Western Cape (0.004). Ibissta shows more notable changes over the southern portion of the escarpment (0.005 increase), Southern Kalahari (0.005 increase) and Northern Namibia (0.02 decrease). P1, P2 and P5 show decreases over the northern portion of the escarpment. Other changes are not consistent and there are some minor changes in adjacent regions, such as south of the southern escarpment in P4.

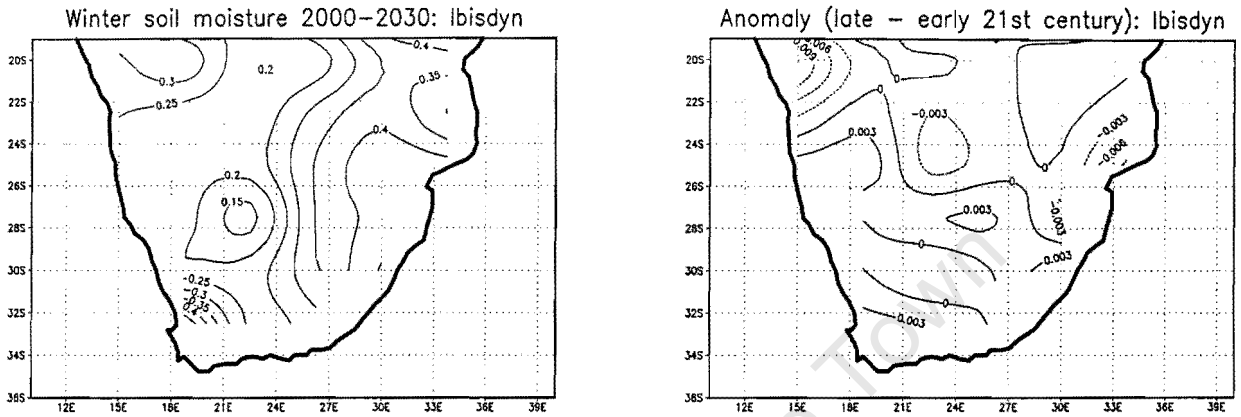

Figure 6.14 Winter soil moisture (fraction) for period 1 and the anomaly for Ibisdyn

6.3.6 Latent heat fluxes

Latent heat fluxes in Ibisdyn (figure 6.15) are highest along the SW, south and east coasts (approximately 40 W m^{-2}), decreasing inland and westwards (to between 0 and 5 W m^{-2}). Fluxes for Ibissta and P1-P5 are similar.

From period 1 to period 2 in Ibisdyn, there is an increase in latent heat fluxes over Northern Namibia (0.5 W.m^{-2}) and the southern (1 W m^{-2}) and northern (0.5 W m^{-2}) portions of SE South Africa on the escarpment. There are latent heat flux decreases over the Southern Kalahari (0.5 W m^{-2}) and changes south of the Mozambiquan plains regions (3.5 W m^{-2}). Ibissta exhibits an increase over the southern portion of the escarpment (1 W m^{-2}), and a decrease to the south of the Mozambiquan plains (4 W m^{-2}), with little change elsewhere. P1, P3 and P5 are in agreement with the increase over the southern escarpment (1 W m^{-2}) and exhibit decreases over the northern escarpment (of between 1 and 2 W m^{-2}) and Mozambiquan plains (1 W m^{-2}). P1 shows a decrease over the Southern Kalahari (0.5 W m^{-2}). Changes in P2 and P4 are dissimilar to the other scenarios, although there is a distinct decrease over the Southern Kalahari (1 W m^{-2}).

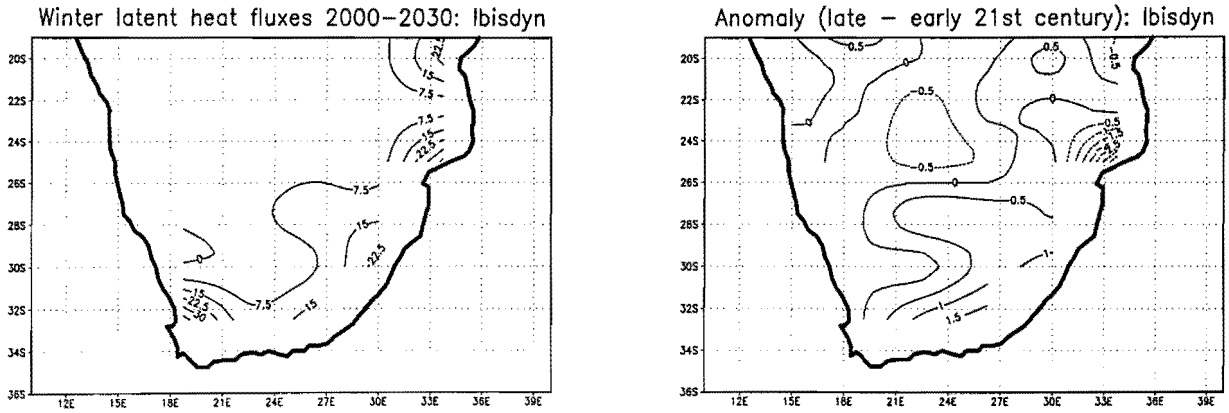

Figure 6.15 Winter latent heat fluxes (W m^{-2}) for period 1 and the anomaly for Ibisdyn

6.3.7 Leaf area index (upper and lower canopies)

Leaf area indices in period 1 for the upper canopy in Ibisdyn (figure 6.16) reflect high values over the SW, east and south coasts (approximately 5) and over the north (1.5), with very low values (less than 0.5) elsewhere. P1-P5 have similar values and patterns.

From period 1 to period 2 Ibisdyn exhibits a decrease in leaf area indices in the upper canopy in the northern portion of SE South Africa on the escarpment (0.6), the Mozambiquan plains (0.8) and south of the southern escarpment (1). P1, P2 and P5 show responses over the same region and in the same direction. P3 and P4 do not present any notable response except south of the southern escarpment (-1). Ibissta shows almost no change.

Lower canopy indices in Ibisdyn (figure 6.17) are high over the north central South Africa (3.3) and northern Namibia (0.9). Values over the SE coast and Mozambiquan plains are between 1.5 and 1.8. Values of 1.8 are also present over the Botswana/Zimbabwe border. P1, P2 and P5 have a similar pattern, while P3 and P4 do not reflect the high values over the Mozambiquan plains. The pattern for Ibissta is different, with the highest indices in the south and east of South Africa, decreasing northwards (from 3 to 0.9), but with high indices over Botswana/Zimbabwe (2.1).

In period 2 in Ibisdyn, there is an increase over the southern escarpment (0.8), northern escarpment (1), Mozambiquan plains (2) and Northern Namibia (0.4). The increase over the southern escarpment and Northern Namibia is reflected in P1-P5. P1, P2 and P5 show an increase over the Mozambiquan plains as well. Ibissta shows little change (generally index increases of less than 0.1 are apparent).

There is a general trend for a decrease in upper canopy leaf area indices and in increase in lower canopy leaf area indices from the early to late 21st century, implying a shift towards vegetation with fewer trees and a reduced amount of tall vegetation.

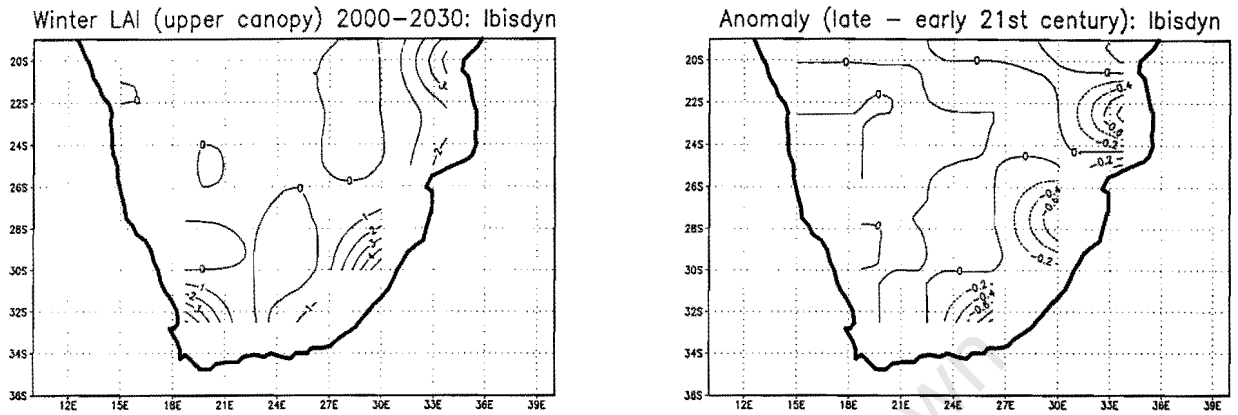

Figure 6.16 Winter LAI (upper canopy) for period 1 and the anomaly for Ibisdyn

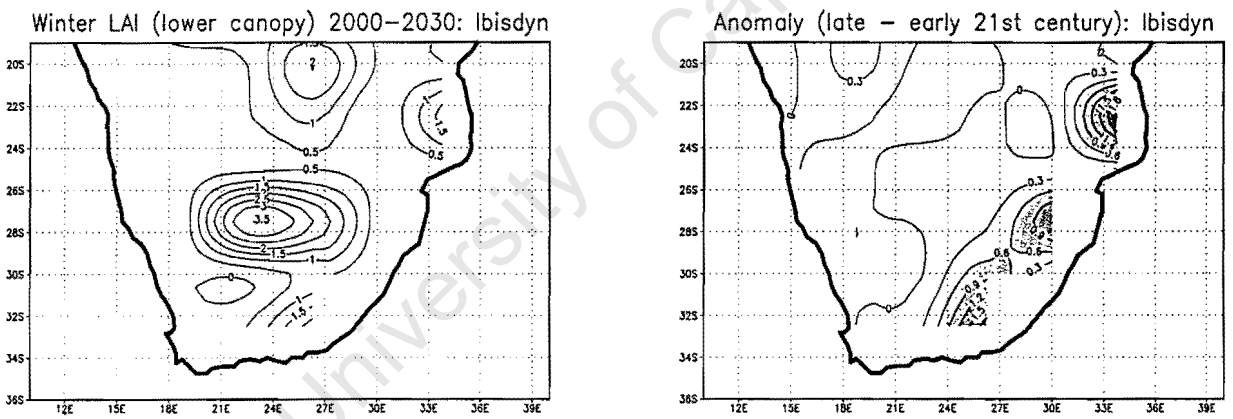

Figure 6.17 Winter LAI (lower canopy) for period 1 and the anomaly for Ibisdyn

6.4 Seasonal and monthly scale trends in IBIS output data

6.4.1 Introduction

Up to this point, analyses have been concerned with a coarse temporal resolution. The section to follow expands on this by considering a higher temporal resolution (i.e. the monthly scale). Sub-seasonal timescales need to be considered in the context of the transition seasons in addition to the conventional summer and winter months of DJF and JJA, since transition seasons may be playing an important role in determining the response and response differences between the different scenarios. In order for examine the important role of the transition seasons, a Principal Components Analysis (PCA) is performed, since it is a favourable means of identifying commonalities in data sets. PCA is beneficial as a linear dimensionality reduction technique and it is also used to identify structure within data. In addition, the PCA allows for a multivariate analysis at a high temporal resolution over the full domain, and can therefore be an effective means of distinguishing detailed commonalities in response. A PCA is therefore a useful tool in this research, since it presents the possibility of distinguishing inter- and intra- scenario response variations over the domain.

The PCA analyses performed here, employ the biosphere model output variables examined in sections 6.1 and 6.2 (*viz.*, average evapotranspiration, leaf area index (upper and lower canopies), latent heat fluxes, net primary productivity, sensible heat fluxes, soil temperature and soil moisture) as well as the IBIS simulated precipitation and relative humidity (determined from the daily derived data, which are averaged into monthly values). Three scenarios, Ibisdyn, P1 and P4, are considered. Ibisdyn has mean temperature, precipitation and relative humidity atmospheric input forcing. In P1, the atmospheric input forcing includes a positive standard deviation from the mean temperature and precipitation, and a negative standard deviation from the mean relative humidity. P4's atmospheric forcing includes a negative standard deviation from the mean temperature and precipitation and a positive standard deviation from the mean relative humidity. P1 and P4 therefore represent input forcing scenario extremes and in terms of annual and seasonal output, the responses of P1 and P4 tend to be most dissimilar. Hence, an examination of Ibisdyn, P1 and P4 reasonably encompasses the range of scenario responses.

6.4.2 Principal Components Analysis Methods

Monthly data from each of these biosphere model output variables over each grid point for the early (2000-2030) and late (2050-2080) 21st century are averaged for each month, and the anomaly calculated for each month of the year over each grid point and for each variable. The anomaly data are then standardized for each variable. The standardized data sets are combined into a matrix where the columns are the grid points (of which there are 29 for the southern African domain south of 20°S) and the rows are the monthly anomaly signals for each of the biosphere output variables. Separate matrices are produced for Ibisdyn, P1 and P4. A schematic diagram showing the structure of the Principal Components Analysis (PCA) matrix is presented in figure 6.18.

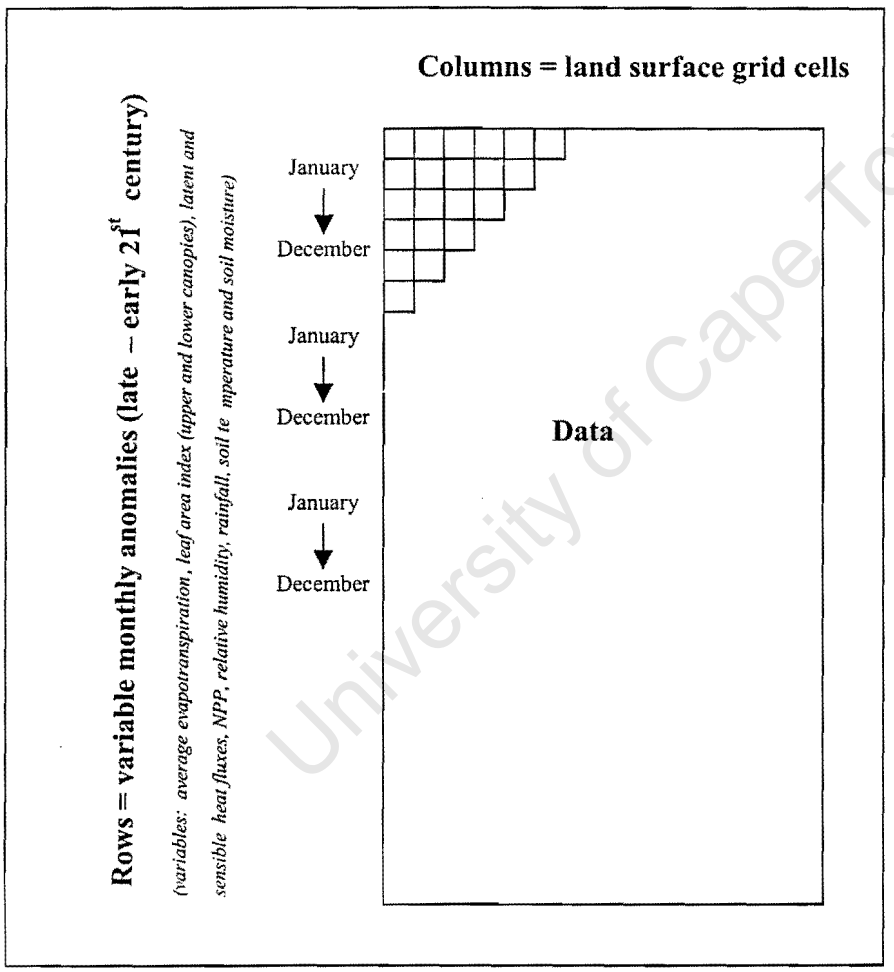

Figure 6.18 Structure of PCA matrix

A separate PCA is performed on each of the scenarios. Principal component (PC) loadings are rotated using varimax rotation (i.e. variances of the squared raw PC loadings across the variables for each PC are maximised) to better fit the data (Richman, 1986). It is common for all components having eigenvectors greater than 1.0 to be retained for rotation, since those

components with values less than 1.0 are accounting for less of the total variance of any one variable (Kaiser in Pocock and Wishart (1969)). This often leads to too many components usefully being retained for rotation. An additional or alternative method for determining the number of PCs to be retained for rotation is the graphical method of the scree plot (Catell, 1966; Jackson, 1991). In this instance, PCs retained are determined from the break of slope of the scree plot of the eigenvalues. In the case of Ibisdyn and P1, 3 PCs are retained, while in the case of P4, 2 PCs are retained, this being based on the scree test (Figures 6.19 a) – c)). Total percentage variance of the retained components and variance of each rotated PC for the 3 model simulations are displayed in table 6.1

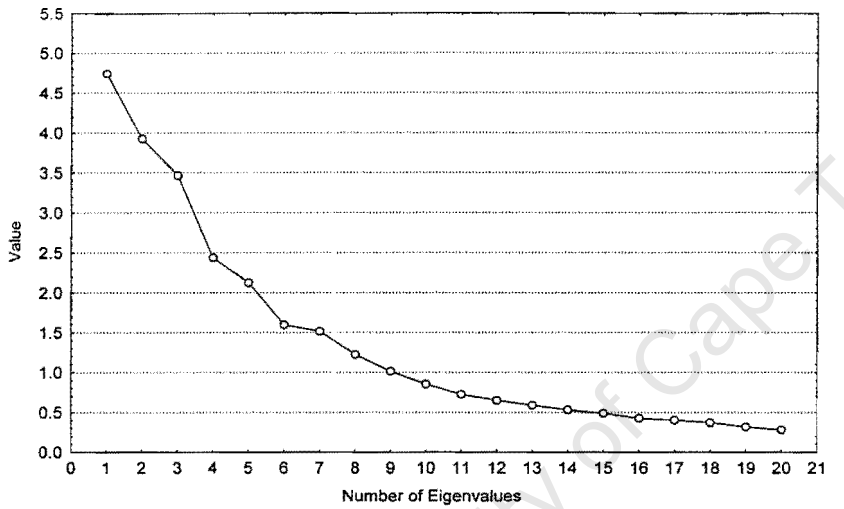

Figure 6.19a) Plot of eigenvalues for Ibisdyn

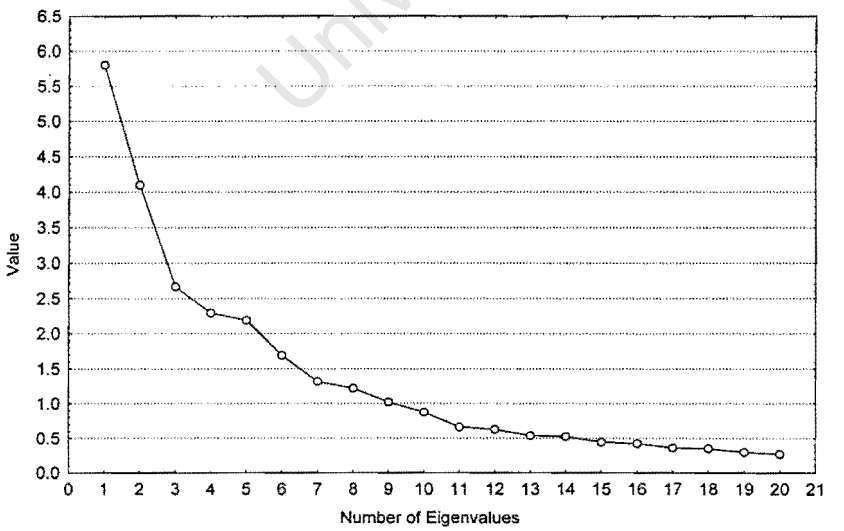

Figure 6.19b) Plot of eigenvalues for P1

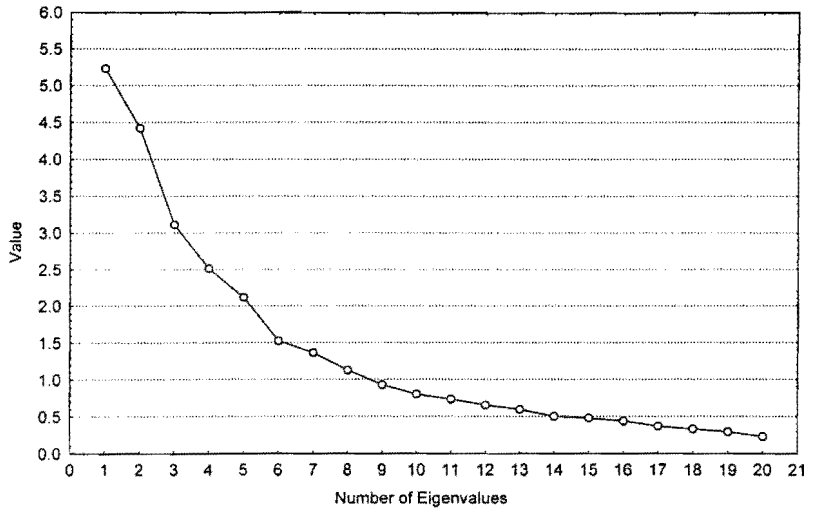

Figure 6.19c) Plot of eigenvalues for P4

Model Simulation	Explained variance of rotated principal components (%)			Total explained variance (%)
	PC 1	PC 2	PC 3	
Ibisdyn	14.96	14.12	12.74	41.82
P1	16.44	15.21	11.68	43.33
P4	17.99	15.29	N/A	33.28

Table 6.1 Percentage variance of each rotated principal component retained

6.4.3 Principal component loading results

Figures 6.20a) – c) are plots of the rotated PC loadings for each of the 3 scenarios. Significant grid cells (which are shaded in the figures) are determined as grid cells with a PC loading of 0.6 or higher (or –0.6 or lower). This translates into the particular PC accounting for at least a third of the grid cell variance. The significant loadings are examined in the context of the vegetation types and tendencies represented in these grid cells for periods 1 and 2. Figures 6.21a) – c) present a summary of the IBIS model simulation vegetation categories (for each scenario's rotated PC loadings) represented in the early and late 21st century for each significant grid cell. Note that each PC loading on the vegetation category maps is represented by a different greyscale shade. PC 1 is shaded the darkest, PC 2 a lighter shade and PC 3 (not applicable for P4) is not shaded. The black dot in the right hand corner of some grid cells indicates those grid cells where the component loadings are negative in sign (a negative component loading implies

an opposite response direction to a positive sign). Vegetation categories in the figures are indicated in the order of frequency of representation. For example, "Open shrubland/Desert/Grassland" should be interpreted as there being a mix of vegetation with Open shrubland occurring most often, followed by Desert and then Grassland.

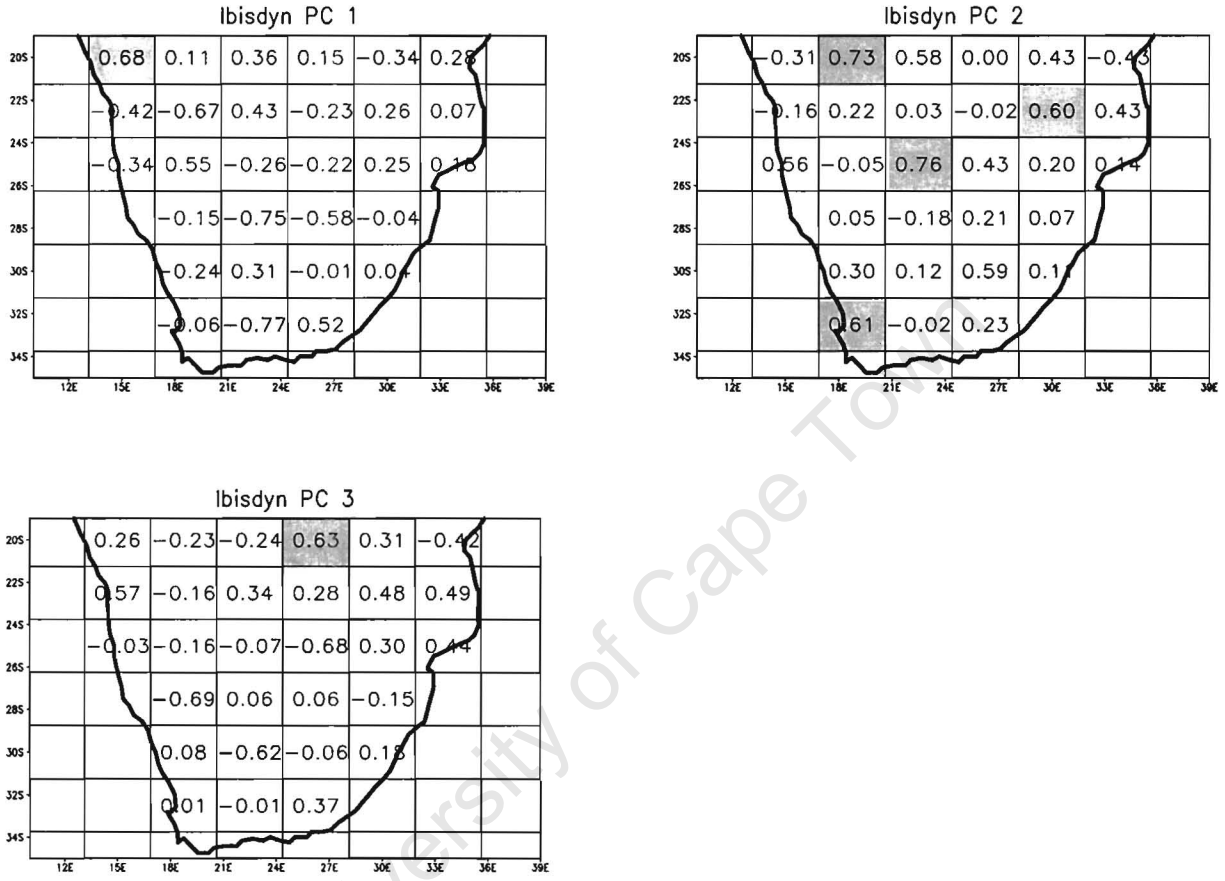

Figure 6.20a) Rotated principal component loadings for Ibisdyn

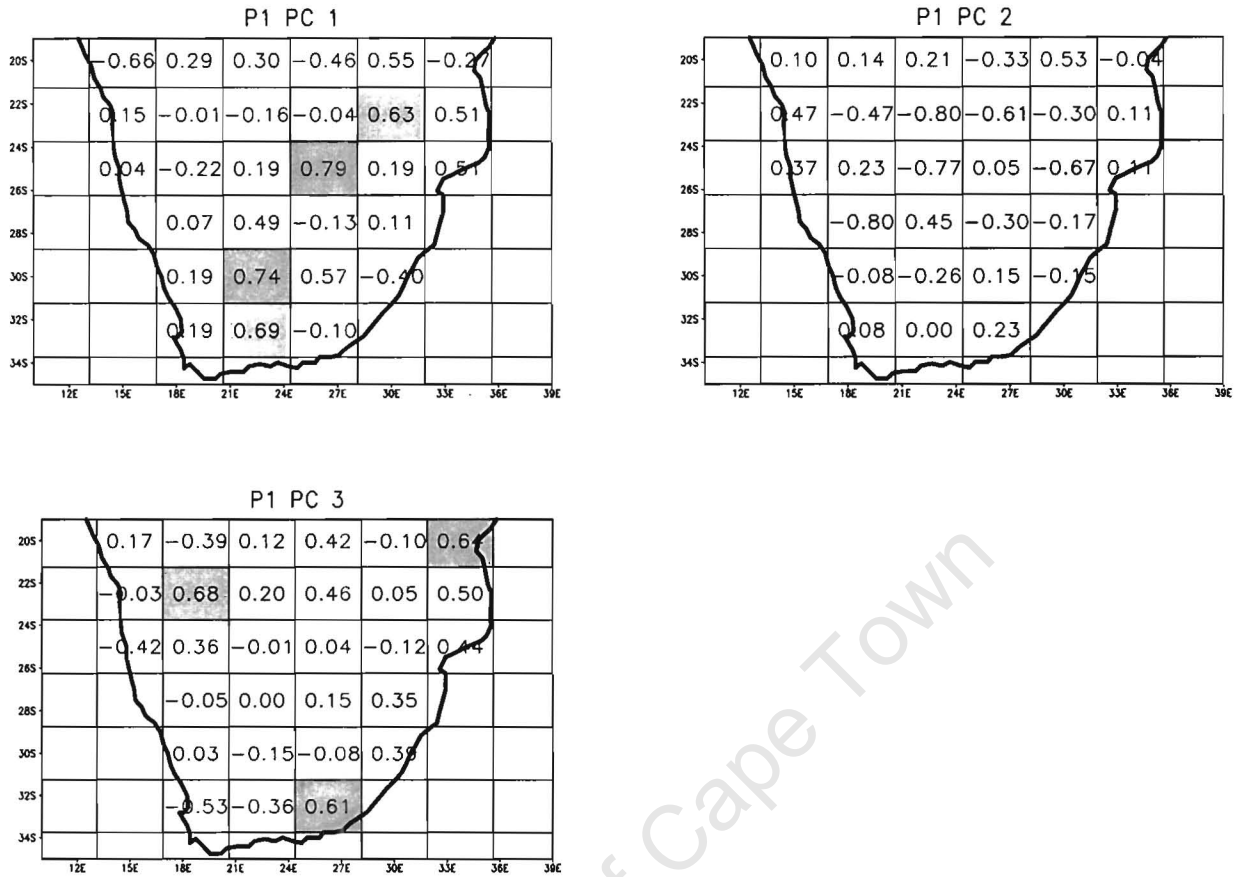

Figure 6.20b) Rotated principal component loadings for P1

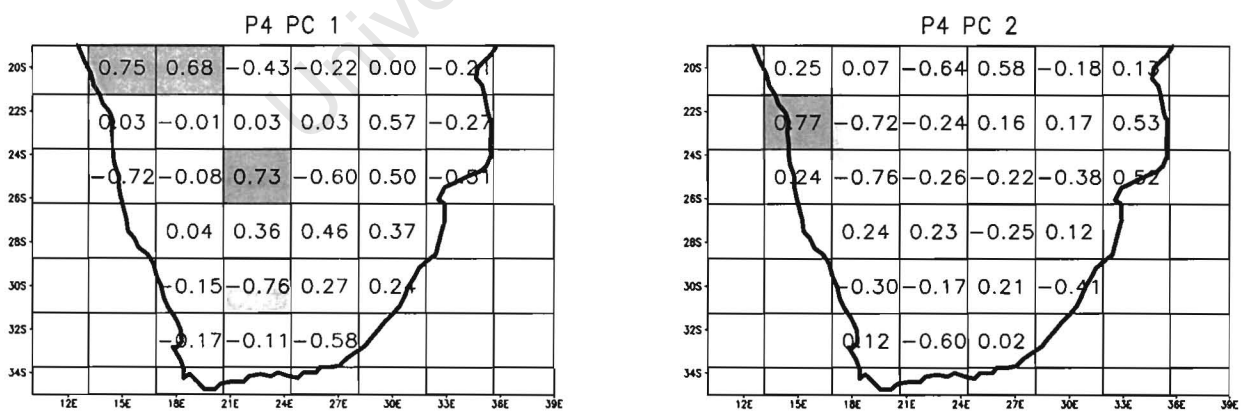

Figure 6.20c) Rotated principal component loadings for P4

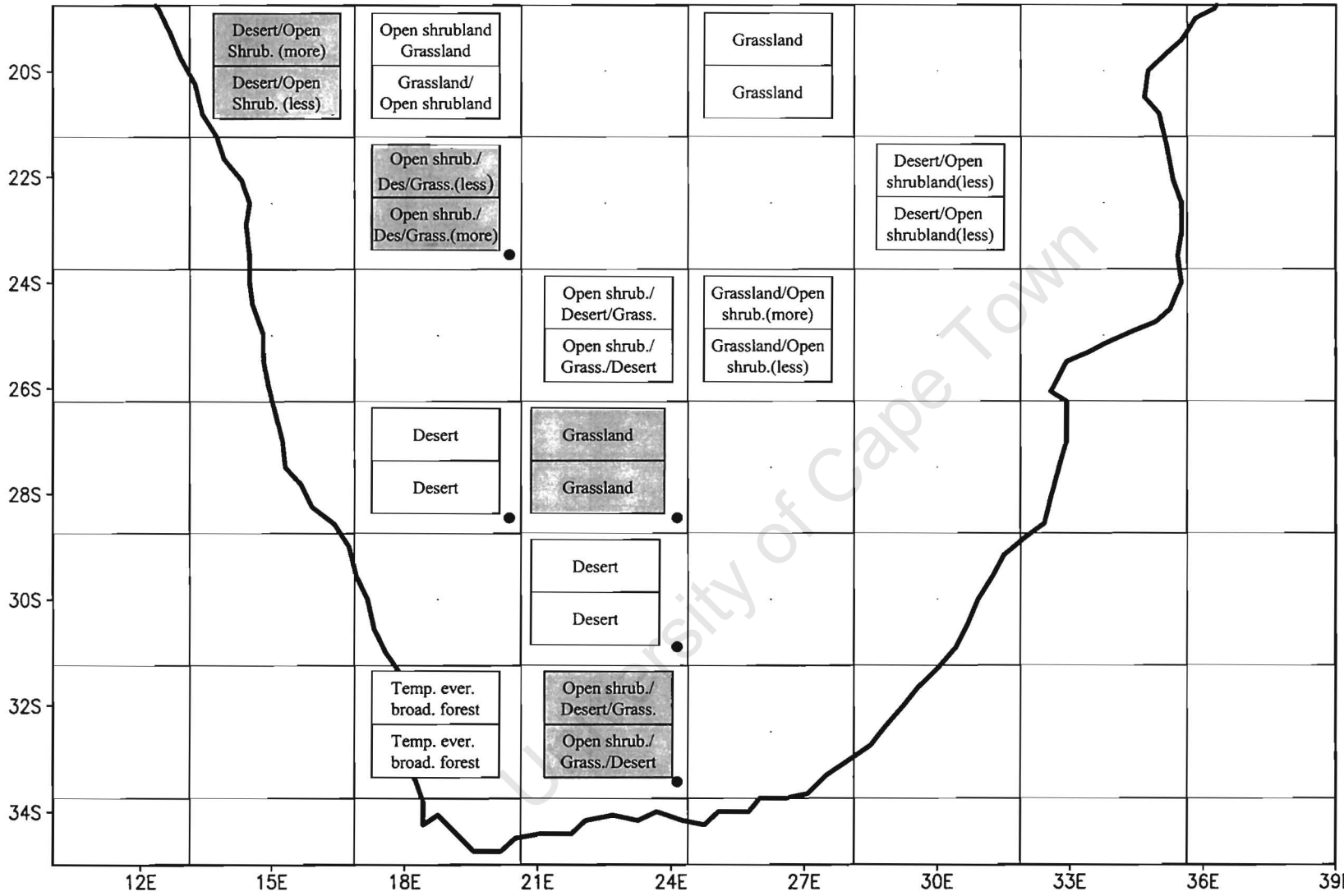

Figure 6.21a) Ibisdyn vegetation categories for each PC for period 1 and period 2. Note: PC 1 is shaded darkest, PC 2 a lighter shade and PC 3 is unshaded. Black dots represent component loadings with a negative sign. The upper box in a grid is period 1 and the lower box is period 2.

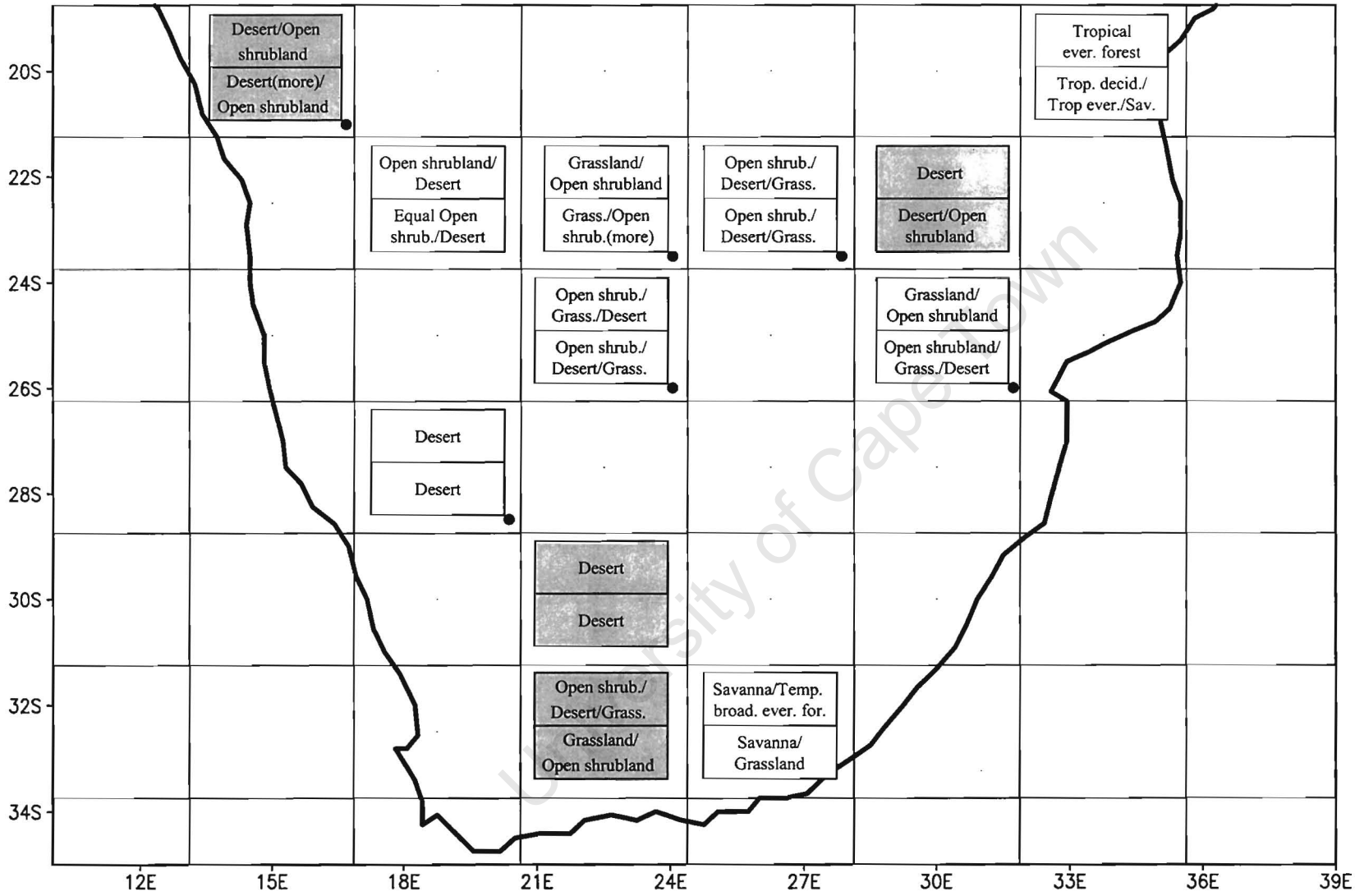

Figure 6.21b) P1 vegetation categories for each PC for period 1 and period 2.

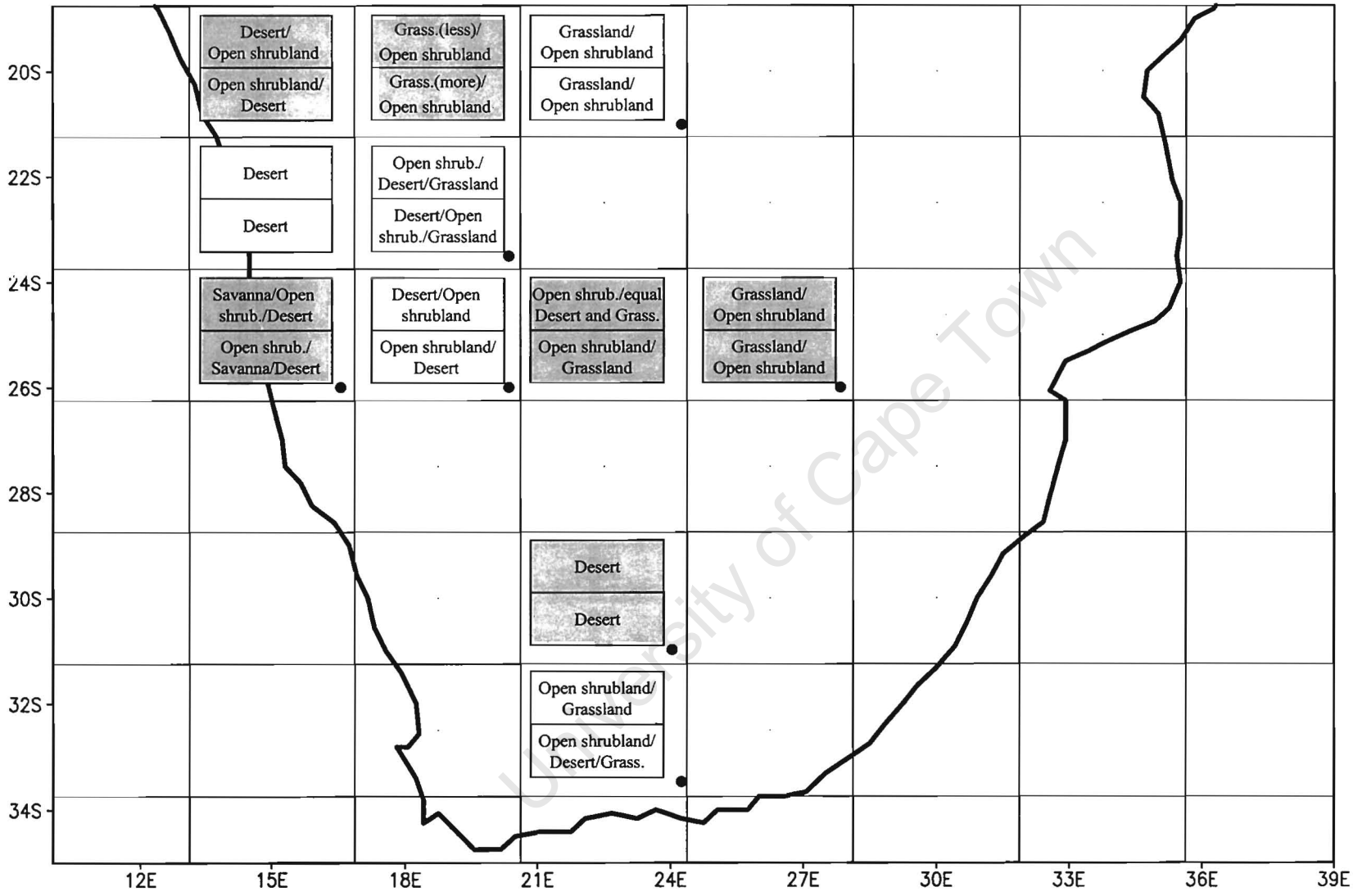

Figure 6.21c) P4 vegetation categories for each PC for period 1 and period 2.

In Ibisdyn, negative loadings of PC 1 (all but one significant loadings are negative) and positive loadings of PC 2 indicate a move away from dryland vegetation or no discernible vegetation class change, from the early to late 21st century. The positive loading of PC 1 indicates a tendency towards dryland vegetation. PC 3 shows no significant vegetation category change for either the positive or negative component loadings, with vegetation largely remaining constant.

P1 shows a distinction between a more dryland and less dryland vegetation category tendency for negative loadings of PC 2 (all significant loadings are negative) and positive loadings (all but one are positive) of PC 1 respectively. The negative loading of PC 1 indicates a move towards dryland vegetation, as is the case in negative loadings of PC 2. PC 3 also indicates a move towards more dryland vegetation categories.

In P4, there is a distinction between a general move away from more dryland vegetation categories (in the case of positive loadings of PC 1) and a general move towards more dryland vegetation categories (in the case of negative loadings of PC 2). Negative loadings of PC 1 (half the significant loadings are negative) show a tendency towards dryland vegetation.

It is therefore evident that in the case of P1 and P4 there is a distinction in the component loadings between more and less productive vegetation categories, with a tendency for a movement towards or away from dryland vegetation. Thus, principal component loadings in P1 and P4 do not necessarily represent a vegetation type/category distinction, but rather a spatial change of vegetation. Further distinctions between the different loadings for the 3 scenarios, can be made by examining the component scores from the PCA in the following section.

6.4.4 Principal component scores results

The PC scores from the PCA are a representation of the anomaly (period 2 minus period 1) seasonal cycle signal, for each PC, of the biosphere variables (see Jackson, 1991). The seasonal cycle (i.e. the scores) of each of the variables for the 3 scenarios (Ibisdyn, P1 and P4) and the different rotated PC loadings are compared, in order to establish whether the scores identify any pattern or seasonal cycle signal changes between periods 1 and 2.

6.4.4.1 Ibisdyn

It is evident from the previous section, that negative loadings of PC 1 (all but one significant loadings are negative loadings) and positive loadings of PC 2 (all loadings are positive) are both indicative of a movement away from dryland vegetation (or no discernible change). Therefore, since Ibisdyn indicates an increase in productivity for both the negative loadings of PC 1 and the positive loadings of PC 2, it cannot simply be productivity that is distinguishing PC 1 from PC 2. It may be the timing of the increase or decrease in productivity that is important. Table 6.2 presents a summary of months showing a component score increase for each variable for the 3 component loadings. Plots of key moisture (average evapotranspiration and soil moisture) and productivity (Net Primary Productivity) variables for each component are presented in figures 6.22a) – c). Note that since PC 1 loadings are (for the most part) negative, score anomalies that are *negative* in sign indicate an *increase*.

In examining the scores of PC 1, there is a clear increase in all variables except sensible heat fluxes and soil temperature (which show a decrease), from approximately February to July/August. March and April show the greatest increase. In PC 2 the anomaly increase for the same variables is from approximately December to April, but with a decrease over this time in the case of sensible heat fluxes and soil temperatures. It is therefore clear that the transition seasons are demonstrating some important changes and that the timing of increases over the 21st century partially distinguishes and differentiates PC 1 from PC 2. PC 3 shows an increase generally in January, April to June, September and October, but with some variations.

IBISDYN (dynamic vegetation mean run)	PC 1 (negative loadings)	PC 2 (positive loadings)	PC 3 (positive loadings)
	Description: Depicts a movement away from dryland vegetation. Greatest productivity and moisture increases in March and April	*Description: Depicts a movement away from dryland vegetation. Increases in productivity and moisture from December to April.*	*Description: Depicts vegetation with little change through the 21st century. Greatest increases in productivity in January, April and May.*
Average evapotranspiration	February → July	December → April	January, April → July, September, October
Leaf area index (lower canopy)	February → July	January → May	April → October
Leaf area index (upper canopy)	March, May, June, October → December	December → May, October	January → March, June → August, October, November
Latent heat fluxes	February → July	December → April	January, April → July, September, October
Net Primary Productivity	February → August	December → April	January, April → June, September, October
Rainfall	February → April, July	December → March	January, March → May, September, December
Relative humidity	February, March, June → August, October	November → February, August	March → May, August → October
Sensible heat fluxes	September → January	May → November	January, February, April → August
Soil temperature	September → January	May → November	February, March, November, December
Soil moisture	March → August	December → April	April → October

Table 6.2 Months showing a variable anomaly *increase* between the early and late 21st century, as represented by score anomalies for Ibisdyn (e.g. there is an increase, from the early to late 21st century, in average evapotranspiration between February and July.)

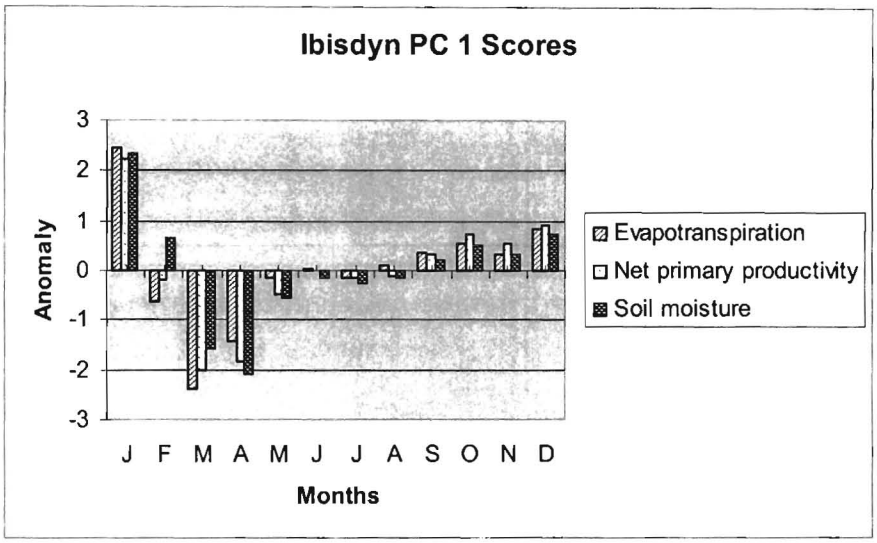

Figure 6.22a) PC 1 monthly score anomalies for Ibisdyn

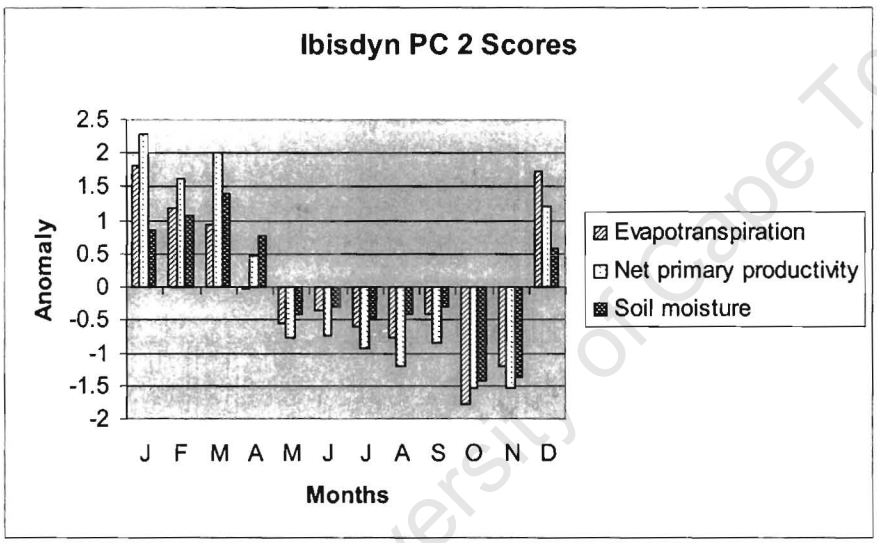

Figure 6.22b) PC 2 monthly score anomalies for Ibisdyn

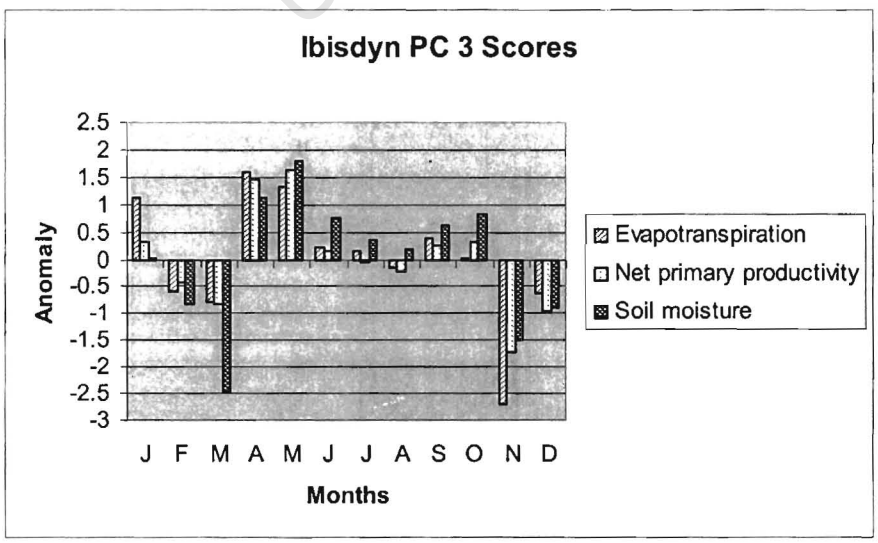

Figure 6.22c) PC 3 monthly score anomalies for Ibisdyn

6.4.4.2 P1

The previous section demonstrated the distinction of PC2 from PC1 being partially due to vegetation spatial change (towards dryland vegetation in the case of PC 2 and away from more dryland in the case of PC 1). However, the distinction between PC 2 and PC 3 cannot be explained in terms of vegetation spatial change, since PC 3 also shows a tendency towards dryland vegetation.

PC 1 for P1 (table 6.3) shows a general increase in most variables from the early to late 21st century for February, March, May, September and October (except in the case of sensible heat fluxes and soil temperatures where there are decreases) with some variations. Greatest increases in productivity and moisture are apparent in March (figure 6.23a)). Negative loadings of PC 2 (all significant loadings are negative) generally indicate an increase from April to September and December. April, May and June show the most significant increases (figure 6.23b)). Therefore, PC loadings 1 and 2 are distinguishing not only between a general overall increase and decrease in productivity but also between a difference in the timing of productivity increases and decreases. PC 3 indicates a general anomaly increase for February/March and September to December (which therefore further differentiates PC 3 from PC 2). There is largely an early summer season productivity and moisture increase (figure 6.23c)), but with a decrease in productivity on a sustained basis (i.e. at other times of the year).

P1 (dynamic vegetation run with standard deviation scenario 1)	PC 1 (positive loadings)	PC 2 (negative loadings)	PC 3 (positive loadings)
	Description: Depicts a movement away from dryland vegetation. Greatest productivity and moisture increases in March.	*Description: Depicts a movement towards dryland vegetation. Increases in productivity from April to September and December, increases in moisture from April to September.*	*Description: Depicts a movement towards dryland vegetation categories. Greatest increases in productivity and moisture in November and December.*
Average evapotranspiration	March, May, October	April → September, December	September → December
Leaf area index (lower canopy)	March → July	June → October	March, June → August, October → December
Leaf area index (upper canopy)	October → May	October → April, July	October → April
Latent heat fluxes	March, May, October	April → September, December	September → December
Net Primary Productivity	February → May	April → September, December	February, July, September → December
Rainfall	February, March, May, September	March → September, December	February, July, September → December
Relative humidity	February, March, May, December	March, May, June, August, October → December	February, September, November, December
Sensible heat fluxes	January, July, August, October → December	January → March, October, November	February, March, August, October → December
Soil temperature	January, February, June → December	January → March, November	January → August
Soil moisture	March → June, August, September	April → September	February, March, September → December

Table 6.3 Months showing a variable anomaly *increase* between the early and late 21st century, as represented by score anomalies for P1

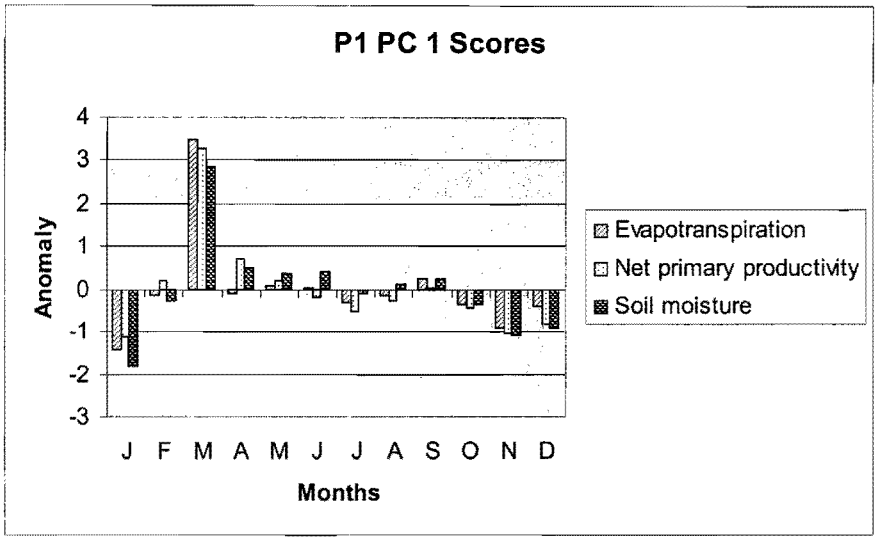

Figure 6.23a) PC1 monthly score anomalies for P1

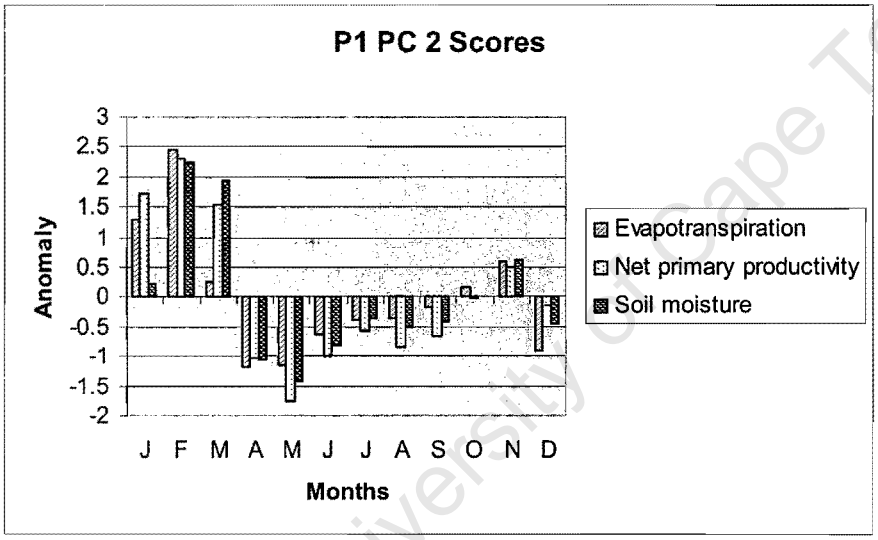

Figure 6.23b) PC 2 monthly score anomalies for P1

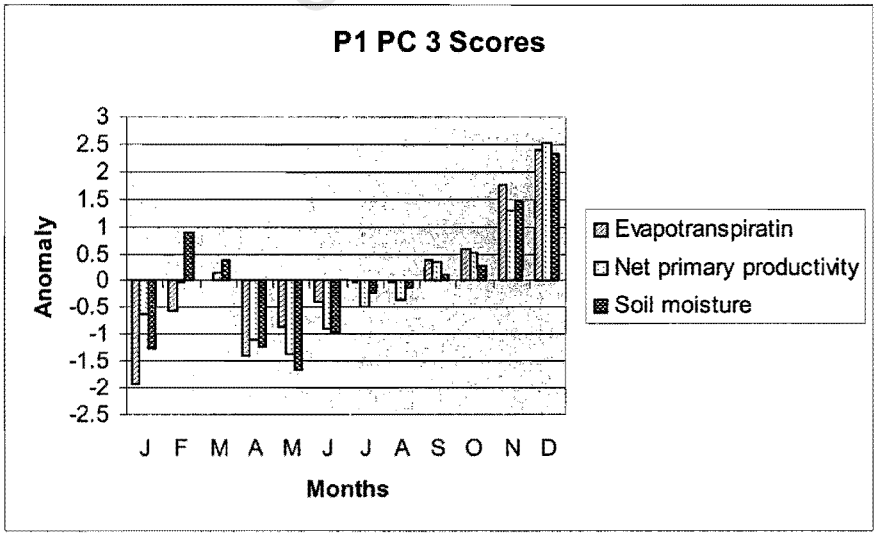

Figure 6.23c) PC 3 monthly score anomalies for P1

6.4.4.3 P4

It is evident from the previous section that vegetation spatial change partially distinguishes PC 1 from PC 2. Positive loadings of PC 1 show a movement away from dryland vegetation categories, while negative loadings of PC 2 show a movement towards dryland vegetation categories. However, approximately half of PC 1's loadings are negative and therefore other factors must distinguish the two principal components.

PC 1 in P4 (table 6.4) indicates the greatest increase of most variables from the early to late 21st century to be in March and April (figure 6.24a)). Negative loadings for PC 2 show an increase primarily from January to March (figure 6.24b)) and thus a general increase in mid to late summer seasonal productivity. However, there is a decrease in overall sustained productivity, evidenced by the decrease in productivity during other months of the year. Thus, the timing of increases is critical in terms of plant growth and productivity changes in P4 and is important in differentiating PC 1 from PC 2.

P4 (dynamic vegetation run with standard deviation scenario 4)	**PC 1 (positive loadings)**	**PC 2 (negative loadings)**
	Description: Depicts a movement away from dryland vegetation. Greatest increase in productivity and moisture in March and April.	*Description: Depicts a movement towards dryland vegetation. Greatest increase in productivity and moisture from January to March.*
Average evapotranspiration	March, April	January → March, July, August
Leaf area index (lower canopy)	February → July	January → April, November
Leaf area index (upper canopy)	February, March, May → September	February → May, September, October
Latent heat fluxes	March, April	February, July, August
Net Primary Productivity	March, April	February, March
Rainfall	February → April, December	February, July → September
Relative humidity	February → May, July, October, December	February, June, July, September
Sensible heat fluxes	January, May, June, August → December	April → June, August → November
Soil temperature	August → February	April → October
Soil moisture	March, April	February, March

Table 6.4 Months showing a variable anomaly *increase* between the early and late 21st century, as represented by score anomalies for P4

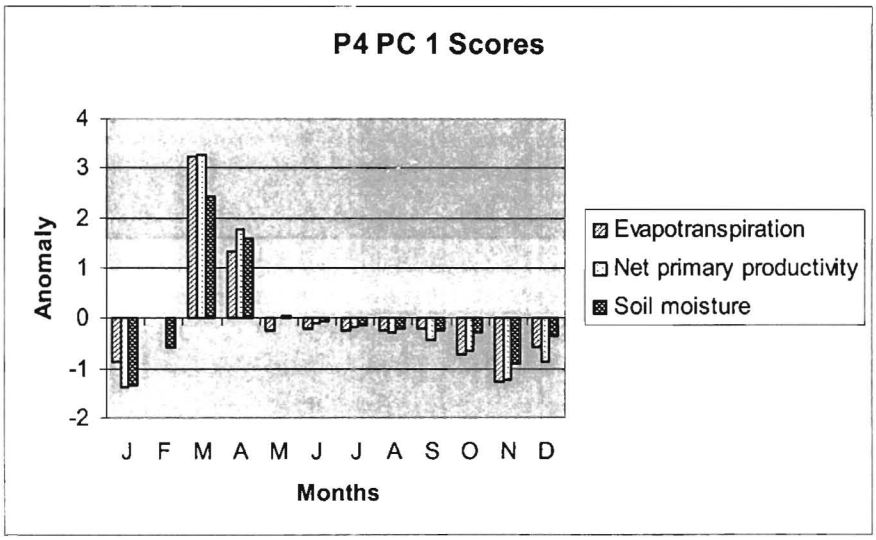

Figure 6.24a) PC 1 monthly score anomalies for P4

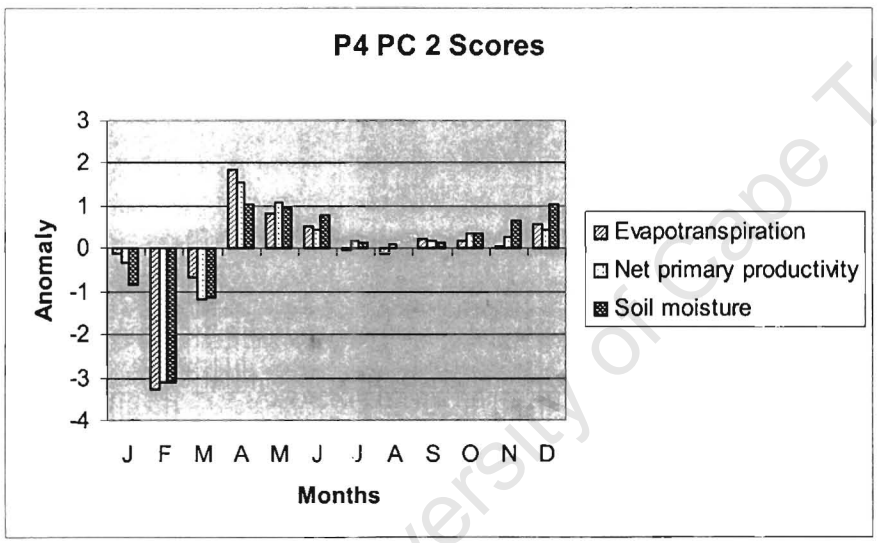

Figure 6.24b) PC 2 monthly score anomalies for P4

6.4.5 Synthesis

It is evident that the transition seasons over the southern African domain demonstrate some important changes and need to be considered in addition to the typically examined winter and summer seasons. The three scenarios presented here (Ibisdyn, P1 and P4) all show intra- and inter- scenario differentiation in terms of seasonal timing of changes in key IBIS model output variables (as represented by the principal component scores) and vegetation response.

As shown by the PCA, atmospheric changes in line with Ibisdyn show differentiation in terms of spatial change of vegetation, and seasonal timing of changes in key IBIS model output variables. PC 1 and PC 2 both indicate a spatial change away from dryland vegetation categories, but

increases in all variables considered (except sensible heat fluxes and soil temperatures, which show a decrease) are from approximately February to July in PC 1, and December to April in PC 2. Productivity increases in PC 2 therefore extend into the winter months and PC 1 into autumn, and demonstrate an extension of the growing season. PC 3 also shows an extension of the growing season through winter and spring.

Atmospheric changes in line with P1 also show differentiation in terms of spatial change in vegetation and timing of changes in key variables. PC 2 and PC 3 both indicate a movement towards dryland vegetation, but are distinguished by the timing of increases in key IBIS model output variables. Productivity, for example, increases most between April and June in the case of PC 2, and in February, March and September to December in the case of PC 3. PC 1, on the other hand, shows the largest changes in March.

Atmospheric changes in line with P4 again show vegetation movement and timing of changes in key variables to be important. Vegetation movement distinguishes PC 1 from PC 2 in part, but seasonal timing of changes in key IBIS model output variables is notably important. In PC 1, most anomaly increases in productivity are in autumn (March, April), while in PC 2, increases are in late summer (January to March).

It may be concluded that over the domain there is a general movement away from dryland vegetation in Ibisdyn and P4, but a mixed response in P1. Therefore differentiation between and within scenarios is partially as a result of spatial change of vegetation over the domain. Another important factor differentiating grid cell response in each scenario, is the time of year at which the changes in variables such as NPP, soil moisture and soil temperature are most pronounced, as well as the direction of change.

It appears from the above and earlier sections, that the transition seasons are crucial considerations, since many of the changes reflected through the 21st century are evident in these shoulder months, rather than merely the conventional summer and winter seasons typically examined. Furthermore the input temperature, precipitation and relative humidity atmospheric forcing driving the IBIS model for the different scenarios are playing a vital role in determining the response, affecting both the timing and the direction of change.

6.5 A case study of vegetation change and process links

In this section a more in depth study is conducted at a particular location, in order to consider some of the processes driving the modelled vegetation change. Based on the results of the annual, summer and transitional seasons presented in Chapters 5 and 6, one region that indicates a common response in almost all cases, the Northern Namibia region (region 5), has been chosen. This region displays a somewhat complex response to the atmospheric forcing evident from the IBIS model simulations. As noted earlier, indications from the model developers are that temperature, relative humidity and precipitation appear to be the primary atmospheric input forcings driving the IBIS model simulations. Process response is hence most likely to be due to these forcing input variables, as demonstrated thus far.

In order to examine the vegetation response variations some important factors related to processes need to be explored. Precipitation is a vital atmospheric forcing factor, regulating the hydrological system and is an important determinant to a large degree, of the processes operating in the earth system. Precipitation has a close association with evapotranspiration, and affects the run-off, storage and underground flow of water. Evapotranspiration is in itself an important process, particularly in the context of the recycling of moisture. Evapotranspiration in IBIS is simulated as the addition of three water vapour fluxes, *viz.* canopy transpiration, soil surface evaporation and evaporation from water intercepted by vegetation canopies (Foley *et al.*, 1996). Through precipitation, much moisture is lost to the atmospheric system, but through evapotranspiration, a large percentage is returned. Evapotranspiration is also important as an energy transferral mechanism. In association with the evapotranspiration processes, are processes operating below the surface, such as soil moisture storage. Soil moisture is critical for its stress relief role during periods of drought, since it provides the necessary moisture source to maintain the surrounding vegetation. The spatial distribution of plant functional types and the relative dominance of grasses and trees are controlled by competition for soil moisture and sunlight (Foley *et al.*, 1996). Six soil layers capture soil moisture variations on an interannual and seasonal basis, with plants drawing water differentially from these layers. Woody plants are able to take up more water from the deeper soil layers, while herbaceous plants take up more water from the shallower layers (Foley *et al.*, 1996).

Bearing the above in mind, region 5 is considered in some degree of detail, in order to demonstrate the intricate processes involved, providing some insight into the complex nature of the processes involved, and how sometimes subtle changes in input forcing can considerably

impact on the regional vegetation characteristics. Region 5, as discussed in previous chapters, shows a general increase in temperature during the 21st century (by up to 5°C), a decline in relative humidity (5%) and a slight decrease in precipitation (although precipitation in period 2 in fact shows an increase). The vegetation categories represented in region 5 are summarised in table 6.5 for ease of reference.

	Period 1 (2000-2030)	**Period 2 (2050-2080)**
Ibissta	Grassland	Grassland
Ibisdyn	Open shrubland with some Grassland	Predominantly Grassland with some Open shrubland
P1	Open shrubland, with some Grassland and cases of Desert	Mix of Grassland and Open shrubland
P2	Open shrubland with some Grassland and cases of Desert	Mix of Grassland and Open shrubland
P3	Predominantly Open shrubland, with an equal mix of Grassland and Desert	Grassland
P4	Grassland with some Open shrubland	Predominantly Grassland with some Open shrubland
P5	Equal mix of Grassland, Open shrubland and Desert	Predominantly Grassland with some Open shrubland

Table 6.5 Summary of vegetation categories represented for periods 1 and 2 in region 5, for the 7 scenarios (Note: Scenarios of similar response are shaded alike)

In the context of region 5, evapotranspiration processes have played a significant role with respect to vegetation categories. In all 7 scenarios evapotranspiration has increased from period 1 to period 2. The tendency of vegetation in region 5 is for a general movement away from more dryland vegetation categories, which would on first impressions suggest an increase in precipitation in the input forcing. However, if the input forcing precipitation is considered (refer to figure 5.10 in Chapter 5), it is evident that there is a subtle decline in precipitation over the period 2000-2080. However, period 2 (2050-2080), as noted earlier, in fact shows an increase in precipitation during that time. If the subtle decline in precipitation during the 21st century is considered alone, then precipitation as a driving force cannot account for the vegetation tendencies apparent. Whilst the increase in temperature may provide the energy required to drive

the evapotranspiration process, some other important processes must be taking place, since precipitation is not notably in contrast between periods 1 and 2. A possible explanation is most likely the recycling of moisture within the earth system, as a consequence of evapotranspiration processes. Evapotranspiration is a contributor to convective uplift processes (which are likely to be common in the Northern Namibian region), and acts as a moisture recycling agent. In close association with this, is soil moisture, which is particularly important during periods of drought.

All 7 scenarios show a tendency towards an increase in soil moisture between the 2 periods. This cannot be explained by a decrease in precipitation as a driving force, and may be related to the increase in vegetation cover between the two periods, since vegetation has a fairly complex interaction with soil moisture (Foley *et al.*, 1996). Furthermore, the increase in soil moisture is an important factor explaining the vegetation tendency to move away from more dryland vegetation categories (see Foley *et al.*, 1996). The recycling function played by the increase in evapotranspiration will provide the necessary moisture source through the potential rainfall associations associated with the convective uplift processes.

On a scenario basis, these processes may be explored further, since vegetation response is scenario dependent. Referring to table 6.5, scenarios Ibisdyn, P3, P4 and P5 are all indicative of a tendency towards a dominance of grassland in period 2. In contrast, P1 and P2 show more of a mix of grassland and open shrubland. Considering the input atmospheric forcing (figure 4.1 in Chapter 4), it is clear that there are some likely explanations for these tendencies. In the case of P1 and P2, the commonality is the relative humidity input forcing, which has a negative standard deviation from the mean relative humidity. This could account for these two scenarios showing less of a tendency towards productive vegetation categories than the other scenarios. Relative humidity is, by definition, an indication of the vapour content of the air as a ratio of the vapour content needed to saturate the air, and is temperature dependent. In the case of P1 and P2, the relative humidity values are lower than the other scenarios, and this probably contributes to a large degree to the apparent difference in vegetation representation in these two scenarios in period 2.

In the case of the other scenarios (Ibisdyn, P3, P4 and P5), the response (a dominance or exclusivity of grassland) is not clear. In P3, precipitation and relative humidity atmospheric forcing inputs both have a positive standard deviation from the mean response, and temperature a negative standard deviation from the mean response (figure 4.1 in Chapter 4). In terms of

vegetation response, this scenario would be expected to simulate the most productive vegetation response, which is in fact the case (grassland). The fact that only grassland is simulated in period 2, is probably as a result of the climatic thresholds for growth of open shrubland being exceeded in their entirety. In the case of scenario simulation P4, relative humidity forcing inputs have a positive standard deviation from the mean and temperature a negative standard deviation from the mean. However, precipitation forcing has a negative standard deviation from the mean. Precipitation forcing alone would indicate a reduction in available moisture for this scenario, and would result in a vegetation response more akin to P1 or P2. However, the relative humidity and temperature inputs have resulted in a response more closely resembling P3 and P5 (where precipitation shows a positive standard deviation from the mean response).

Thus, while the processes of evaptranspiration and soil moisture storage are operating in the same direction, the differences in vegetation response between scenarios are more closely linked to some of the input forcings driving the IBIS simulation. Therefore, while there is a link on a more general scale between vegetation and the processes such as evapotranspiration and soil moisture storage in the IBIS model physics described by Foley *et al.* (1996), differences between scenarios are more easily accounted for and explained in terms of the atmospheric input forcings. Hence, processes cannot be considered in isolation, but need to be examined in an interconnected manner.

It is clear from this case study for region 5 that the processes involved are intricately interlinked and in order to understand the link mechanisms and processes, it is necessary to consider many factors in order to obtain a detailed understanding. . It is evident that with monthly and yearly variations in atmospheric input forcing, there is a tendency for there to be a switch between vegetation categories in different years, for example, the vegetation in period 2 in region 5 is shifting between the thresholds imposed by open shrubland and grassland. This case study presents an explanation for the process response in one region, but it is likely that other regions will have different response tendencies to the processes involved, since thresholds and climatic conditions in these regions will differ. An interesting follow-on from this research would be to consider the relative importance of each process and atmospheric input forcing variable for each scenario, in other regions of notable response.

CHAPTER 7

IMPLICATIONS OF LAND SURFACE SENSITIVITY IN THE CONTEXT OF GLOBAL CLIMATE CHANGE SCENARIOS

CHAPTER 7

IMPLICATIONS OF LAND SURFACE SENSITIVITY IN THE CONTEXT OF GLOBAL CLIMATE CHANGE SCENARIOS

7.1 Consequences and impacts

7.1.1 A global context

The climate can change in a number of ways. The changes may be large or small scale, natural or anthropogenic and over a long or short term (Parry and Carter, 1998). The current anthropogenically induced climate change may be thought of as a debate on what is not known, since it concerns what *could* occur in the future. There are unexpected effects that models cannot account for or which are not natural extensions of present trends, for instance a new scientific finding outside our range of expectations, stemming from our incomplete understanding of social and physical systems (Darmstadter and Toman, 1993). An example of such an unexpected effect is a totally unanticipated deterioration in agricultural productivity or biodiversity, as a consequence of temperature or rainfall shifts (Darmstadter and Toman, 1993).

An important element of surprise concerns non-linear change, which is one that is disproportionate with respect to one of the driving variables. A good example of non-linearity is the relationship between CO_2 and photosynthesis. In C_4 plants (e.g. maize), photosynthesis starts at low CO_2 concentrations, rises quickly to the concentration presently in the atmosphere, and then rises a small amount more (Waggoner, 1993). In C_3 plants (e.g. wheat), photosynthesis starts at a much later stage, but rises at a considerably faster rate than maize. C_4 plants will therefore have greater yields under current conditions, but a future CO_2 environment may be of more benefit to C_3 plants (Waggoner, 1993). Recent results from a fully-coupled 3-dimensional carbon-climate model show that carbon-cycle feedbacks could notably accelerate climate change over the 21st century (Cox *et al.*, 2000).

With regard to climate forcing of the land surface, it is possible that there is more than one climate state that could exist given a particular forcing scenario (Goodess *et al.*, 1992), a response characteristic of an intransitive system. Under such conditions, the climate will be in a stable state until an external factor (such as a change in solar radiation) causes a shift to a new

climate state (Goodess *et al.*, 1992). This makes modelling of intransitive systems extremely difficult, if not impossible.

Furthermore, clouds, which are important regulators of the earth's temperature, are one of the primary uncertainties with respect to climate change, since they may be negative or positive in feedback depending on cloud elevation (Rosenberg, 1993). The present day net effect is a surface cooling of 5°C (Rossow and Zhang, 1995). If climate change results in cloud displacement to higher levels this will result in an increase in energy retained in the atmosphere, while a displacement to lower levels will have the reverse effect (Rosenberg, 1993).

There is also uncertainty with respect to the interactive effect between the climate and biosphere, since changes in either system resonate through both systems. This and the factors discussed above make the examination of the effects of land surface changes within a climate change context more complex and difficult than they already are.

Factors such as soil moisture holding capacity, soil depth, seasonal temperature variability, species competition and carbon losses from organic matter are some of the many factors making analysis of vegetation in a climate change context challenging (Darmstadter and Toman, 1993). However, attempts at understanding the changes and the important processes underlying such changes can be made. Climate change affects hydrological cycles in a number of ways. If temperatures increase in the growing season, without a complementary increase in moisture within the atmosphere, soil moisture demands will increase (Clark and Reid, 1993). Although plants may become more efficient in water use, an increase in CO_2 could result in increased water interception and use, through a leaf area increase (Clark and Reid, 1993).

There is a correlation between leaf area index and water availability and a correlation between leaf expansion and temperature (Woodward, 1987). The influence of climate on leaf area index will have consequences for plant growth as well as the casting of shade (Woodward, 1987). Plant growth, nutrient cycles and carbon exchange with the atmosphere are largely determined by water availability, since water is essential in maintaining chemical and physiological processes in plants and for energy exchange (Schulze, 1997). Water constitutes a major percentage of plant tissues, it is the major reagent in photosynthesis, it is transpired through leaves, it is the primary transport mechanism in plants and it exerts an influence on growth (Woodward, 1987).

Soil moisture storage (shallow soils have a lower storage capacity) often tends to be a better productivity indicator than precipitation, since storage is important in relieving moisture stress in short-term droughts (Clark and Reid, 1993). However, precipitation is also important, since precipitation increases in previously drier months and the associated increase in the length of the growing season could result in an increase in overall productivity. An increase in the availability of moisture, through both soil storage capability and directly through precipitation, could increase net primary production where moisture has been limited previously.

7.1.2 Land surface sensitivity and impacts over southern Africa

It is clear that a change in moisture availability and productivity levels, for example, may have significant repercussions in a global context over the local environment. It is evident from previous chapters, that there is not always consistency (in terms of vegetation and other biosphere model output variables) with respect to response regions and response trend directions over southern Africa in summer and winter. A sensitivity study such as that presented in this thesis is therefore important in studies concerned with climate change impacts. The section to follow considers some of the key variables over southern Africa, specifically, evapotranspiration, leaf area indices and soil moisture. These will be discussed as a means of illustrating the possible consequences and impacts changes within the climate system may have over the region.

Moisture is replenished in the atmosphere through evaporation from the soil and plants, and through transpiration from plant leaves. *Evapotranspiration* is a vitally important process, since it is the primary boundary layer moisture feed into the atmosphere from the surface hydrological system (Briggs and Smithson, 1985). The contribution by recycling through evapotranspiration generally accounts for a large proportion of precipitation received. In the Amazon, for example, the contribution is 50% (Salati, 1987), while in central Africa the contribution is a larger 75-95% (Brinkman, in Biodiversity Support Program (1993)). Southern Africa would most likely fall somewhere between these two in terms of the evapotranspiration recycling contribution to precipitation (Hewitson, *pers. comm.*). Evapotranspiration is a major heat energy transfer from vegetation into the atmosphere and results in an increase in energy available for the processes of convective uplift and hence convective rainfall potential. An increase in evapotranspiration leads to an increase in available moisture, which may contribute to a potential increase in the energy available for convection. The IBIS model simulates increases in evapotranspiration from the

early to late 21st century, of up to 15% over Northern Namibia and the southern escarpment region. Therefore this is indicative of a significant increase in available energy and moisture for convective processes in these regions.

The 3 scenarios considered in the PCA in Chapter 6, *viz.* P1, P4 and Ibisdyn (which represent reasonably the range of scenario responses) are considered in terms of their potential convective rainfall changes as a consequence of altered evapotranspiration rates. As discussed in Chapter 6, 3 PCs were retained for rotation in Ibisdyn and P1, while 2 PCs were retained for rotation in P4. Component scores, which represent the anomaly seasonal cycle, have been plotted in order to display months of increase and decrease (from the early to late 21st century) in score anomalies (figures 6.22-6.24). The discussion to follow is based on these score anomaly increases and decreases (refer to Chapter 6 for further details). In Ibisdyn, PC 1 regions show an increase in average evapotranspiration from February to July, which may result in an increase in convective rainfall during this time (through greater energy available for convective processes). Thus, late seasonal productivity increases could be anticipated for such regions. Regions of increase for PC 2 are from December to April, which may indicate a mid-season rainfall increase. PC 3 shows an average evapotranspiration increase primarily in the winter months. Thus convective rainfall during the summer growing season is unlikely to be influenced. In P1, increases in average evapotranspiration for PC 1 are during March, May and October. There are therefore indications for a late seasonal increase in convective rainfall. Regions represented by PC 2 indicate an average evapotranspiration increase during the winter season predominantly (April to September) and these regions are thus perhaps not as important in terms of convective rainfall increases, since convective uplift is minimal during the winter months. In P4, average evapotranspiration for PC 1 shows a late summer increase (March, April) and therefore convective rainfall increases in late summer could perhaps be anticipated. In the case of PC 2, potential convective rainfall increases are most likely from January to March. The evident lack of inter- and intra- scenario response consistency highlights the importance of sensitivity studies incorporating a range of responses, particularly when considering impacts and consequences of climate change.

It is also informative to compare losses through evapotranspiration with the precipitation amounts over the sub-continent. Considering summer average evapotranspiration (refer to figure 6.3 in Chapter 6) and the summer HadCM2 input precipitation driving the IBIS simulation (refer to figure 3.10 in Chapter 3), some interesting observations can be made. HadCM2 precipitation

from the early to late 21st century has generally decreased over most of the domain, whilst evapotranspiration displays notable increases over a large portion of the domain. Hence, this suggests a notable and important increase in the moisture recycling from the land surface to the atmosphere through evapotranspiration[1].

Leaf area indices (of upper and lower canopies) are important within the local climate, since they are linked to albedo. With a decrease in leaf area index, there is greater albedo (for example, by increased soil exposure). This is a contributory factor to desertification in arid areas. In most scenarios and regions there is a tendency for a movement away from more arid vegetation types (a sensitivity to precipitation rather than temperature input forcing) and therefore lower albedo values and less of a tendency towards desertification. Leaf area indices are also associated with water availability, since plant growth is dependent on water.

Soil moisture is a good productivity indicator as soil moisture storage is vital in relieving stress during periods of drought. Soil moisture changes affect both the local and regional environments and they are closely linked to run-off. Greater soil moisture levels will imply greater run-off potential. There is a variation in soil moisture between regions and scenarios over southern Africa. Therefore the run-off potential within the local system is variable and critically linked to changes in key atmospheric variables such as precipitation (a major determinant of soil moisture levels) and temperature (increases will place increased demands on stored soil moisture). Soil moisture and leaf area indices together may reflect desertification and may be used as indicators of productivity levels in the local system.

It is therefore evident that there are a number of interlinking factors at the local level, which may have impacts on the locally and regionally specific response. Therefore the input climate forcing parameters for the IBIS model simulation (precipitation, temperature, relative humidity etc.) are crucial in determining the response variations and directions in different locations. Changes in one localised area could have impacts on adjacent areas, through, for example, run-off potential and the potential alteration of the local climate through change in vegetation structure and other land surface properties. Processes are interlinked and interdependent and the consequences and impacts will therefore be complex and both locally and regionally specific. There is therefore a delicate balance existing in each region and a change in one variable (such as temperature,

[1] This raises an important future research question concerning the relationship of moisture recycling (through changes in evapotranspiration) to rainfall processes over southern Africa.

precipitation or evapotranspiration) in the system will have a series of effects on and relationships to other variables. The effect this may have will, of course, depend on the degree and direction of change.

Therefore, the biosphere and atmosphere should not be considered in isolation, but rather as a whole, and changes should be viewed within this context. This furthermore enforces the need for developers of general circulation models (GCMs) to place much emphasis on better representing the interactions between the land surface and the climate. There are a range of future climate scenario projections and many different GCMs and therefore a variety of projected future consequences and impacts over the southern African region. In the light of this, some of the different GCM climate forcing scenarios need to be considered here in order to place the HadCM2 simulation within the context of other GCM simulations.

7.2 The latest emission scenarios

7.2.1 Background

The IPCC IS92 emission scenarios were monumental in their time, since they were the first global emission scenarios to provide estimates of the full range of greenhouse gases. Since this time, however, understanding of plausible future greenhouse gas emissions and climate change has greatly improved. The 1996 Plenary of the IPCC therefore requested a Special Report on Emissions Scenarios (SRES). As a result, new emission scenarios were developed which would provide useful input to the IPCC third assessment report.

The driving forces of future greenhouse gas emissions, such as demographic development, socio-economic development and technological change, are complex and dynamic. Thus, there becomes a need for scenarios representing the range of driving forces and emissions (IPCC, 2000). Surprise and disaster type scenarios are the only exclusions. Four different storylines (described in more detail in figure 7.1) were developed, each representing different social, technological, demographic and environmental developments for the next 100 years (IPCC, 2000). These four storylines are given names A1, A2, B1 and B2, each of which includes several different scenarios (figure 7.2). In total there are 40 SRES scenarios.

A1

- Rapid economic growth
- Global population at a maximum in the mid 2000s, declining thereafter
- New more efficient technologies introduced expeditiously
- Capacity building
- Increased interactions (cultural and social)
- Decrease in regional income difference
- There are 3 scenario groups, viz. fossil intensive, non-fossil energy sources and balanced energy sources

A2

- Heterogeneous world
- Self-reliance and preservation
- Continuously increasing global population
- Regionally oriented economic development
- Economic growth and technological advancement which is slower than other storylines

B1

- Global population at a maximum in the mid 2000s, declining thereafter
- Rapid movement towards service and information economy
- Clean and resource-efficient technologies
- Improved equity with global solutions in sustainability (social, environmental and economic)

B2

- Local solutions to economic, environmental and social sustainability
- Increasing global population, but at a lower rate than A2
- Economic development is intermediate
- Technological change is not a fast and more diverse than B1 and A1
- Focus on local and regional levels

Figure 7.1 Description of the 4 storylines as described in IPCC (2000).

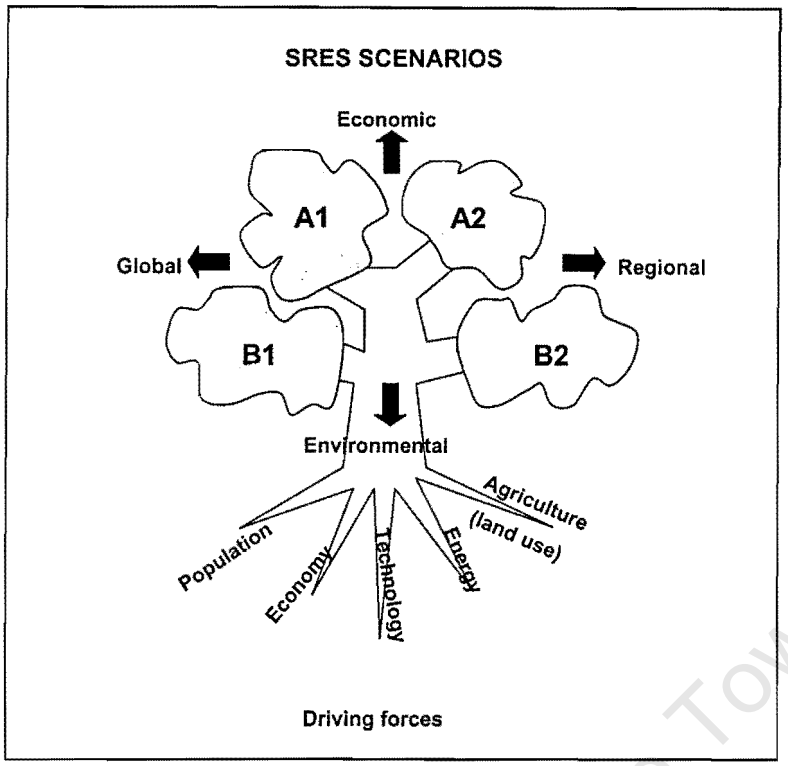

Figure 7.2 The SRES scenarios tree (modified from IPCC, 2000).

7.2.2 The SRES scenarios of current models

The HadCM2 model run used in driving the IBIS model is placed in the context of the latest emission scenarios. Two key atmospheric variables for driving the IBIS model have been identified as precipitation and temperature. Therefore, future response differences of these variables between models are an important consideration, in order to obtain a perspective on the HadCM2 response. The A2 and B2 storyline results for 8 GCM simulations were available for examination in terms of their precipitation (except in the case of the GFDL model) and temperature anomaly responses at a (regridded) 2.5° by 2.5° horizontal resolution. The present day in these data is taken as being the average of 1961 to 1990 and the future as 2071 to 2100. Anomaly difference maps for A2 and B2 for each GCM for the 2 atmospheric variables are produced for summer and winter. The anomaly difference maps for the full suite of models are included in Appendix C; some maps are included in this chapter where appropriate.

The 8 GCMs considered are as follows:

- The Canadian Centre for Climate Modelling and Analysis (CCCma or CGCM1)
- The Australian Commonwealth Scientific and Industrial Research Organisation (CSIRO)
- The US NCAR Climate System Model (CSM)

- The US Geophysics Fluid Dynamics Laboratory (GFDL)
- The Japanese Meteorological Research Institute (MRI2)
- The Japanese CCSR National Institute for Environmental Studies (NIES)
- The US NCAR Parallel Climate Model (PCM)
- The UK Hadley Centre for Climate Prediction and Research (HadCM3)

The A2 and B2 storylines within a particular model generally show much the same pattern of response for a particular season (summer or winter), but the magnitude of response tends to be greater in the A2 storyline. Thus, a storyline is important in underlining the variation in response magnitude that could be expected for a given model under varying future emission scenarios.

7.2.2.1 Precipitation

The HadCM3 model (figure 7.3), a model simulation subsequent to HadCM2, shows a precipitation decrease of greatest extent over the NW in summer. This decrease is 1.8 mm day^{-1} in the A2 storyline and 1.4 mm day^{-1} in the B2 storyline. Decreases in winter are over central South Africa (0.6 mm day^{-1} for A2 and 0.4 mm day^{-1} for B2). The MRI2 model indicates a decrease over most of the domain, but to a lesser extent than in HadCM3. The CCCma model also shows a decrease over the southern African domain, but without a peak in the NW in summer. The CSIRO model indicates a slight increase in winter over the SE and a general decrease over the north central interior of South Africa; there is an increase to the NE of this. The NIES (figure 7.4) and CSM models are both notable in that they both indicate only precipitation anomaly increases during the summer months, as opposed to the general decreases evidenced in some areas in other models. The NIES model shows a slight winter decrease over the southern portion of South Africa, while the CSM and CSIRO models show a slight increase. Response patterns along the coastline, such as that of the NIES model simulates in summer may well be as a consequence of the boundary layer moisture calculations. Anomaly increases for summer in the CSM being largely in the north, is perhaps due to the very active ITCZ in the model. The PCM model indicates a precipitation decrease over the west and an increase to the east of this in summer.

It is apparent that there are some very different response directions and differences between the 8 different models, perhaps explained by the differences in their treatment of various physical parameters. The varying precipitation anomaly responses between models lends much justification to the choice of including, in this study, standard deviation scenarios P1 to P5 (i.e.

variation in precipitation standard deviations from the mean response). It is clear that there is not certainty or consistency in response, in either response region or response trend (increase or decrease) in summer and winter. Thus, a sensitivity study such as that presented in this thesis is important in studies considering the impacts and consequences of climate change.

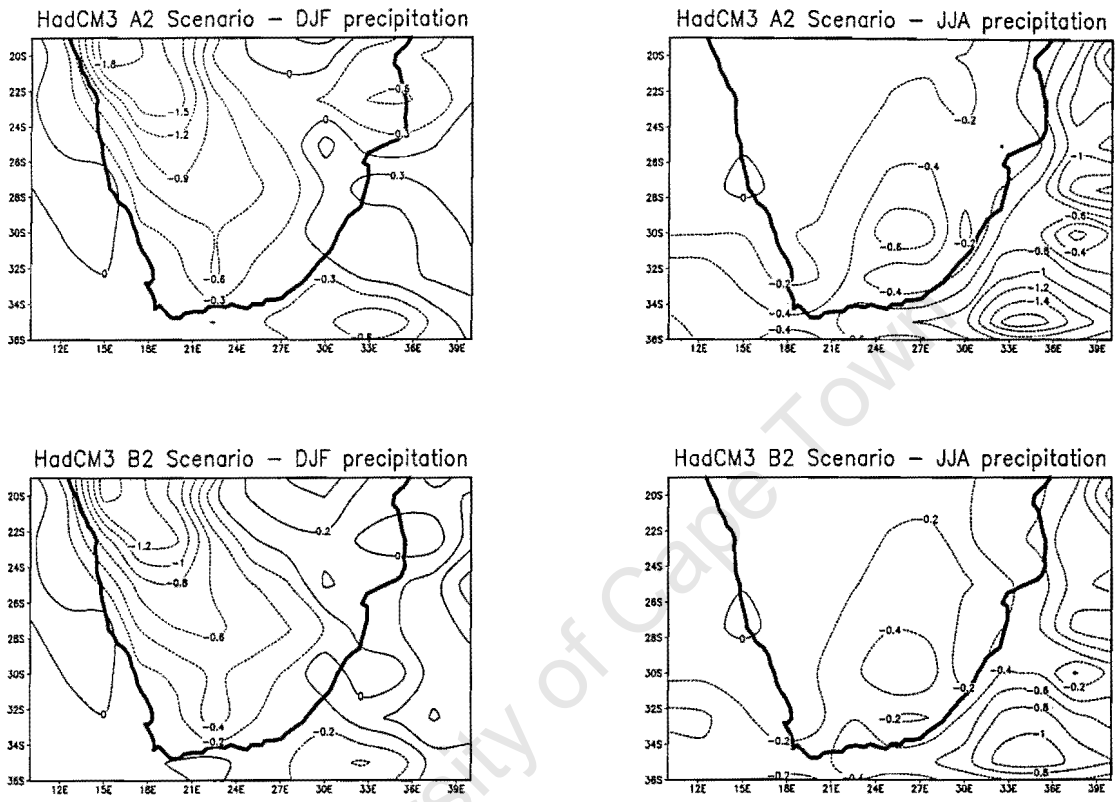

Figure 7.3 HadCM3 precipitation anomaly simulation (mm day^{-1}) for the A2 and B2 storylines

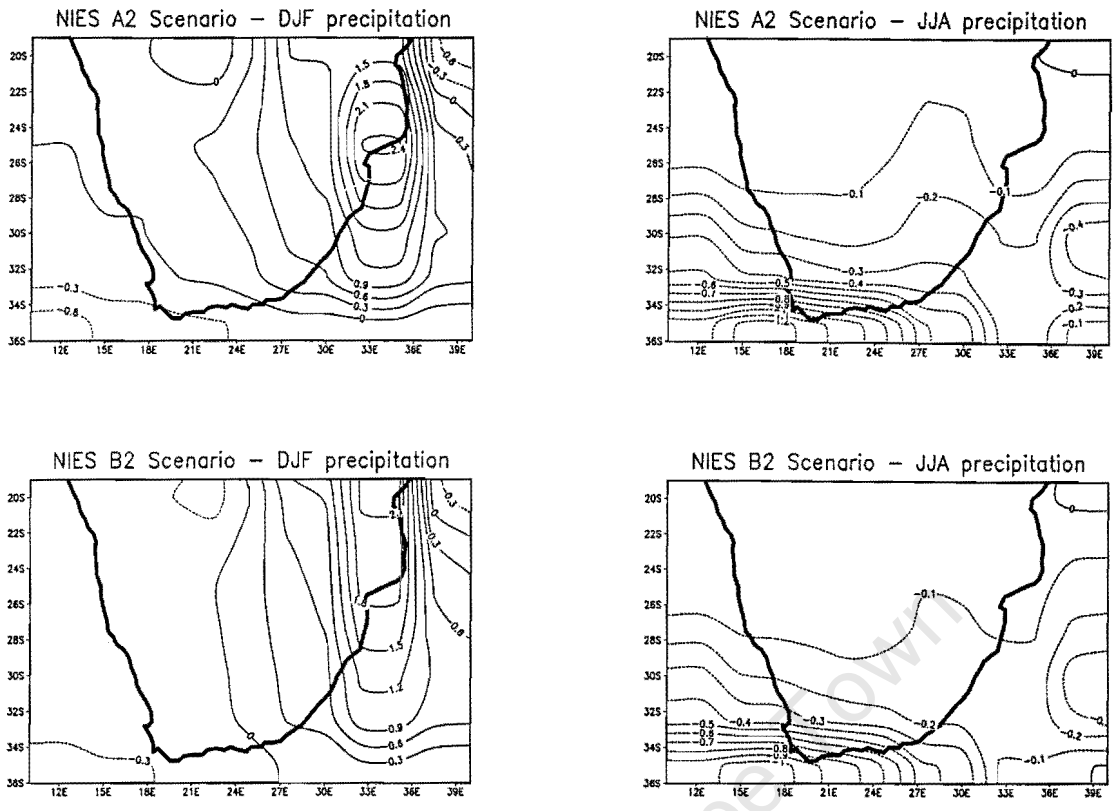

Figure 7.4 NIES precipitation anomaly simulation (mm day^{-1}) for the A2 and B2 storylines

7.2.2.2 Temperature

All models show an increase in temperature from the present day to the end of the 21st century, but the increase amount is variable. For summer, HadCM3 (figure 7.5) shows the greatest overall anomaly increase within the southern African domain (6 K for A2 and 4 K for B2), followed by NIES, CCCma, CSIRO, GFDL, CSM, PCM and then MRI2. The increase for MRI2 is only of the order of 1.5 K. Anomaly increases are greatest over the interior, decreasing towards the coast and southwards. Increases in some models (e.g. HadCM3 and NIES) are greater to the west and northwest interior, while in others the increases are greatest in the north (e.g. GFDL). The pattern increase for the CSM shows the greatest anomaly increases to be over the NE, in contrast to other models.

Winter anomaly increases tend to be slightly higher than in summer, except in the case of HadCM3, where the increases are generally similar in magnitude. The NIES model shows the greatest anomaly increase (6.5 K for A2 and 5.1 K for B2), followed by HadCM3, CCCma, GFDL, CSIRO, PCM, CSM and MRI2. The increase for MRI2 is only of the order of 1.9 K for A2 and 1.4 K for B2.

It is clear that temperature anomaly responses are more consistent than the precipitation anomaly responses, in the sense that all models show a temperature increase from the present day to the end of the 21st century. However, the anomaly increases amounts are variable in magnitude between the different models. The change amount therefore again lends justification to sensitivity studies, which include standard deviation variations from the mean response.

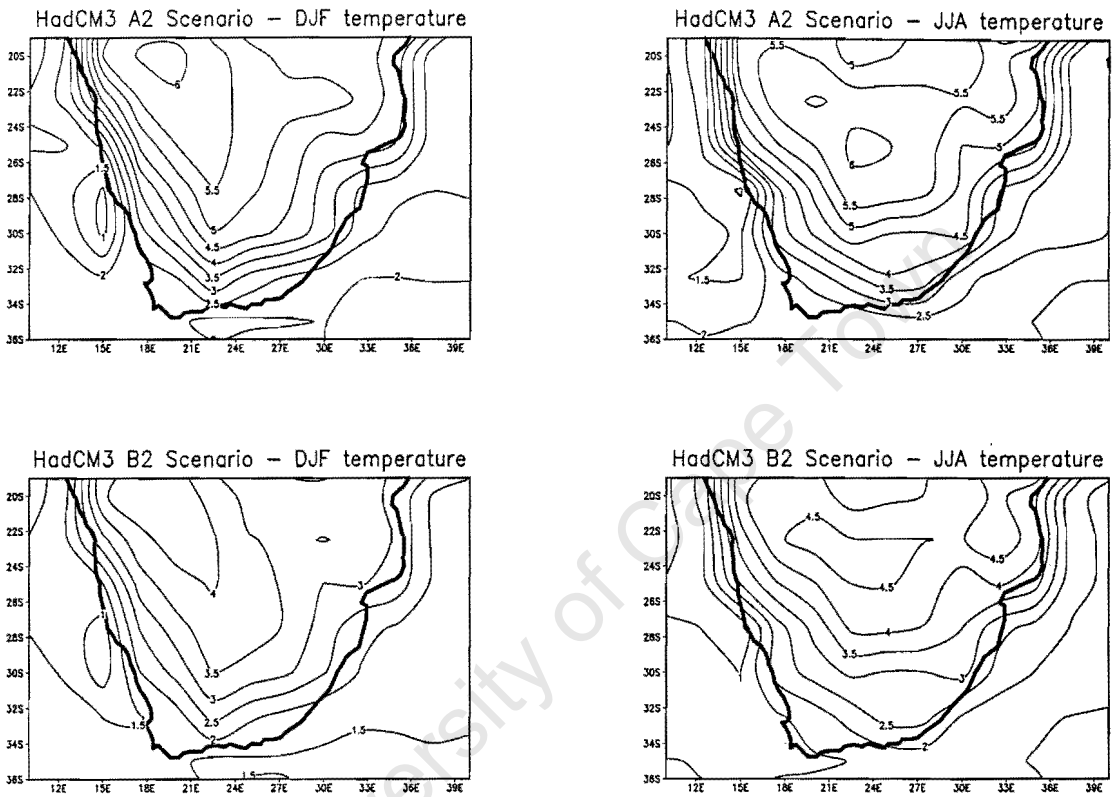

Figure 7.5 HadCM3 temperature anomaly simulation (K) for the A2 and B2 storylines

7.2.2.3 The HadCM2 model in the context of current SRES scenarios

The HadCM2 is a forerunner to the HadCM3 model (described by Gordon *et al.*, 2000) and differs most notably by the fact that HadCM3 does not require "flux adjustments" whereas the HadCM2 does (prescribed adjustments, or "flux adjustments" are made to heat and water fluxes in the HadCM2, in order to minimise errors in the present day simulation as a result of climate drifts). In addition there are some other changes in HadCM3, such as a new radiation scheme (Edwards and Slingo, 1996) and a new land surface scheme (Cox *et al.*, 1999). The new radiative scheme has 6 and 8 spectral bands in the short and long wave respectively. Minor greenhouse gas radiative effects (i.e. those in addition to CO_2, water vapour and ozone) are represented explicitly. The land surface scheme allows freezing and melting of soil moisture,

surface run-off and drainage; evaporation is dependent on stomatal resistance to CO_2, temperature and vapour pressure. The ocean component of the HadCM3 is also operated at a finer horizontal resolution (1.25° x 1.25°) than its predecessor, therefore allowing for improved heat transport[2]. Therefore there should be some differences in the simulations produced using the HadCM2 and HadCM3 model runs. Although anomaly maps for HadCM2 are not available for the exact same time periods considered in the SRES scenarios, the pattern response and response directions for the HadCM2 model could be compared quantitatively to the HadCM3 and other models.

Chapter 3 presented the early and late 21st century response differences in precipitation and mean temperature for summer and winter for HadCM2. (Refer to figures 3.1 and 3.2 in Chapter 3). As highlighted in the chapter, temperature increases were of the order of 2.7 to 2.8 K for summer and winter respectively. The response patterns for HadCM2 are similar to HadCM3, with an increase in interior mean temperature, and greater increases in the NW. Considering the period of the anomalies (i.e. a difference between the period 2050-2080 and 2000-2030), the increases are fairly substantial in contrast to climate projections such as MRI2 (which shows a lower increase over a much longer time period). Precipitation in HadCM2 shows little notable change or slight decreases over most of the domain in summer, except in the SE (0.6 mm day^{-1} decrease). In winter there is a precipitation increase over the SE (0.6 mm day^{-1}). HadCM3 shows the same direction of response as HadCM2 in summer, but an opposite response direction in winter. The HadCM2 winter precipitation compares more favourably with the anomaly increases evident for the CSIRO and MRI2 models.

Therefore the HadCM2 model, despite being driven with the older IS92a forcing scenarios, does not compare unfavourably with simulations forced by current emission scenarios, since these simulations are notably variable between GCMs. Therefore a sensitivity study approach where a range of temperature and precipitation increases and decreases are examined is most beneficial, instructive and informative. In this particular study, positive and negative temperature and precipitation standard deviations from the mean scenarios (P1 to P5) have been considered in addition to the mean response. This is a useful way forward, since the responses as a consequence of a range of temperature and precipitation change amounts are examined and evaluated.

[2] http://ipcc-ddc.cru.uea.ac.uk/

CHAPTER 8

SUMMARY AND CONCLUSIONS

CHAPTER 8

SUMMARY AND CONCLUSIONS

8.1 Overview

The importance of the land surface to the climate system should not be underestimated. Exchanges of moisture, momentum and heat are vital factors impacting on our livelihood. It is therefore important to examine the interactions between the biosphere and the climate system, such that a greater understanding of the sensitivities between the two systems is achieved. This is particularly relevant in the context of future climate change.

In this investigation the sensitivity (in terms of fluxes and other land surface features) between the biosphere and the atmosphere has been examined over the southern African domain. This domain is highly variable in time and space, and there is a range of vegetation types adapted to suit the climate. Research studies on climate and biosphere interactions have received little attention in this region and have become an important consideration particularly in the context of climate change.

The primary aim of this thesis has been to improve our understanding of the sensitivity of the land surface to changes in climate forcing, such as might be anticipated in a future climate change scenario. This has been approached from a modelling perspective. A biosphere model, the Integrated Biosphere Simulator (IBIS), has been used in conjunction with a general circulation model (GCM). IBIS has been driven with climate change data (specifically temperature, precipitation, relative humidity and wind speed) derived from the Hadley Centre HadCM2 transient GCM simulation.

Two baseline mean vegetation climate change runs were initiated, one using the static (Ibissta) and one the dynamic (Ibisdyn) vegetation option. These differ in that in the static vegetation simulation, vegetation is fixed and therefore does not vary on an inter-annual basis with changed input data. In the dynamic vegetation simulation, vegetation responds over time to the input forcing variables. In addition to the two baseline runs, a further 5 simulations were conducted using forcing fields constructed from the positive and negative standard deviations from the mean climate change data (specifically precipitation, temperature and relative humidity). These 5 plausible climate change scenarios (P1-P5) use the dynamic vegetation option of IBIS. In this

manner some range in the response to climate change could be obtained. Regions most susceptible to change have been identified and examined on both an annual and seasonal basis.

8.2 Summary of results

The main finding of this research is that there is a marked sensitivity evident between the biosphere and the climate, in a climate change context, over the southern African region. The Hadley Centre HadCM2 transient simulation, data from which are used as input forcing for the IBIS model simulation, is a non-sulphate greenhouse gas integration with historic CO_2 from 1860-1989 and a 1% compound increase in CO_2 from 1990-2099. The CO_2 emission scenario falls favourably within the range of current emission scenarios.

This GCM simulation suggests a southwards extension of the southern Hadley Cell. There is an associated zonal increase in sea level pressure to the south of the hemispheric high pressure belt. Mean temperatures have increased over the region, with greater increases in winter than summer. Such increases may promote continental drying. Wind speed increases to the west of southern Africa in summer (with implications for coastal upwelling) and decreases to the south in winter (which will lead to a decrease in mid-latitude westerly flow). Relative humidity and precipitation suggest a summer drying, although specific humidity indicates a moisture availability increase of 10% in the atmospheric column over the entire domain. This increase in specific humidity may negate the soil drying effect of temperature increases and precipitation decreases during the summer months. Winter precipitation indicates an increase over the eastern interior, which may have implications for an extension of the growing season.

Output data from the IBIS model simulations forced with climate change data from the Hadley Centre transient simulation are examined annually and seasonally. The annual results of the IBIS model simulation indicate that precipitation input forcing is vital in determining the broad scale vegetation response *across* scenarios. Indications are for a general change towards a more productive vegetation environment. Vegetation response differences *between* scenarios tend to be dependent on changes in temperature and relative humidity input forcing data. The annual response of the mean dynamic (Ibisdyn) and static (Ibissta) vegetation simulation variables is similar in most respects, except in terms of sensible heat fluxes. This may be attributed to model differences in albedo and soil moisture.

Seasonally, response sensitivity of the IBIS model simulations is most pronounced in summer, which is the primary growing season. There is a spatial change in favour of a more productive vegetation environment and an extension of the growing season is indicated. There are a number of implications of the land surface sensitivity to climate change evident from the IBIS model output. Evapotranspiration, for example, has increased over most of the domain, with implications for an increase in available energy and moisture for convective processes. Some more specific results follow.

8.2.1 The Hadley Centre transient run simulation

The Hadley Centre HadCM2 transient run simulation uses the IS92a forcing scenario, which has modest assumptions tending to offset one another (e.g. an economic growth of about 2.3% per annum between 1990 and 2100, a population of 11.3 billion by 2100 and utilization of conventional and renewable energy sources). Two periods, the early 21st century (defined as 2000-2030) and late 21st century (defined as 2050-2080) are considered over the southern African domain. Some general broad scale tendencies are the following:

- The Hadley Centre HadCM2 model suggests a southwards extension of the subsidence region of the southern Hadley Cell over the Southern Hemisphere through the 21st century.
- The global mean temperature response is a 2.5°C increase. Mean temperatures over southern Africa have increased, more so in winter than summer.
- Wind speeds have increased to the south of the sub-continent in summer, related to the southwards extension of the southern Hadley Cell.
- Relative humidity and precipitation indicate a summer drying over the domain.

8.2.2 Mean annual IBIS results

Mean annual results from the IBIS simulation are examined in terms of the following variables: vegetation type, average evapotranspiration, net primary productivity, sensible heat fluxes, soil temperature and soil moisture. The anomaly differences between the early (2000-2030) and late (2050-2080) 21st century are considered.

- Five regions of notable response in most variables over southern Africa emerge, *viz.*, Northern Namibia, the Mozambiquan plains, the South African escarpment regions and the southern Kalahari.
- The IBIS model appears to be most responsive to precipitation input forcing *across* all scenarios and there are indications for a movement towards a more productive vegetation environment. Although there is no general marked increase or decrease in annual

precipitation input forcing data, there appears to be a change in seasonality towards wetter winters.

- The sensitivity to precipitation is supported by P1, P3 and P5 (which include a negative standard deviation from the mean precipitation input forcing) being distinct from P2, P4 (which include a positive standard deviation from the mean precipitation input forcing) and Ibisdyn in terms of response pattern, direction and amount.
- Vegetation response differences *between* scenarios are related to relative humidity and temperature input forcing scenarios.
- The sensitivity to relative humidity and temperature is supported by P1, P2 and P5 (which include a positive standard deviation from the mean temperature, and mean or negative standard deviation from the mean relative humidity input forcing) and Ibisdyn being distinct from P3 and P4 (which include a negative standard deviation from the mean temperature and positive standard deviation from the mean relative humidity input forcing) in vegetation response.
- Sensible heat fluxes are most dependent on vegetation being set as static or dynamic and this may be ascribed to differences in albedo and soil moisture.

8.2.3 Seasonal and intra-seasonal results

Seasonal results are considered in terms of the conventionally examined summer and winter months as well as in terms of monthly scale trends. The following variables have been considered in the seasonal analysis: net primary productivity, average evapotranspiration, sensible heat fluxes, soil temperature, soil moisture, latent heat fluxes and leaf area index (upper and lower canopies). At time scales shorter than a year, response regions and signals are complex and therefore the monthly scale is an important consideration, since the transition seasons (e.g. March and September) may be playing a vital role. The monthly analysis has been approached using principal components analysis (PCA) of the variables outlined above (as well as model simulated precipitation and relative humidity, determined from daily-derived calculations), over the entire southern African domain. PCA is useful in this research, since it provides a means of distinguishing inter- and intra- scenario variations in response. P1, P4 and Ibisdyn represent the range of scenario responses in terms of the variables considered in the seasonal analysis, and are therefore considered in the PCA analyses.

- The sensitivity of the variables considered shows a seasonal bias in response. The response is most prominent during the summer months, since summer is the main growing season over the majority of the domain.

- Temperature and relative humidity input forcings are important in determining the response groupings between scenarios for leaf area indices and net primary productivity, while precipitation is important in determining the response groupings between scenarios in terms of sensible and latent heat fluxes.
- Principal component (PC) loadings (which group grid regions of similarity) from the principal components analyses (of monthly data) performed on Ibisdyn, P1 and P4 tend to be high in Northern Namibia, central Botswana and central South Africa in particular. This suggests these 3 regions to be important regions of change.
- An analysis of vegetation changes between the early and late 21st century indicates PC loadings to be distinguishing, in part, the spatial change of vegetation. Regions showing a spatial change towards and away from a more productive vegetation environment are isolated in the PC loadings.
- Component scores, which are a representation of the anomaly seasonal cycle, highlight the importance of seasonal timing and duration of increases and decreases in key variables, in determining vegetation response and response differences between the different principal components and scenarios.
- Component scores highlight the importance of transition seasons, since many of the notable changes in key variables are evident in these shoulder months.

8.2.4 Implications of land surface sensitivity in a climate change context

The climate may change in a variety of ways and the climate change debate is really a debate of unknowns. Therefore, an examination of changes in the land surface is complex and challenging. The local climate could be altered through a change in land surface properties, as indicated by changes in evapotranspiration, leaf area indices and soil moisture.

- Changes in evapotranspiration are important, since evapotranspiration is the primary process feeding boundary layer atmospheric moisture. Indications over the southern African domain are for an increase in average evapotranspiration through the 21st century, with implications for an increase in the available moisture and energy to drive convective processes.
- Leaf area indices are linked to albedo, with decreases implying an increased albedo, contributing towards desertification in arid areas. A reduced albedo is suggested from the results of the simulations, and hence there is a decreased tendency towards desertification.
- Soil moisture is a useful indicator of productivity and soil moisture storage is crucial in alleviating stress during extended dry spells. There is some variation in soil moisture

between regions and scenarios and therefore some variability in run-off and storage potentials.

In order to place the HadCM2 simulation into the context of the latest emission scenarios (with respect to precipitation and temperature), preliminary results from GCMs simulated using the Special Report on Emissions Scenarios (SRES) A2 and B2 storylines, have been examined. In summary:

- The HadCM2 temperature and precipitation projected scenarios fall favourably within the range of the current emission scenarios, even though driven by the older IS92a scenarios.
- There are variable precipitation response directions and patterns existing in the 8 GCMs, with no clear consistency at the regridded (2.5° by 2.5°) horizontal resolution considered.
- The magnitude of temperature increase from the present day to the end of the 21st century is variable between GCMs.

8.3 Caveats

As with any research, there are invariably constraints to which attention should be drawn, since results need to be assessed in the context of these limitations. Some of the caveats identified are as follows:

- The IBIS model has been run at a resolution of 2.5° latitude by 3.75° longitude and therefore results are an indication of broad scale sensitivity only. Simulations at a finer spatial resolution may provide further insight with respect to the somewhat complex interactions, at the local scale. Hence, this research should be viewed in the light of the broad spatial scale considered.
- The research uses GCM and biosphere model output data and is therefore reliant on the accuracy of the model representation. Large-scale features are well simulated by GCMs, but the GCM resolution prevents the examination of sub-grid scale and more subtle changes. Since GCM grid cell input forcing is used in IBIS, the sub-grid scale interactive sensitivity skill is greatly reduced.
- IBIS represents modelled as opposed to observed vegetation and therefore does not capture the full precision of observed vegetation boundaries. In addition, a proportion of land over southern Africa is under agriculture, used as pasture or is categorised as urban settlement, rather than natural vegetation as assumed in IBIS. Results presented here isolate the modelled vegetation interactive sensitivity to climate and should therefore be viewed in this context.

- The effect of CO_2 fertilization is not included in the IBIS model. This may be important under future conditions, which are anticipated to be of more benefit to C_3 plants than C_4 plants.
- IBIS does not account for seasonal burning, an important component in savanna ecosystems in particular. Therefore some regions, which may support savanna type vegetation, could be misrepresented.

8.4 Conclusions

It is important to remember that the land surface is vital to the climate system in terms of exchanges of moisture, momentum and heat and that our livelihood is largely dependent on these interactions. There is therefore the need for a better understanding of the interactive sensitivity between the climate and biosphere systems, particularly within the context of future climate change. The findings presented here highlight the importance, for the biosphere, of subtle changes in atmospheric forcing variables (such as precipitation, temperature and relative humidity) over the southern African region.

There are 5 regions showing a notable sensitivity on an annual scale, while on a seasonal scale the response has appeared to be more spatially complex. There is a general trend towards more productive vegetation categories, which is a response to precipitation atmospheric forcing. Vegetation response differences between scenarios are largely attributed to temperature and relative humidity atmospheric forcing. At the monthly and seasonal scale, seasonal timing and duration of increases in key variables (e.g. average evapotranspiration, net primary production and soil moisture) are shown to be important distinguishing factors for response differences between different scenarios and regions over the southern African domain. Transition seasons have generally shown the most notable increases or decreases. The interactive sensitivity between the biosphere and atmosphere over southern Africa can also be viewed within the context of impacts and consequences, with the local climate being altered through a change in land surface properties.

There are a number of uncertainties to which attention must be drawn. Feedbacks, such as clouds, are one of the primary uncertainties in terms of a future climate change, since they may be negative or positive (depending on cloud height). This is particularly relevant in the context of the regulatory role clouds play with respect to the earth's temperature. Moreover, GCMs have problems with respect to appropriately representing cloud physics and hence precipitation. There

are also unexpected effects, which models cannot account for, or which do not conform to present trends. There may well be more than one climate state that could possibly exist and modelling of such a system is virtually impossible. Furthermore, non-linear changes, such as the relationship between CO_2 and photosynthesis (C_3 versus C_4 plants), may introduce an element of future surprise.

A number of recommendations for future research emerge from this study. Foremost, there is the need for the inclusion of both fire (particularly with respect to savanna ecosystems) and CO_2 fertilization effects on vegetation into a land surface model, such that the important effects of these two elements are accounted for. It would also be advisable to incorporate urban settlement (which is associated with heat island effects) and agriculture into a land surface model, in order to more accurately reflect the observed land use. In conjunction with this, model simulations at a finer resolution would greatly benefit our understanding of the interactive sensitivity between the climate and land surface systems over the southern African domain. A more local as opposed to broad scale understanding of the interactions between the two systems may then be achieved. It would also be informative to conduct IBIS model simulations using other GCM transient simulation scenarios, in order to determine the spatial and temporal consistency between GCMs.

The research presented here has ascertained that the land surface over the southern African domain is indeed sensitive to subtle changes in atmospheric forcing, and that in a climate change context these modifications may be significant and should not be neglected or ignored.

REFERENCES

REFERENCES

Aber, J.D. 1992. Terrestrial Ecosystems, In: Trenberth, K.E. (editor), *Climate System Modeling*. Cambridge University Press, London, 788pp.

Bergengren, J.C., Thompson, S.L., Pollard, D. and De Conto, R.M. 2000. The Equilibrium Vegetation Ecology Model (EVE): Modeling the effects of vegetation change on climate sensitivity to doubling CO_2. Submitted to *Climatic Change*.

Biodiversity Support Program, 1993. *Central Africa global climate change and development overview*. Corporate Press, Maryland, 108pp.

Boer, G.J., Flato, G., Reader, M.C. and Ramsden, D. 2000. A transient climate change simulation with greenhouse gas and aerosol forcing: projected climate for the 21st century. *Climate Dynamics* **16**, 405-425.

Briggs, D. and Smithson, P. 1985. *Fundamentals of Physical Geography*. Hutchinson, London, 558pp.

Catell, R.B. 1966. The scree test for the number of factors. *Multivariate Behavioral Research* **1**, 245-276.

Clark, J.S. and Reid, C.D. 1993. Sensitivity of unmanaged ecosystems to global change. In: Darmstadter, J. and Toman, M.A., *Assessing Surprises and Nonlinearities in Greenhouse Warming, Proceedings of an Interdisciplinary Workshop*. Resources for the Future, Washington DC, 158pp.

Cox, P., Betts, R., Bunton, C., Essery, R., Rowntree, P.R. and Smith, J. 1999. The impact of new land surface physics on the GCM simulation of climate and climate sensitivity. *Climate Dynamics* **15**, 183-203.

Cox, P.M., Betts, R.A., Jones, C.D, Spall, S.A. and Totterdell, I.J. 2000. Acceleration of global warming due to carbon-cycle feedbacks in a coupled climate model. *Nature* **408**, 184-187.

Cullen, M.J.P. 1993. The Unified forecast/climate model. *The Meteorological Magazine* **122**, 81-95.

Darmstadter, J. and Toman, M.A. 1993. Nonlinearities and surprises in climate change: An introduction and overview. In: Darmstadter, J. and Toman, M.A. (editors), *Assessing surprises and nonlinearities in greenhouse warming, Proceedings of an Interdisciplinary Workshop.* Resources for the Future, Washington DC, 158pp.

De Noblet, N.I., Prentice, I.C., Joussaume, S., Texier, D., Botta, A., Haxeltine, A. 1996. Possible role of atmosphere-biosphere interactions in triggering the last glaciation. *Geophysical Research Letters* **23**(22), 3191-3194.

Dickinson, R.E. 1984. Modelling evapotranspiration for three-dimensional global climate models. Climate processes and climate sensitivity. In: Hansen, J.E. and Takahashi, T. (editors), *Geophysical Monographs of the American Geophysical Union* **29**, 58-72.

Dickinson, R.E., Henderson-Sellers, A., Kennedy, P.J. and Wilson, M.F. 1986. Biosphere-atmosphere transfer scheme (BATS) for NCAR Community Climate Model for the Western United States. *Climatic Change* **15**, 383-422.

Dickinson, R.E. 1992. Land surface. In: Trenberth, K.E. (editor), *Climate System Modeling.* Cambridge University Press, London, 788pp.

Edwards, J.M. and Slingo, A. 1996. Studies with a flexible new radiation code. I: Choosing a configuration for a large scale model. *Quarterly Journal of the Royal Meteorological Society* **122**, 689-719.

Foley, J.A. 1994a. The sensitivity of the terrestrial biosphere to climatic change: A simulation of the middle Holocene. *Global Biogeochemical Cycles* **8**(4), 505-525.

Foley, J.A. 1994b. Net primary productivity in the terrestrial biosphere: The application of a global model. *Journal of Geophysical Research* **99**, 20773-30783.

Foley, J.A., Kutzbach, J.E., Coe, M.T. and Levis, S. 1994. Feedbacks between climate and boreal forests during the Holocene epoch. *Nature* **371**, 52-55.

Foley, J.A., Prentice, I.C., Ramankutty, N., Levis, S., Pollard, D. Sitch, S. and Haxeltine, A. 1996. An integrated biosphere model of land surface processes, terrestrial carbon balance, and vegetation dynamics. *Global Biogeochemical Cycles* **10**(4), 603-628.

Foley, J.A., Levis, S., Prentice, I.C., Pollard, D. and Thompson, S.L. 1998: Coupling dynamic models of climate and vegetation. *Global Change Biology* **4**, 561-579.

Gates, W.L. 1992. AMIP: The Atmospheric Model Intercomparison Project. *Bulletin of the American Meteorological Society* **73**(12), 1962-1970.

Giorgi, F., Brodeur, C.S. and Bates, G. 1994. Regional climate change scenarios over the United States produced with a nested regional climate model. *Journal of Climate* **7**, 375-399.

Goodess, C.M., Palutikof, J.P. and Davies, T.D. 1992. *The Nature and Causes of Climate Change Assessing the long-term future.* Lewis Publishers, London, 248pp.

Gordon, C., Cooper, C., Senior, C.A., Banks, H., Gregory, J.M., Johns, T.C., Mitchell, J.F.B., Wood, R.A. 2000. The simulation of SST, sea ice extents and ocean heat transports in a version of the Hadley Centre coupled model without flux adjustments. *Climate Dynamics* **16**(2/3), 147-168.

Gregory, D. and Rowntree, P.R. 1990. A mass flux convection scheme with representation of cloud ensemble characteristics and stability dependent closure. *Monthly Weather Review* **118**, 1483-1506.

Hansen, J., Johnson, D., Lacis, A., Lebedeff, S., Lee, P., Rind, D. and Russell, G. 1981. Climate impacts of increasing atmospheric carbon dioxide. *Science* **213**(4511), 975-976.

Harrison, S.P., Kutzbach, J.E., Prentice, I.C. Behling, P.J. and Sykes, M.T. 1995. The response of northern hemisphere extratropical climate and vegetation to orbitally induced changes in insolation during the last interglaciation. *Quaternary Research* **43**(2), 174-184.

Hasselmann, K., Sausen, R., Maier-Reimer, E. and Voss, R. 1993. On the cold start problem in transient simulations with coupled atmosphere-ocean models. *Climate Dynamics* **9**, 53-61.

Haxeltine, A. and Prentice, I.C. 1996. BIOME3: An equilibrium terrestrial biosphere model based on ecophysiological constraints, resource availability, and competition among plant functional types. *Global Biogeochemical Cycles* **10**(4), 693-710.

Heimann, M. 1998: Biota in biogeochemistry. *IPCC Workshop on Rapid non-linear Climate Change*, Noordwijkerhout, the Netherlands, 31 March - 2 April 1998 (Unpublished Workshop Report).

Henderson-Sellers, A. and McGuffie, K. 1987. *A Climate Modelling Primer*. John Wiley and Sons, Suffolk, 217pp.

Henderson-Sellers, A., Yang, Z.-L. and Dickinson, R.E. 1993. The Project for Intercomparison of Land-surface Parameterization Schemes. *Bulletin of the American Meteorological Society* **74**(7), 1335-1349.

Intergovernmental Panel on Climate Change (IPCC). 1990. *The IPCC Scientific Assessment.* (Working Group 1). Houghton, J.T., Jenkins, G.J. and Ephraums, J.J. (editors), Cambridge University Press, Cambridge, 365pp.

Intergovernmental Panel on Climate Change (IPCC). 1992. *Climate Change 1992, The Supplementary Report to the IPCC Scientific Assessment.* Houghton, J.T., Callander, B.A. and Varney, S.K. (editors), Cambridge University Press, Cambridge, 200pp.

Intergovernmental Panel on Climate Change (IPCC). 1996. *Climate Change 1995 – The Science of Climate Change: Contribution of Working Group 1 to the Second Assessment Report of the Intergovernmental Panel on Climate Change.* Houghton, J.T., Meira Filho, L.G., Callander, B.A., Harris, N., Kattenberg, A. and Maskell, K. (editors), Cambridge University Press, Cambridge, 572pp.

Intergovernmental Panel on Climate Change (IPCC). 2000. *Emissions Scenarios*. Cambridge University Press, Cambridge, 599pp.

Jackson, J.E. 1991. *A User's Guide to Principal Components*. Wiley, New York, 569pp.

Johns, T.C., Carnell, R.E., Crossley, J.F., Gregory, J.M, Mitchell, J.F.B., Senior, C.A., Tett, S.F.B. and Wood, R.A. 1997. The second Hadley Centre coupled ocean-atmosphere GCM: model description, spinup and validation. *Climate Dynamics* **13**, 103-134.

Joubert, A.M. 1997. Simulations by the Atmopsheric Model Intercomparison Project of atmospheric circulation over southern Africa. *International Journal of Climatology*, **17**(11), 1129-1154.

Kalnay, E., Kanamitsu, M., Kistler, R., Collins, W., Deaven, D., Gandin, L., Iredell, M., Saha, S., White, G., Woollen, J., Zhu, Y., Chelliah, M., Ebisuzaki, W., Higgins, W., Janowiak, J., Mo, K.C., Ropelewski, C., Wang, J., Leetma, A., Reynolds, R., Jenne, R. and Joseph, D. 1996. The NCEP/NCAR 40-year reanalysis project. *Bulletin of the American Meteorological Society* **77**(3), 437-471.

Kutzbach, J., Bonan, G., Foley, J. and Harrison, S.P. 1996. Vegetation and soils feedbacks on the response of the African monsoon to orbital forcing in the early to middle Holocene. *Nature* **384**, 623-626.

Lambert, S.J. and Boer, G.J. 2000. CMIP1 Evaluation and intercomparison of coupled climate models. Submitted to *Climate Dynamics*.

Leemans, R. 1998: Biogeochemical and Biogeophysical feedbacks: Changes in vegetation distribution. *IPCC Workshop on Rapid non-linear Climate Change*, Noordwijkerhout, the Netherlands, 31 March - 2 April 1998 (Unpublished Workshop Report).

Leemans, R. and Cramer, W. 1991. *The IIASA database for monthly mean values of temperature, precipitation and cloudiness of a global terrestrial grid*. International Institute for Applied Systems Analysis (IIASA). RR-91-18.

Levis, S., Foley, J.A., Brovkin, V. and Pollard, D. 1999. On the stability of the high-latitude climate-vegetation system in a coupled atmosphere-biosphere model. *Global Ecology and Biogeography* **8**, 489-500.

Macdonald, I.A.W. 1991. Man's role in changing the face of southern Africa. In: Huntley, B.J. (editor), *Biotic Diversity in Southern Africa Concepts and Conservation*. Oxford University Press, Cape Town, 380pp.

McGuffie, K. and Henderson-Sellers, A. 1999: *A Climate Modelling Primer* (second edition). John Wiley and Sons, Chichester, 253pp.

Meehl, G.A. 1992. *Global coupled models: atmosphere, ocean, sea ice*. In Trenberth, K.E. (editor). *Climate System Modeling*. Cambridge University Press, London, 788pp.

Meehl, G.A, Washington, W.M. and Karl, T.R. 1993. Low-frequency variablility and CO_2 transient climate change. *Climate Dynamics* **8**, 117-133.

Midgley, G.F. and O'Callaghan, M. 1993. *Review of the Likely Impacts of Climate Change on South African Flora and Vegetation*. Report prepared for the southern African Nature Foundation, 23pp.

Monserud, R.A. 1990. Methods for comparing global vegetation maps. *IIASA WP-90-40*. International Institute for Applied Systems Analysis, Laxenburg, Austria.

Murphy, J.M. 1995. Transient response of the Hadley Centre coupled ocean-atmosphere model to increasing carbon dioxide. Part I, Control climate and flux adjustment. *Journal of Climate* **8**, 36-56.

Murphy, J.M. and Mitchell, J.F.B. 1997. Transient response of the Hadley Centre coupled ocean-atmosphere model to increasing carbon dioxide. Part II. Spatial and temporal structure of response. *Journal of Climate* **8**, 57-80.

Noilhan, J. and Planton, S. 1989. A Simple parameterization of land surface processes for meteorological models. *Monthly Weather Review* **117**, 536-549.

Parry, M. and Carter, T. 1998. *Climate Impact and Adaptation Assessment*. Earthscan publications, London, 166pp.

Peixoto, J.P. and Oort, A.H. 1992. *Physics of Climate*. American Institute of Physics, New York, 520pp.

Phillips, N.A. 1956. The general circulation of the atmosphere: A numerical experiment. *Quarterly Journal of the Royal Meteorological Society* **82**, 123-164.

Pocock, D.C.D and Wishart, D. 1969. Methods of deriving multi-factor uniform regions. *Transactions Institute of British Geographers* **47**, 73-98.

Pollard, D. and Thompson, S.L. 1995a. A Global Climate Model (GENESIS) with a Land-Surface Transfer Scheme (LSX). Part 1: Present Climate Simulation. *Journal of Climate* **8**(4), 732-761.

Pollard, D. and Thompson, S.L. 1995b. Use of a Land-Surface-Transfer Scheme (LSX) in a Global Climate Model: The Response to Doubling Stomatal Resistance. *Global and Planetary Change* **10**, 129-161.

Prentice, I.C., Cramer, W., Harrison, S.P., Leemans, R., Monserud, R.A. and Solomon, A.M. 1992. A global biome model based on plant physiology and dominance, soil properties and climate. *Journal of Biogeography* **19**, 117-134.

Richman, M.B. 1986. Rotation of principal components. *Journal of Climatology* **6**, 293-335.

Roeckner, E.L., Bengtsson, L., Feitcher, J., Lelieveld, J. and Rodhe, H. 1999. Transient climate change with a coupled atmosphere-ocean GCM including the tropospheric sulfur cycle. *Journal of Climate* **12**, 3004-3032.

Rosenberg, N.J. 1993. Facts and uncertainties of Climate Change. In: Darmstadter, J. and Toman, M.A. (editors), *Assessing Surprises and Nonlinearities in Greenhouse Warming, Proceedings of an Interdisciplinary Workshop*. Resources for the Future, Washington DC, 158pp.

Rossow, W.B. and Zhang, Y.-C. 1995. Calculations of surface and top-of-atmosphere radiative fluxes from physical quantities based on ISCCP datasets: 2. Validation and first results. *Journal of Geophysical Research* **100**, 1167-1197.

Rutherford, M.C. 1997. Categorization of Biomes. In: Cowling, R.M. and Richardson, D.M. and Pierce, S.M. (editors), *Vegetation of Southern Africa*. Cambridge University Press, Cambridge, 615pp.

Rutherford, M.C. and Westfall, R.H. 1986. Biomes of southern Africa – An Objective Categorization. *Memoirs of the Botanical Survey of South Africa No.***54**, Botanical Research Institute, Department of Water Supply, South Africa, 98pp.

Salati, E. and Vose, P.B. 1987. Amazon Basin: a system in equilibrium. *Science* **225**, 129-137.

Sato, N., Sellers, P.J., Randall, D.A., Schneider, E.K., Shukla, J., Kinter III, J.L., Hou, Y.-T. and Albertazzi, E. 1989. Effects of implementing the Simple Biosphere Model in a general circulation model. *Journal of the Atmospheric Sciences* **46**(18), 2757-2782.

Schulze, R.E. 1997. Climate. In: Cowling, R.M. and Richardson, D.M. and Pierce, S.M. (editors). *Vegetation of Southern Africa*. Cambridge University Press, Cambridge, 615pp.

Sellers, P.J., Mintz, Y., Sud, Y.C. and Dalcher, A. 1986. A Simple Biosphere Model (SiB) Using Point Micrometeorological and Biophysical Data. *Journal of Applied Meteorology* **26**, 622-651.

Sellers, P.J., Randall, D.A., Collatz, G.J., Berry, J.A., Field, C.B., Dazlich, D.A., Zhang, C., Collelo, G.D. and Bounoua, L. 1996a. A revised land surface parameterization (SiB2) for atmospheric GCMs, Part 1: Model formulation. *Journal of Climate* **9**, 676-705.

Sellers, P.J., Los, S.O., Tucker, C.J., Justice, C.O., Dazlich, D.A., Collatz, G.J. and Randall, D.A. 1996b. A revised land surface parameterization (SiB2) for atmospheric GCMs. Part 2: The generation of global fields of terrestrial biophysical parameters from satellite data. *Journal of Climate* **9**, 706-737.

Sellers, P.J., Dickinson, R.E., Randall, D.A., Betts, A.K., Hall, F.G., Berry, J.A., Collatz, G.J., Denning, A.S., Mooney, H.A., Nobre, C.A., Sato, N., Field, C.B., Hendeson-Sellers, A. 1997. Modeling the exchanges of energy, water, and carbon between continents and the atmosphere. *Science* **275**, 502-509.

Sellers, P.J. 1998: Recent Progress and Future Challenges in modeling and observing biosphere-atmosphere interactions. *IPCC Workshop on Rapid non-linear Climate Change*, Noordwijkerhout, the Netherlands, 31 March - 2 April 1998 (Unpublished Workshop Report).

Smagorinsky, J. 1963. General circulation experiments with the primitive equations. 1. The basic experiment. *Monthly Weather Review* **91**, 99-164.

Smith, R.N.B. 1990. A scheme for predicting layer clouds and their water content in a general circulation model. *Quarterly Journal of the Royal Meteorological Society* **116**, 435-460.

Slingo, A. and Wilderspin, R.C. 1986. Development of a revised long-wave radiation scheme for an atmospheric general circulation model. *Quarterly Journal of the Royal Meteorological Society* **112**, 371-386.

Stouffer, R.J. and Manabe, S. 1999. Response of a coupled ocean-atmosphere model to increasing atmospheric carbon dioxide: Sensitivity to the rate of increase. *Journal of Climate* **12**(1), 2224-2237.

TEMPO (Testing Earth Systems Models with Palaeo-Observations) 1996. Potential role of vegetation feedbacks in the climate sensitivity of high-latitude regions: A case study at 6000 years B.P. *Global Biogeochemical Cycles* **10**(4), 727-736.

Trenberth, K.E. 1996. Coupled Climate System Modelling, in Giambelluca, T.W. and Henderson-Sellers, A. (editors) 1996. *Climate Change Developing Southern Hemisphere Perspectives*. John Wiley and Sons, West Sussex, England, 475pp.

Verseghy, D.L. 1991. CLASS: A Canadian Land Surface Scheme for GCMs, I. Soil Model. *International Journal of Climatology* **11**, 111-133.

Verseghy, D.L. 1993. CLASS: A Canadian Land Surface Scheme for GCMS, II: Vegetation Model and Coupled Runs. *International Journal of Climatology* **13**, 347-370.

Waggoner, P.E. 1993. Nonlinearities and suprises in the links of farming to climate or weather. In: Darmstadter, J. and Toman, M.A. (editors), *Assessing Surprises and Nonlinearities in Greenhouse Warming, Proceedings of an Interdisciplinary Workshop*. Resources for the Future, Washington DC, 158pp.

Webb, R.S., Rosenzweig, C.E. and Levine, E.R. 1993. Specifying land surface characteristics in general circulation models: Soil profile data set and derived water-holding capacities. *Global Biogeochemical Cycles* **7**, 97-108.

Whittow, J. 1984. *The Penguin Dictionary of Physical Geography*. Penguin Group, London, 591pp.

Woodward, F.I. 1987. *Climate and plant distribution*. Cambridge University Press, Cambridge, 174pp.

Woodward, F.I. and Cramer, W. 1996. Plant functional types and climatic changes: Introduction. *Journal of Vegetation Science* **7**, 306-308.

Woodward, F.I., Smith, T.M. and Emanuel, W.R. 1995. A global land primary productivity and phytogeography model. *Global Biogeochemical Cycles* **9**, 471-490.

APPENDICES

APPENDIX A

ACRONYMS

AMIP	Atmospheric Model Intercomparison Project
BATS	Biosphere-Atmosphere Transfer Scheme
CCCma	Canadian Centre for Climate Modelling and Analysis
CLASS	Canadian Land Surface Scheme
CMIP	Coupled Model Intercomparison Project
CSIRO	Commonwealth Scientific and Industrial Research Organisation
CSM	Climate System Model
EVE	Equilibrium Vegetation Ecology Model
GCM	General Circulation Model
GENESIS	Global Environmental and Ecological Simulation of Interactive Systems
GFDL	Geophysical Fluid Dynamics Laboratory
IBIS	Integrated Biosphere Simulator
IPCC	Intergovernmental Panel on Climate Change
ITCZ	Intertropical Convergence Zone
LSX	Land Surface Transfer Scheme
MRI	Meteorological Research Institute
NCAR	National Center for Atmospheric Research
NCEP	National Centers for Environmental Prediction
NIES	National Institute for Environmental Studies
NPP	Net Primary Production
PCA	Principal Components Analysis
PCM	Parallel Climate Model
SiB	Simple Biosphere Model
SRES	Special Report on Emissions Scenarios

APPENDIX B

TREND GRAPHS

Trend graphs for the 5 regions defined in Chapter 5 are included in the Appendix for Ibissta (static vegetation mean run) and P1-P5 for the early (period 1, defined as 2000-2030) and late (period 2, defined as 2050-2080) 21st century for the following annual variables:

- average evapotranspiration
- net primary productivity
- sensible heat fluxes
- soil temperature
- soil moisture

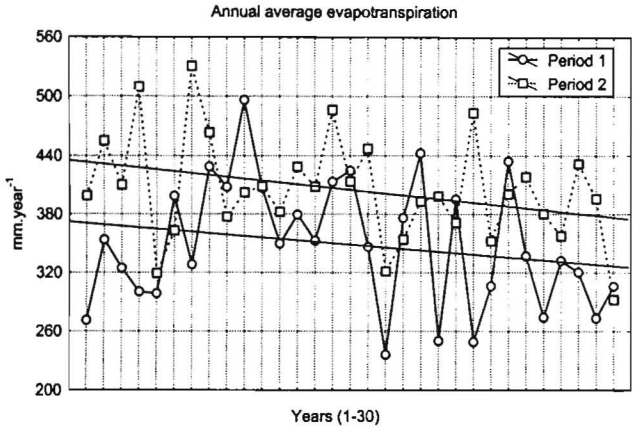

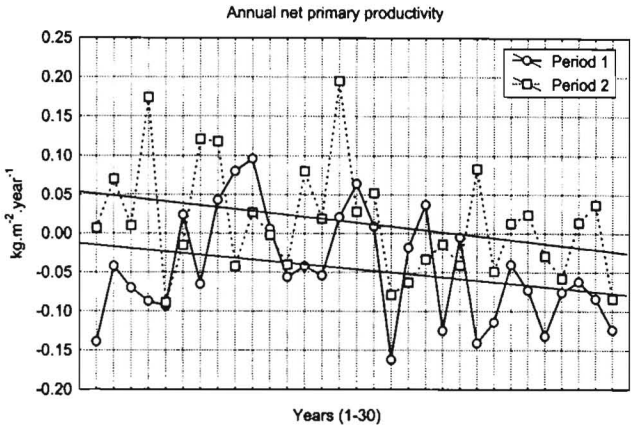

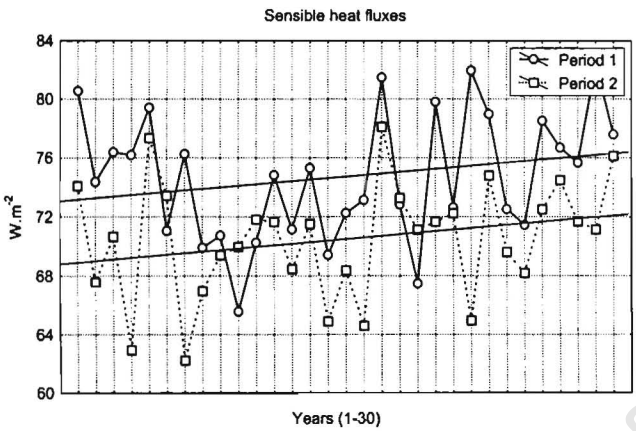

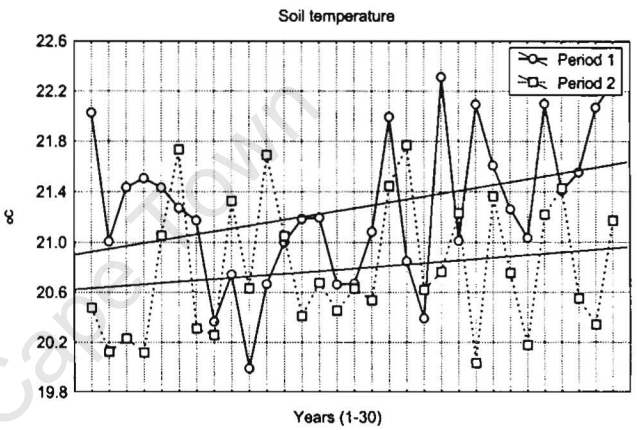

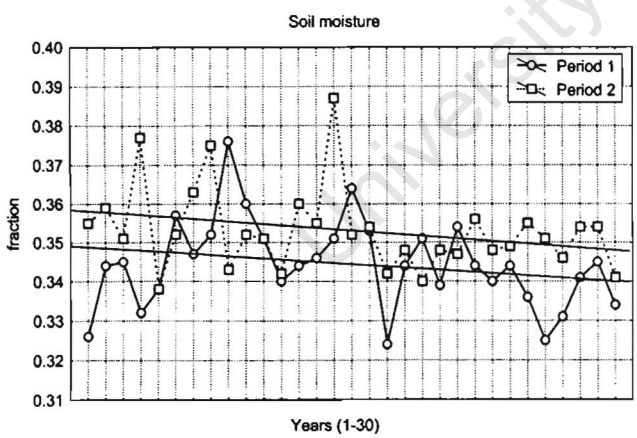

Trend graphs for region 1 for Ibissta

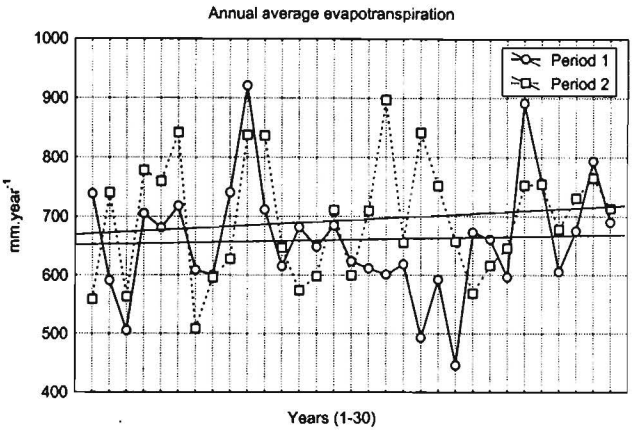

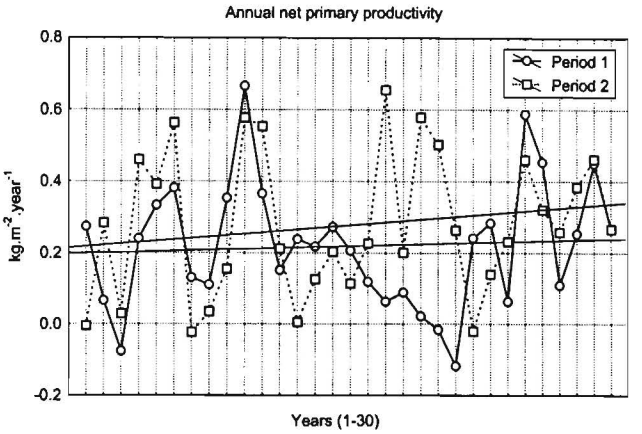

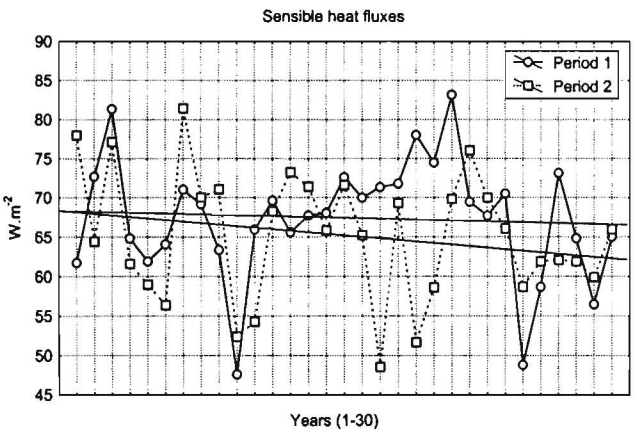

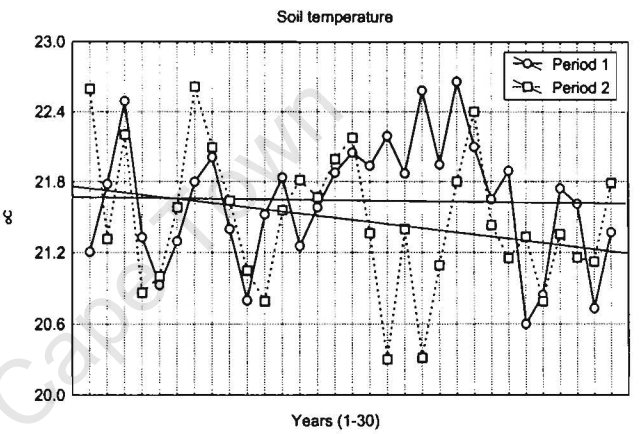

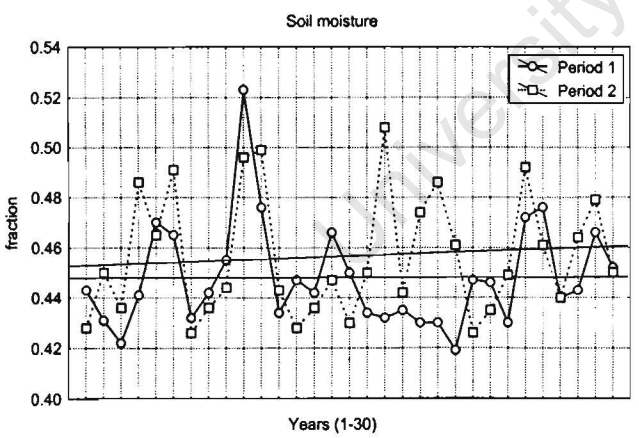

Trend graphs for region 2 for Ibissta

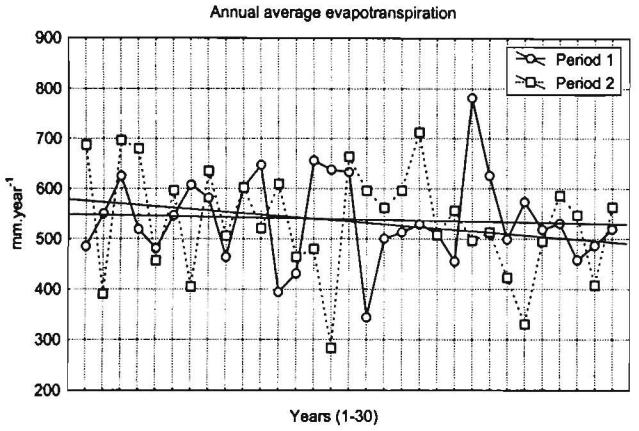

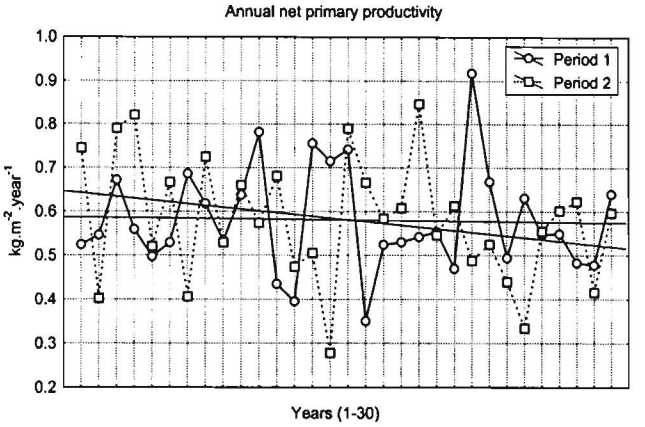

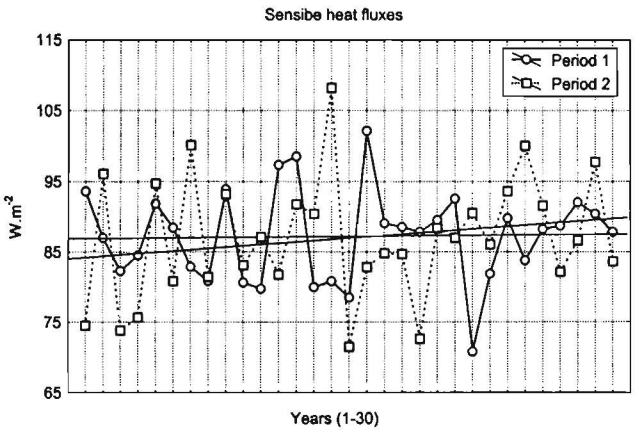

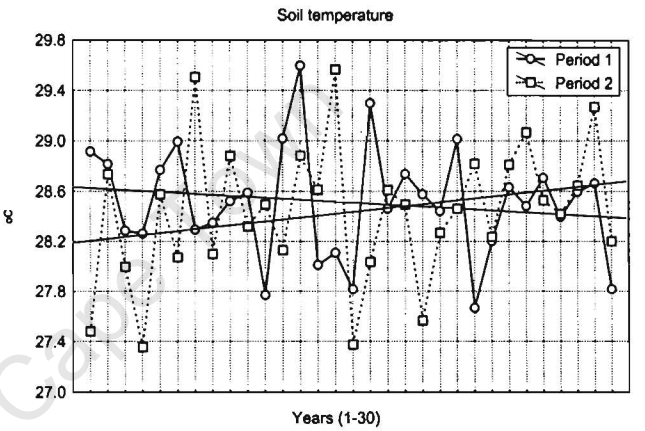

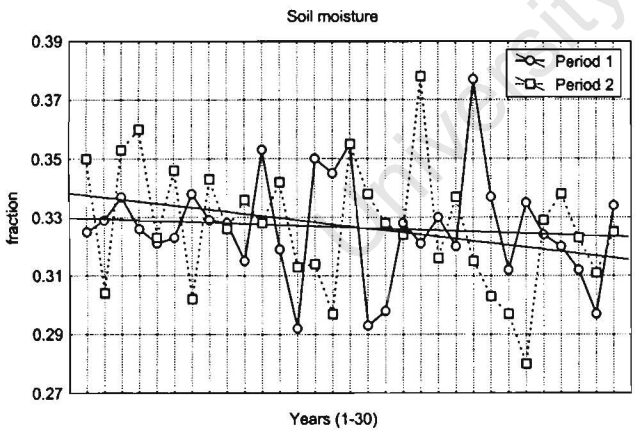

Trend graphs for region 3 for Ibissta

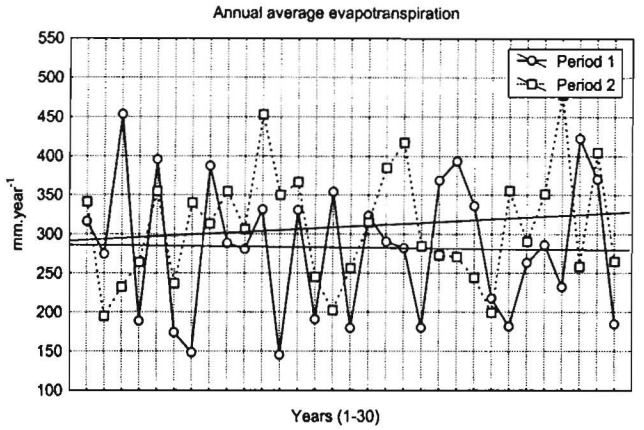

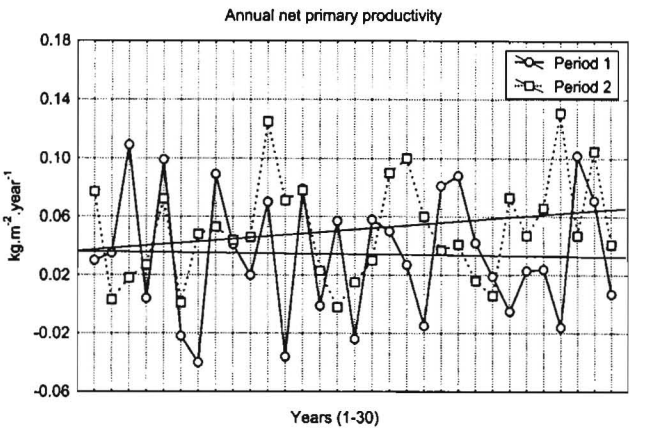

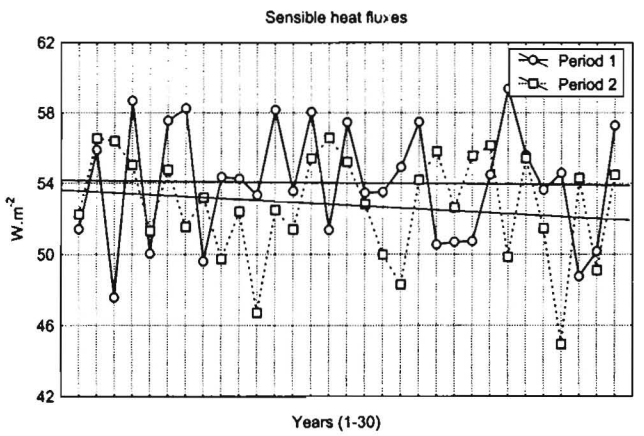

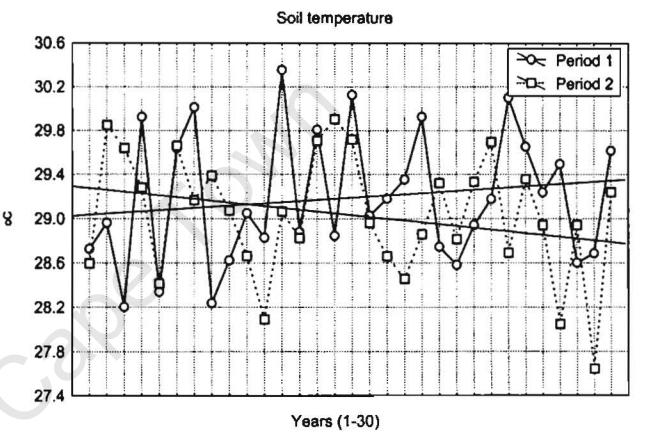

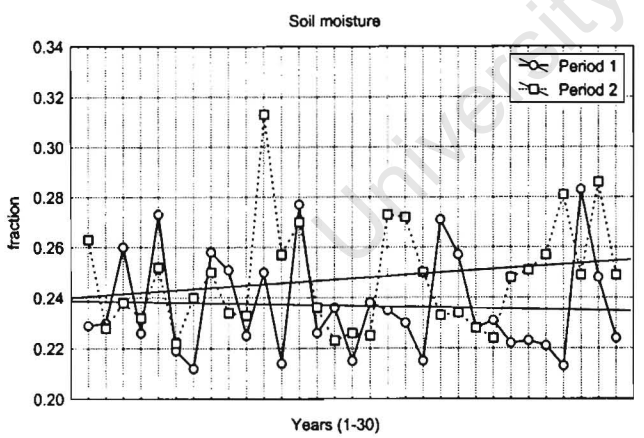

Trend graphs for region 4 for Ibissta

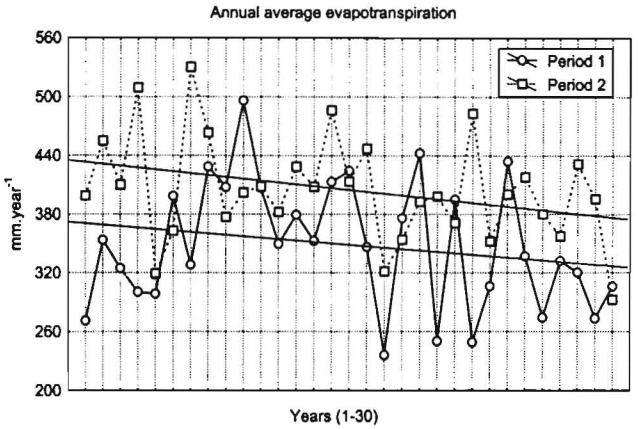

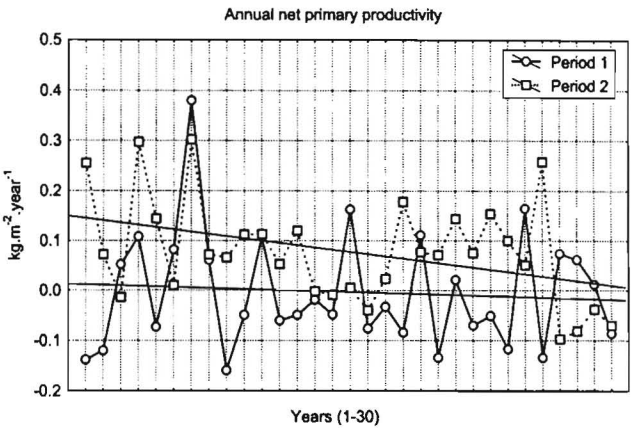

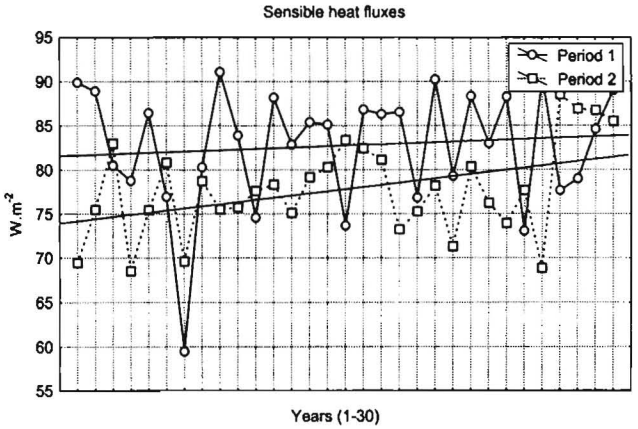

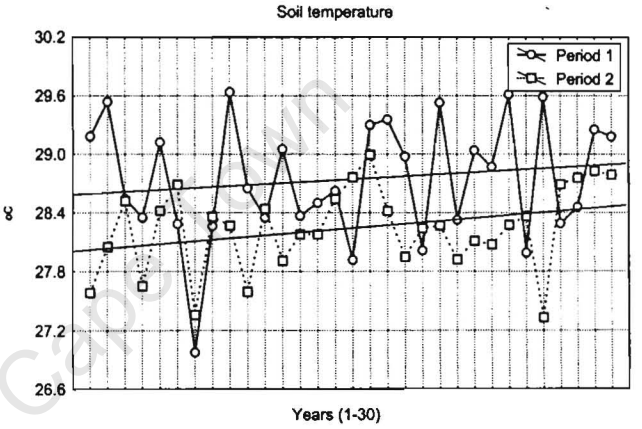

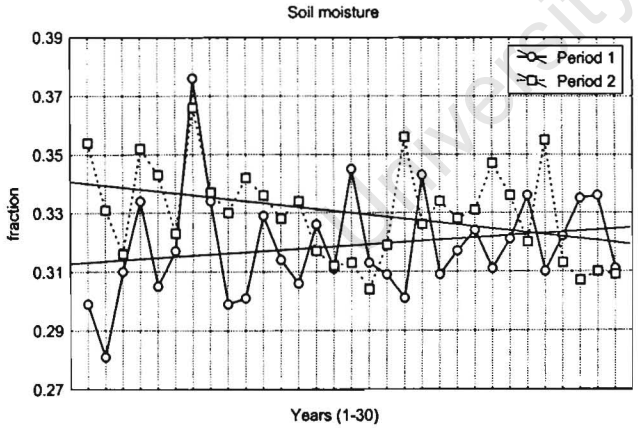

Trend graphs for region 5 for Ibissta

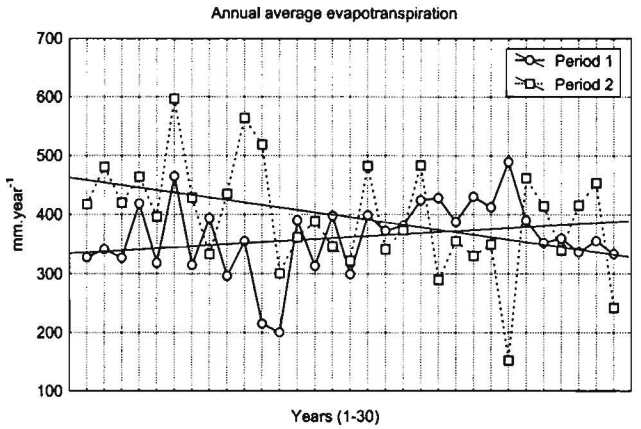

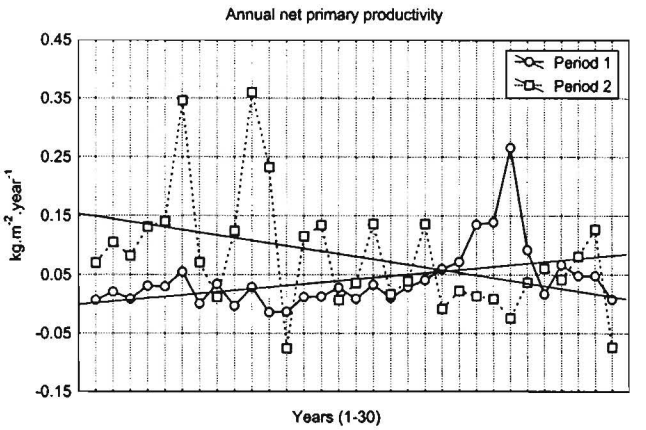

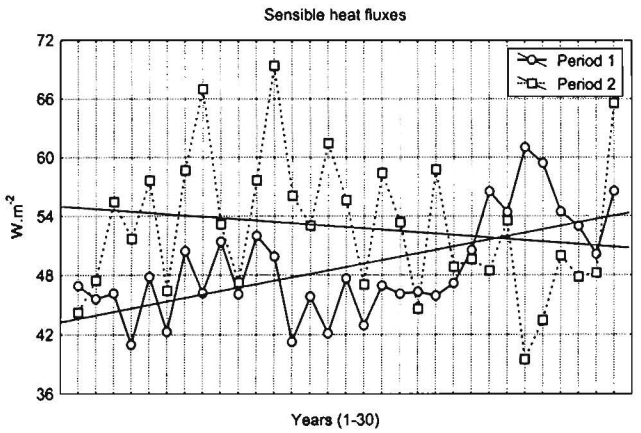

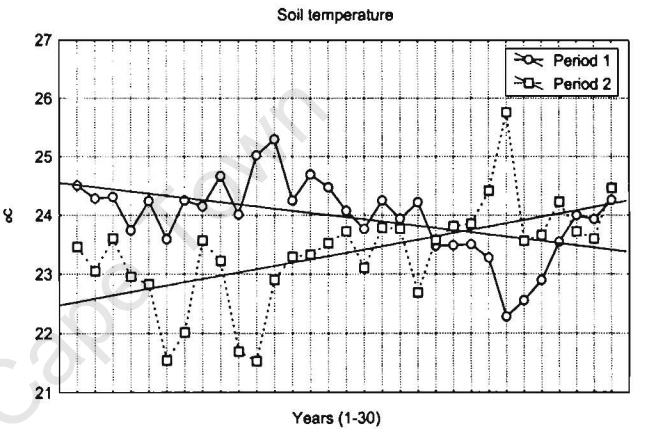

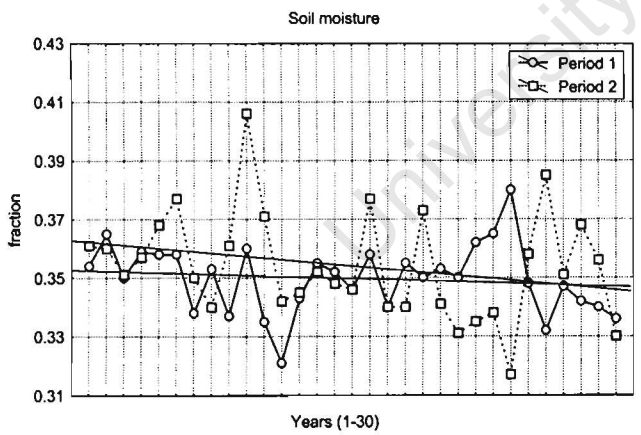

Trend graphs for region 1 for P1

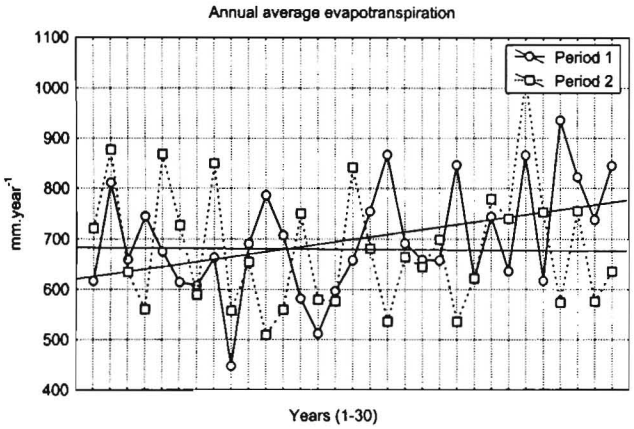

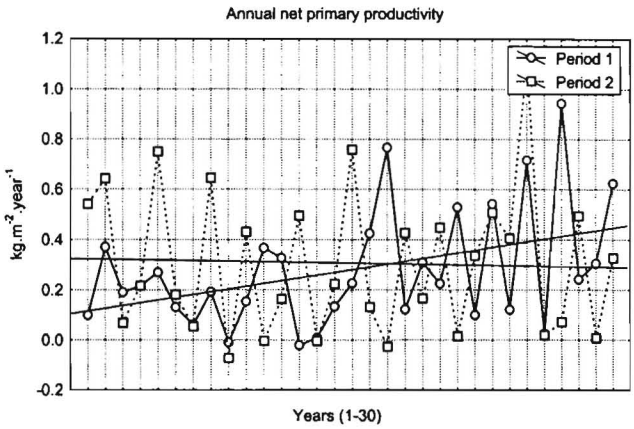

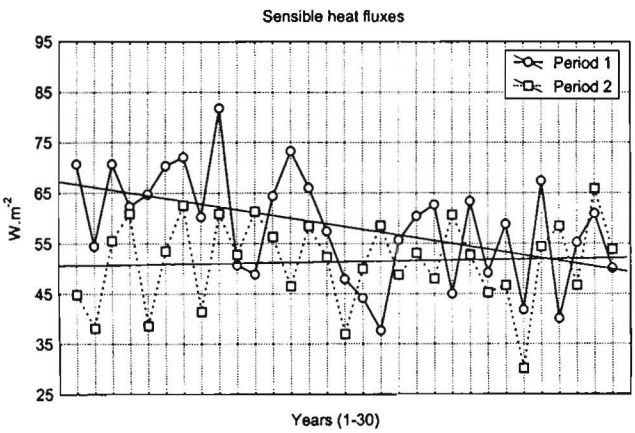

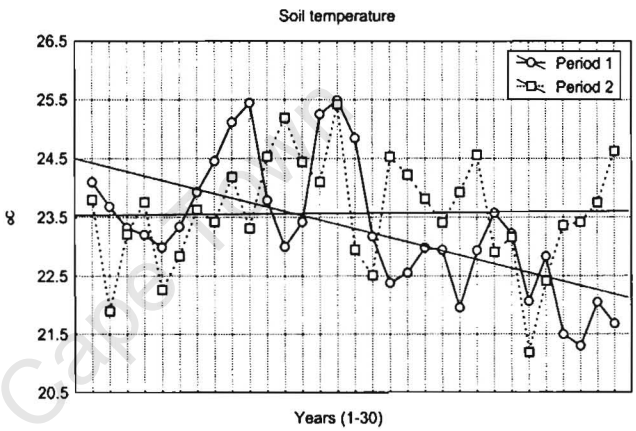

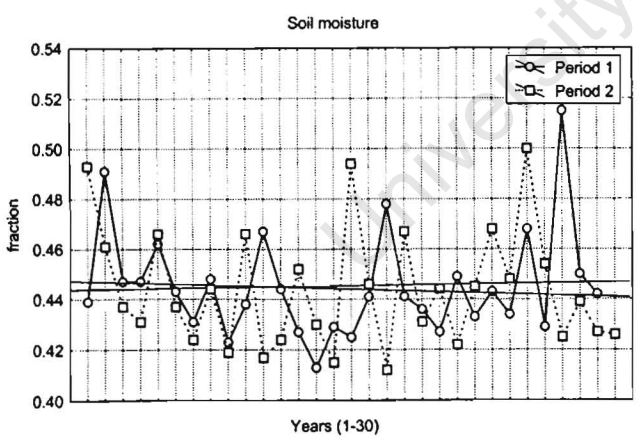

Trend graphs for region 2 for P1

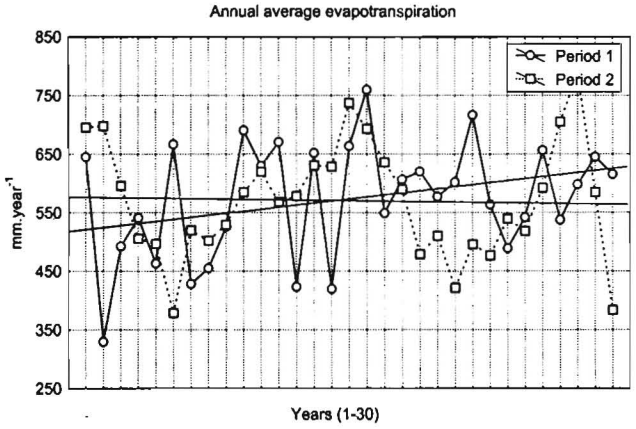

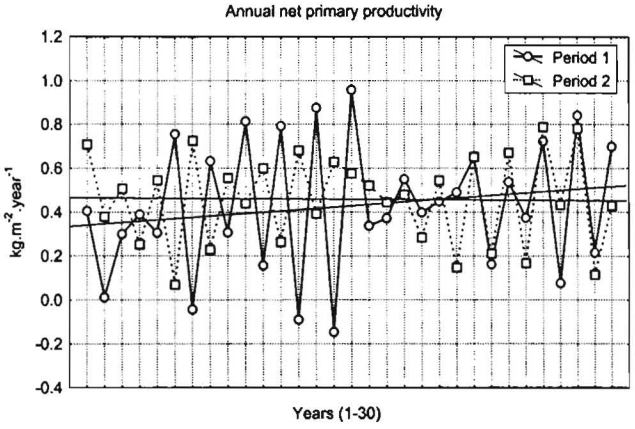

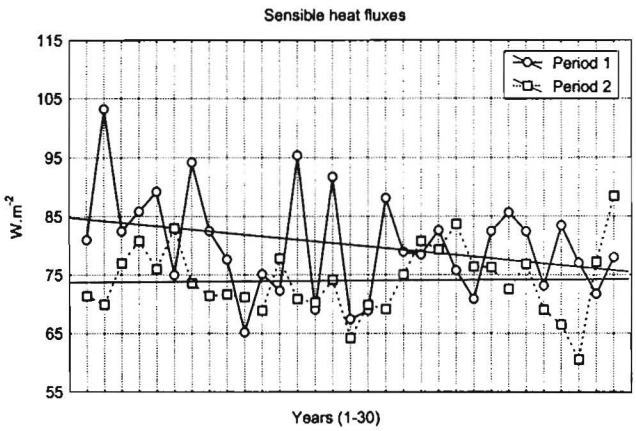

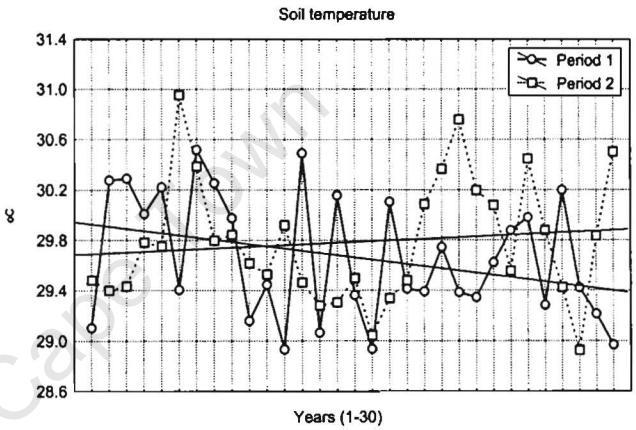

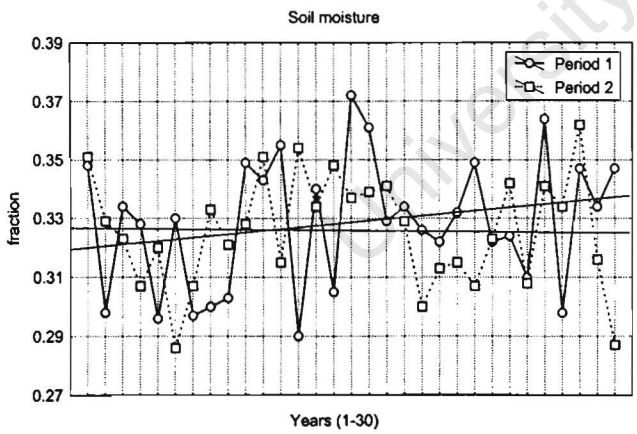

Trend graphs for region 3 for P1

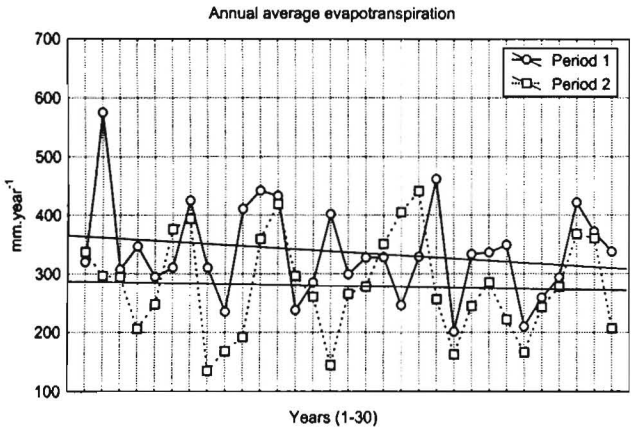

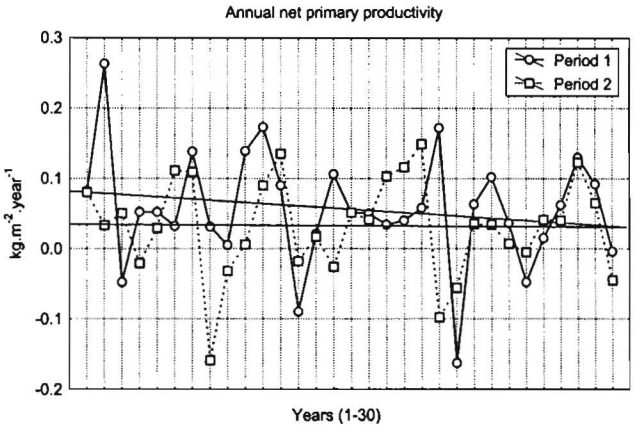

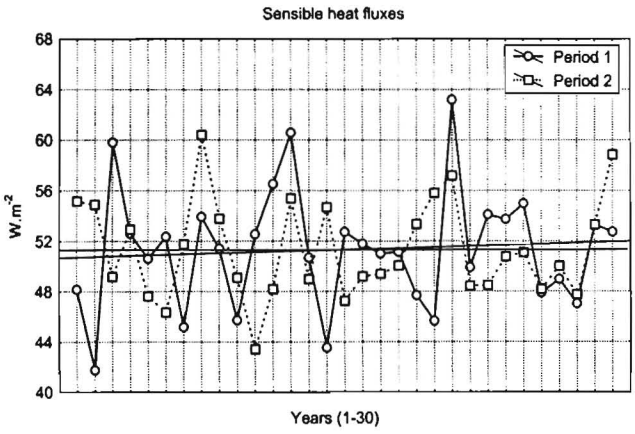

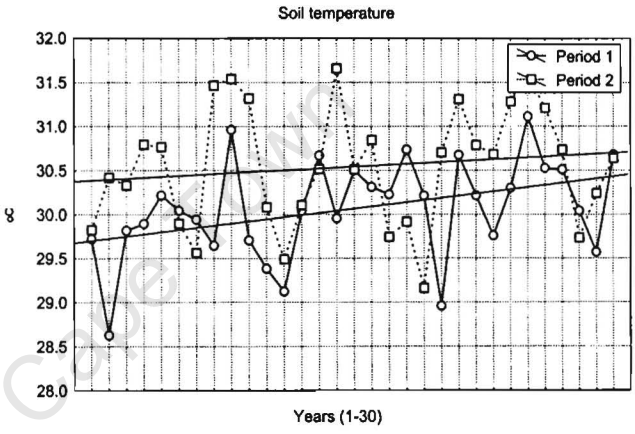

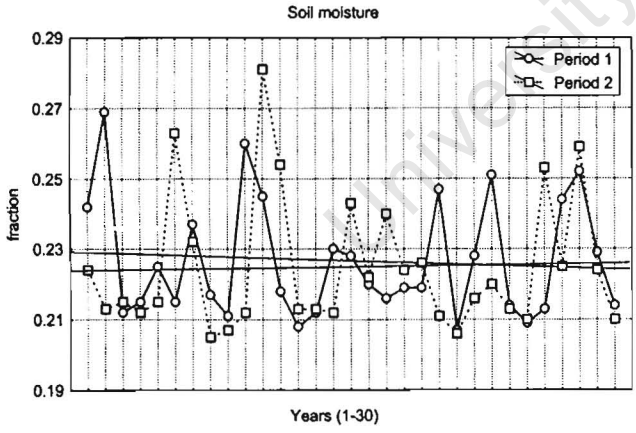

Trend graphs for region 4 for P1

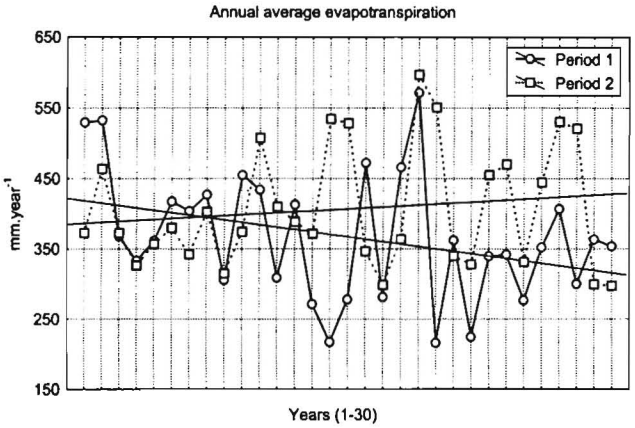

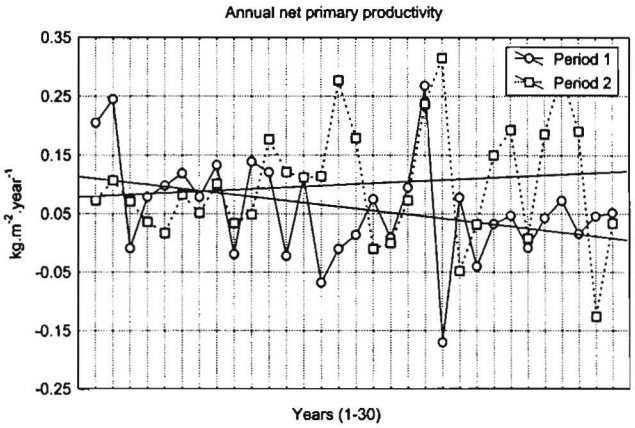

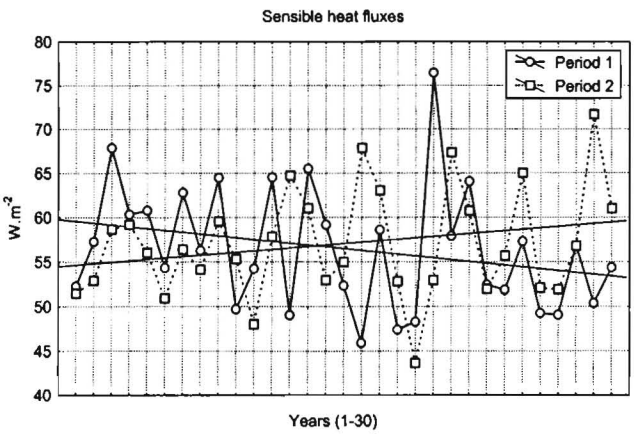

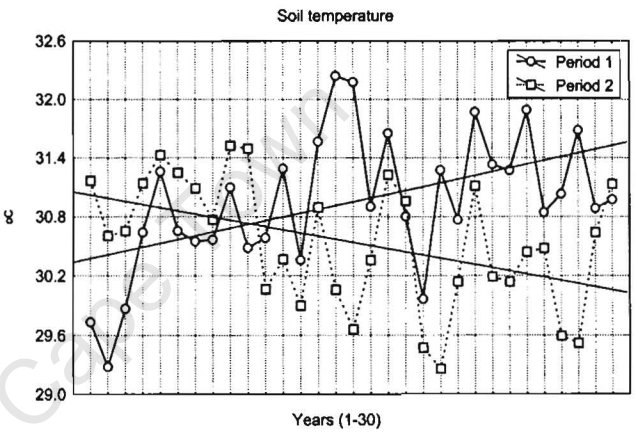

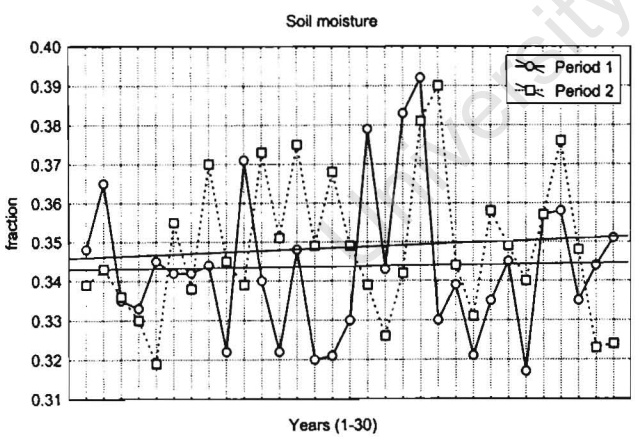

Trend graphs for region 5 for P1

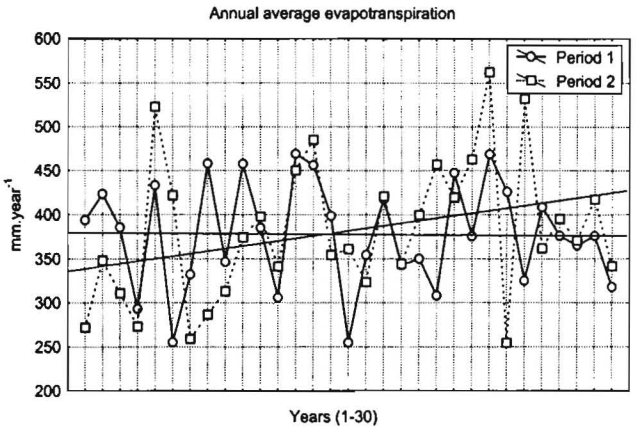

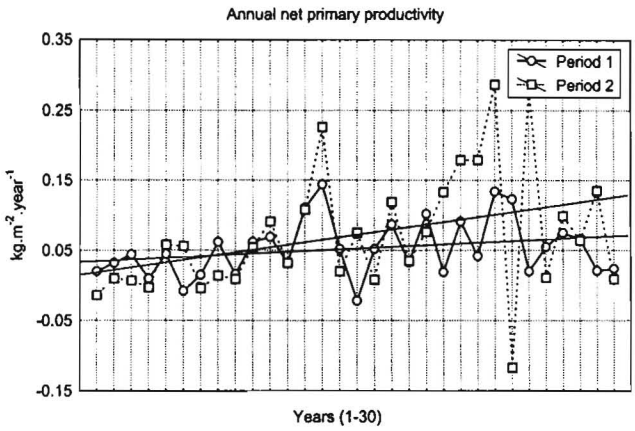

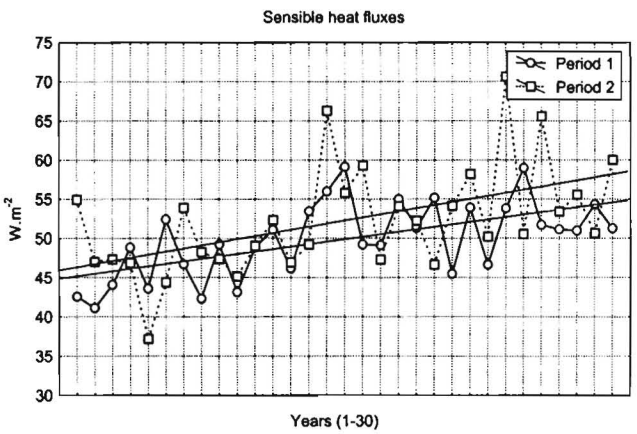

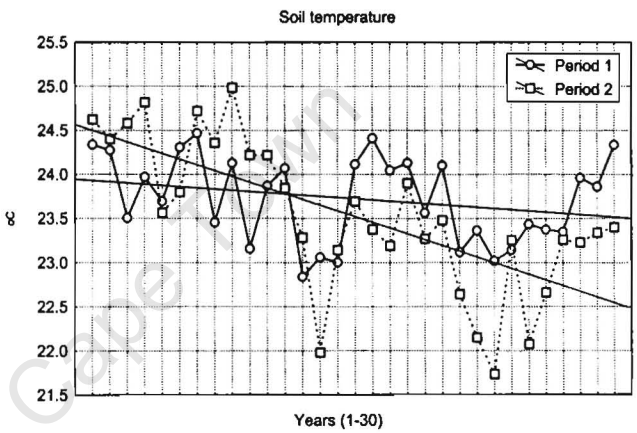

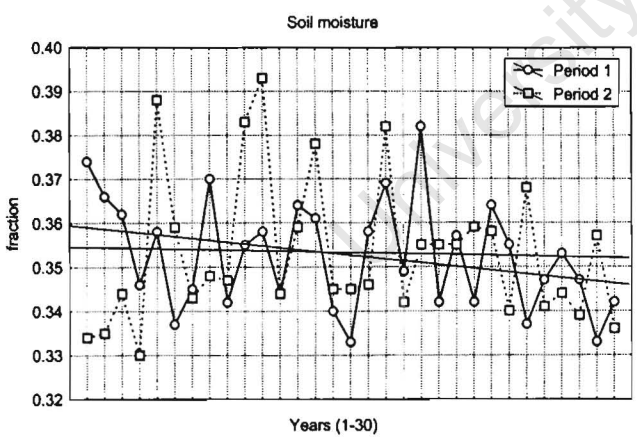

Trend graphs for region 1 for P2

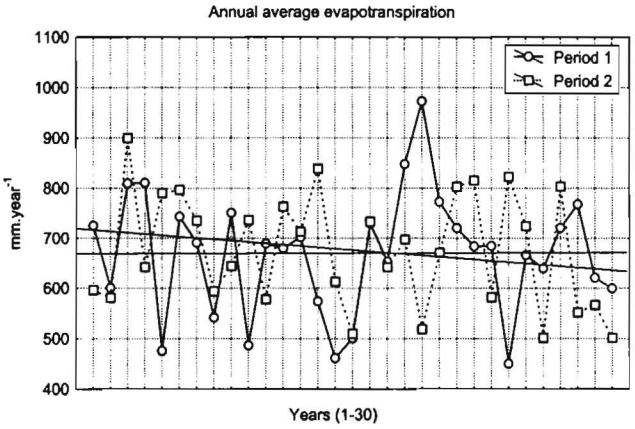

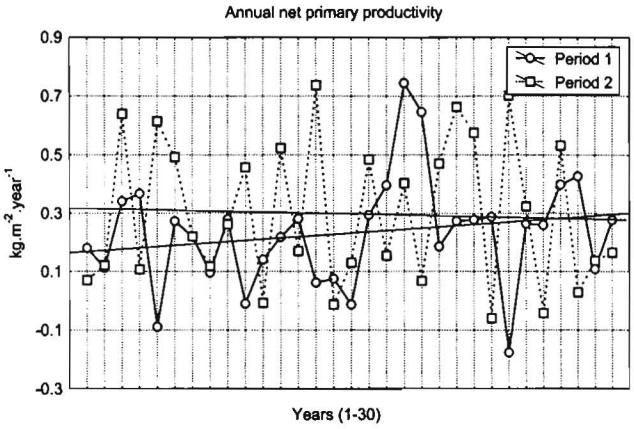

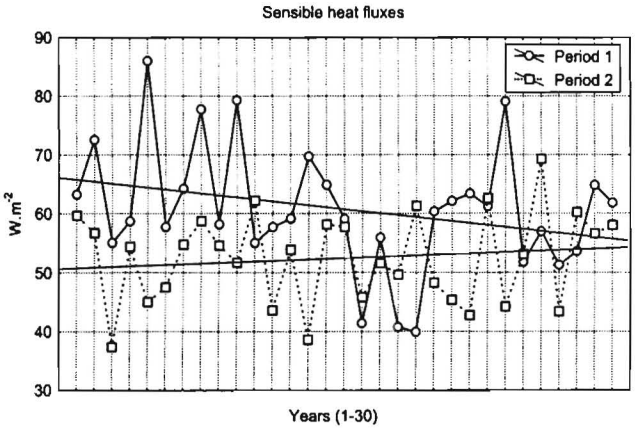

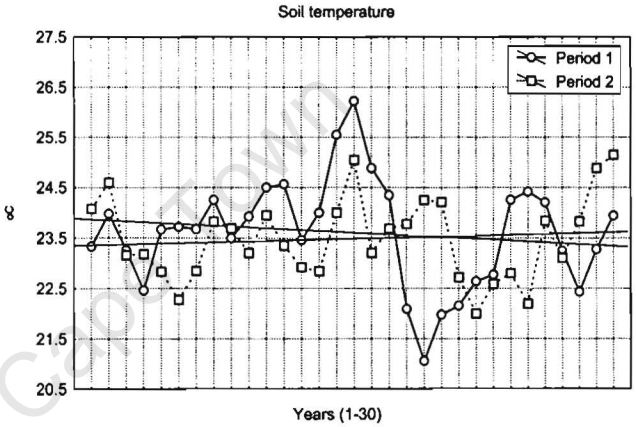

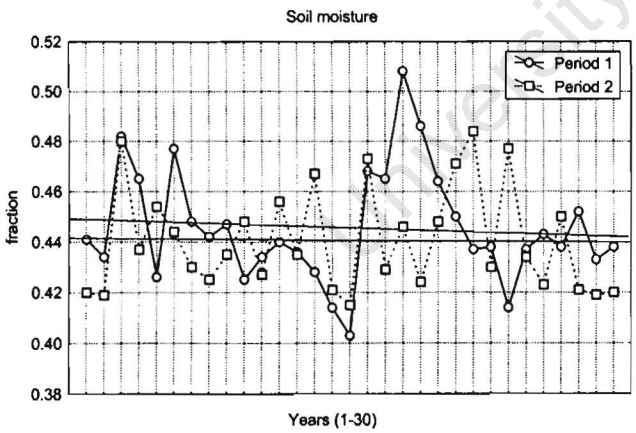

Trend graphs for region 2 for P2

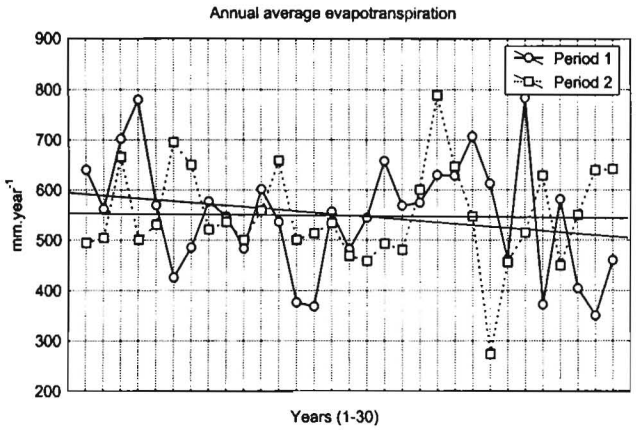

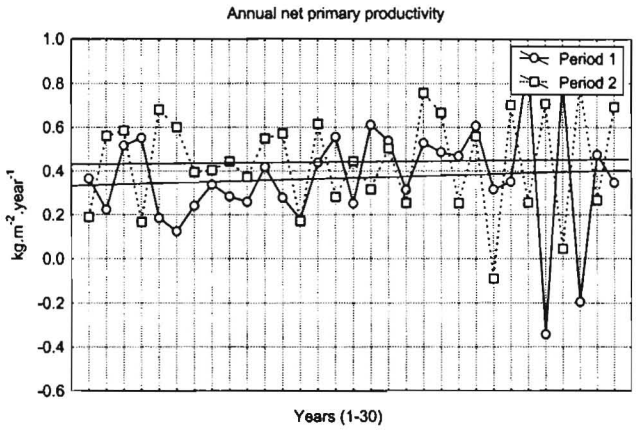

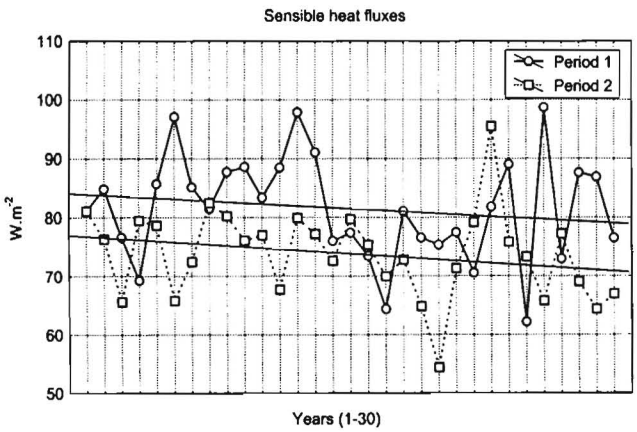

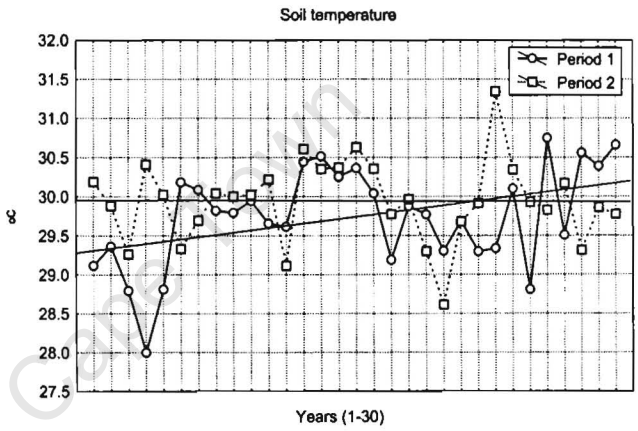

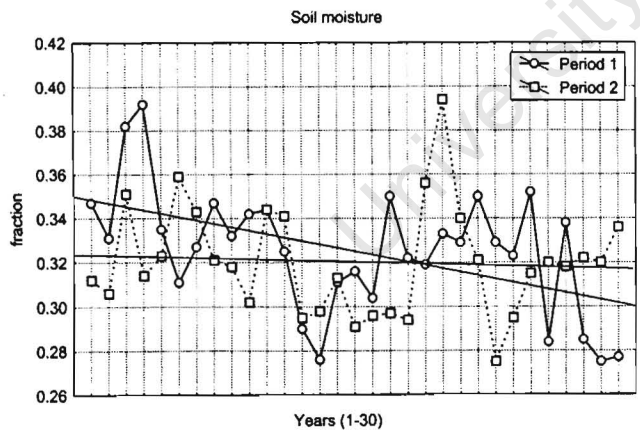

Trend graphs for region 3 for P2

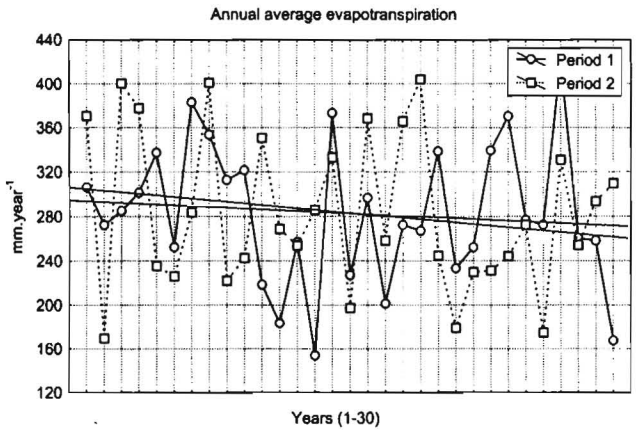

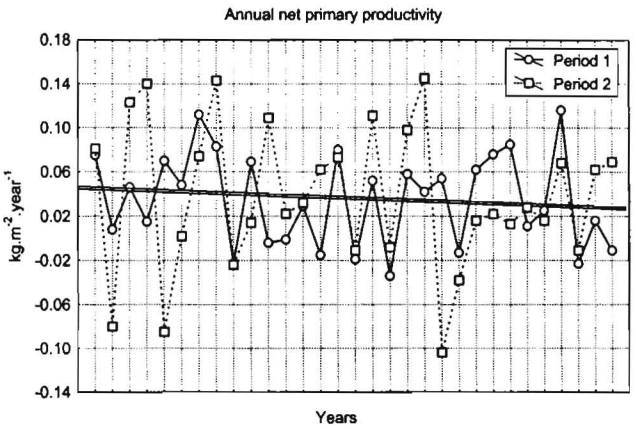

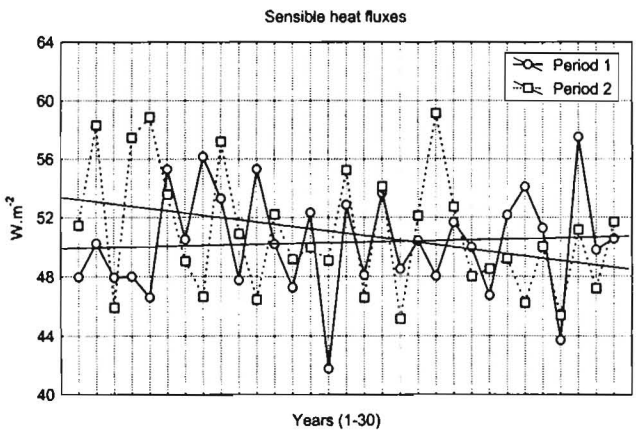

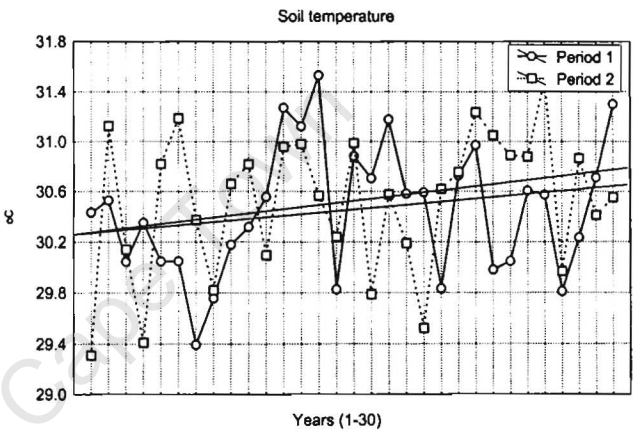

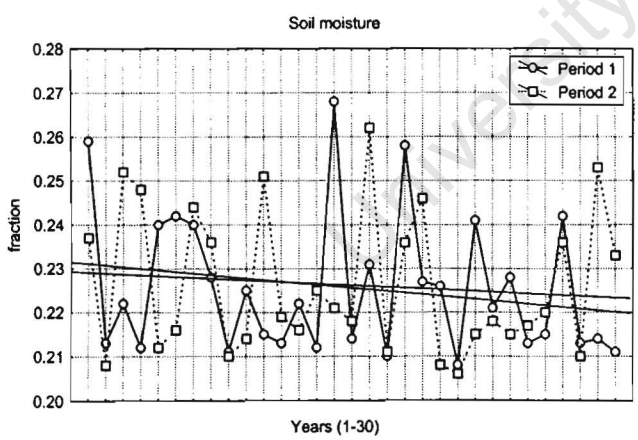

Trend graphs for region 4 for P2

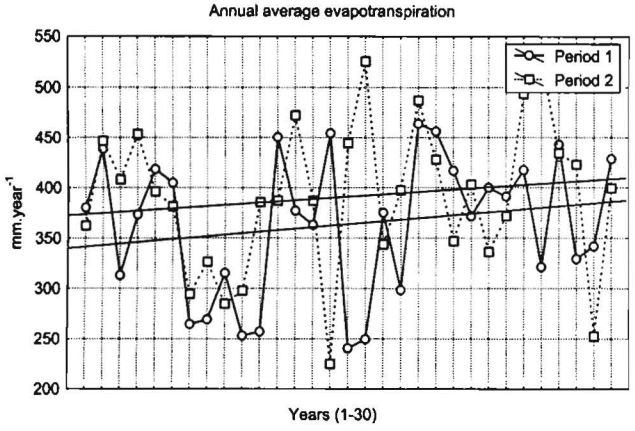

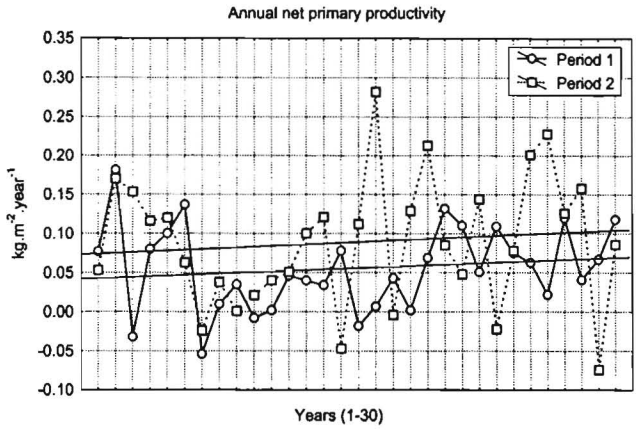

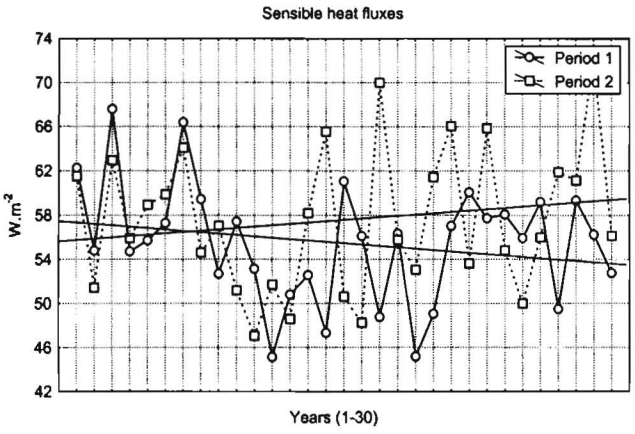

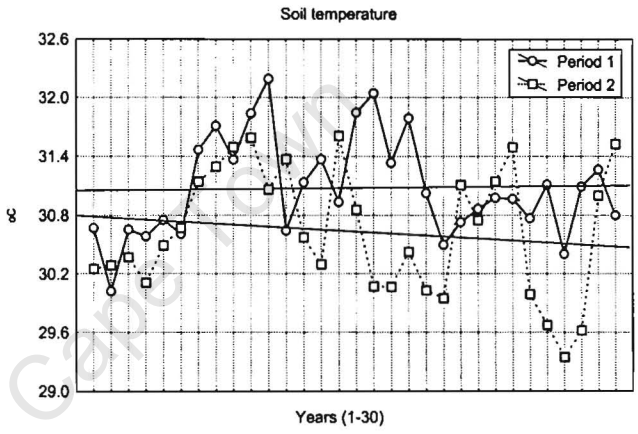

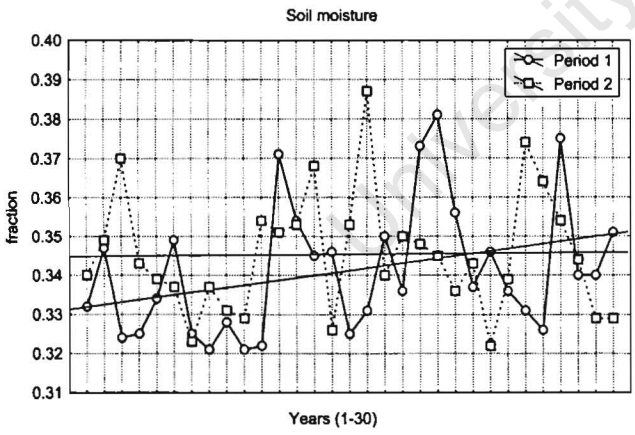

Trend graphs for region 5 for P2

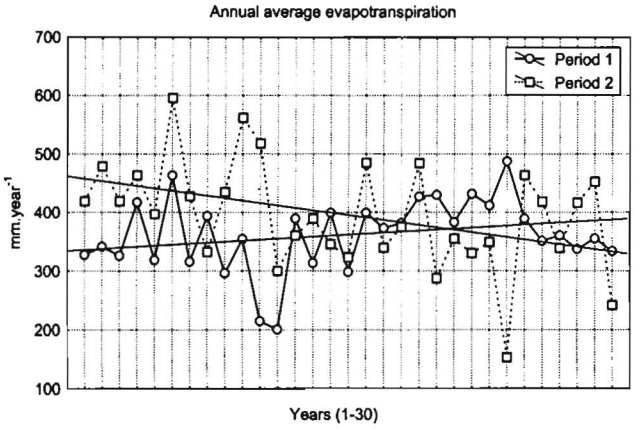

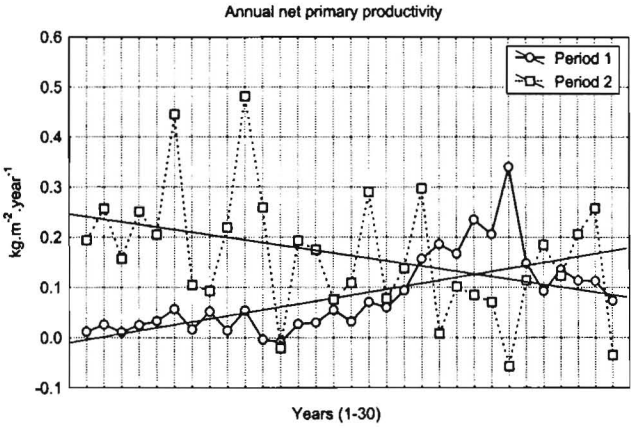

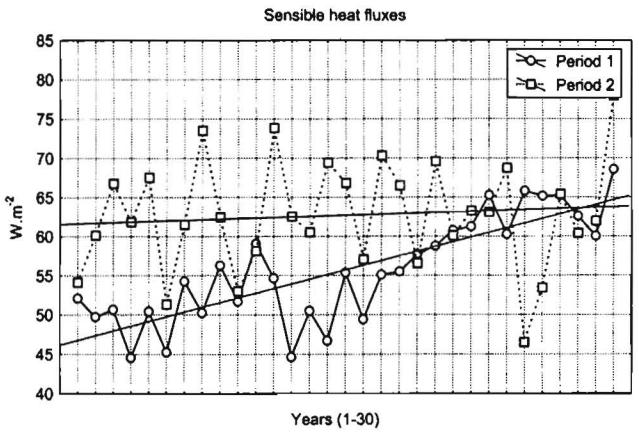

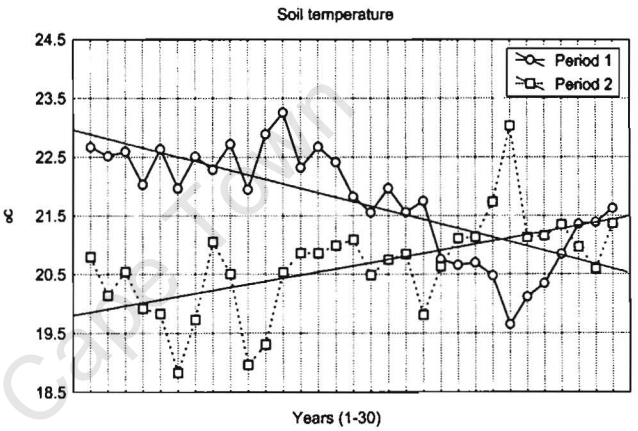

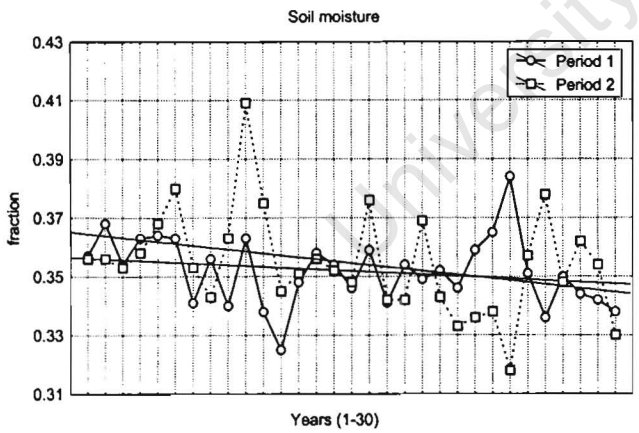

Trend graphs for region 1 for P3

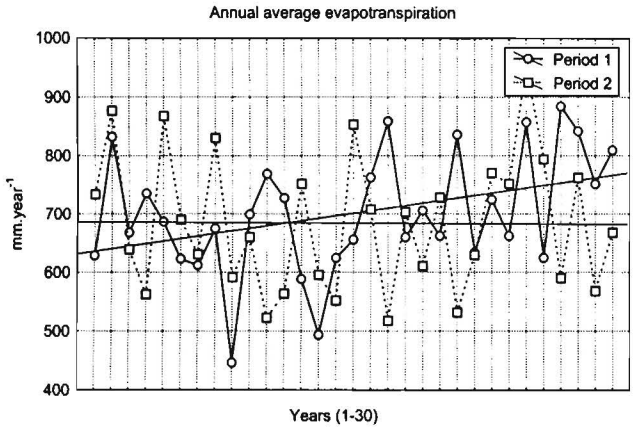

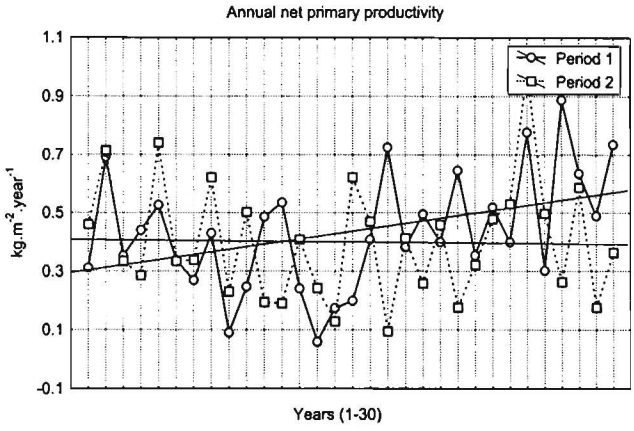

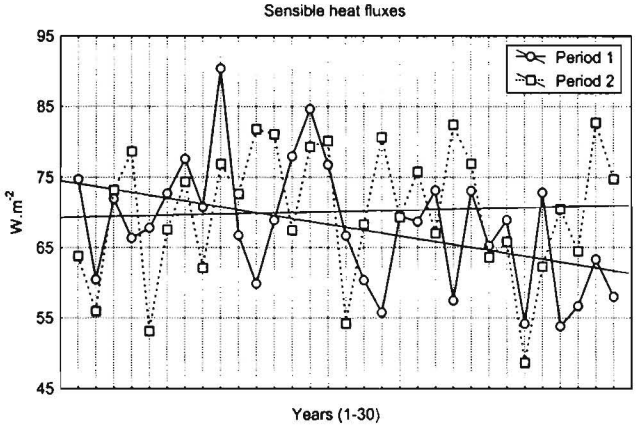

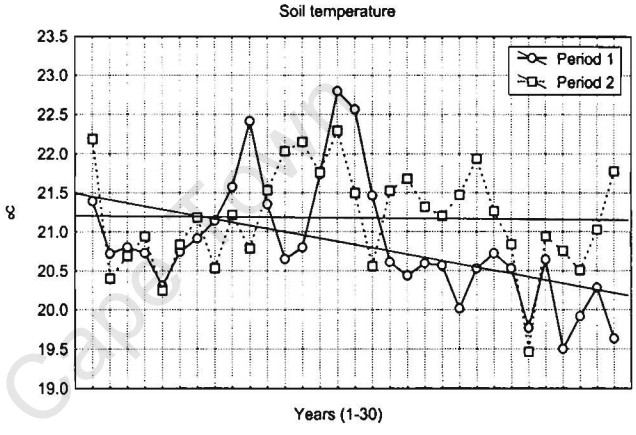

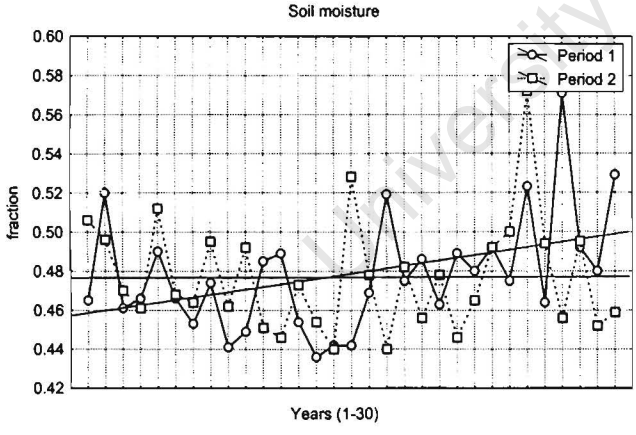

Trend graphs for region 2 for P3

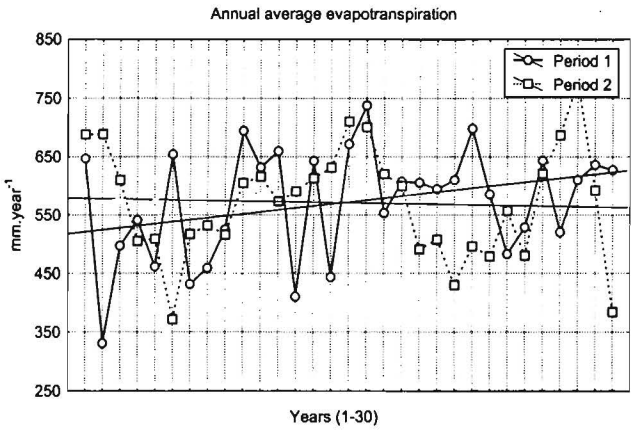

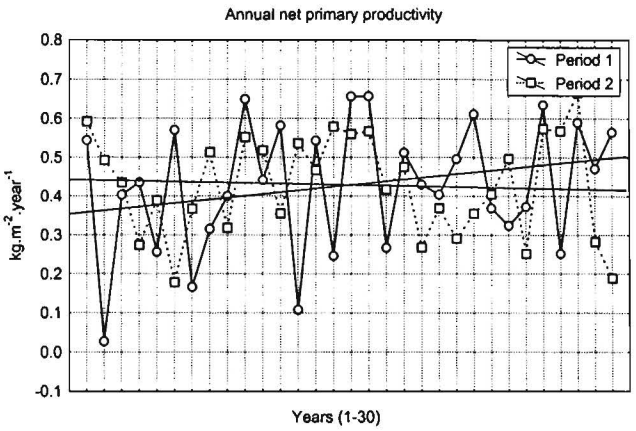

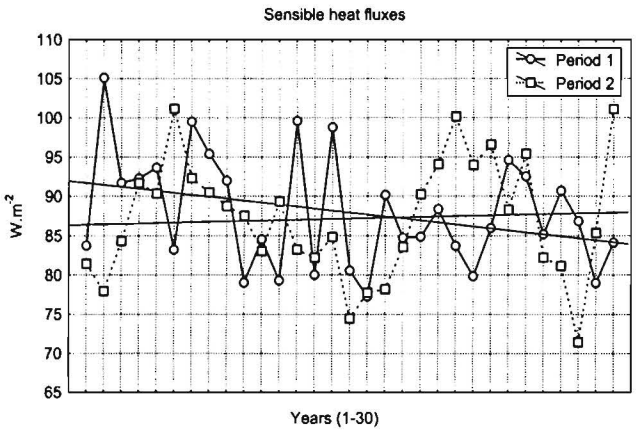

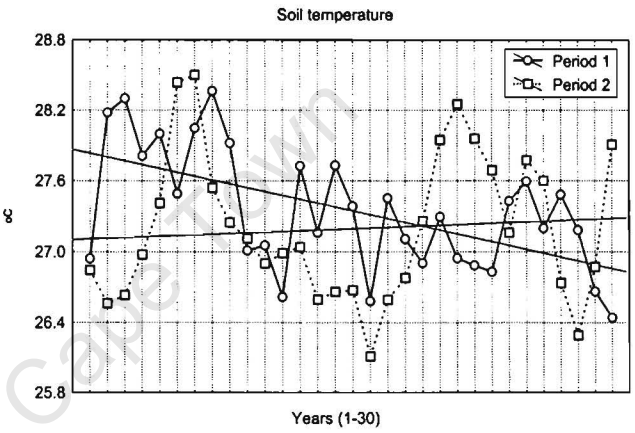

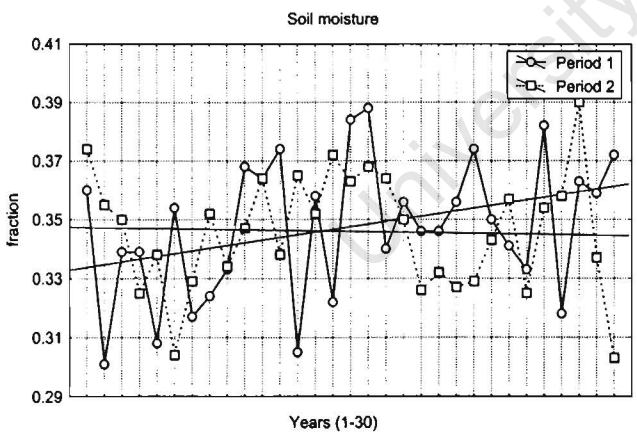

Trend graphs for region 3 for P3

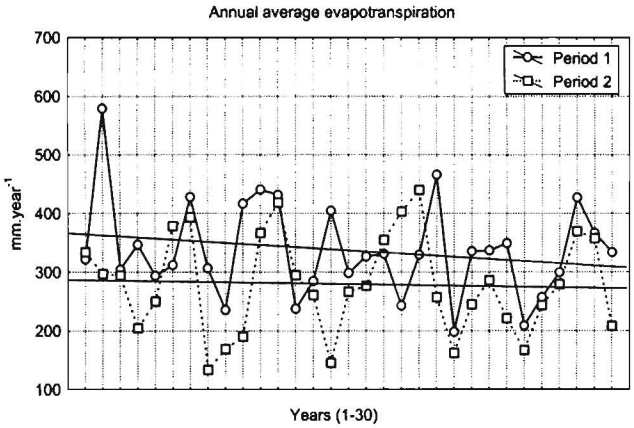

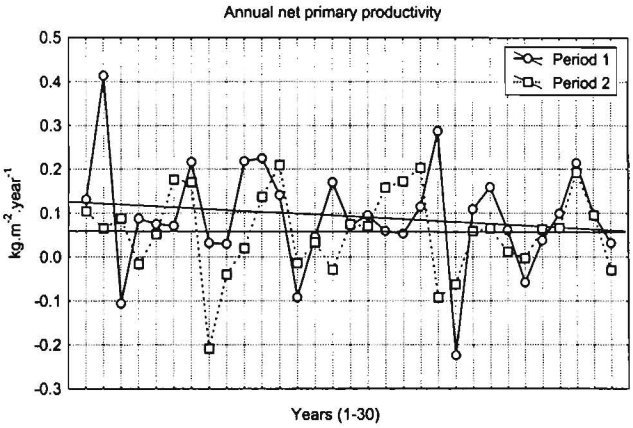

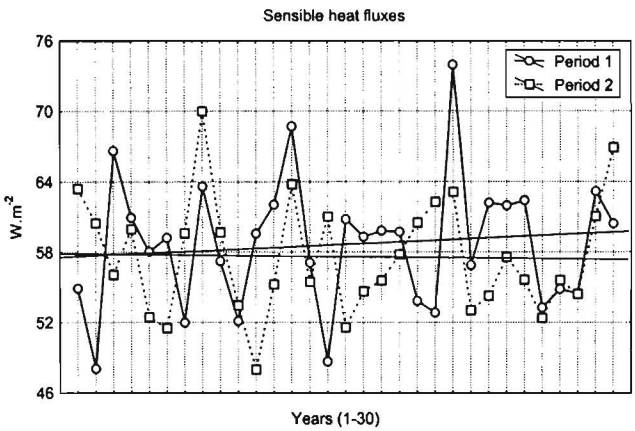

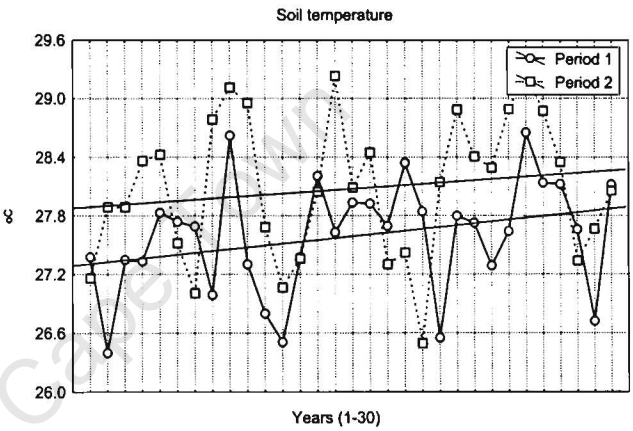

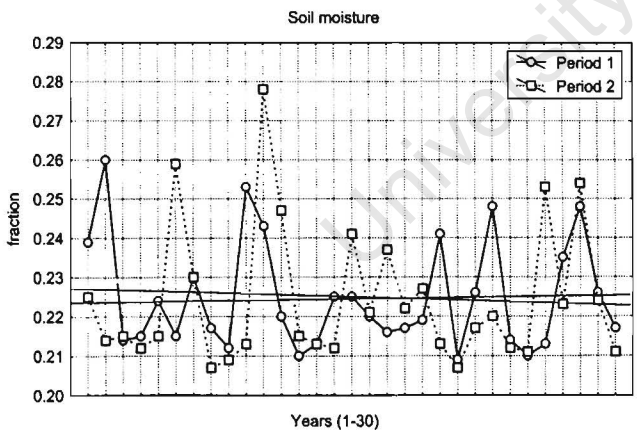

Trend graphs for region 4 for P3

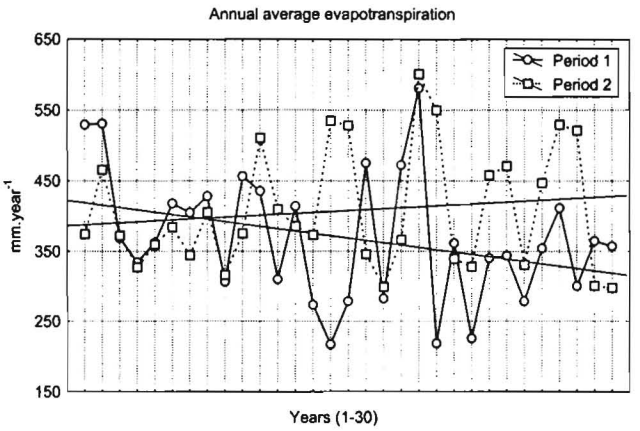

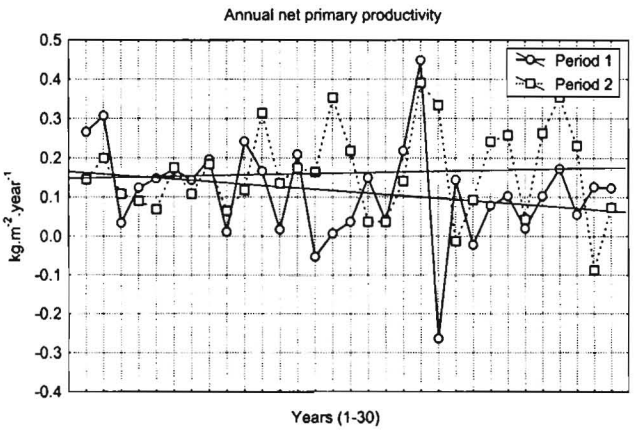

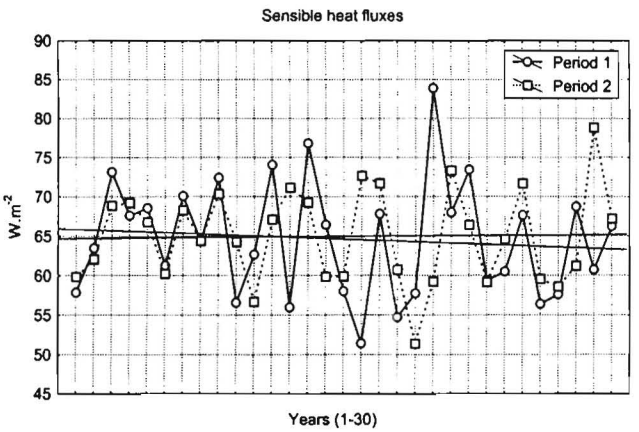

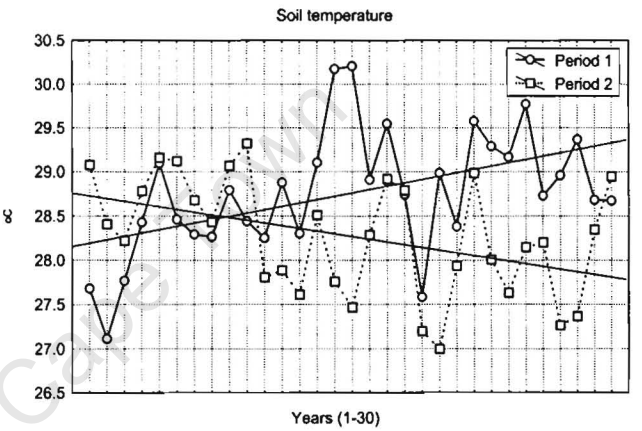

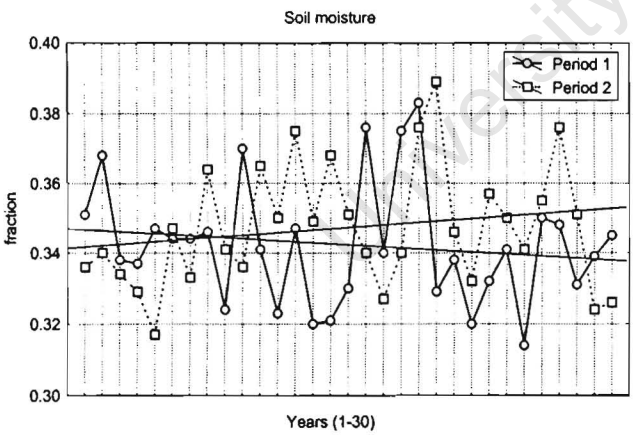

Trend graphs for region 5 of P3

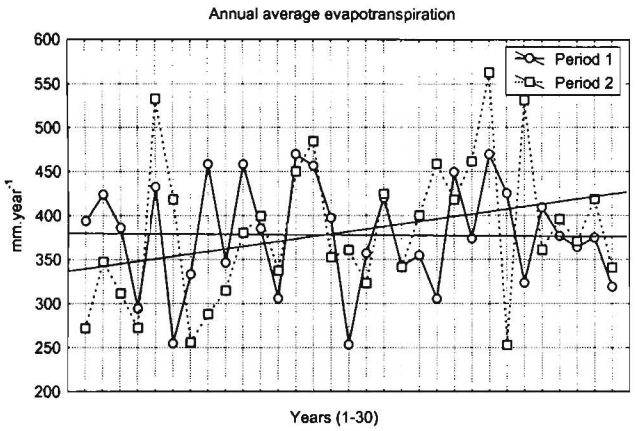

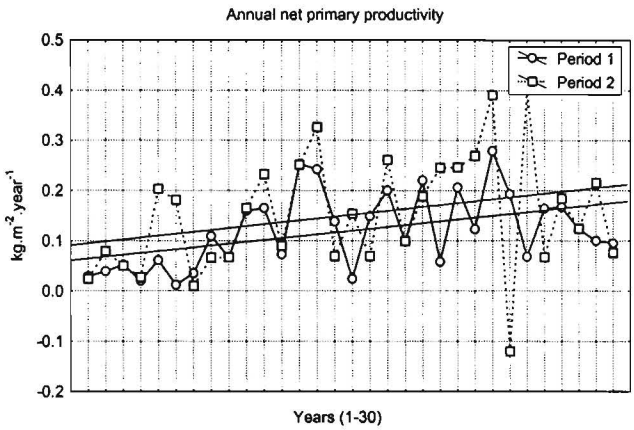

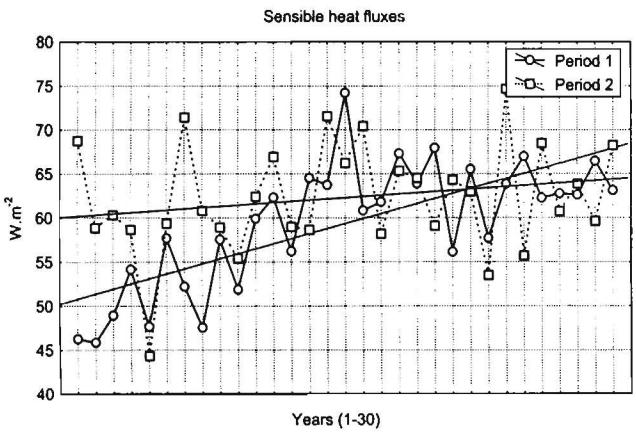

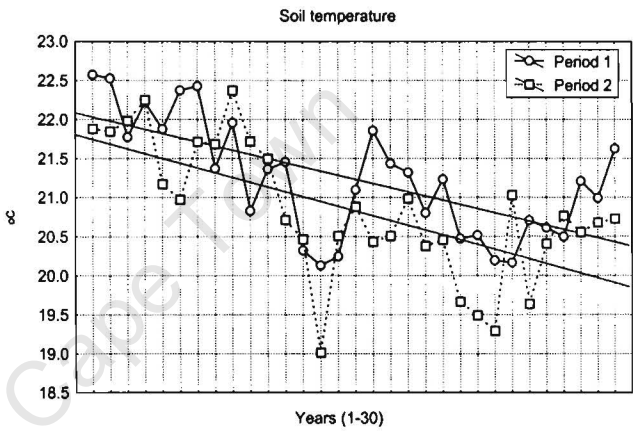

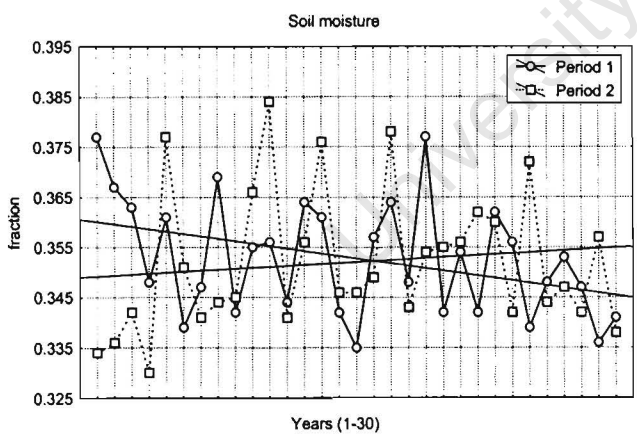

Trend graphs for region 1 for P4

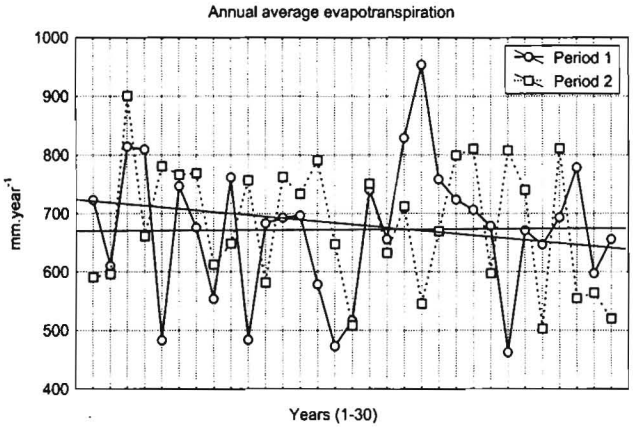

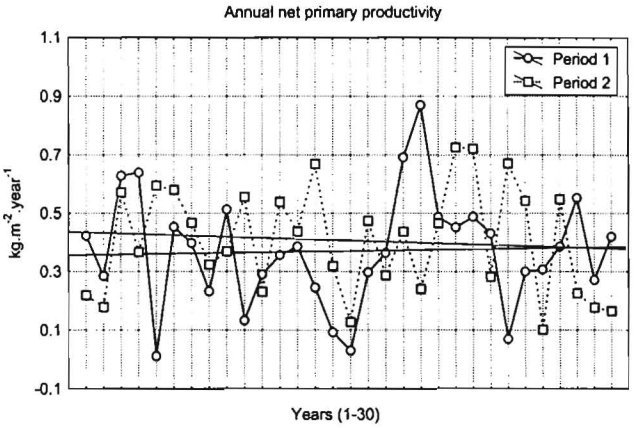

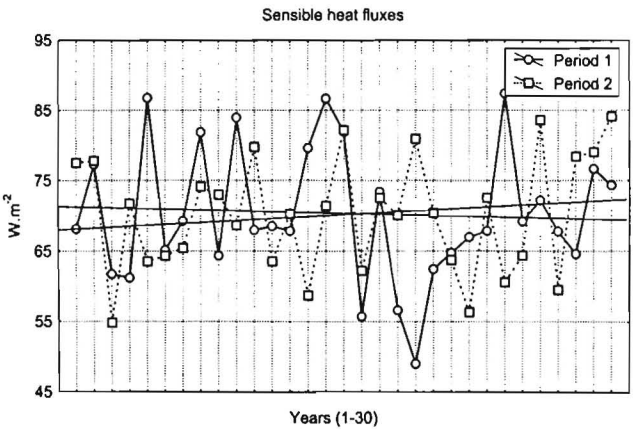

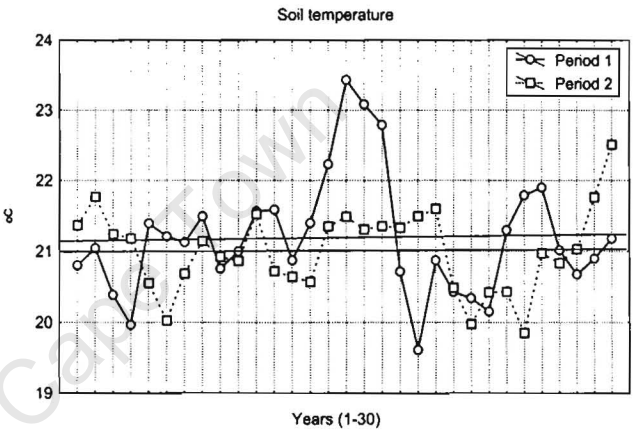

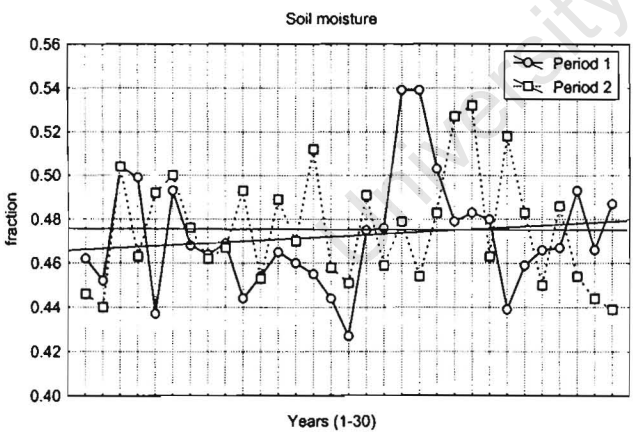

Trend graphs for region 2 for P4

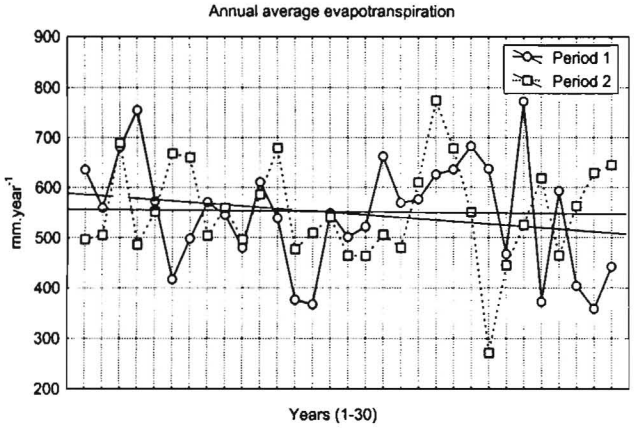

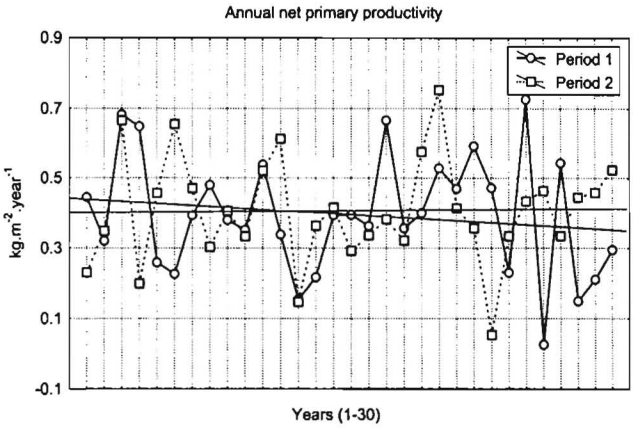

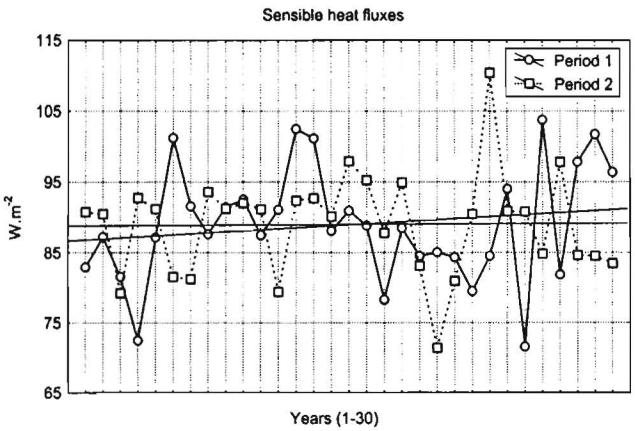

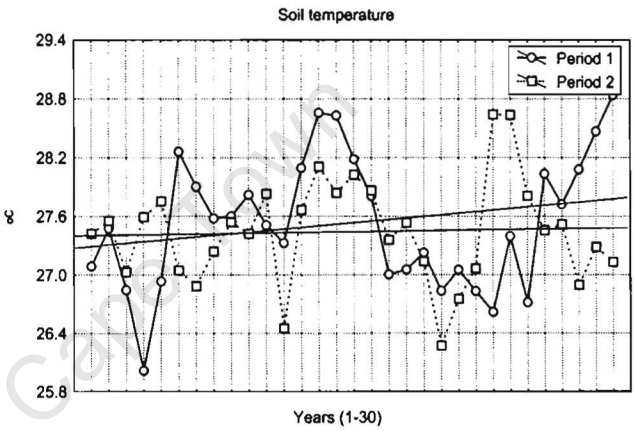

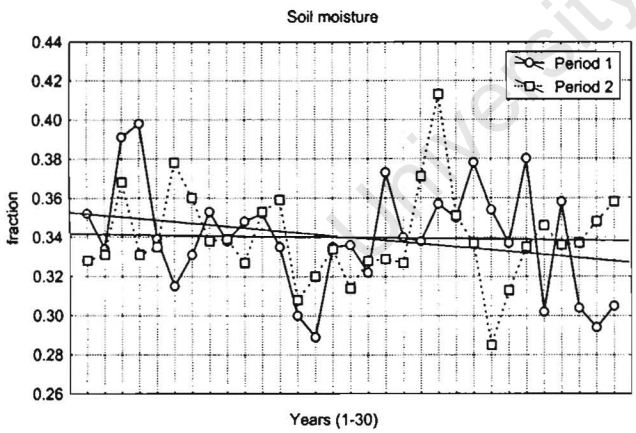

Trend graphs for region 3 for P4

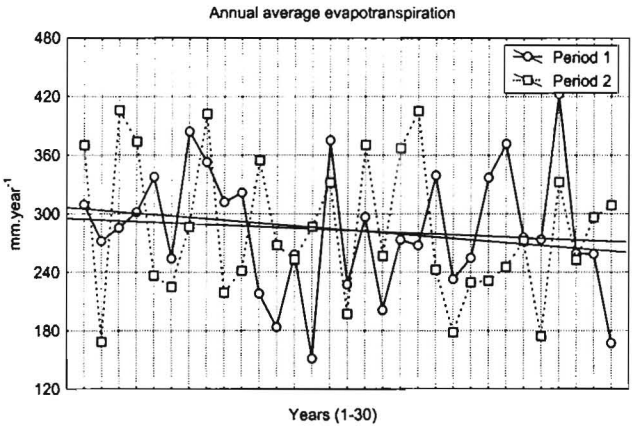

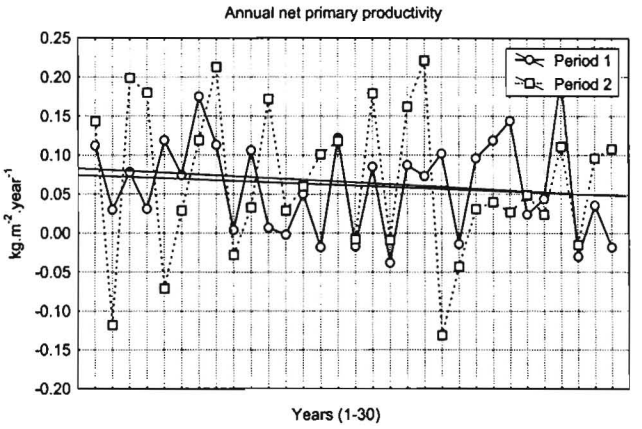

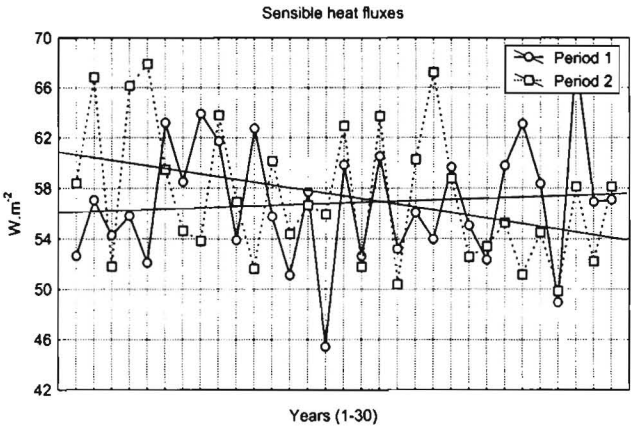

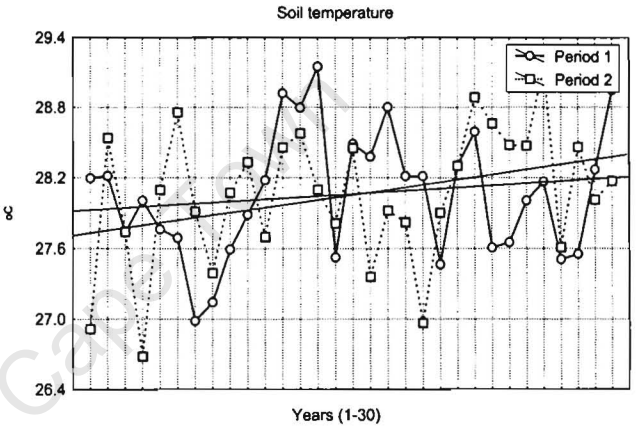

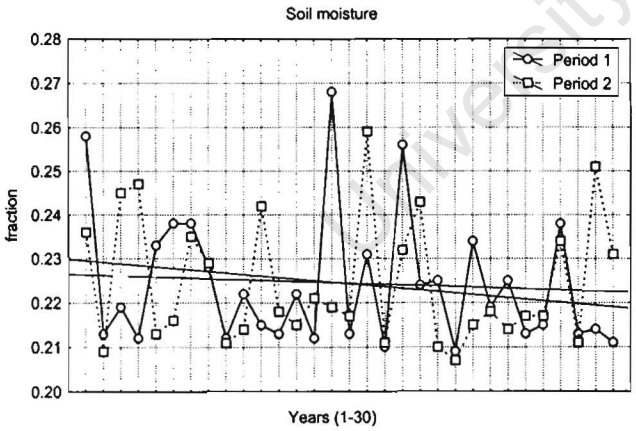

Trend graphs for region 4 for P4

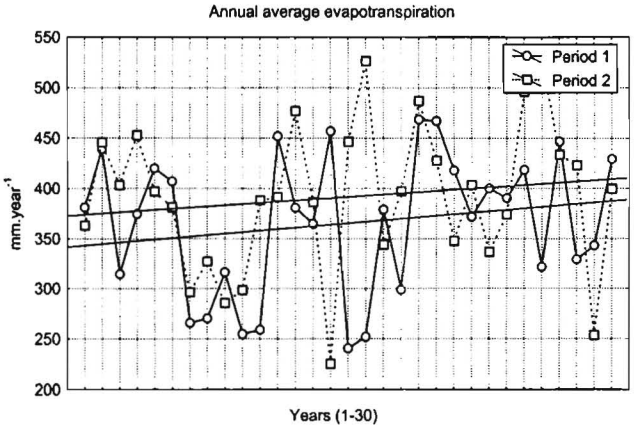

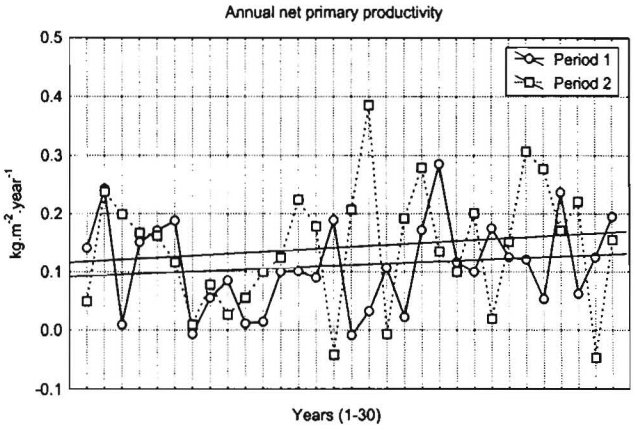

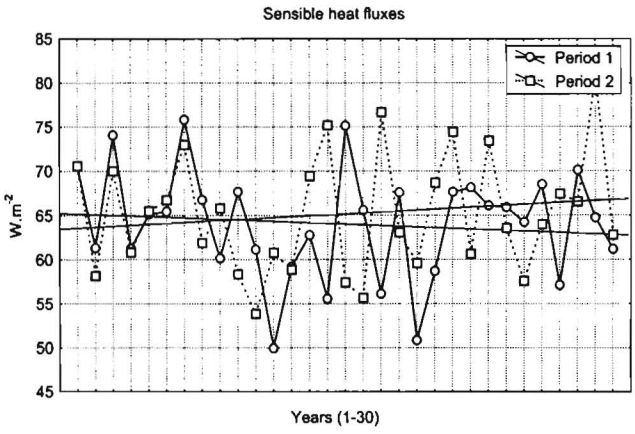

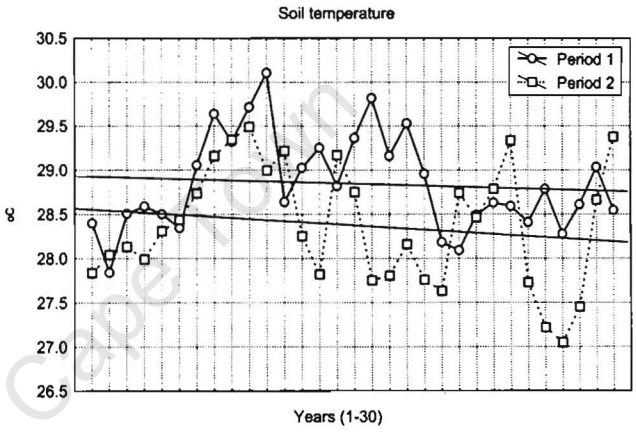

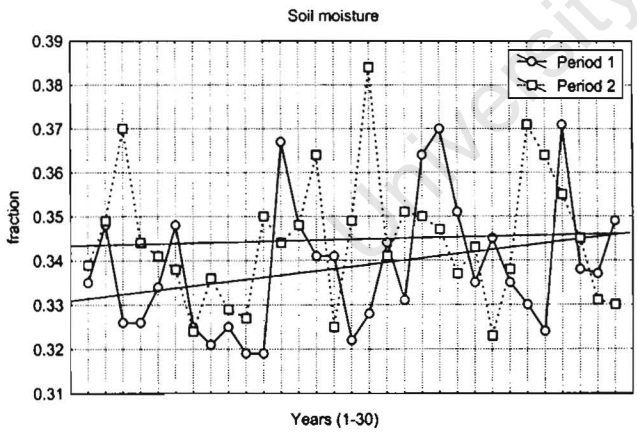

Trend graphs for region 5 for P4

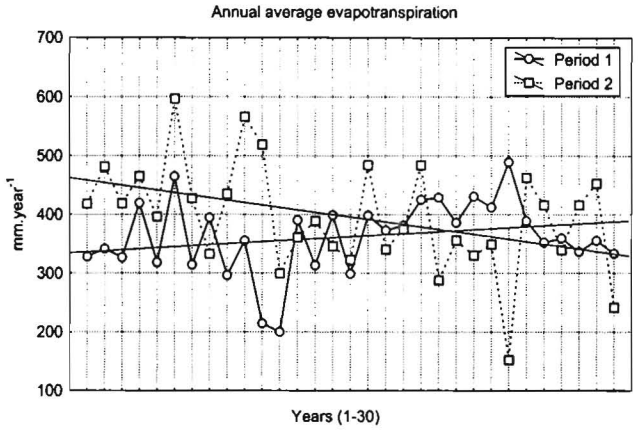

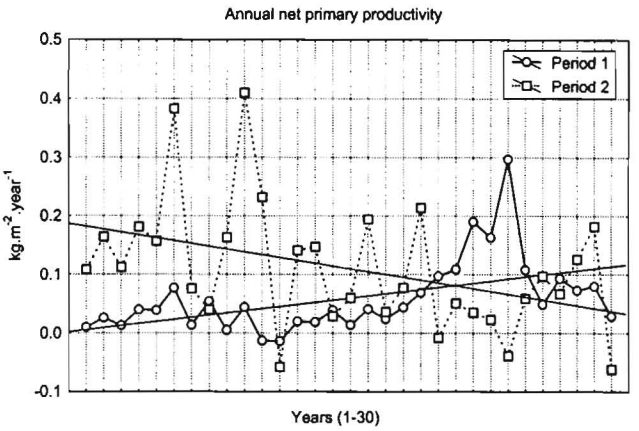

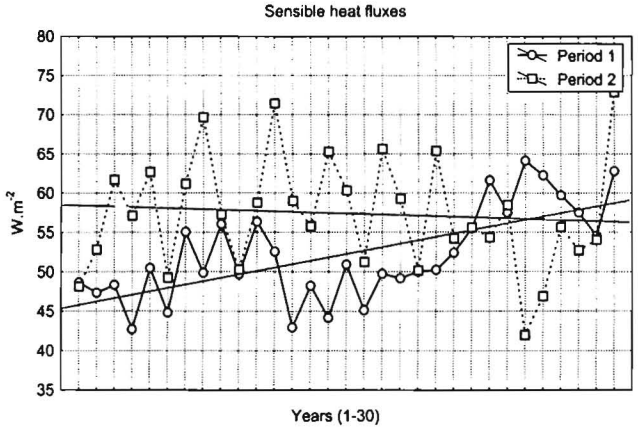

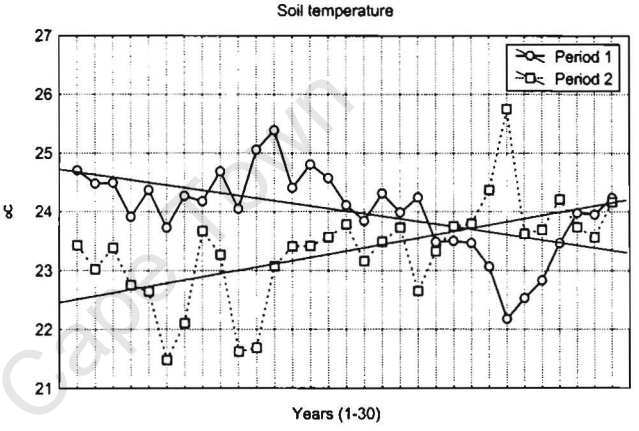

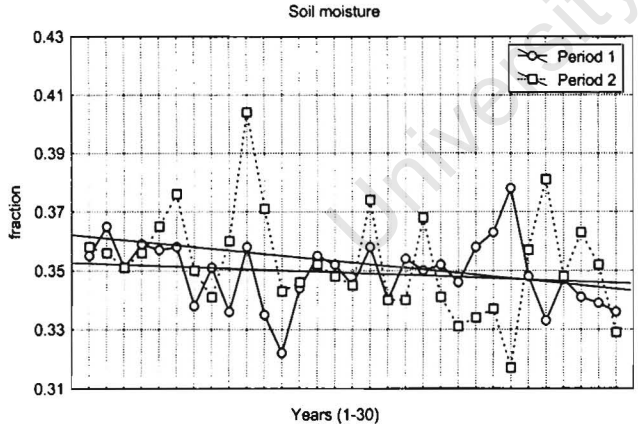

Trend graphs for region 1 for P5

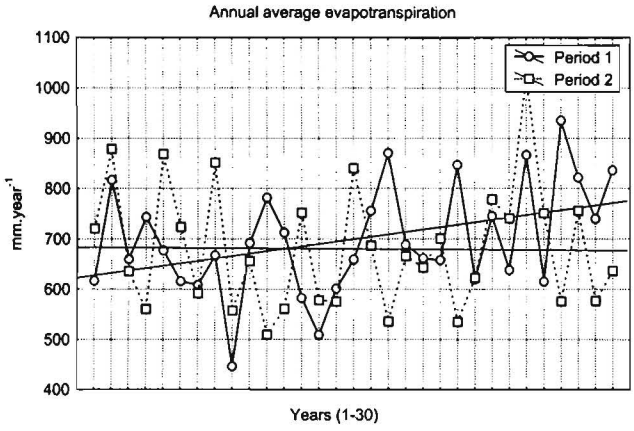

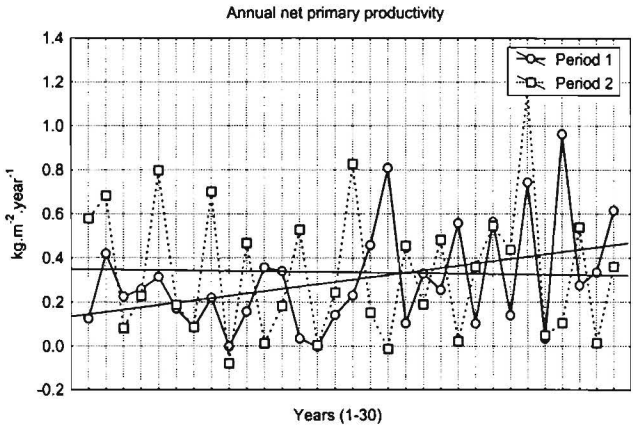

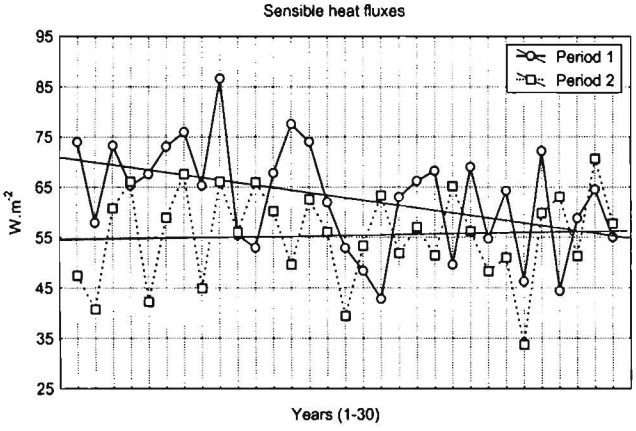

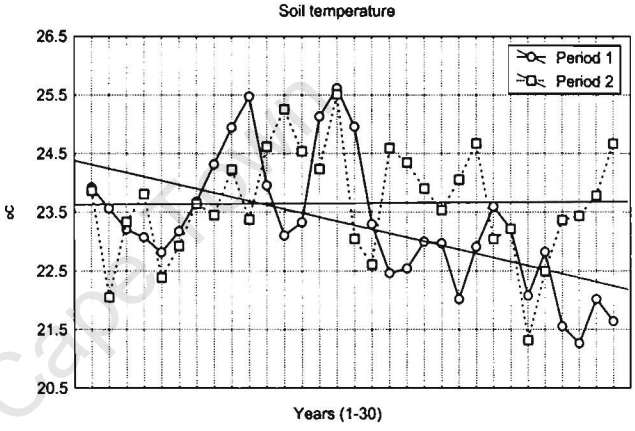

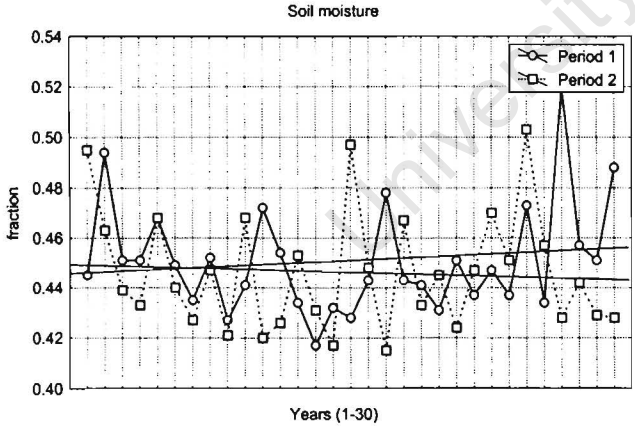

Trend graphs for region 2 for P5

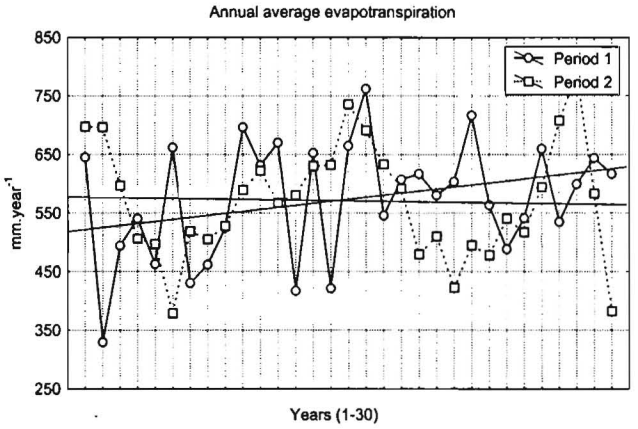

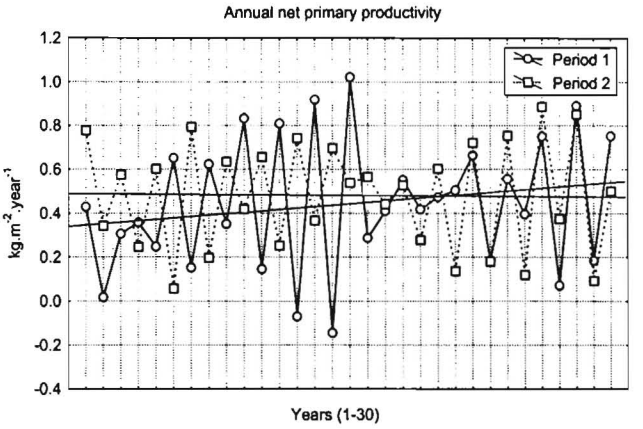

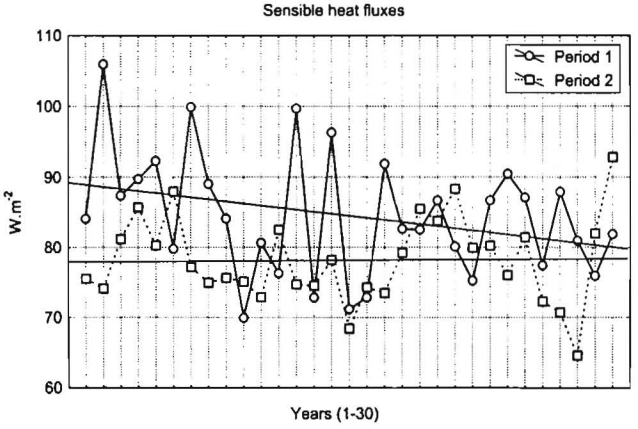

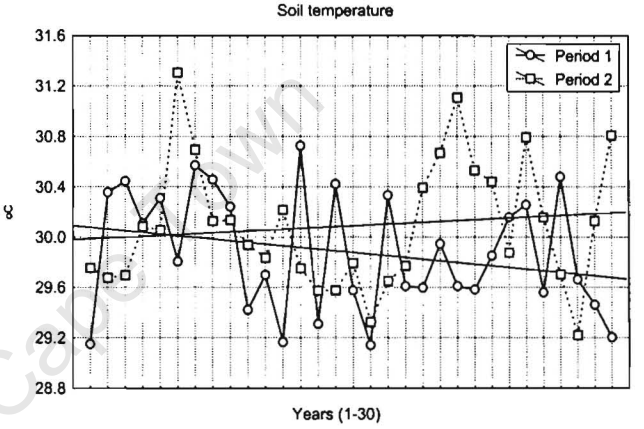

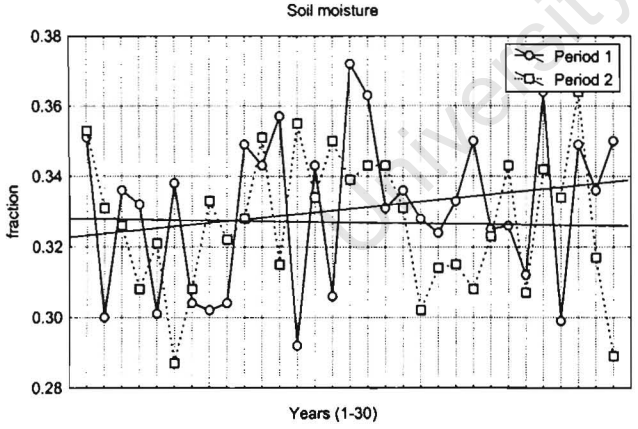

Trend graphs for region 3 for P5

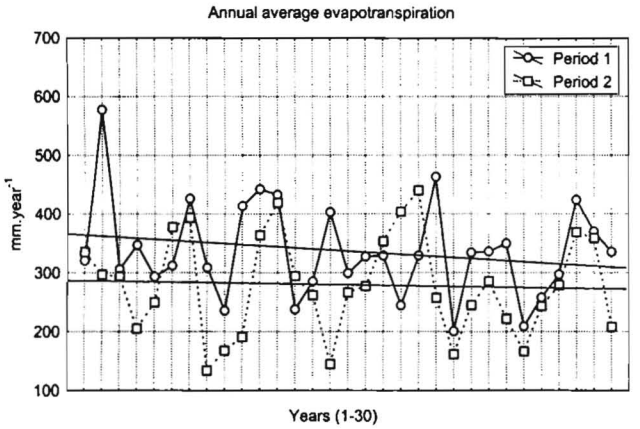

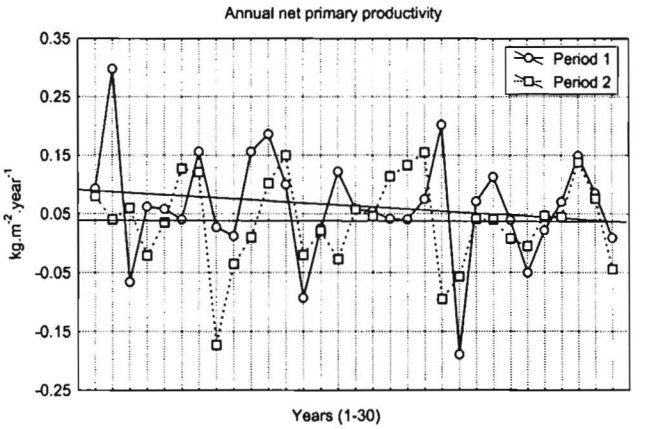

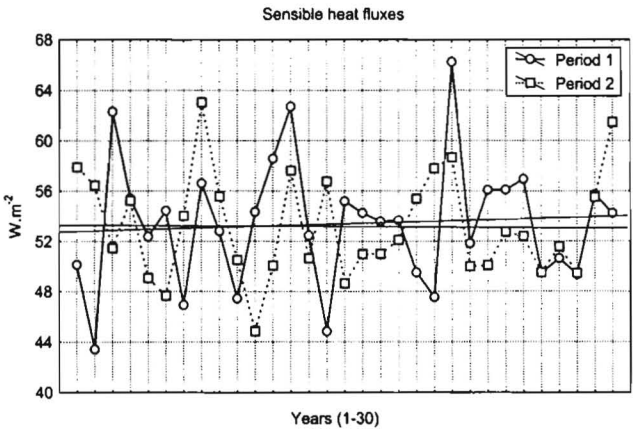

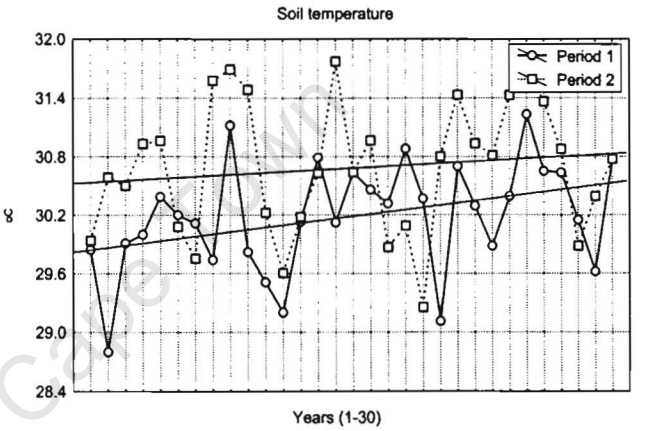

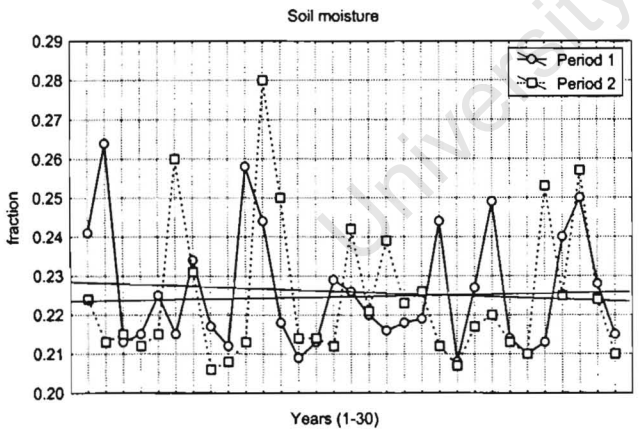

Trend graphs for region 4 for P5

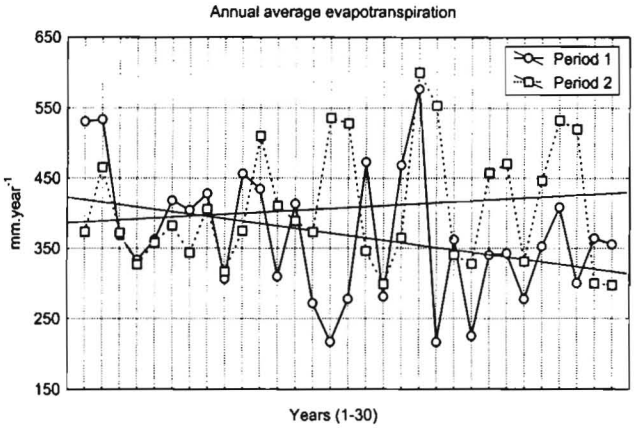

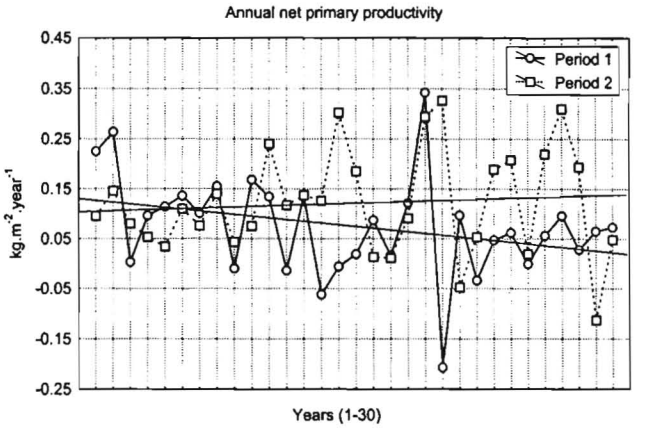

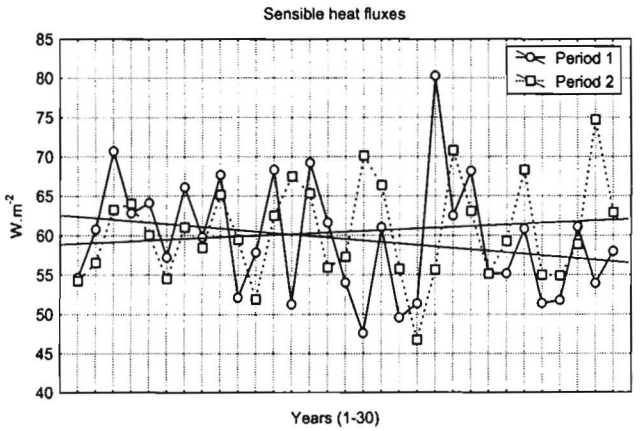

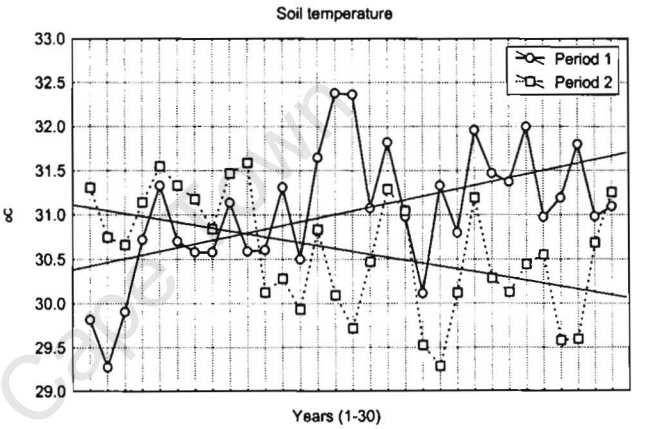

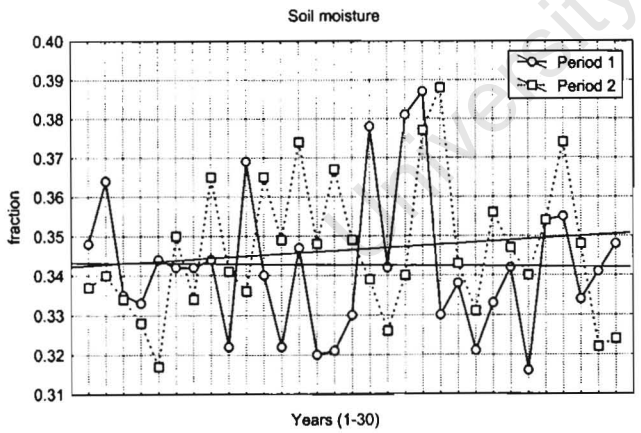

Trend graphs for region 5 for P5

APPENDIX C

SPECIAL REPORT ON EMISSIONS SCENARIOS A2 AND B2 STORYLINES FOR DIFFERENT GENERAL CIRCULATION MODELS

The precipitation (mm day^{-1}) and temperature (K) anomaly fields for summer (DJF) and winter (JJA) from eight different recent models, simulated using of the Special Report on Emissions Scenarios (SRES) A2 and B2 storylines, are included in the Appendix.

The GCMs are as follows:

- The Canadian Centre for Climate Modelling and Analysis (CCCma or CGCM1)
- The Australian Commonwealth Scientific and Industrial Research Organisation (CSIRO)
- The US NCAR Climate System Model (CSM)
- The Japanese Meteorological Research Institute (MRI2)
- The Japanese CCSR National Institute for Environmental Studies (NIES)
- The US NCAR Parallel Climate Model (PCM)
- The UK Hadley Centre for Climate Prediction and Research (HadCM3)
- The US Geophysics Fluid Dynamics Laboratory (GFDL)

z

CCCma A2 Scenario – DJF precipitation

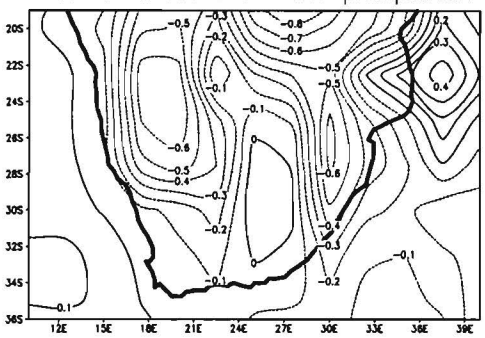

CCCma A2 Scenario – JJA precipitation

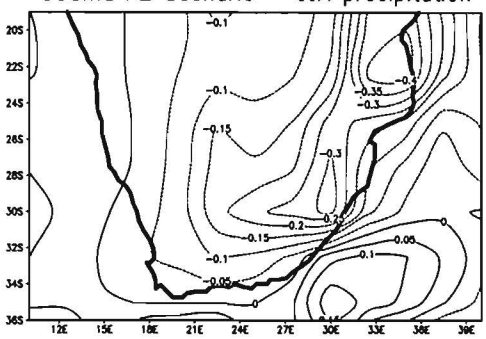

CCCma B2 Scenario – DJF precipitation

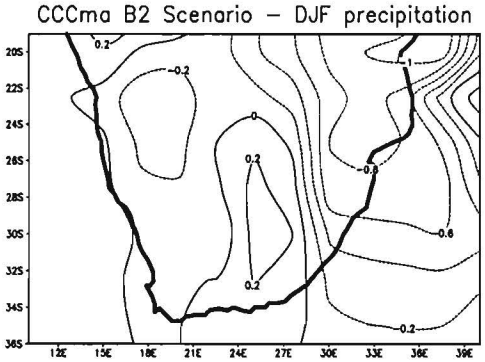

CCCma B2 Scenario – JJA precipitation

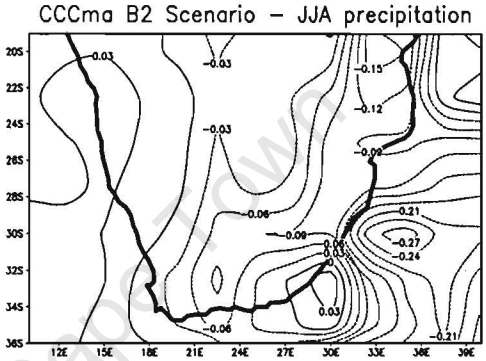

CCCma A2 Scenario – DJF temperature

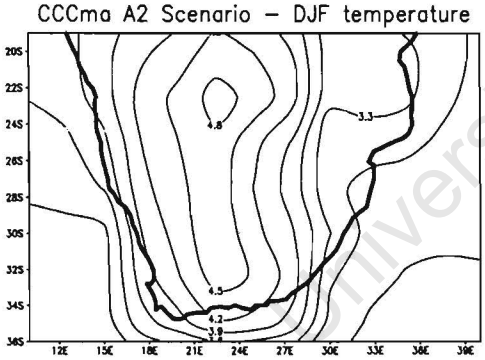

CCCma A2 Scenario – JJA temperature

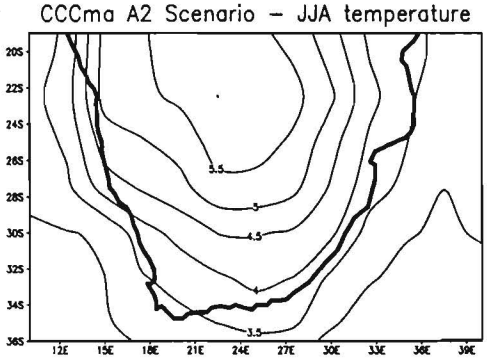

CCCma B2 Scenario – DJF temperature

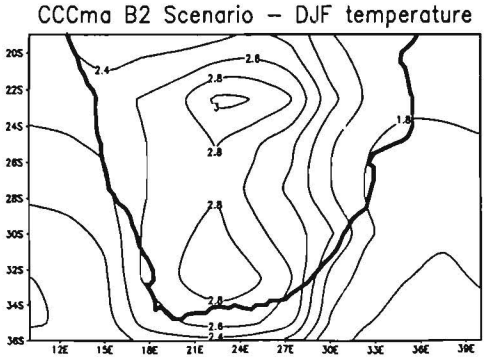

CCCma B2 Scenario – JJA temperature

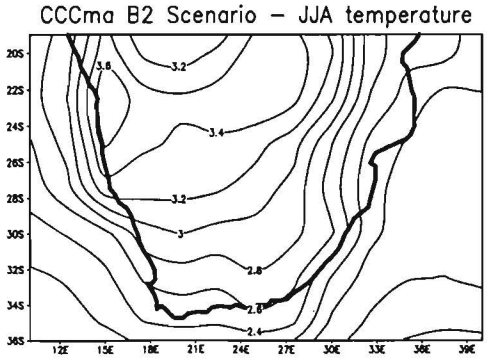

CSIRO A2 Scenario – DJF precipitation

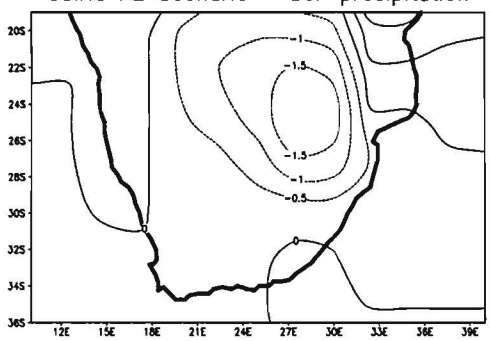

CSIRO A2 Scenario – JJA precipitation

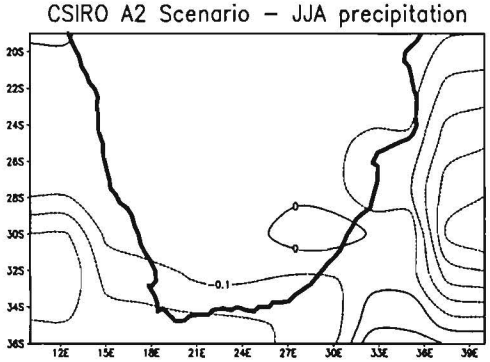

CSIRO B2 Scenario – DJF precipitation

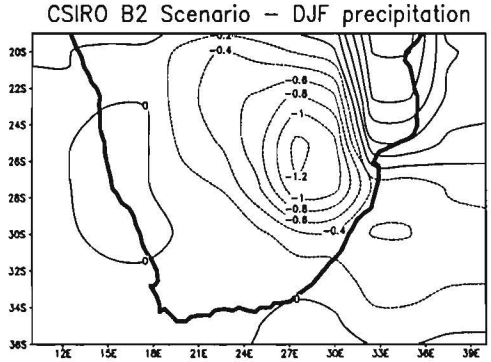

CSIRO B2 Scenario – JJA precipitation

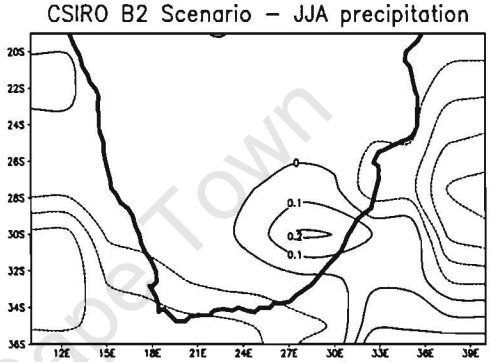

CSIRO A2 Scenario – DJF temperature

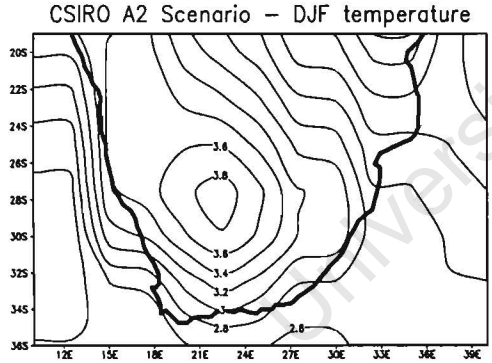

CSIRO A2 Scenario – JJA temperature

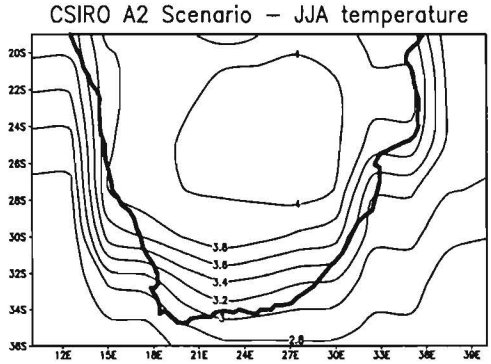

CSIRO B2 Scenario – DJF temperature

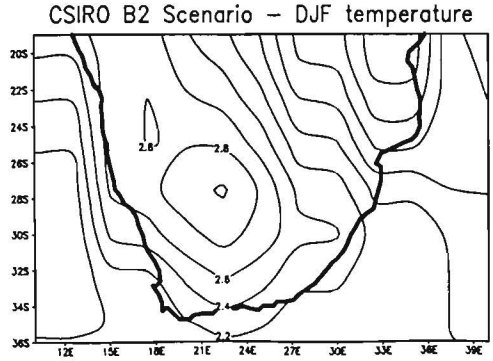

CSIRO B2 Scenario – JJA temperature

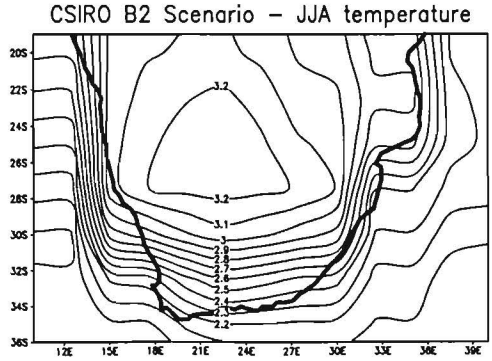

CSM A2 Scenario – DJF precipitation

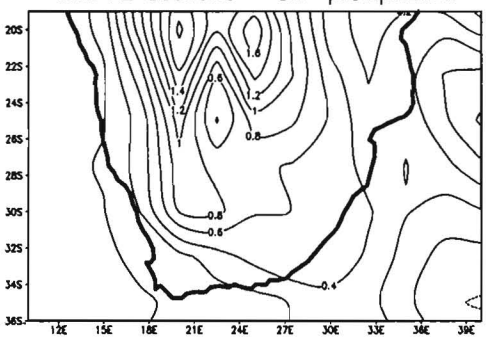

CSM A2 Scenario – JJA precipitation

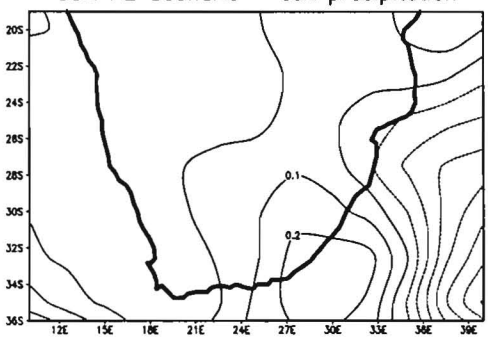

CSM B2 Scenario – DJF precipitation

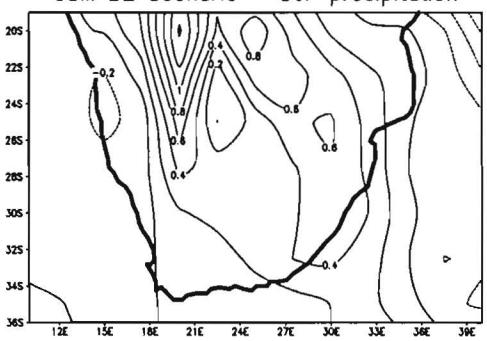

CSM B2 Scenario – JJA precipitation

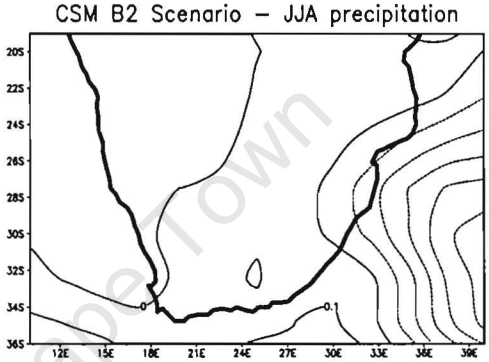

CSM A2 Scenario – DJF temperature

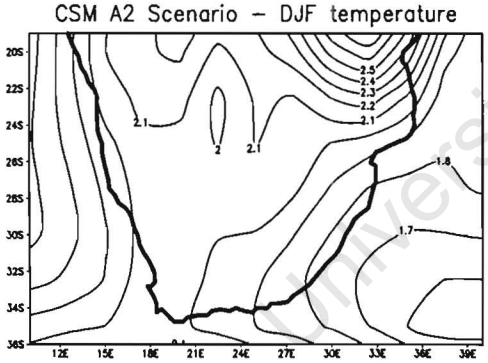

CSM A2 Scenario – JJA temperature

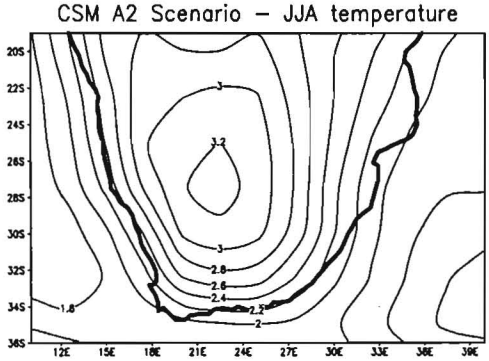

CSM B2 Scenario – DJF temperature

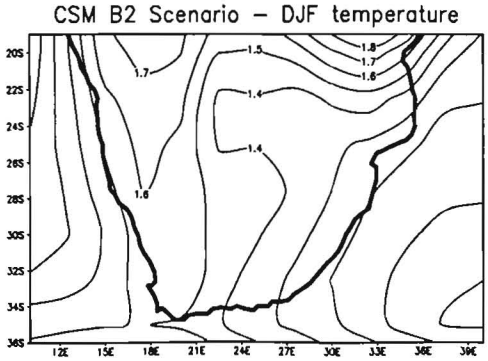

CSM B2 Scenario – JJA temperature

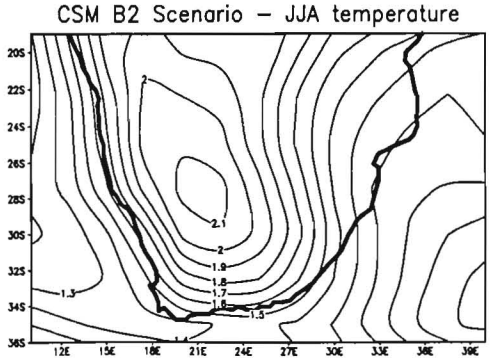

MRI2 A2 Scenario – DJF precipitation

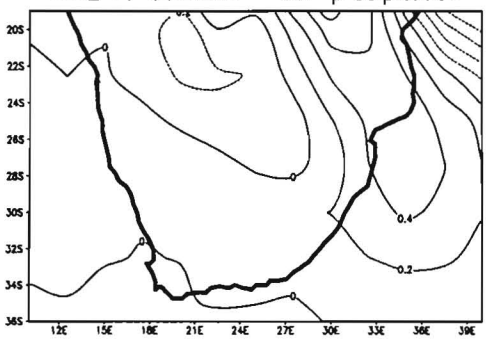

MRI2 A2 Scenario – JJA precipitation

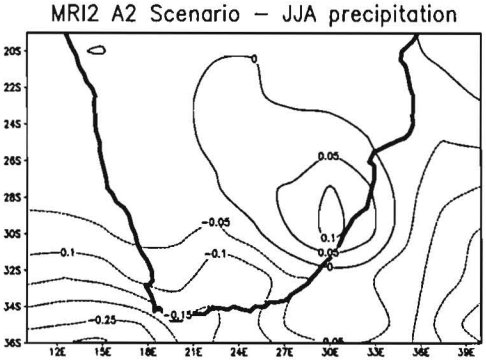

MRI2 B2 Scenario – DJF precipitation

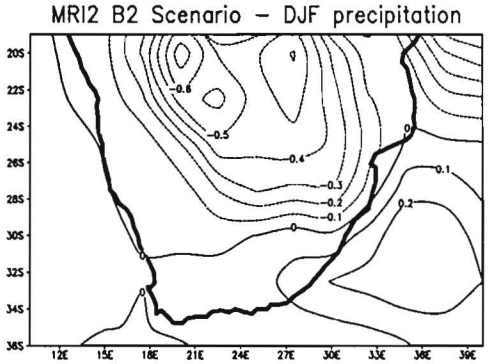

MRI2 B2 Scenario – JJA precipitation

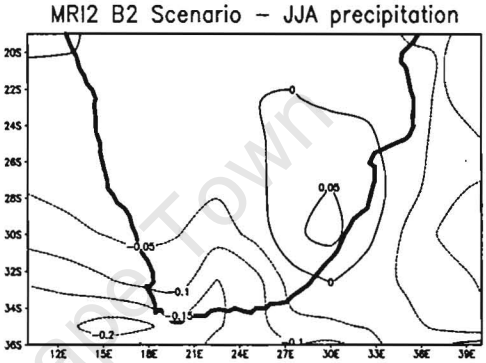

MRI2 A2 Scenario – DJF temperature

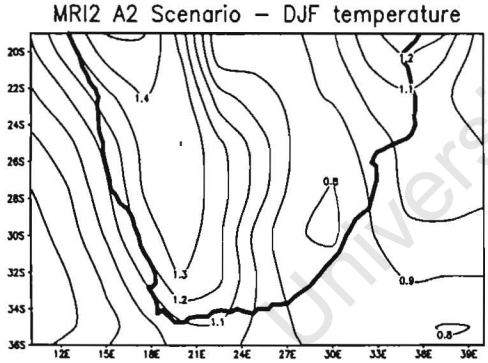

MRI2 A2 Scenario – JJA temperature

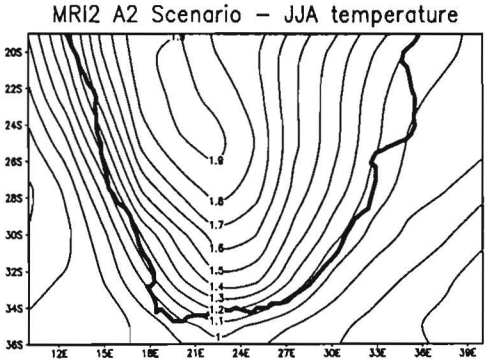

MRI2 B2 Scenario – DJF temperature

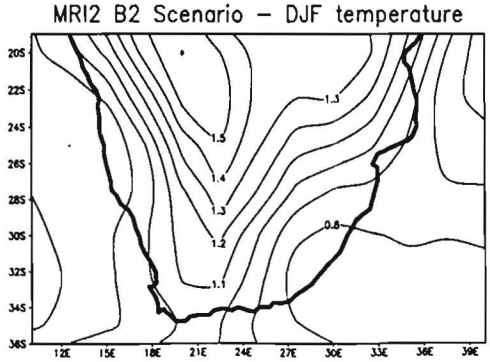

MRI2 B2 Scenario – JJA temperature

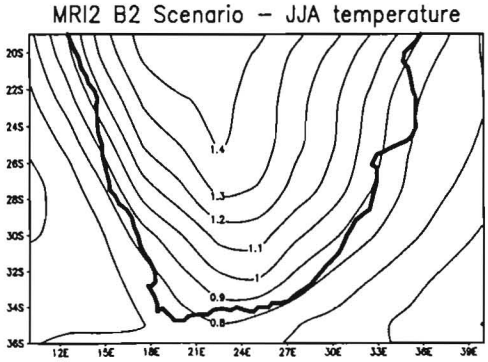

NIES A2 Scenario – DJF precipitation

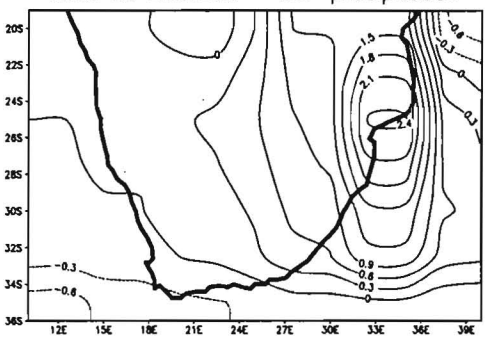

NIES A2 Scenario – JJA precipitation

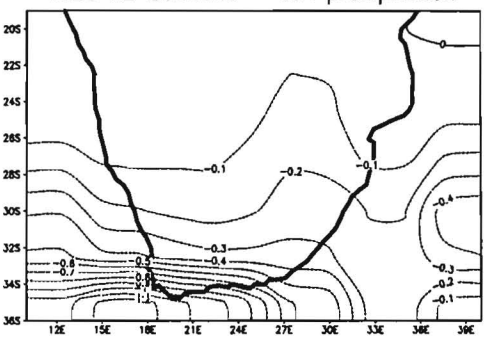

NIES B2 Scenario – DJF precipitation

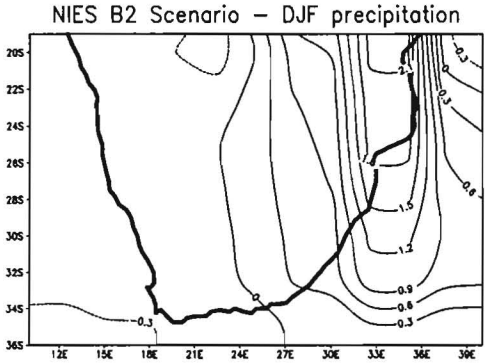

NIES B2 Scenario – JJA precipitation

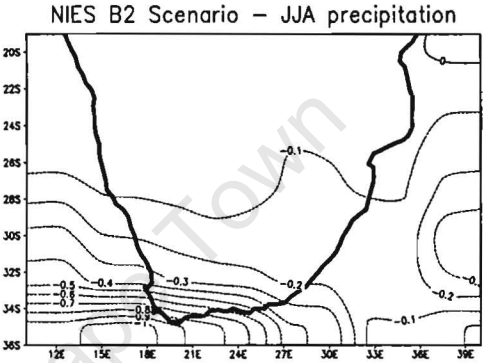

NIES A2 Scenario – DJF temperature

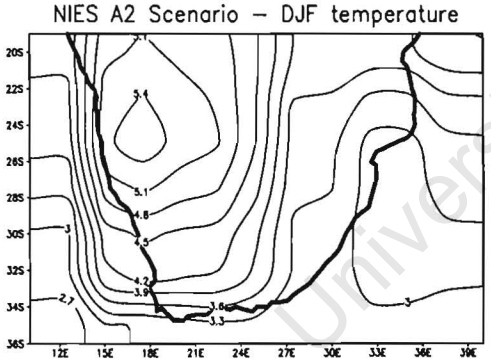

NIES A2 Scenario – JJA temperature

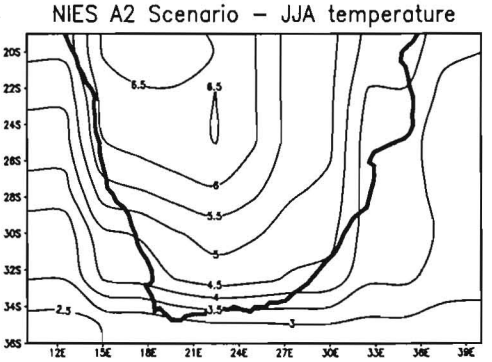

NIES B2 Scenario – DJF temperature

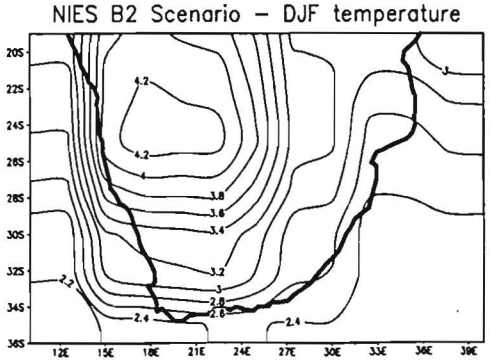

NIES B2 Scenario – JJA temperature

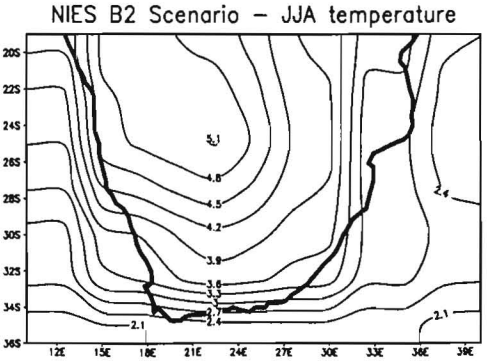

PCM A2 Scenario – DJF precipitation

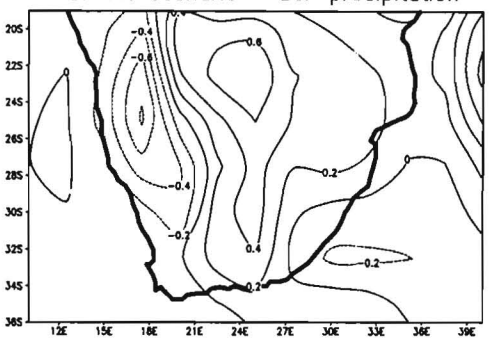

PCM A2 Scenario – JJA precipitation

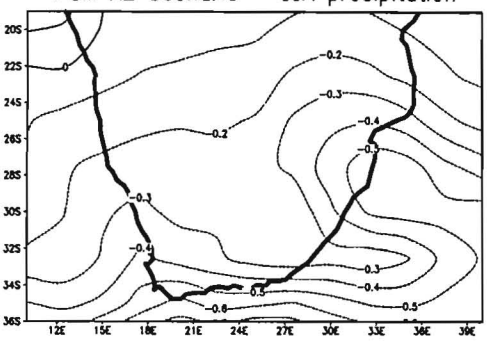

PCM B2 Scenario – DJF precipitation

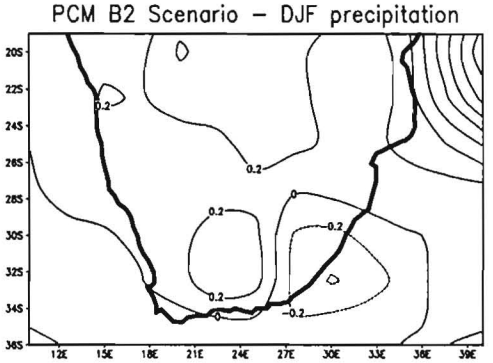

PCM B2 Scenario – JJA precipitation

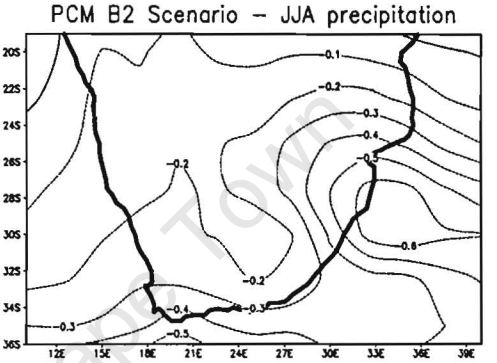

PCM A2 Scenario – DJF temperature

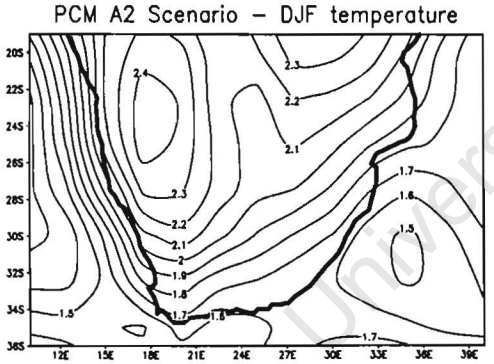

PCM A2 Scenario – JJA temperature

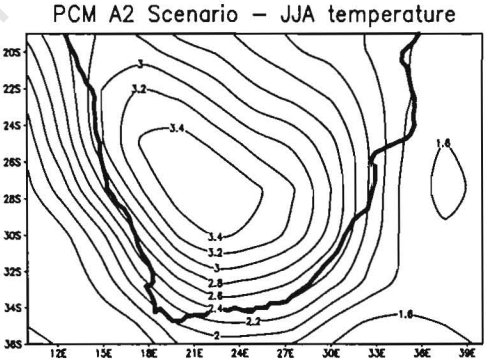

PCM B2 Scenario – DJF temperature

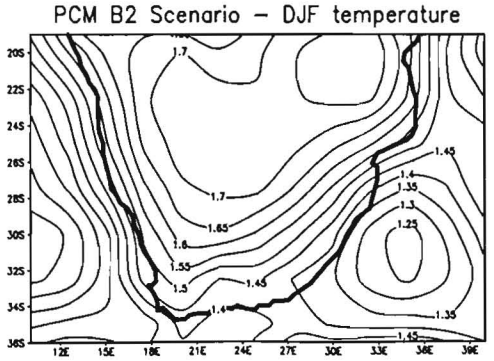

PCM B2 Scenario – JJA temperature

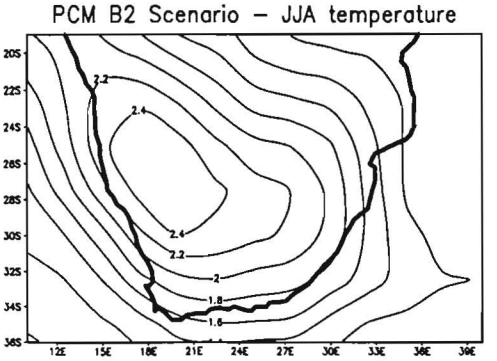

HadCM3 A2 Scenario – DJF precipitation

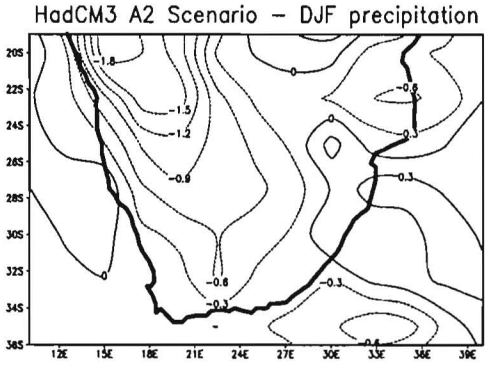

HadCM3 A2 Scenario – JJA precipitation

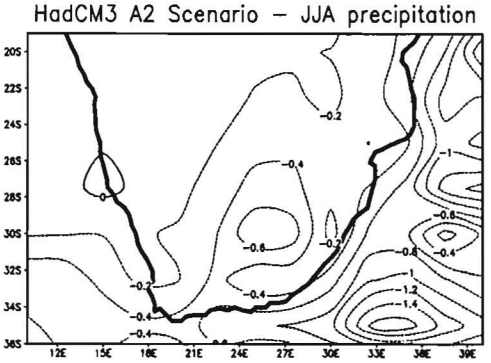

HadCM3 B2 Scenario – DJF precipitation

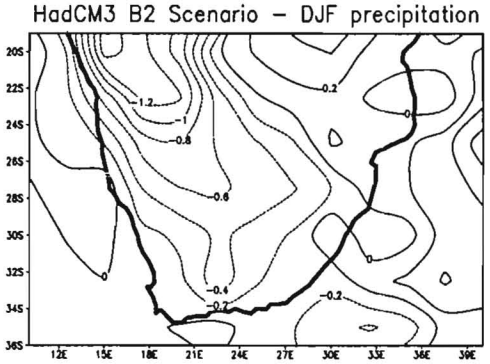

HadCM3 B2 Scenario – JJA precipitation

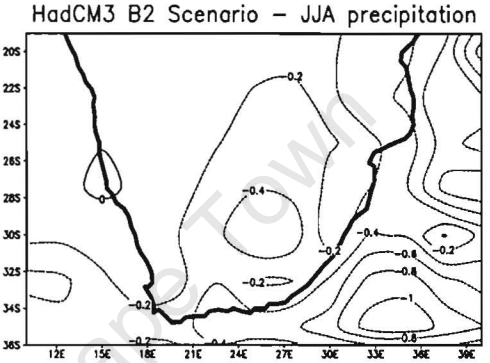

HadCM3 A2 Scenario – DJF temperature

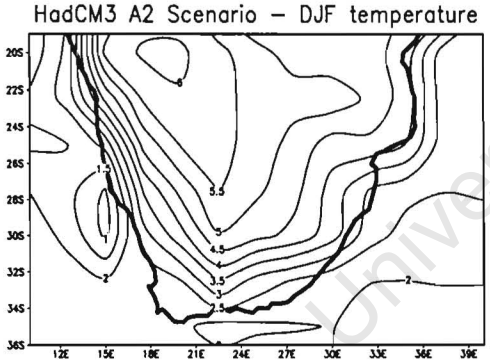

HadCM3 A2 Scenario – JJA temperature

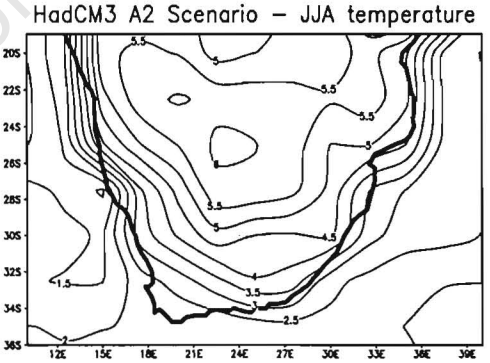

HadCM3 B2 Scenario – DJF temperature

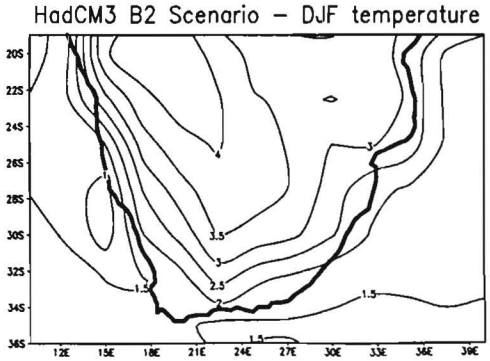

HadCM3 B2 Scenario – JJA temperature

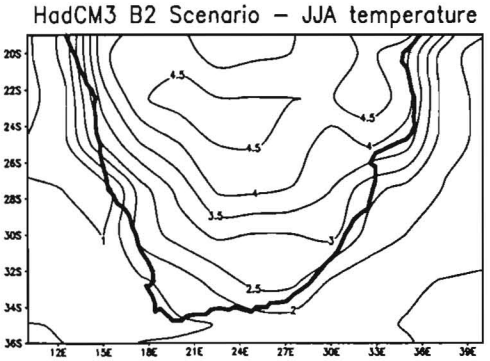

GFDL A2 Scenario – DJF temperature

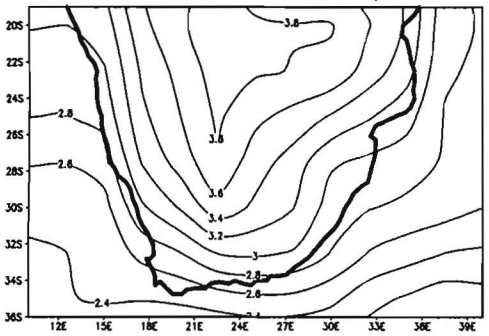

GFDL A2 Scenario – JJA temperature

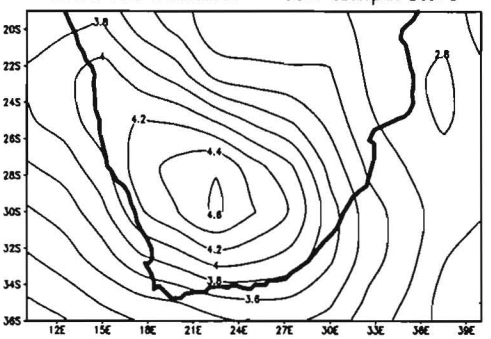

GFDL B2 Scenario – DJF temperature

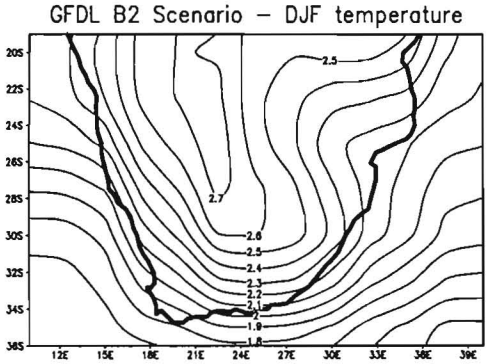

GFDL B2 Scenario – JJA temperature

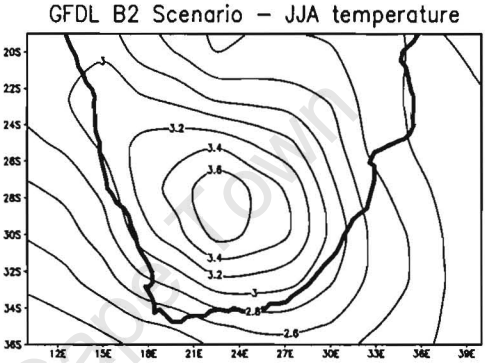

APPENDIX D

SUMMER SEASONAL DIFFERENCES BETWEEN THE EARLY AND LATE 21ST CENTURY

The summer seasonal mean and anomalies for the following scenarios:

- Ibissta
- P1
- P2
- P3
- P4
- P5

and the following variables:

- Net primary productivity
- Average evapotranspiration
- Sensible heat fluxes
- Soil temperatures
- Soil moisture
- Latent heat fluxes
- Leaf area index (upper and lower canopies)

are included in the Appendix.

Summer NPP 2000–2030: Ibissta

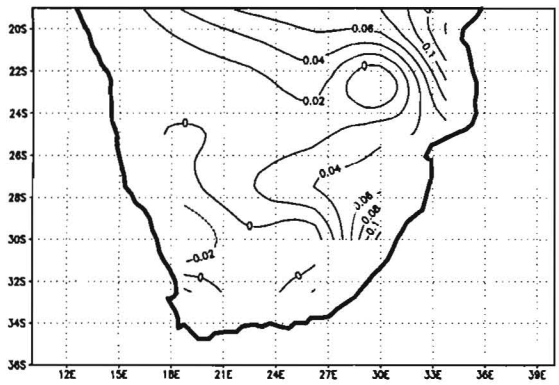

Anomaly (late – early 21st century): Ibissta

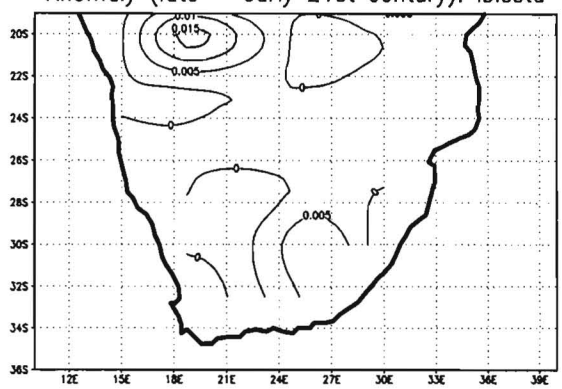

Summer NPP 2000–2030: P1

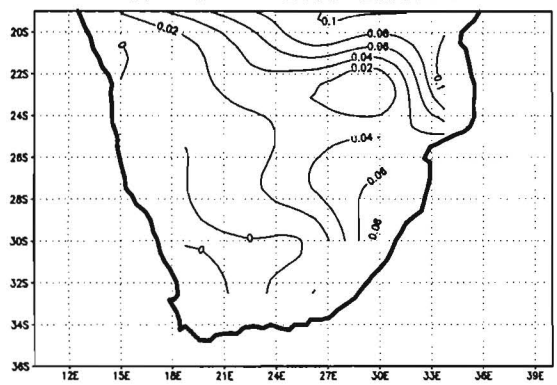

Anomaly (late – early 21st century): P1

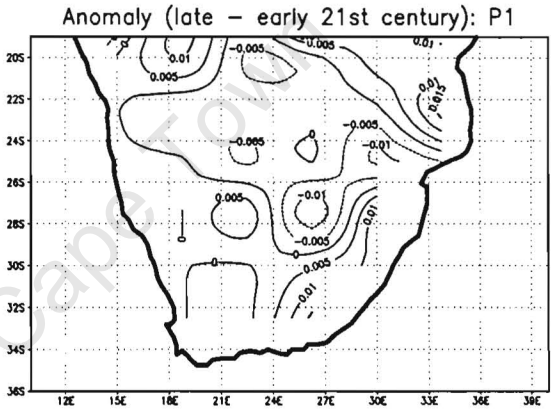

Summer NPP 2000–2030: P2

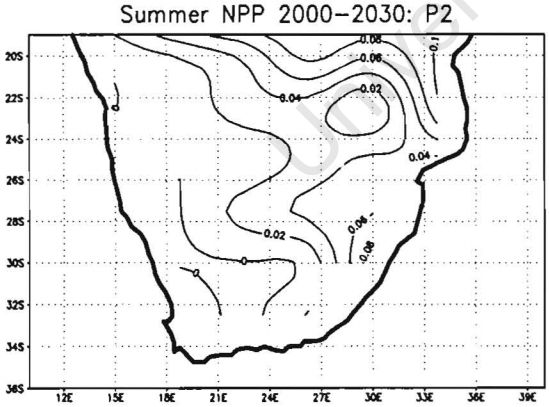

Anomaly (late – early 21st century): P2

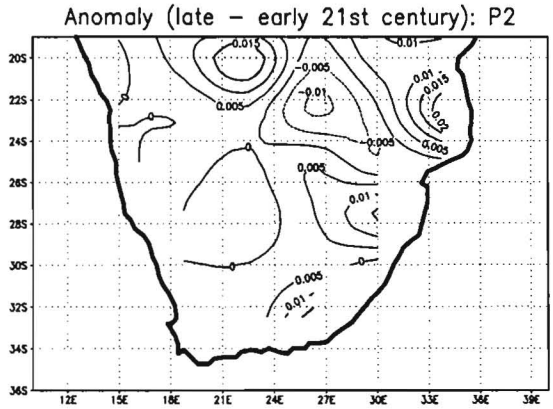

Summer NPP 2000–2030: P3

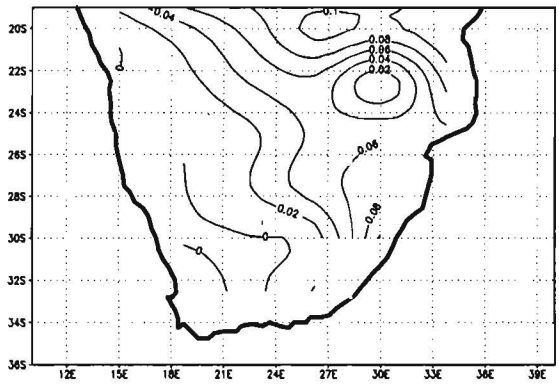

Anomaly (late – early 21st century): P3

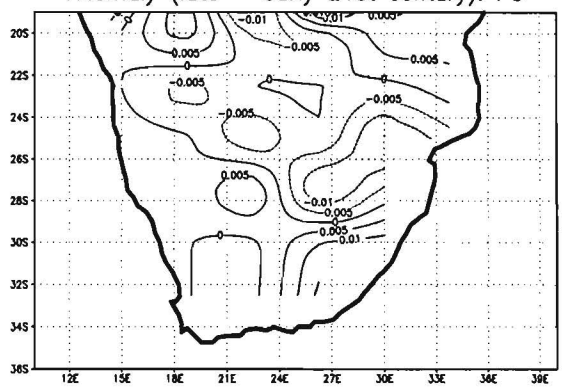

Summer NPP 2000–2030: P4

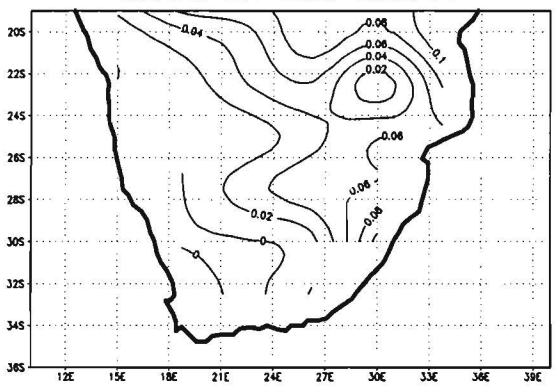

Anomaly (late – early 21st century): P4

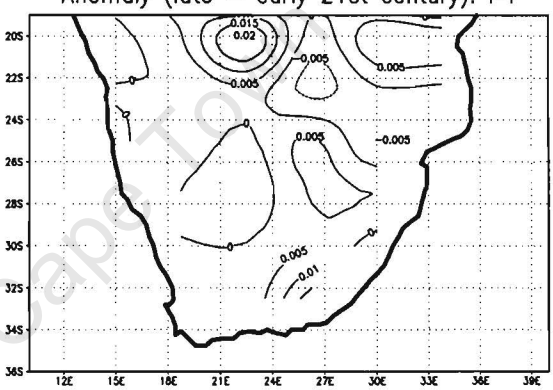

Summer NPP 2000–2030: P5

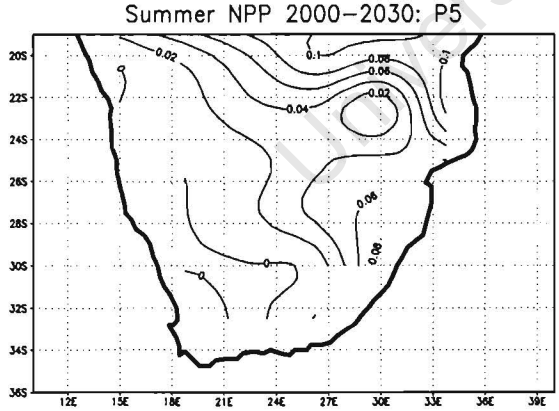

Anomaly (late – early 21st century): P5

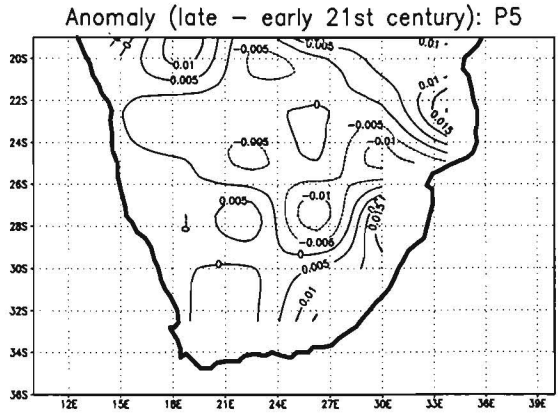

Summer avg. evapotransp. 2000–2030: Ibissta

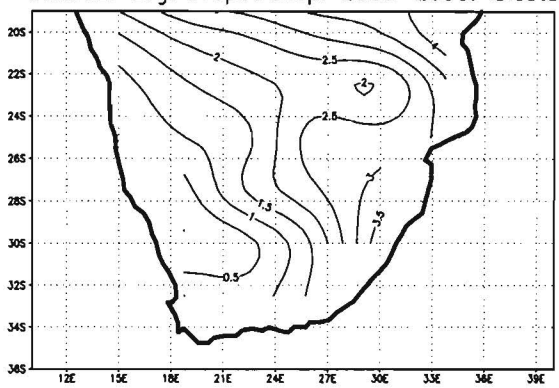

Anomaly (late – early 21st century): Ibissta

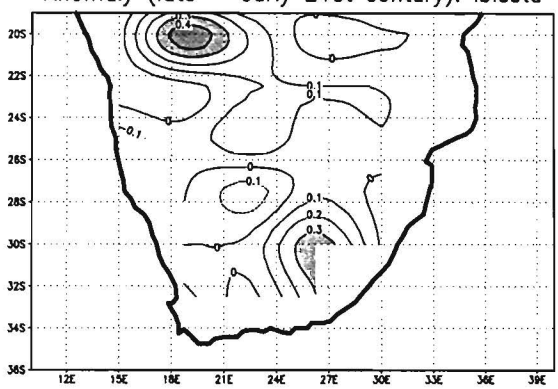

Summer avg. evapotransp. 2000–2030: P1

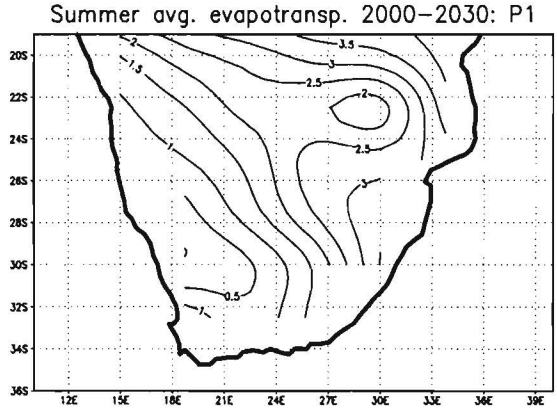

Anomaly (late – early 21st century): P1

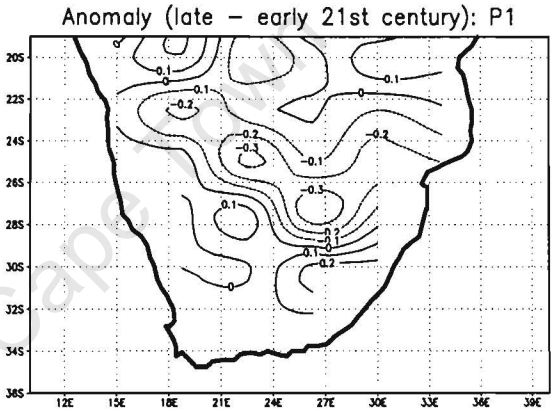

Summer avg. evapotransp. 2000–2030: P2

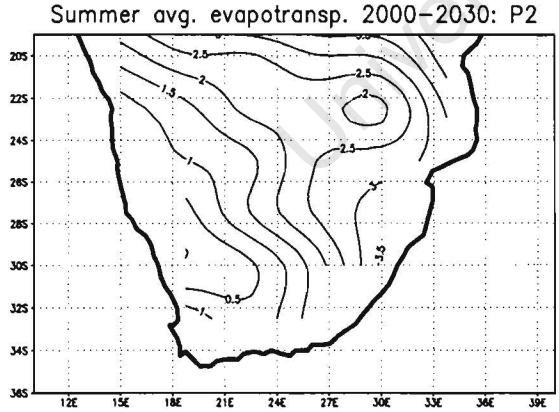

Anomaly (late – early 21st century): P2

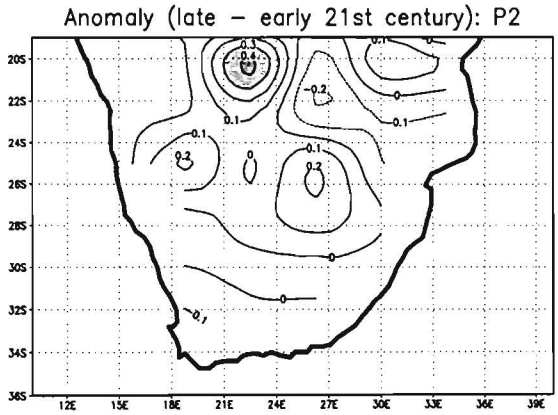

Summer avg. evapotransp. 2000–2030: P3

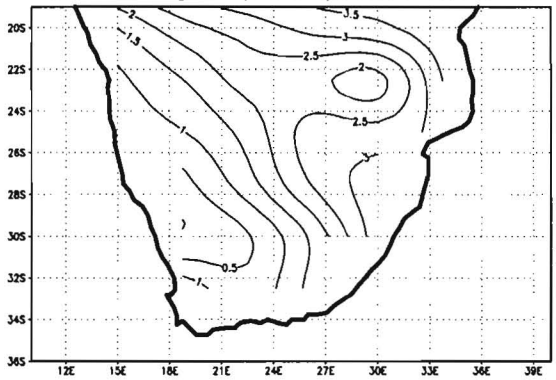

Anomaly (late – early 21st century): P3

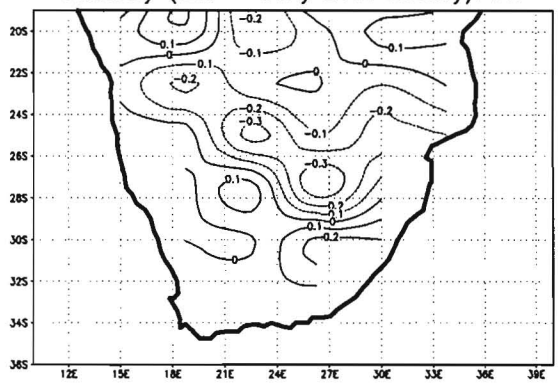

Summer avg. evapotransp. 2000–2030: P4

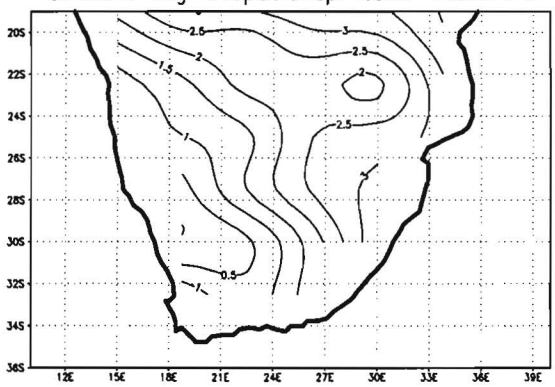

Anomaly (late – early 21st century): P4

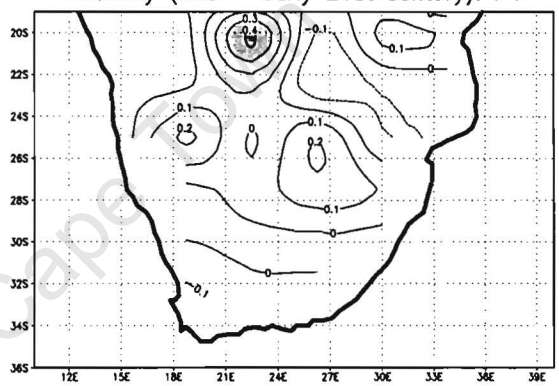

Summer avg. evapotransp. 2000–2030: P5

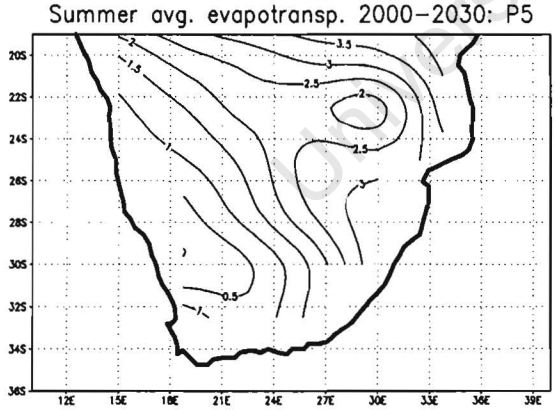

Anomaly (late – early 21st century): P5

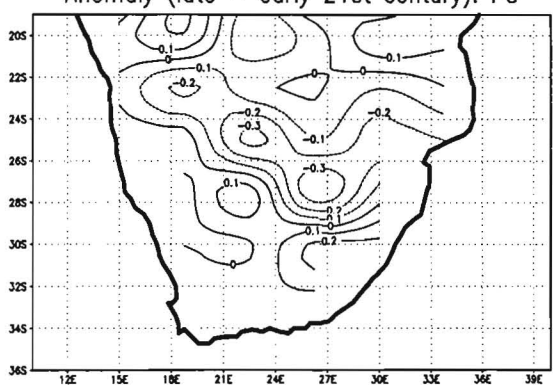

Summer sensible heat fluxes 2000–2030: Ibissta

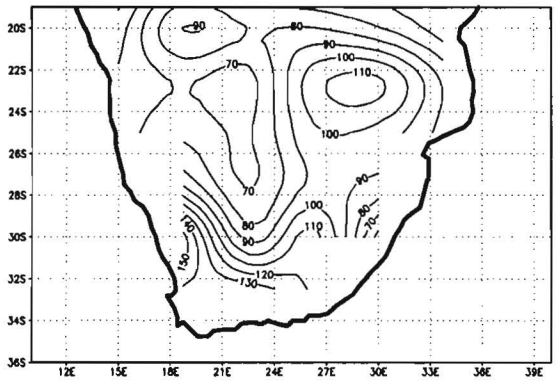

Anomaly (late – early 21st century): Ibissta

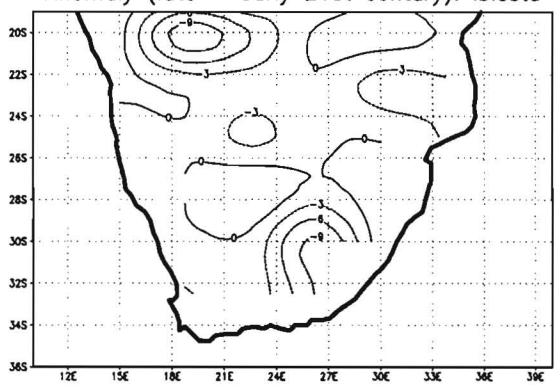

Summer sensible heat fluxes 2000–2030: P1

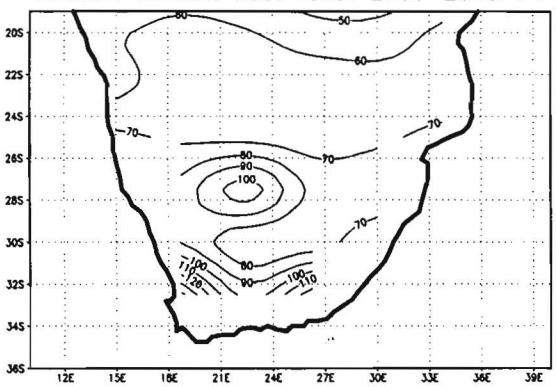

Anomaly (late – early 21st century): P1

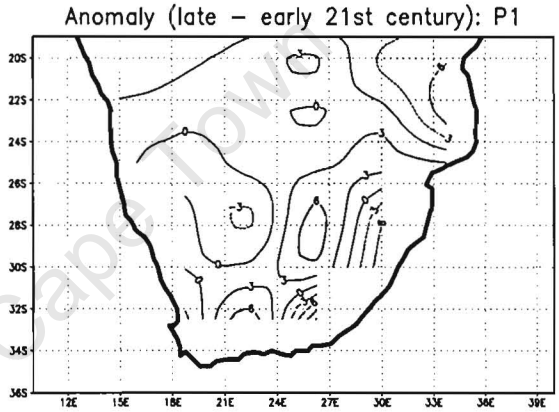

Summer sensible heat fluxes 2000–2030: P2

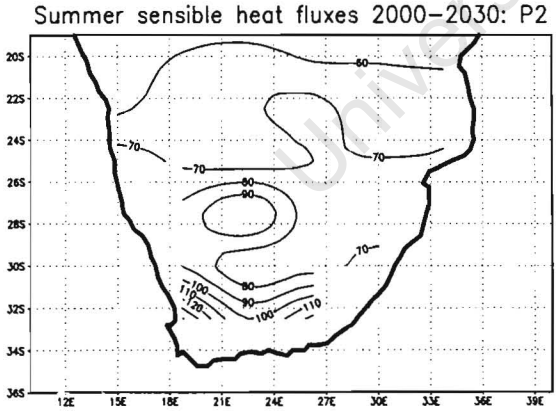

Anomaly (late – early 21st century): P2

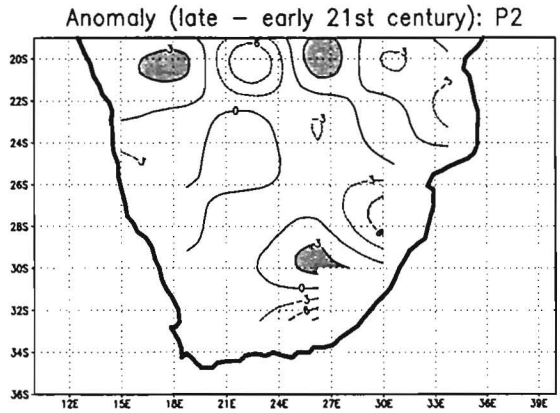

Summer sensible heat fluxes 2000–2030: P3

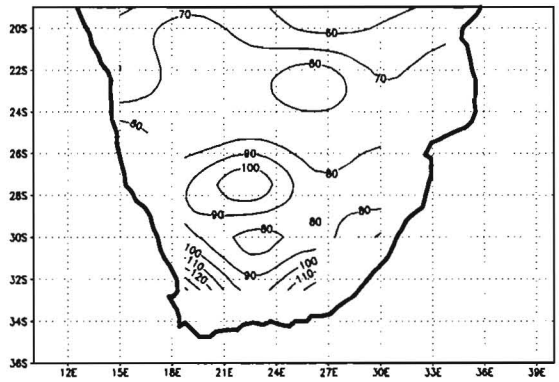

Anomaly (late – early 21st century): P3

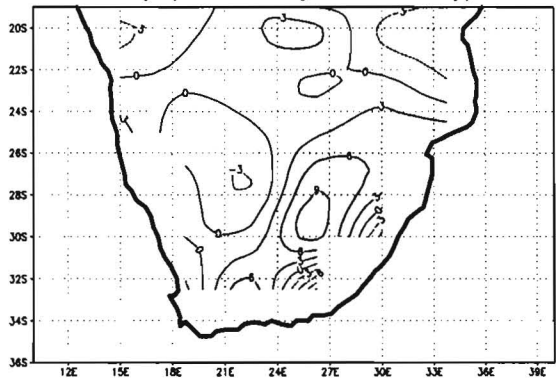

Summer sensible heat fluxes 2000–2030: P4

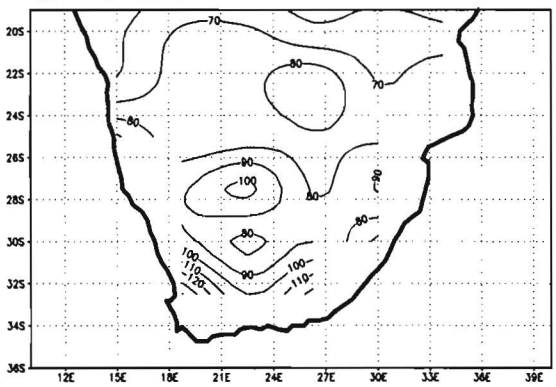

Anomaly (late – early 21st century): P4

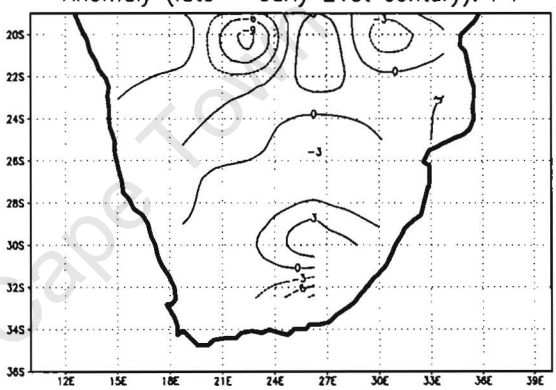

Summer sensible heat fluxes 2000–2030: P5

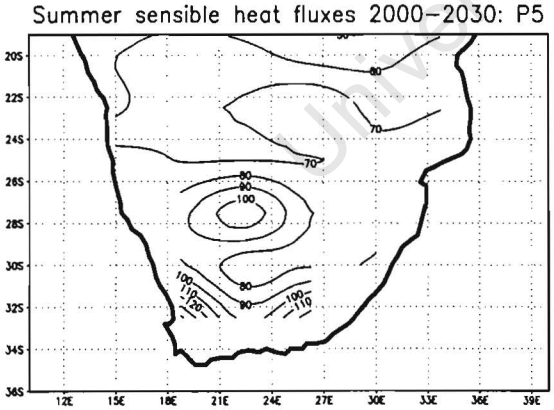

Anomaly (late – early 21st century): P5

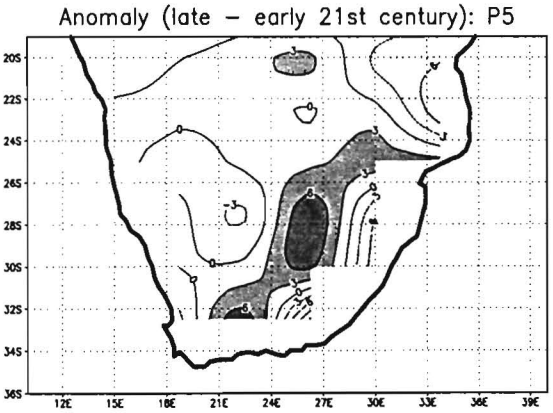

Summer soil temperatures 2000–2030: Ibissta

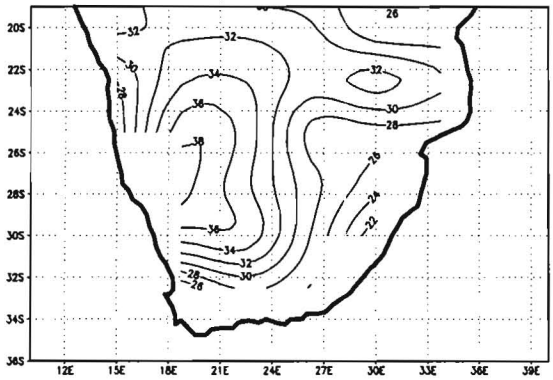

Anomaly (late – early 21st century): Ibissta

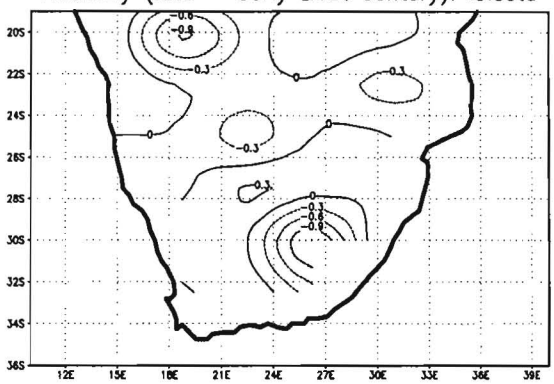

Summer soil temperatures 2000–2030: P1

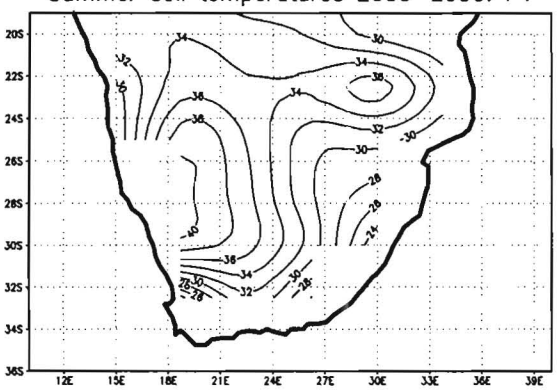

Anomaly (late – early 21st century): P1

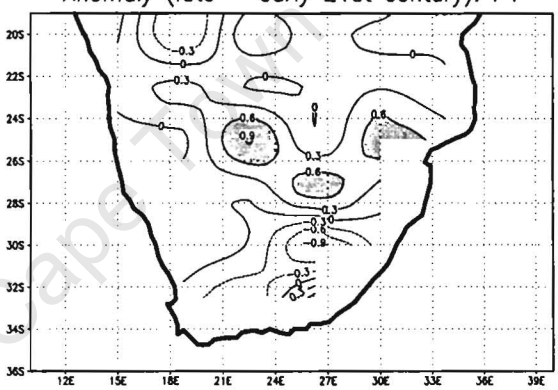

Summer soil temperatures 2000–2030: P2

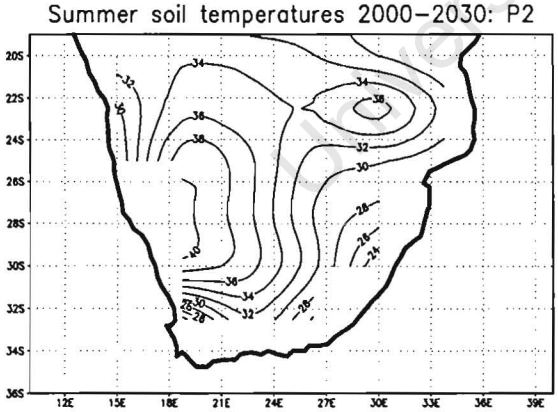

Anomaly (late – early 21st century): P2

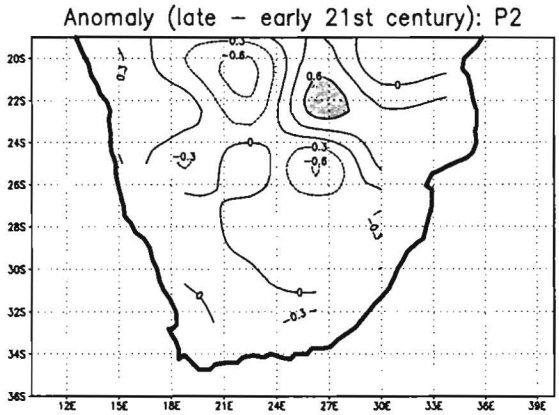

Summer soil temperatures 2000–2030: P3

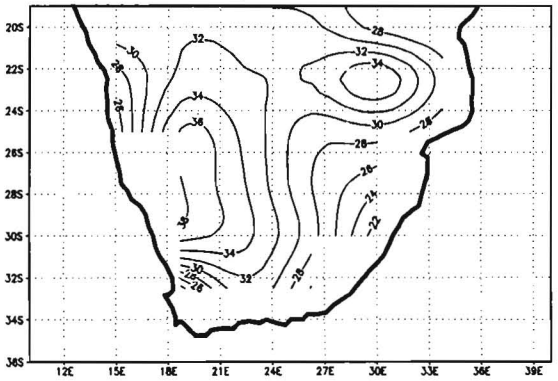

Anomaly (late – early 21st century): P3

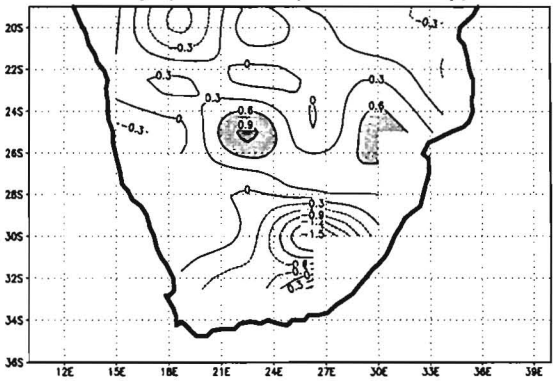

Summer soil temperatures 2000–2030: P4

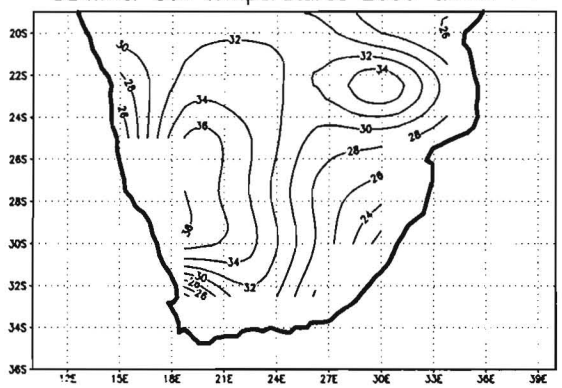

Anomaly (late – early 21st century): P4

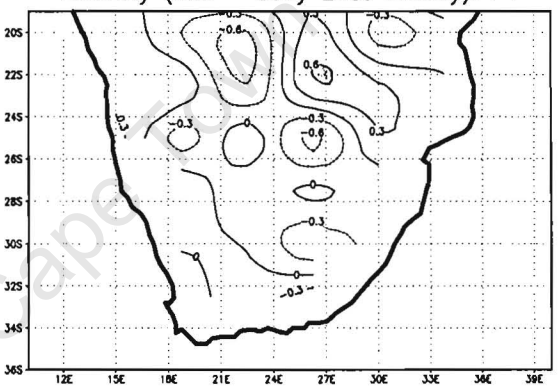

Summer soil temperatures 2000–2030: P5

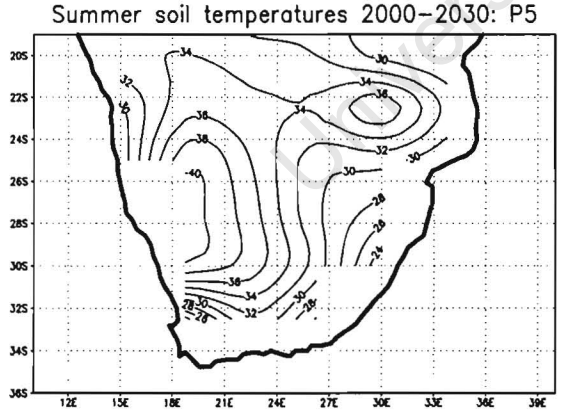

Anomaly (late – early 21st century): P5

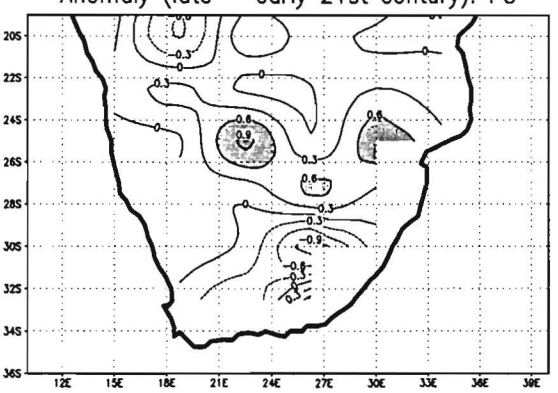

Summer soil moisture 2000–2030: Ibissta

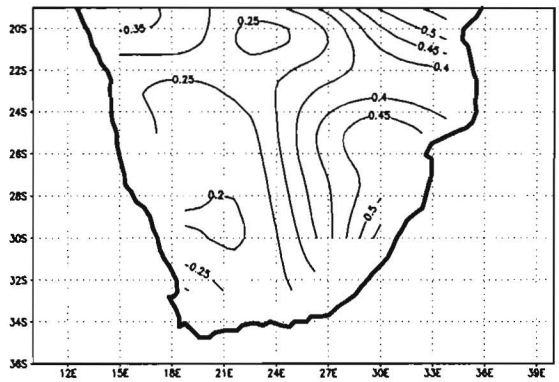

Anomaly (late – early 21st century): Ibissta

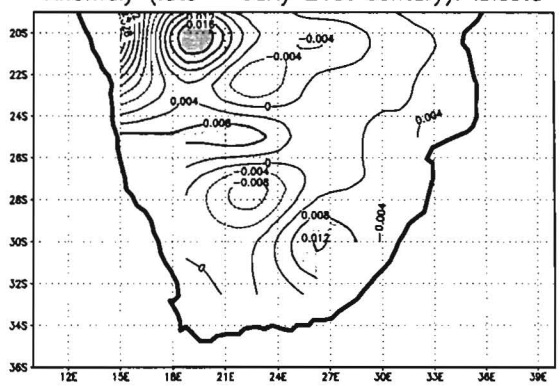

Summer soil moisture 2000–2030: P1

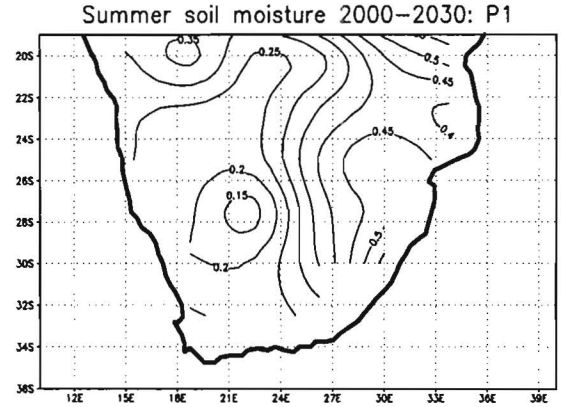

Anomaly (late – early 21st century): P1

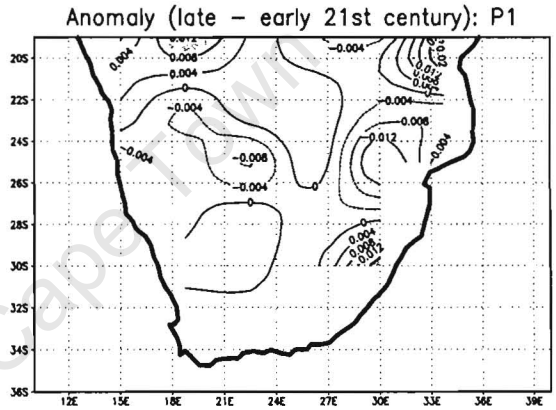

Summer soil moisture 2000–2030: P2

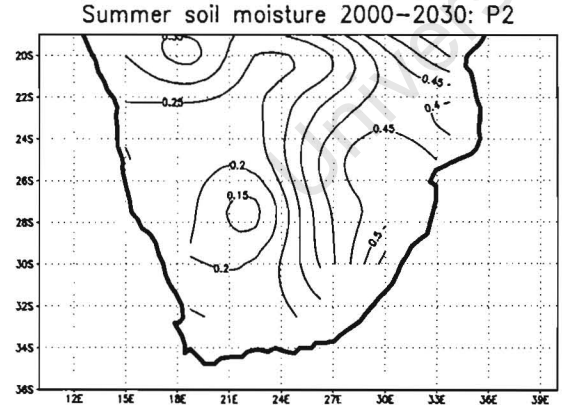

Anomaly (late – early 21st century): P2

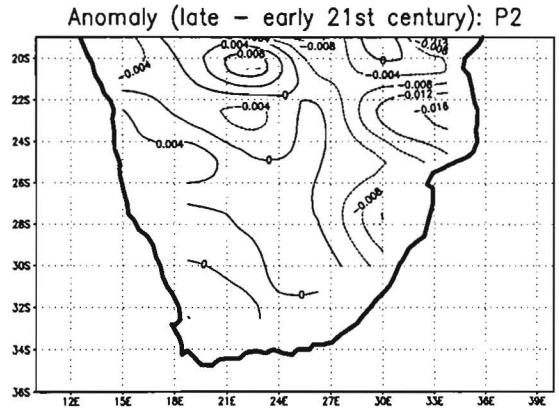

Summer soil moisture 2000–2030: P3

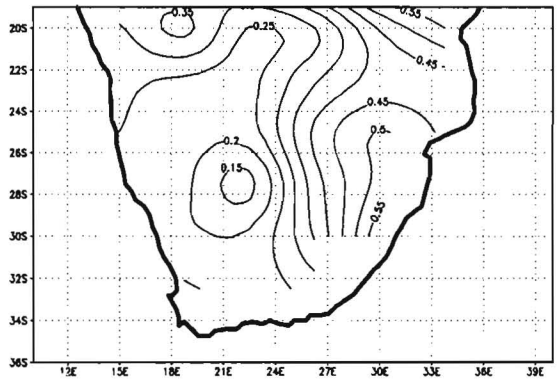

Anomaly (late – early 21st century): P3

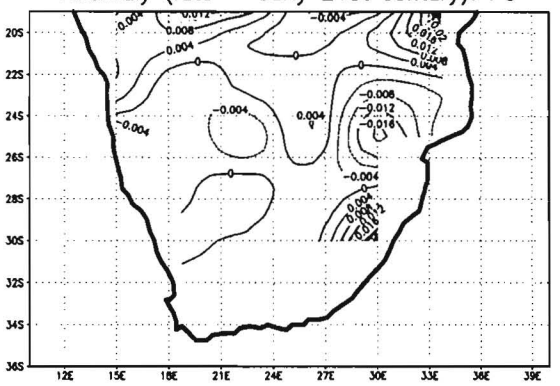

Summer soil moisture 2000–2030: P4

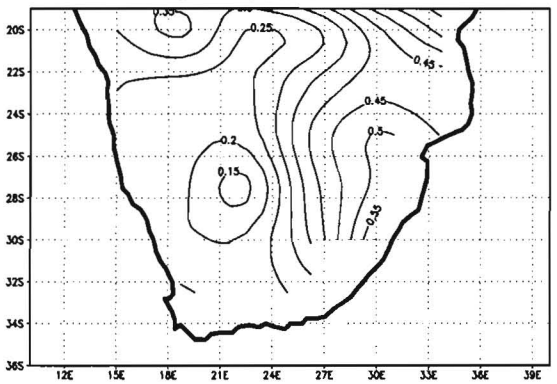

Anomaly (late – early 21st century): P4

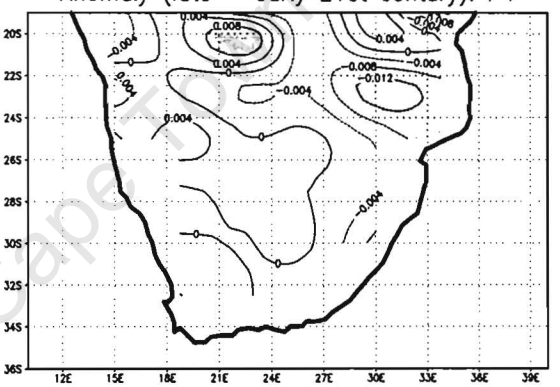

Summer soil moisture 2000–2030: P5

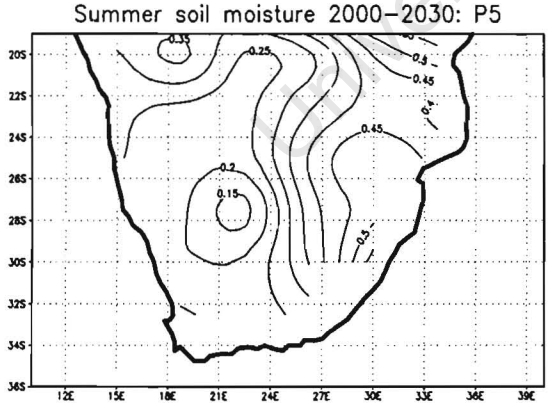

Anomaly (late – early 21st century): P5

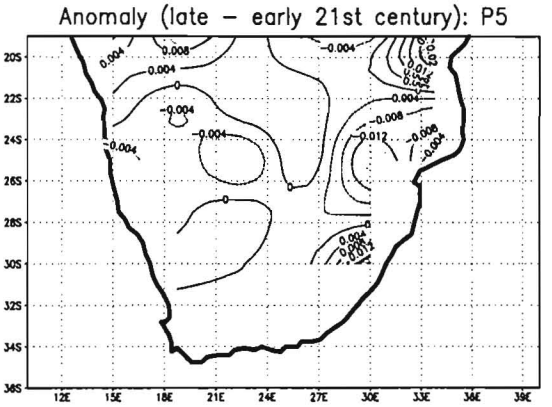

Summer latent heat fluxes 2000–2030: Ibissta

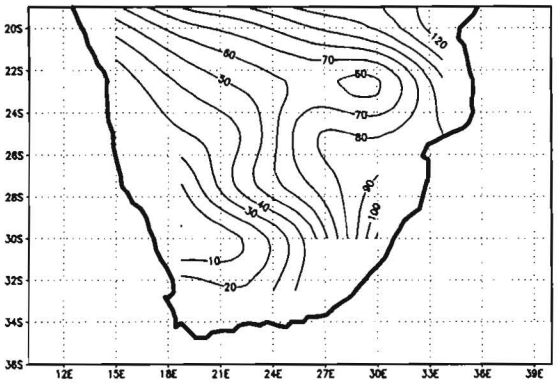

Anomaly (late – early 21st century): Ibissta

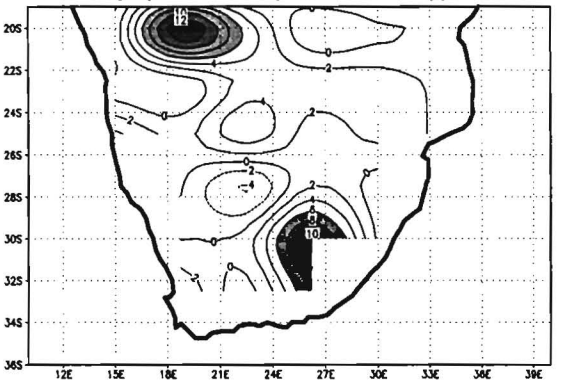

Summer latent heat fluxes 2000–2030: P1

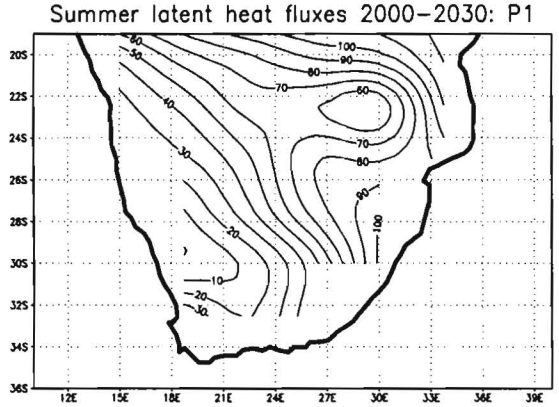

Anomaly (late – early 21st century): P1

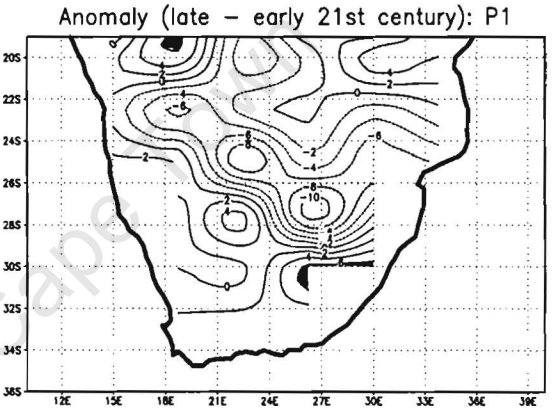

Summer latent heat fluxes 2000–2030: P2

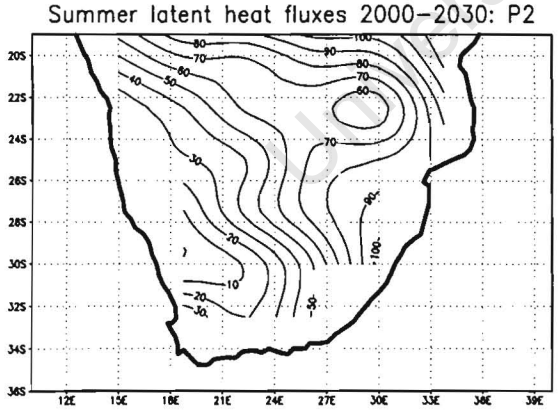

Anomaly (late – early 21st century): P2

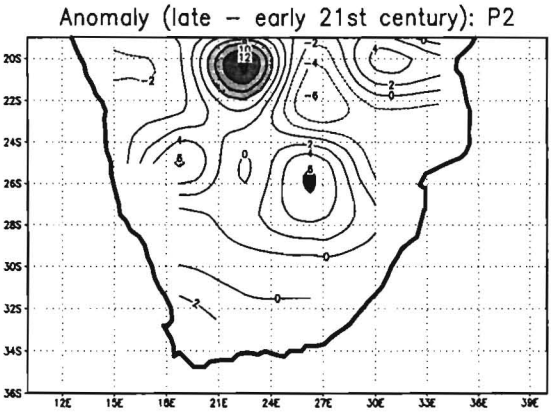

Summer latent heat fluxes 2000–2030: P3

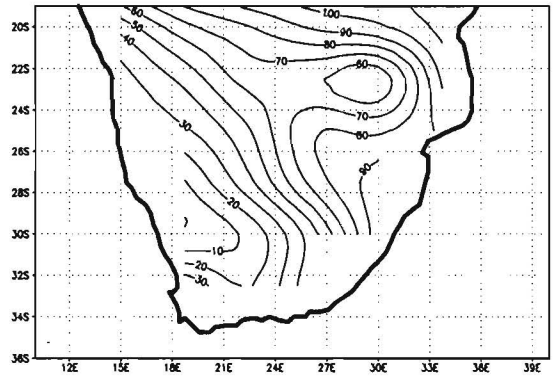

Anomaly (late – early 21st century): P3

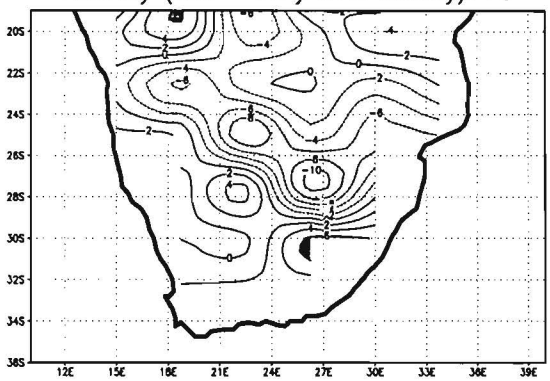

Summer latent heat fluxes 2000–2030: P4

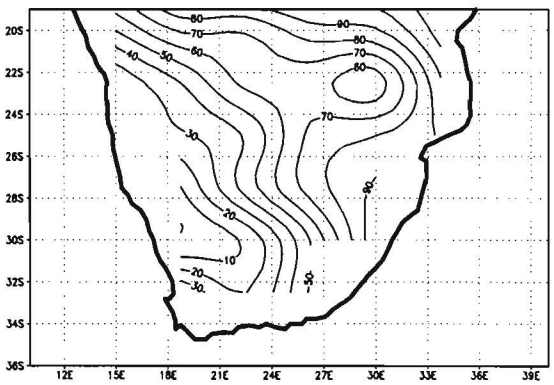

Anomaly (late – early 21st century): P4

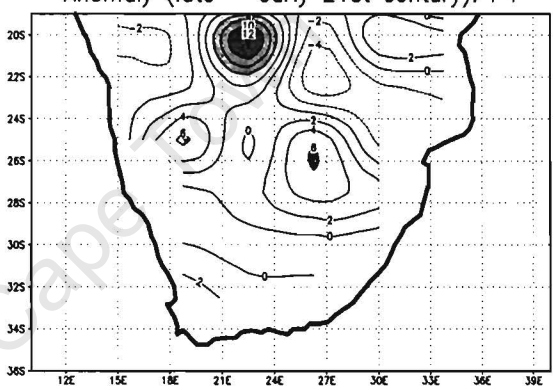

Summer latent heat fluxes 2000–2030: P5

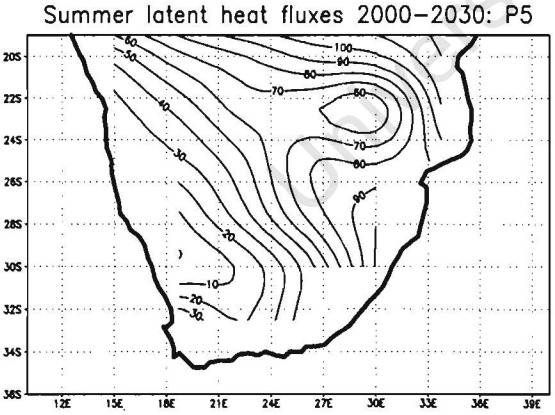

Anomaly (late – early 21st century): P5

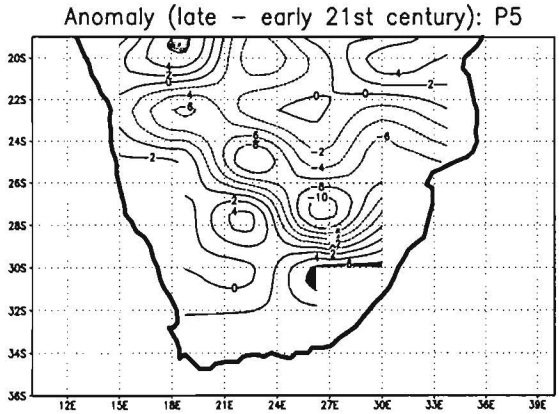

Summer LAI (upper canopy) 2000–2030: Ibissta

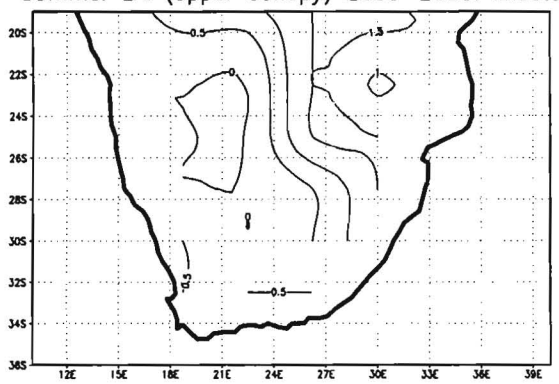

Anomaly (late – early 21st century): Ibissta

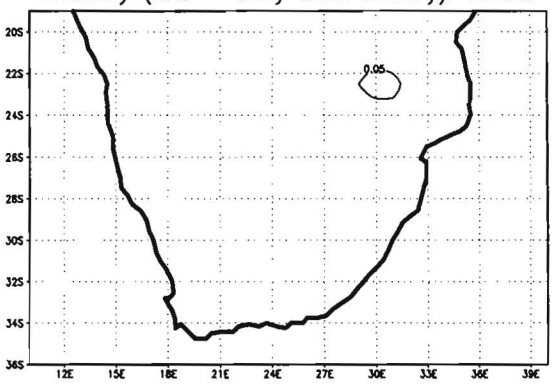

Summer LAI (upper canopy) 2000–2030: P1

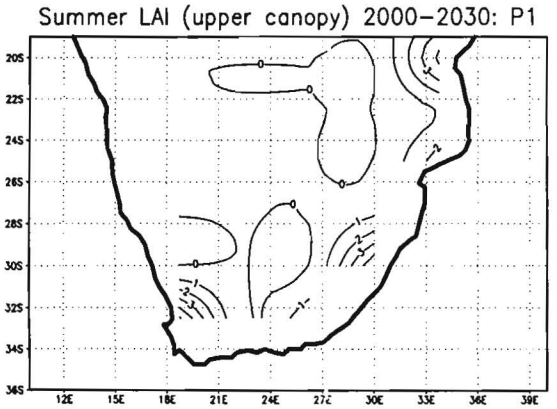

Anomaly (late – early 21st century): P1

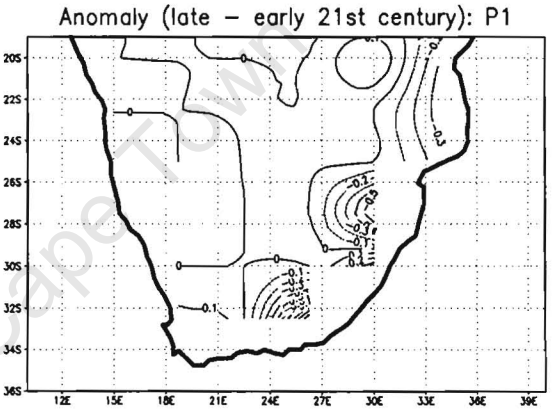

Summer LAI (upper canopy) 2000–2030: P2

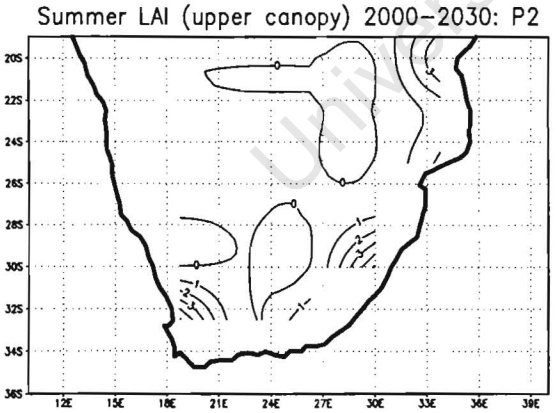

Anomaly (late – early 21st century): P2

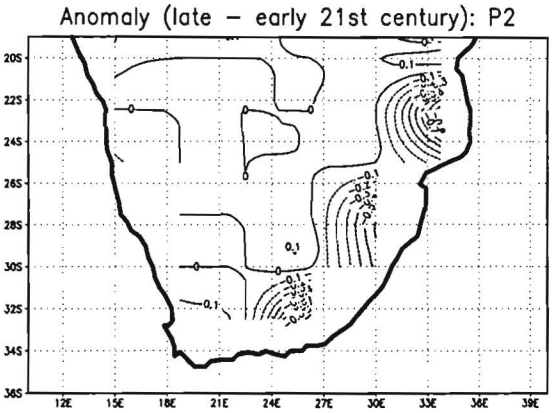

Summer LAI (upper canopy) 2000–2030: P3

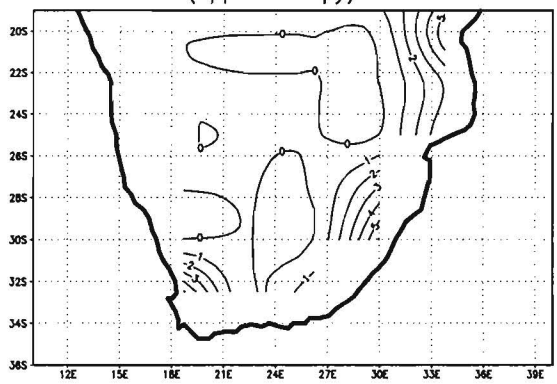

Anomaly (late – early 21st century): P3

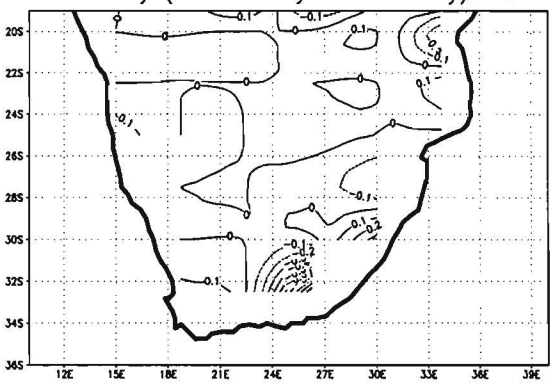

Summer LAI (upper canopy) 2000–2030: P4

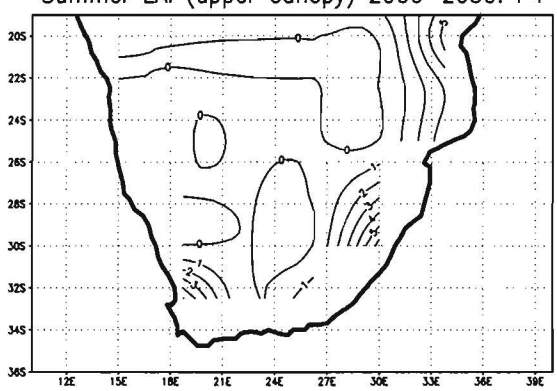

Anomaly (late – early 21st century): P4

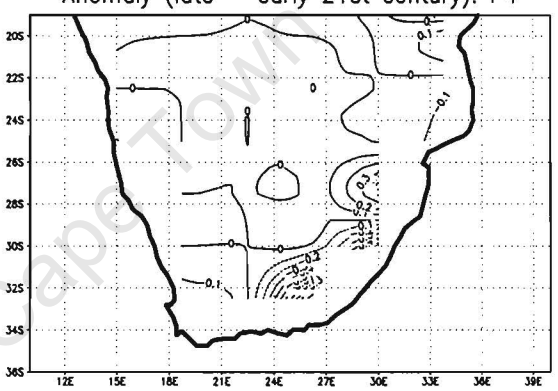

Summer LAI (upper canopy) 2000–2030: P5

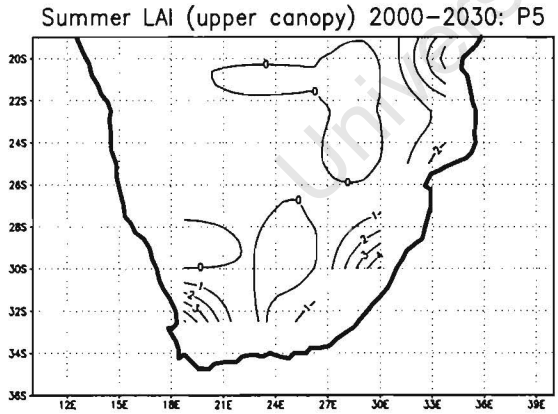

Anomaly (late – early 21st century): P5

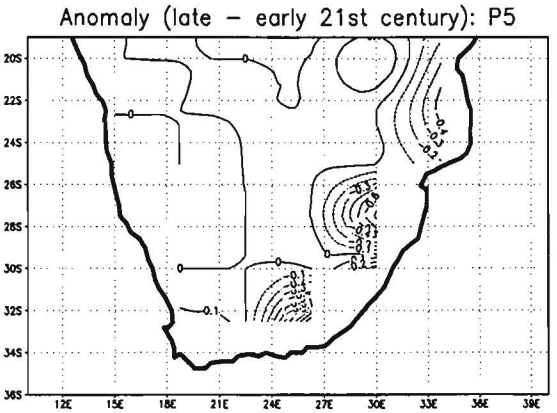

Summer LAI (lower canopy) 2000–2030: Ibissta

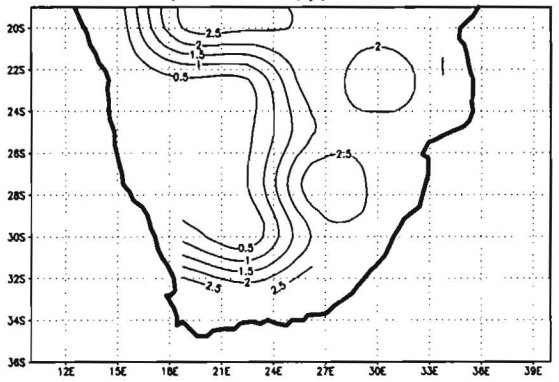

Anomaly (late – early 21st century): Ibissta

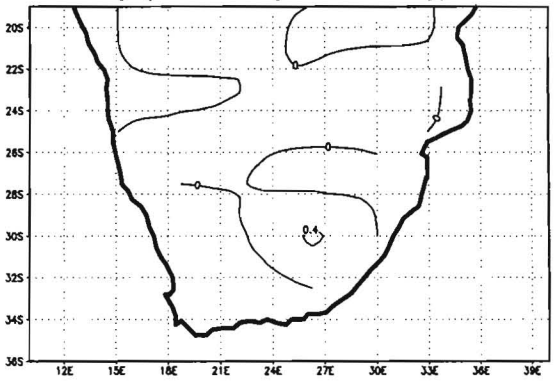

Summer LAI (lower canopy) 2000–2030: P1

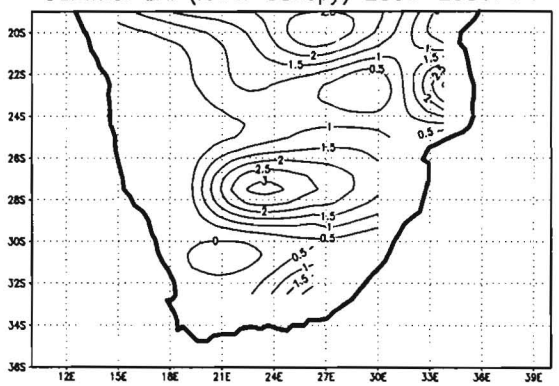

Anomaly (late – early 21st century): P1

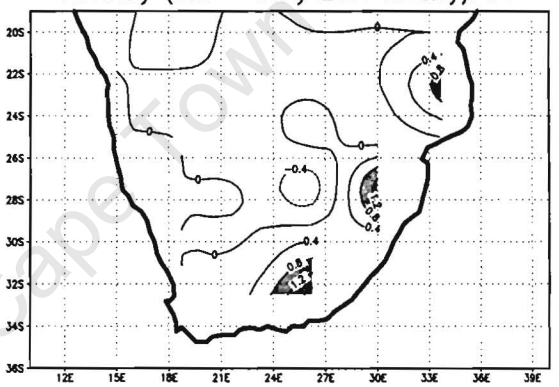

Summer LAI (lower canopy) 2000–2030: P2

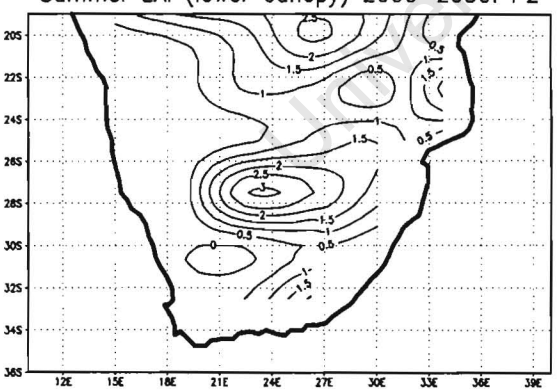

Anomaly (late – early 21st century): P2

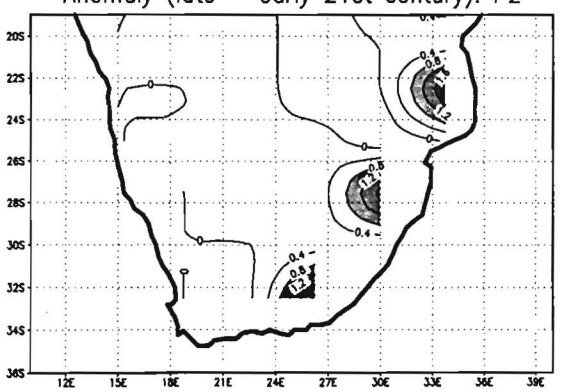

Summer LAI (lower canopy) 2000–2030: P3

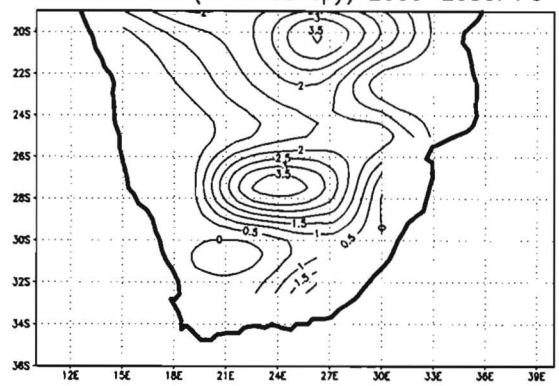

Anomaly (late – early 21st century): P3

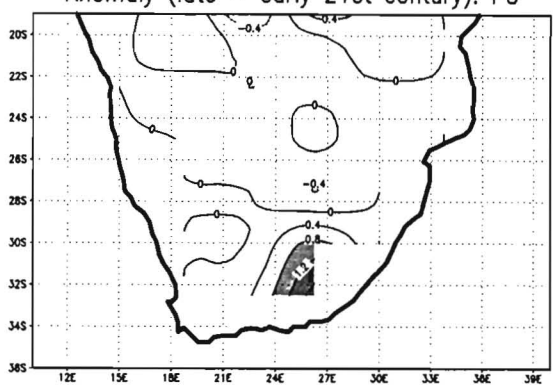

Summer LAI (lower canopy) 2000–2030: P4

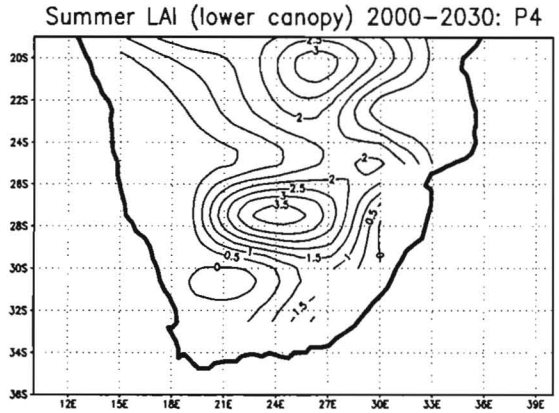

Anomaly (late – early 21st century): P4

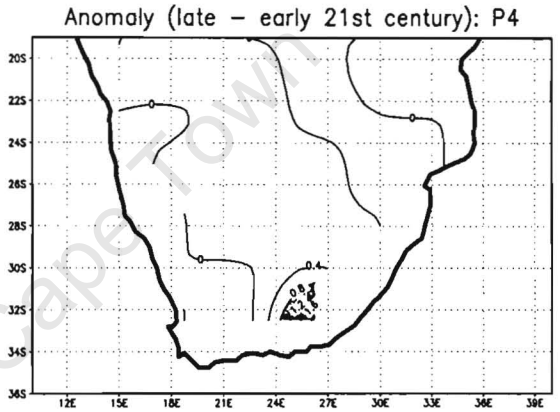

Summer LAI (lower canopy) 2000–2030: P5

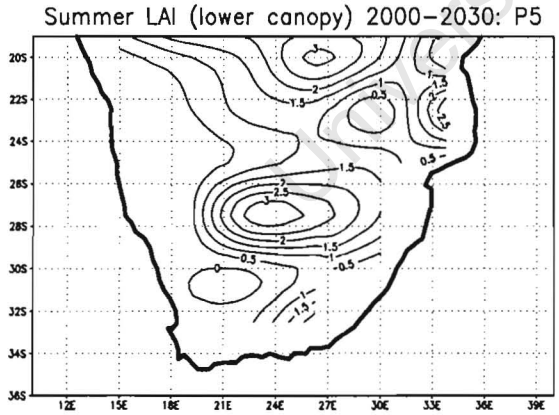

Anomaly (late – early 21st century): P5

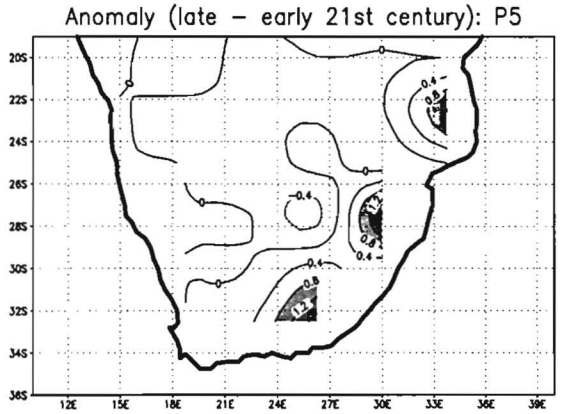

APPENDIX E

WINTER SEASONAL DIFFERENCES BETWEEN THE EARLY AND LATE 21ST CENTURY

The winter seasonal mean and anomalies for the following scenarios:

- Ibissta
- P1
- P2
- P3
- P4
- P5

and the following variables:

- Net primary productivity
- Average evapotranspiration
- Sensible heat fluxes
- Soil temperatures
- Soil moisture
- Latent heat fluxes
- Leaf area index (upper and lower canopies)

are included in the Appendix.

Winter NPP 2000–2030: Ibissta

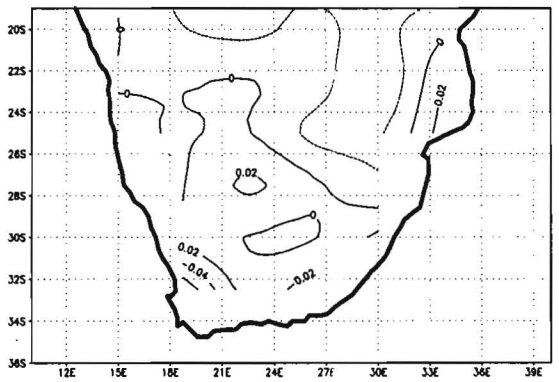

Anomaly (late – early 21st century): Ibissta

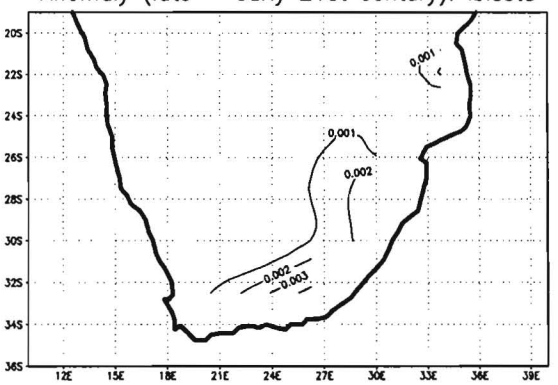

Winter NPP 2000–2030: P1

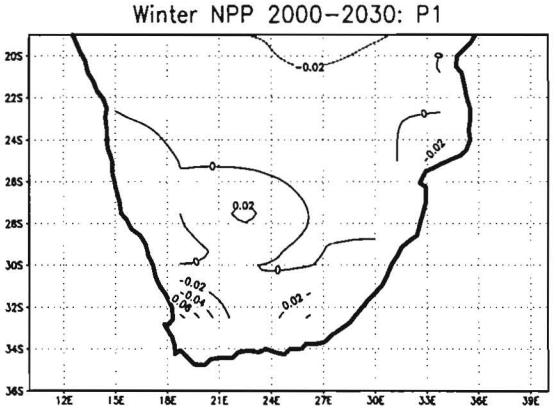

Anomaly (late – early 21st century): P1

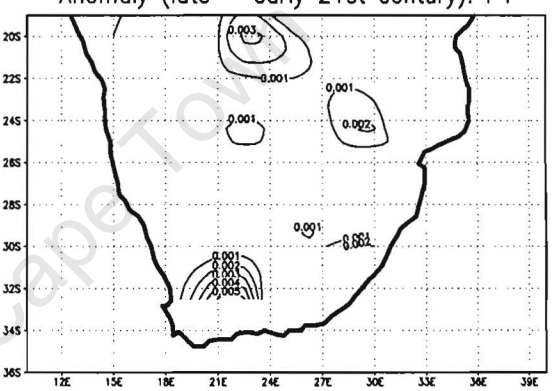

Winter NPP 2000–2030: P2

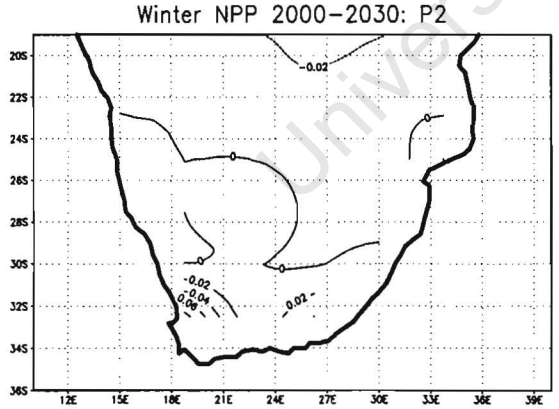

Anomaly (late – early 21st century): P2

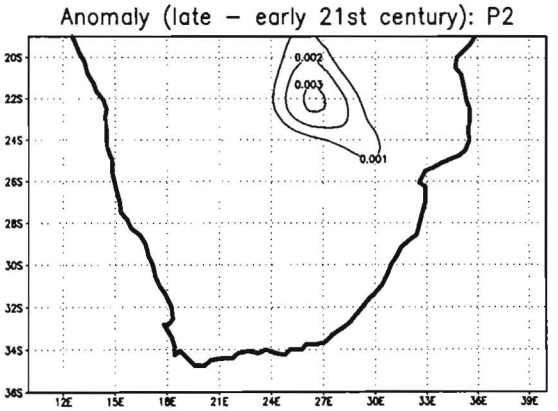

Winter NPP 2000–2030: P3

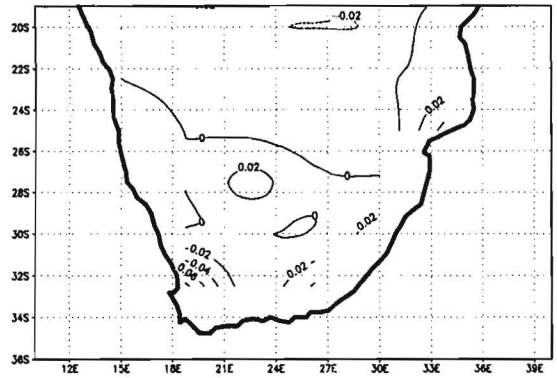

Anomaly (late – early 21st century): P3

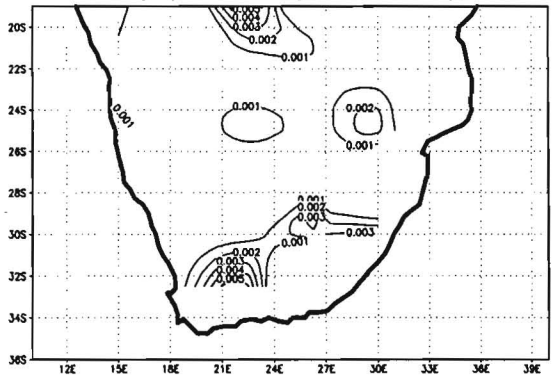

Winter NPP 2000–2030: P4

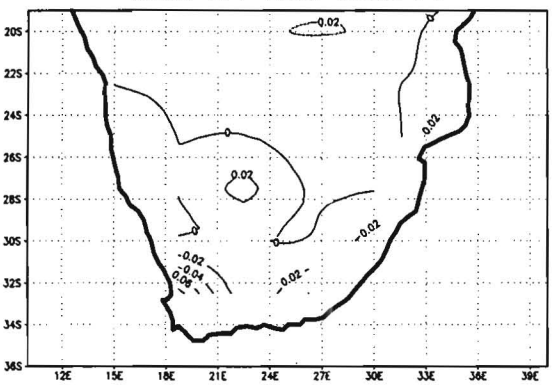

Anomaly (late – early 21st century): P4

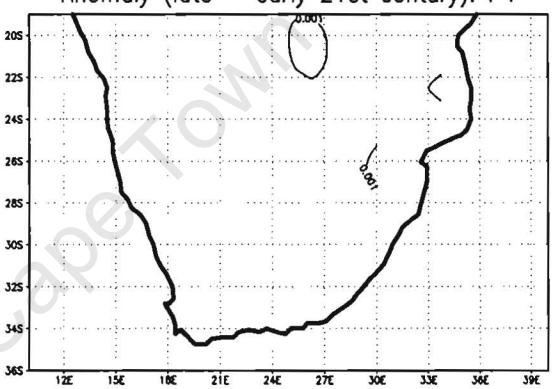

Winter NPP 2000–2030: P5

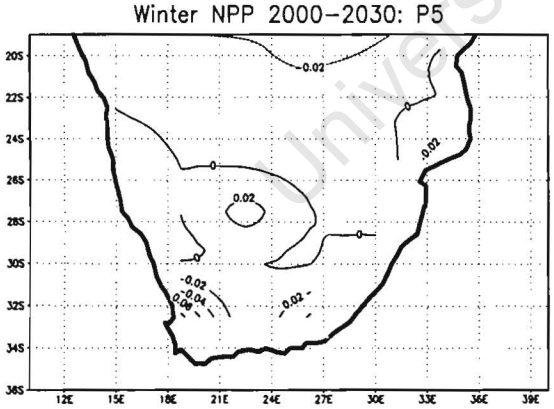

Anomaly (late – early 21st century): P5

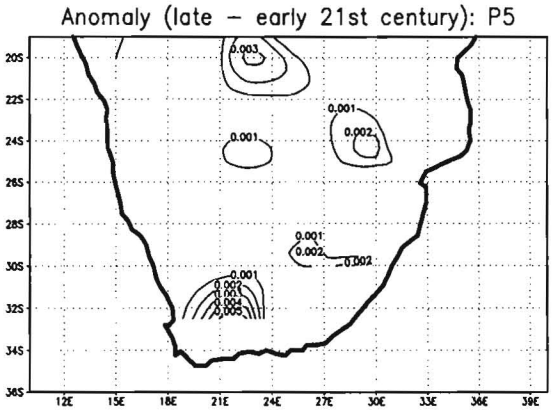

Winter avg. evapotransp. 2000–2030: Ibissta

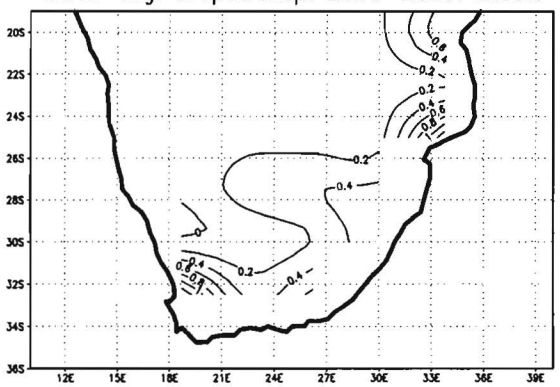

Anomaly (late – early 21st century): Ibissta

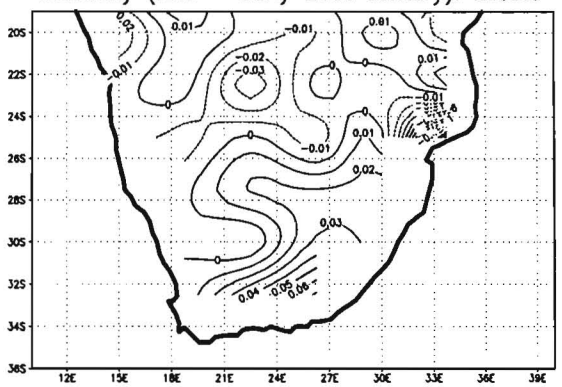

Winter avg. evapotransp. 2000–2030: P1

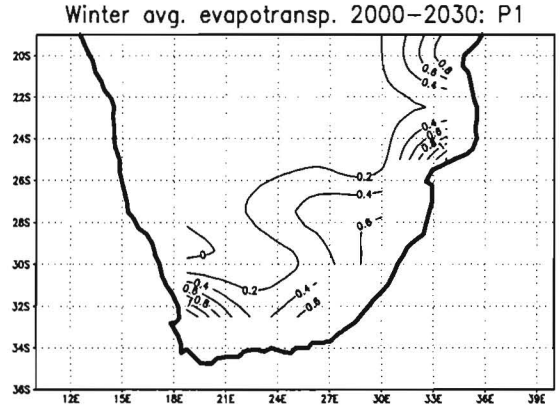

Anomaly (late – early 21st century): P1

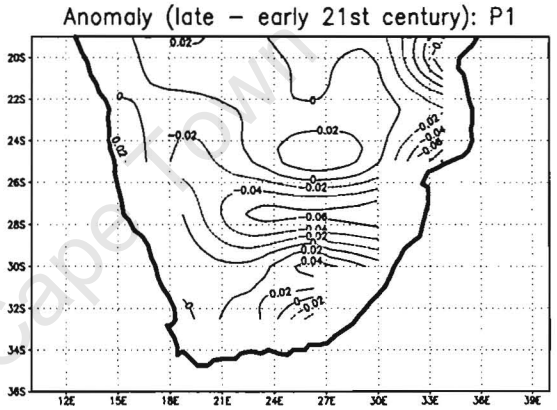

Winter avg. evapotransp. 2000–2030: P2

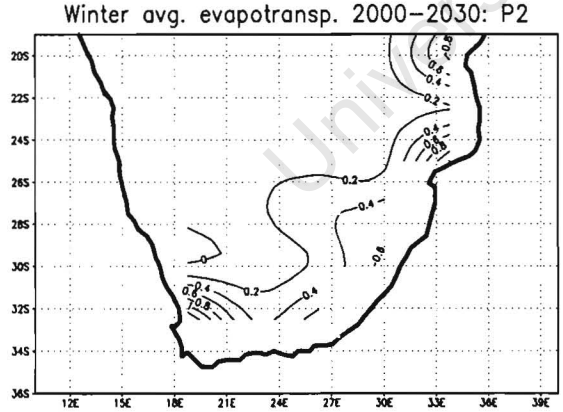

Anomaly (late – early 21st century): P2

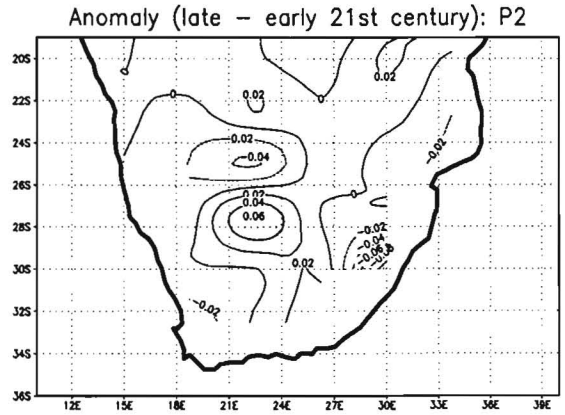

Winter avg. evapotransp. 2000–2030: P3

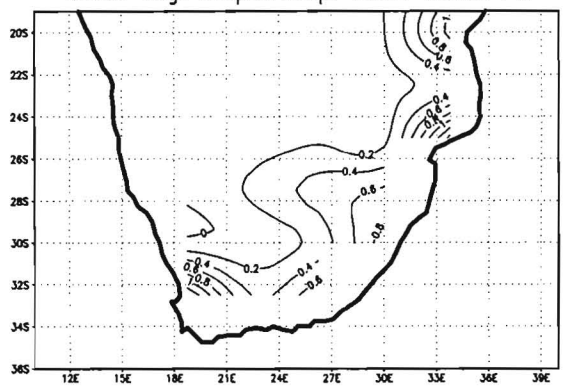

Anomaly (late – early 21st century): P3

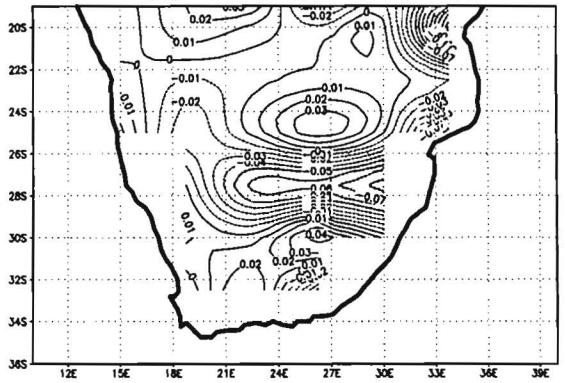

Winter avg. evapotransp. 2000–2030: P4

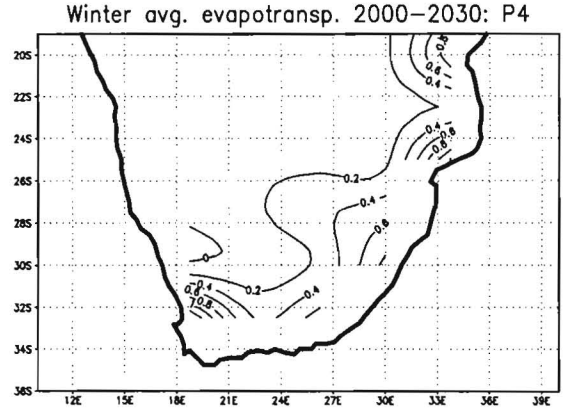

Anomaly (late – early 21st century): P4

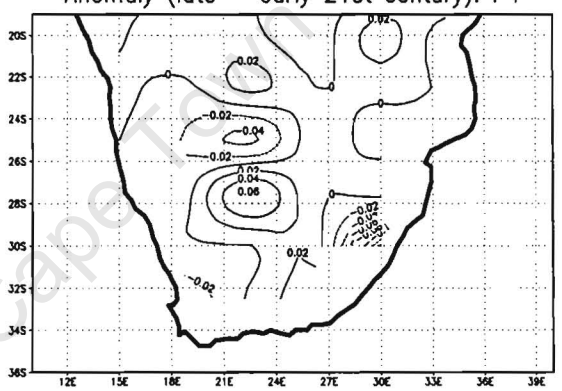

Winter avg. evapotransp. 2000–2030: P5

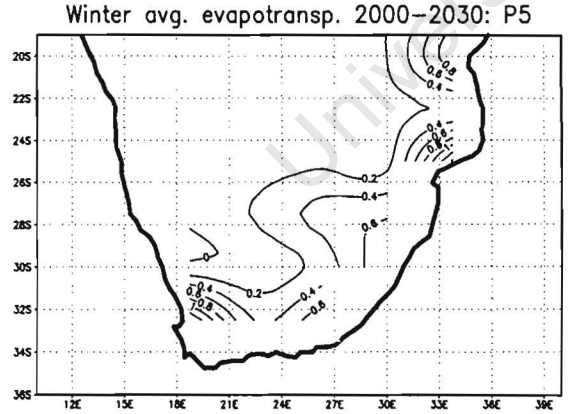

Anomaly (late – early 21st century): P5

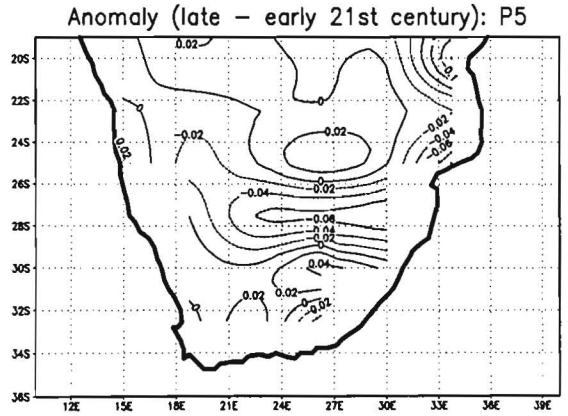

Winter sensible heat fluxes 2000–2030: Ibissta

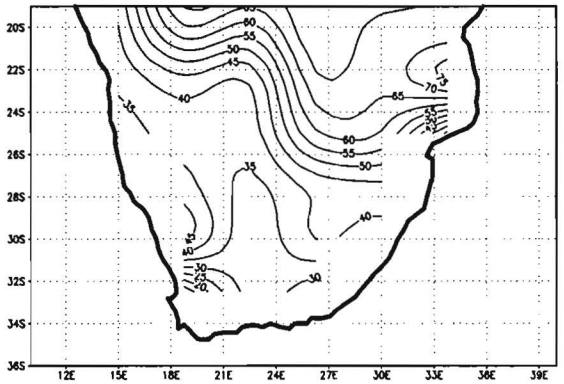

Anomaly (late – early 21st century): Ibissta

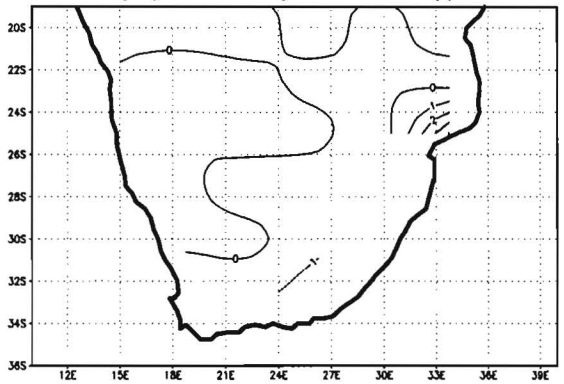

Winter sensible heat fluxes 2000–2030: P1

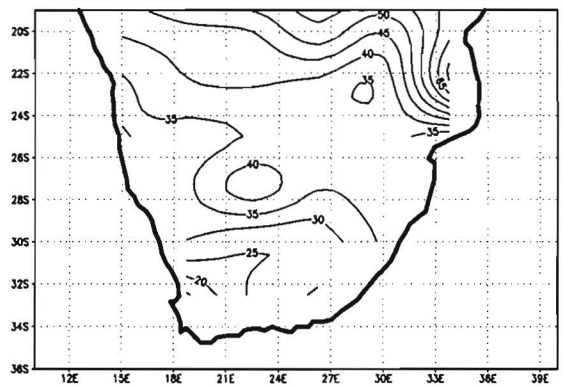

Anomaly (late – early 21st century): P1

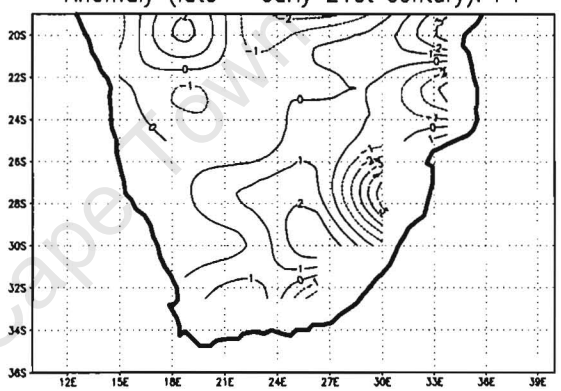

Winter sensible heat fluxes 2000–2030: P2

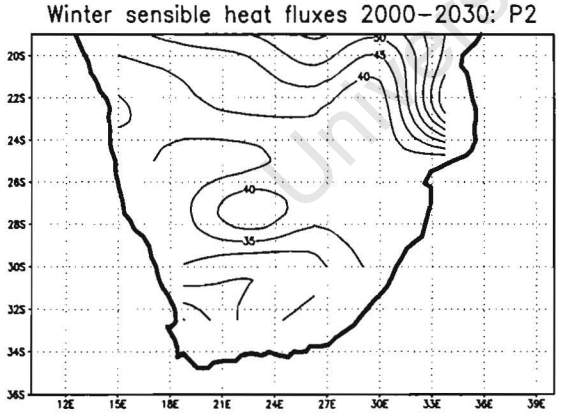

Anomaly (late – early 21st century): P2

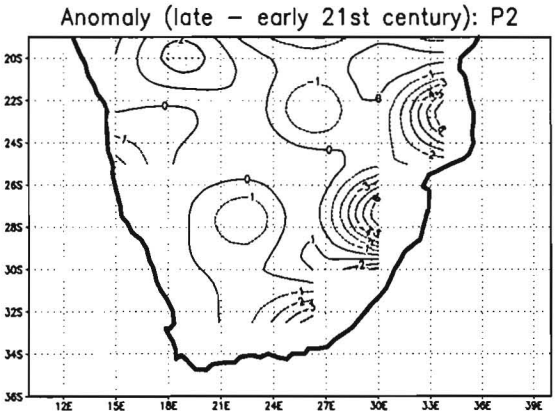

Winter sensible heat fluxes 2000–2030: P3

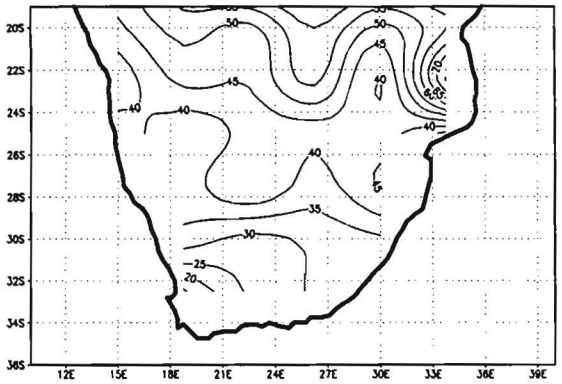

Anomaly (late – early 21st century): P3

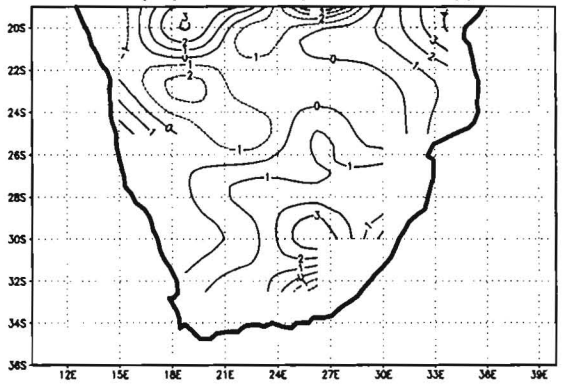

Winter sensible heat fluxes 2000–2030: P4

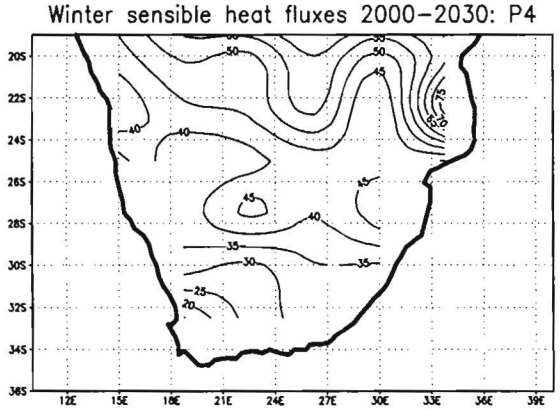

Anomaly (late – early 21st century): P4

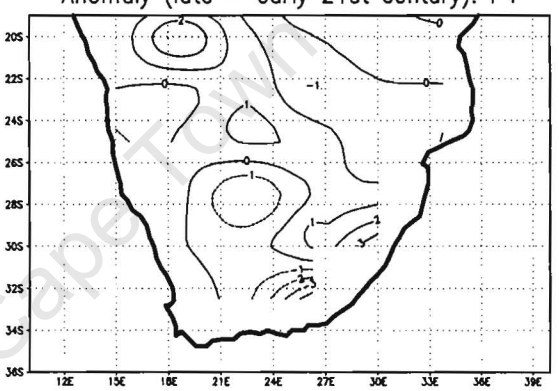

Winter sensible heat fluxes 2000–2030: P5

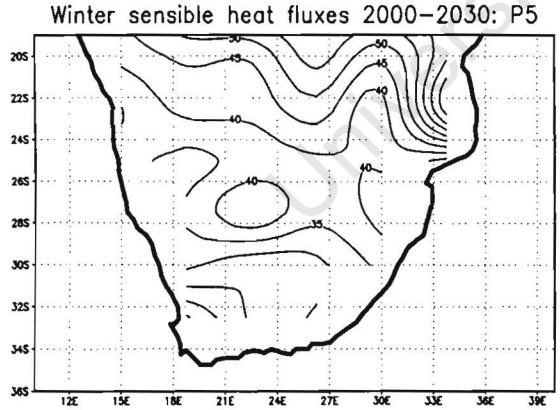

Anomaly (late – early 21st century): P5

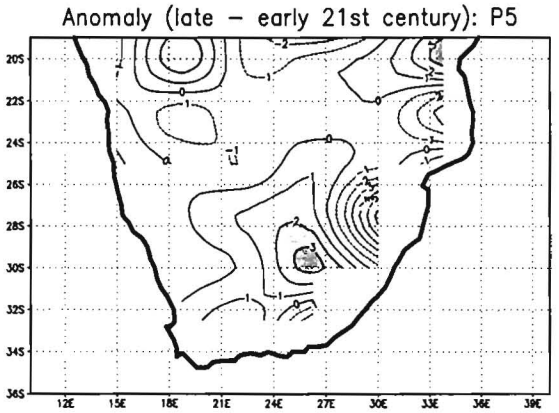

Winter soil temperatures 2000–2030: Ibissta

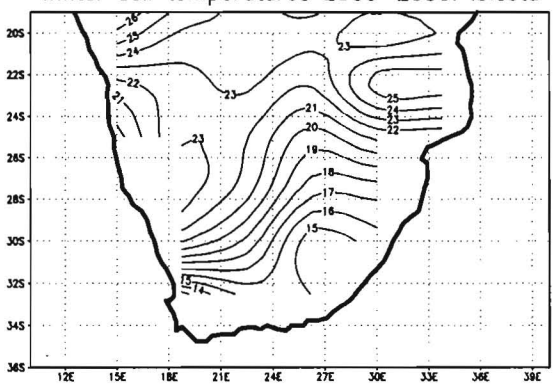

Anomaly (late – early 21st century): Ibissta

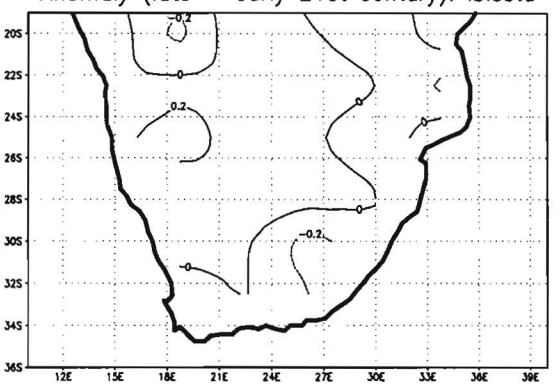

Winter soil temperatures 2000–2030: P1

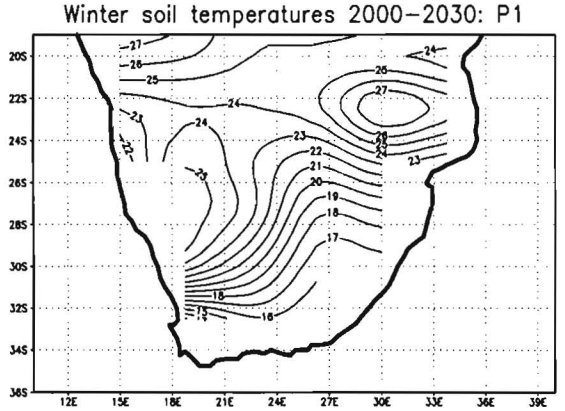

Anomaly (late – early 21st century): P1

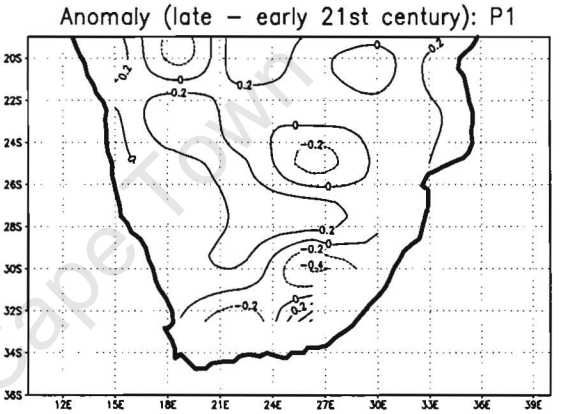

Winter soil temperatures 2000–2030: P2

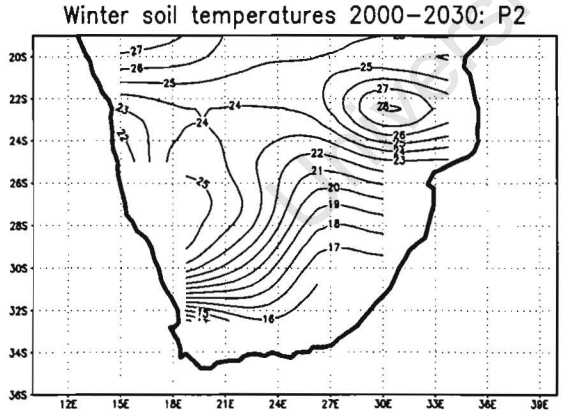

Anomaly (late – early 21st century): P2

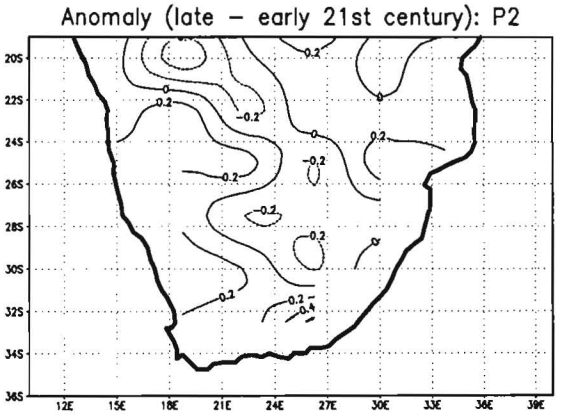

Winter soil temperatures 2000–2030: P3

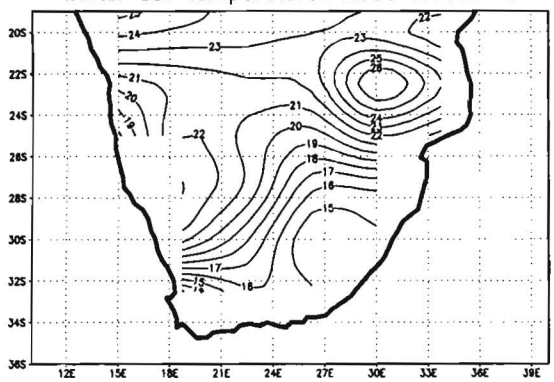

Anomaly (late – early 21st century): P3

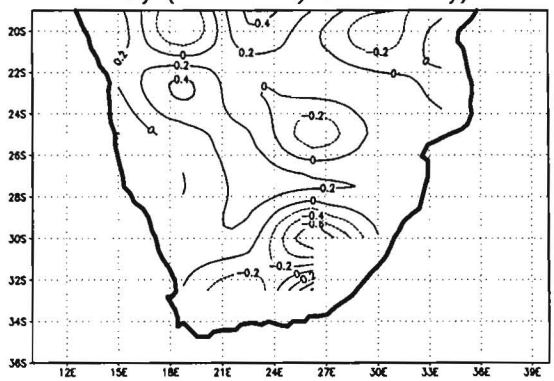

Winter soil temperatures 2000–2030: P4

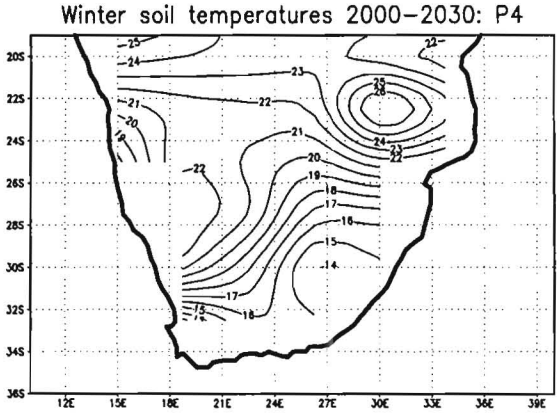

Anomaly (late – early 21st century): P4

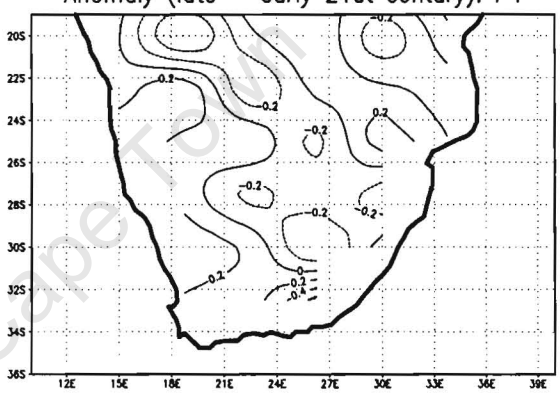

Winter soil temperatures 2000–2030: P5

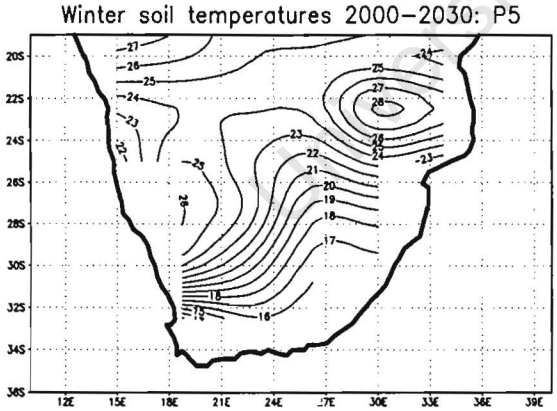

Anomaly (late – early 21st century): P5

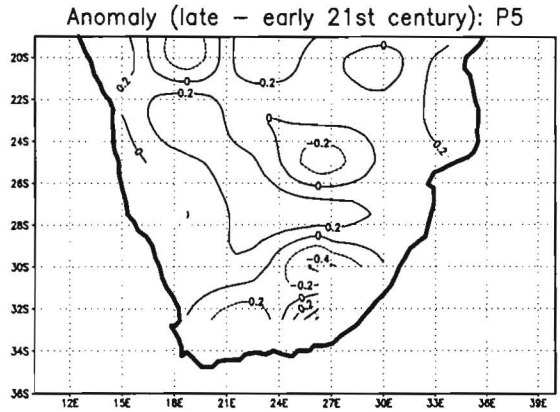

Winter soil moisture 2000–2030: Ibissta

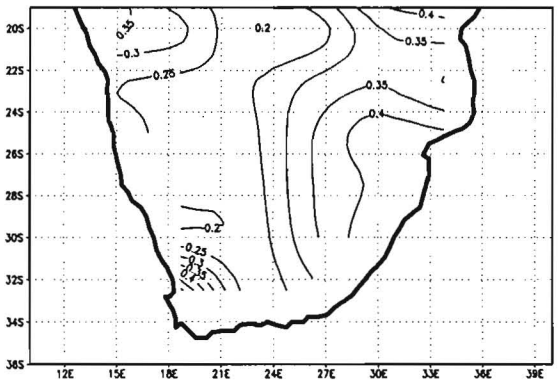

Anomaly (late – early 21st century): Ibissta

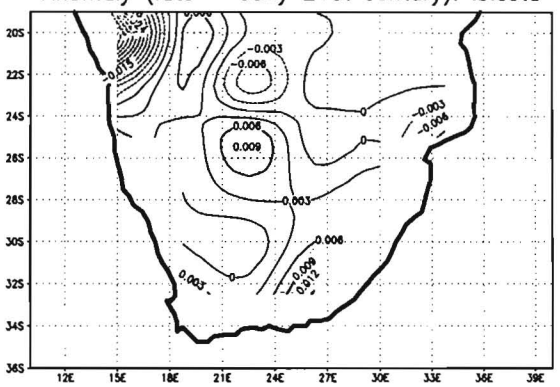

Winter soil moisture 2000–2030: P1

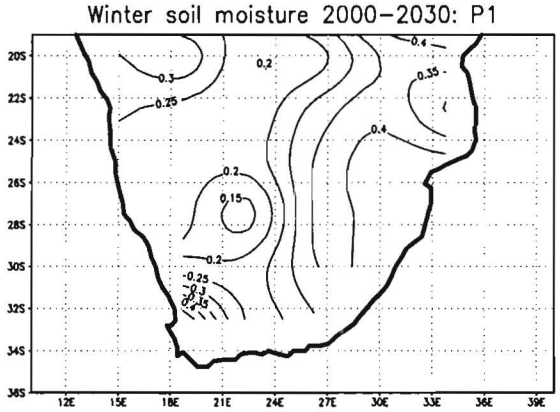

Anomaly (late – early 21st century): P1

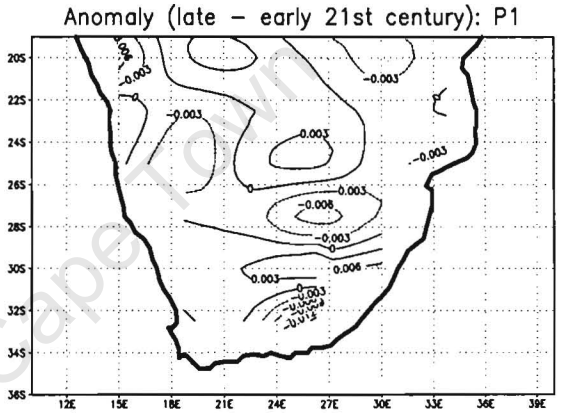

Winter soil moisture 2000–2030: P2

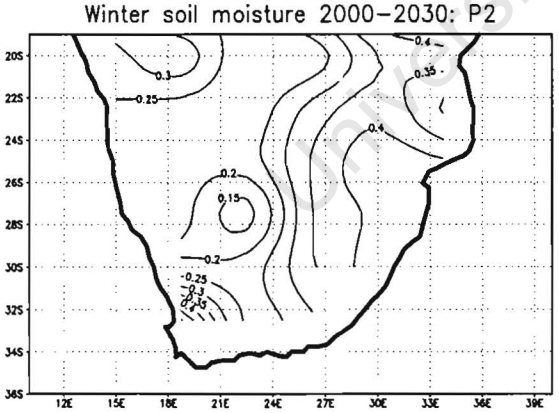

Anomaly (late – early 21st century): P2

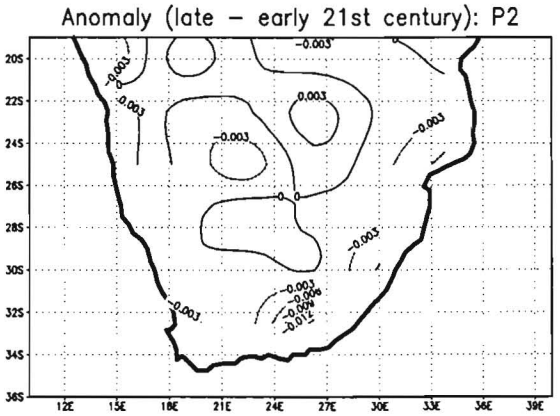

Winter soil moisture 2000–2030: P3

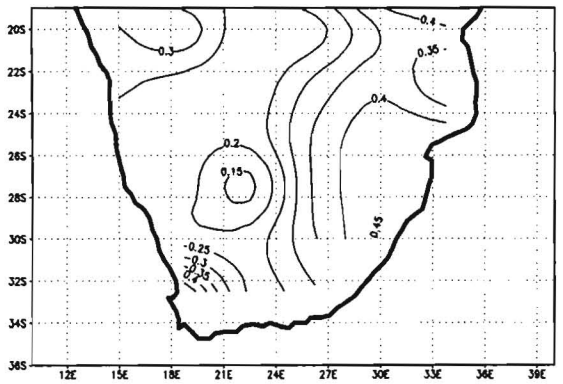

Anomaly (late – early 21st century): P3

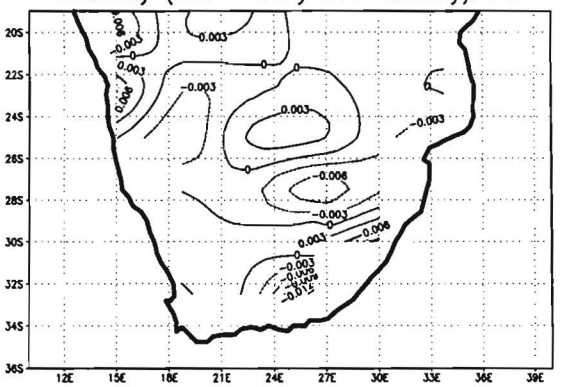

Winter soil moisture 2000–2030: P4

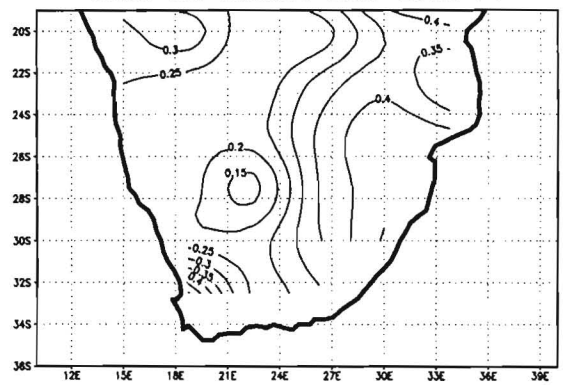

Anomaly (late – early 21st century): P4

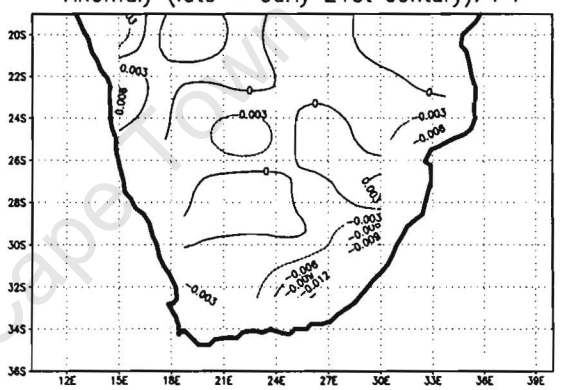

Winter soil moisture 2000–2030: P5

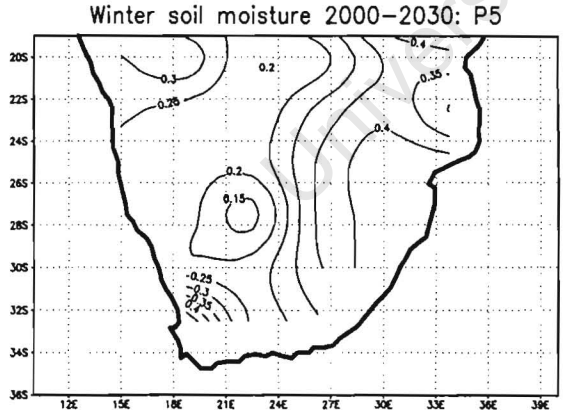

Anomaly (late – early 21st century): P5

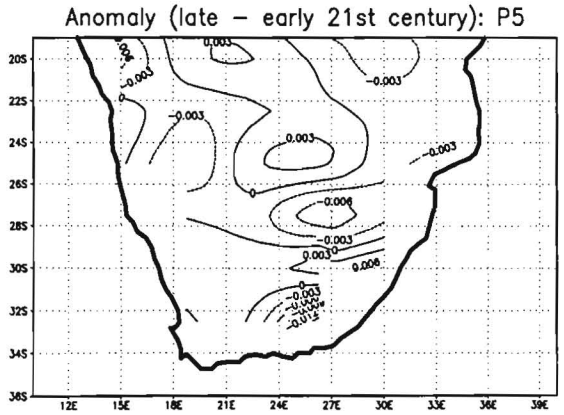

Winter latent heat fluxes 2000–2030: Ibissta

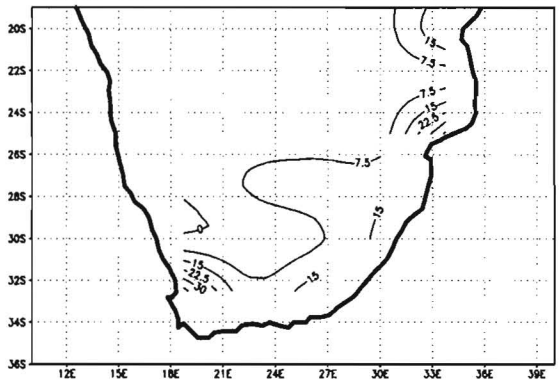

Anomaly (late – early 21st century): Ibissta

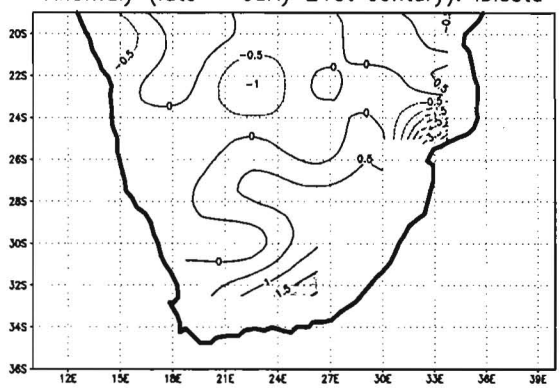

Winter latent heat fluxes 2000–2030: P1

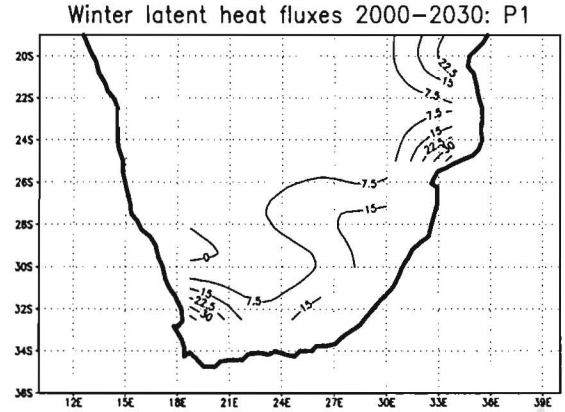

Anomaly (late – early 21st century): P1

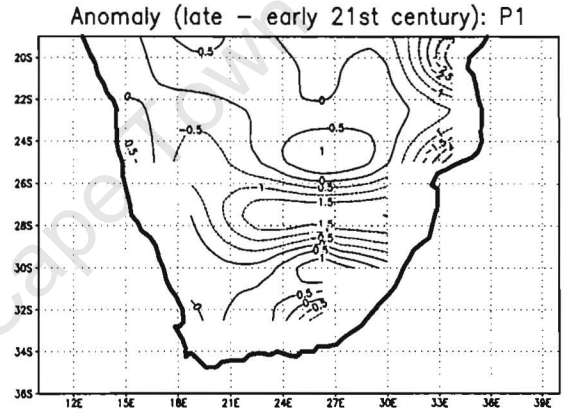

Winter latent heat fluxes 2000–2030: P2

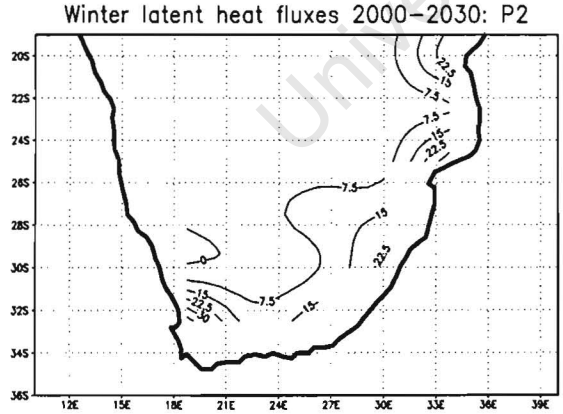

Anomaly (late – early 21st century): P2

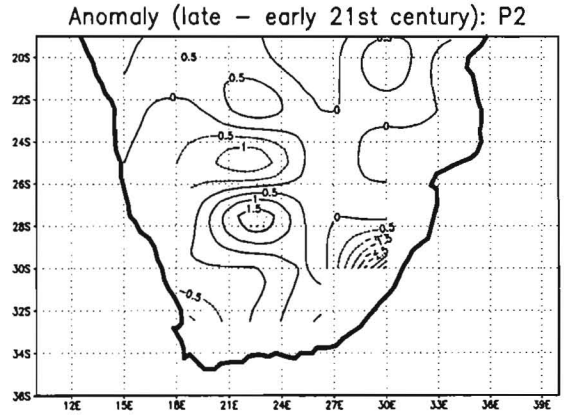

Winter latent heat fluxes 2000–2030: P3

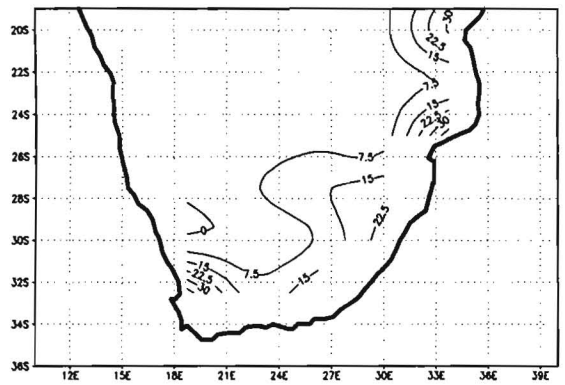

Anomaly (late – early 21st century): P3

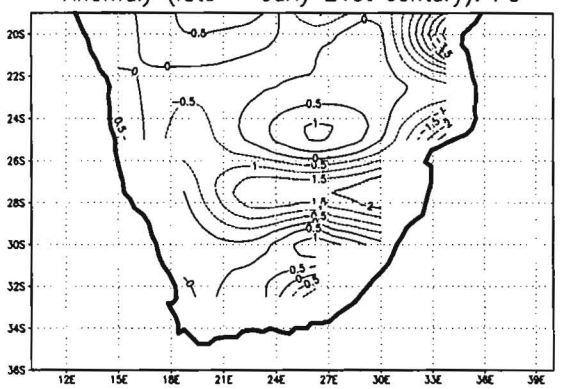

Winter latent heat fluxes 2000–2030: P4

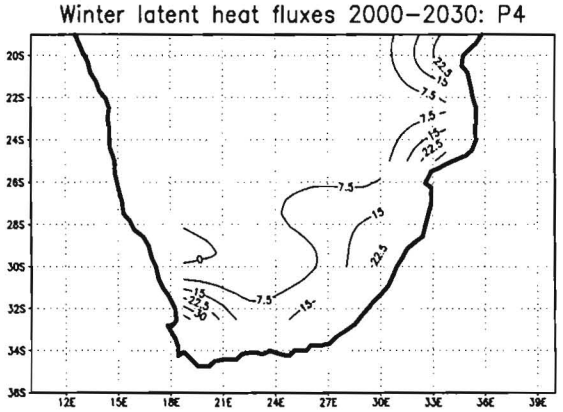

Anomaly (late – early 21st century): P4

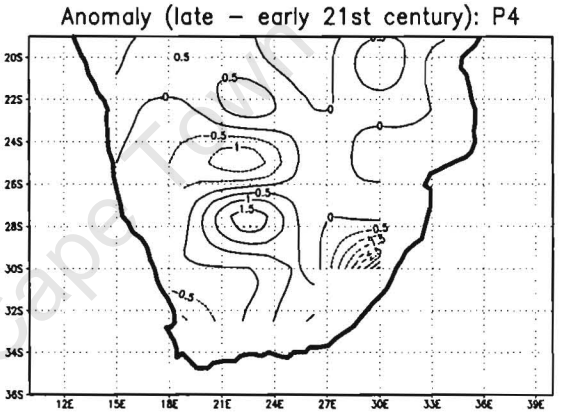

Winter latent heat fluxes 2000–2030: P5

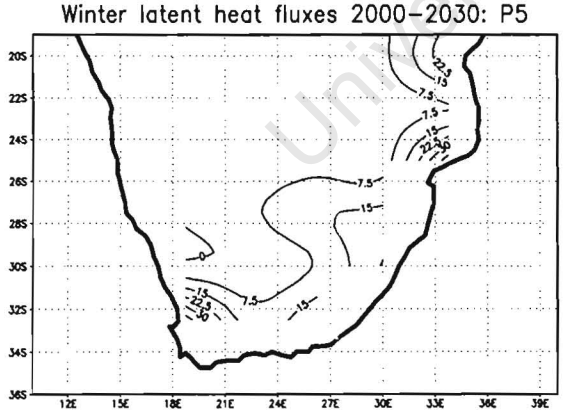

Anomaly (late – early 21st century): P5

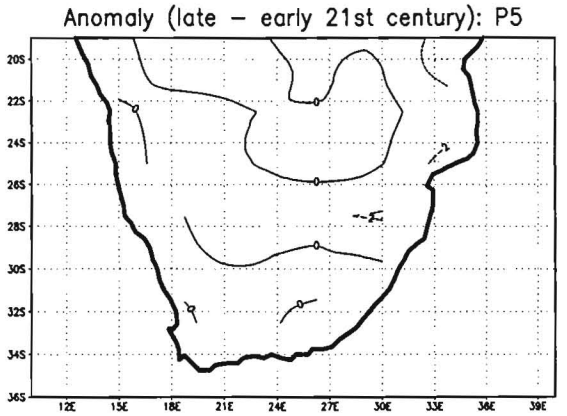

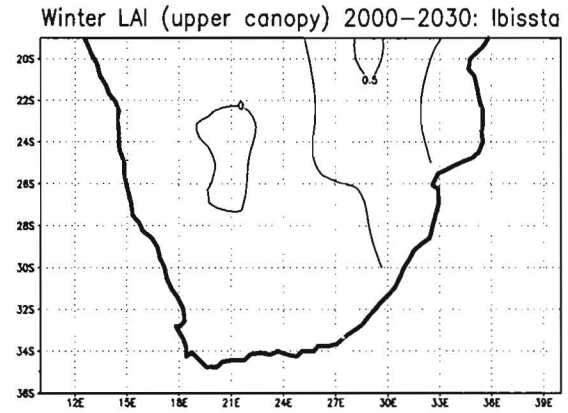

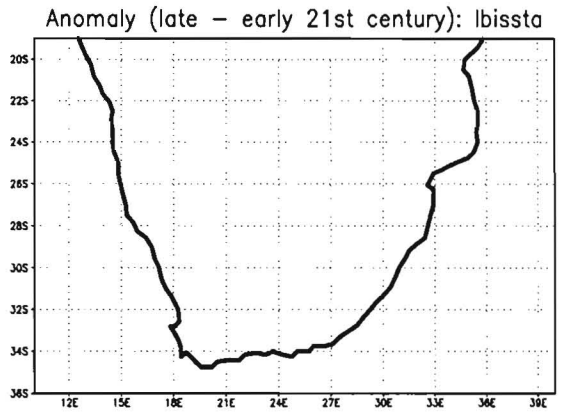

(No notable change in anomaly)

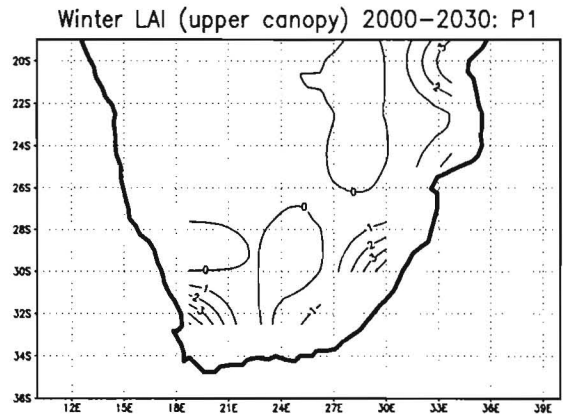

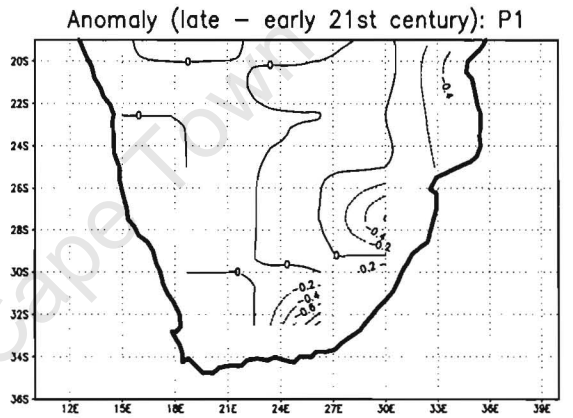

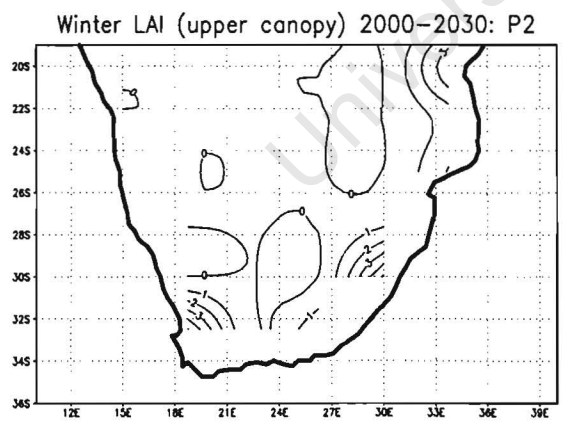

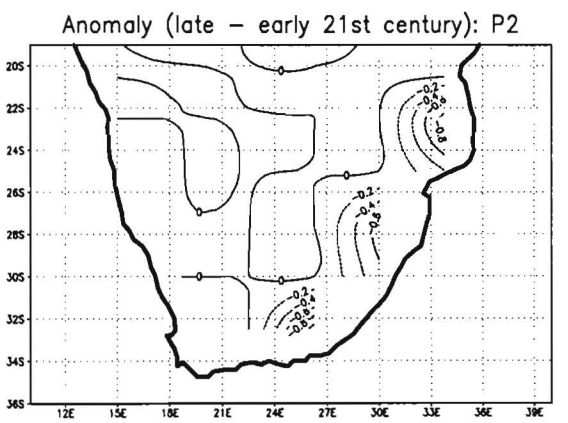

Winter LAI (upper canopy) 2000–2030: P3

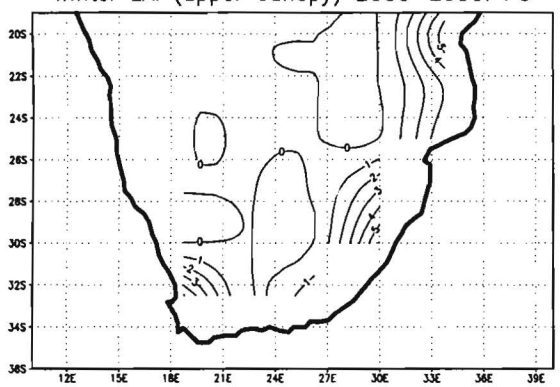

Anomaly (late – early 21st century): P3

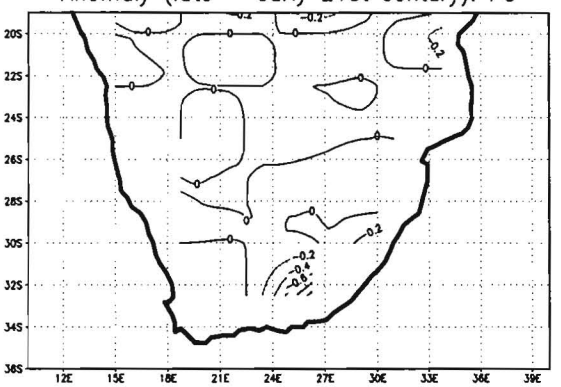

Winter LAI (upper canopy) 2000–2030: P4

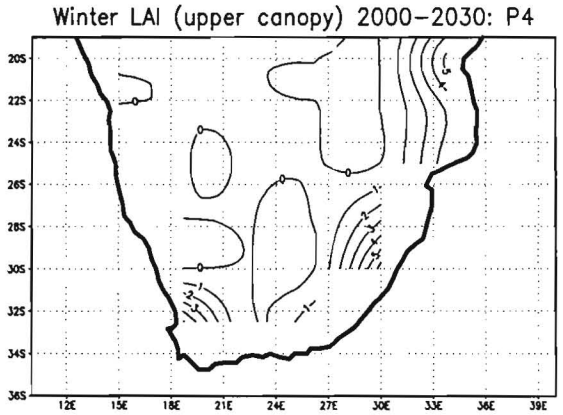

Anomaly (late – early 21st century): P4

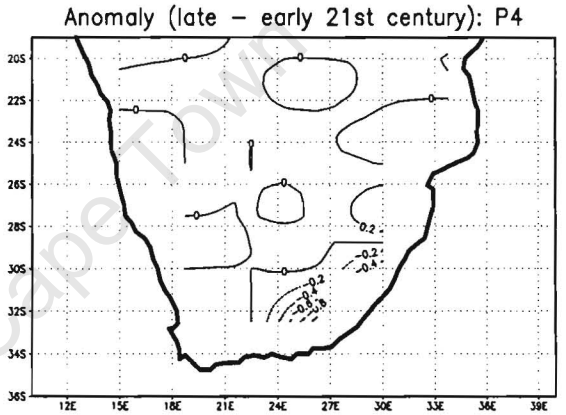

Summer LAI (upper canopy) 2000–2030: P5

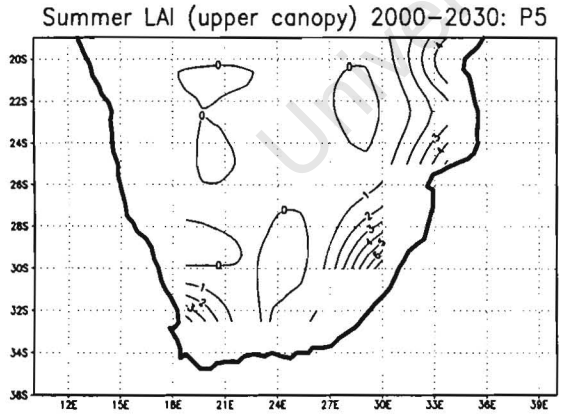

Anomaly (late – early 21st century): P5

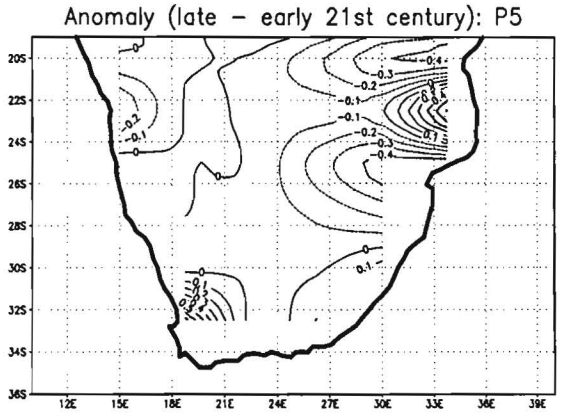

Winter LAI (lower canopy) 2000–2030: Ibissta

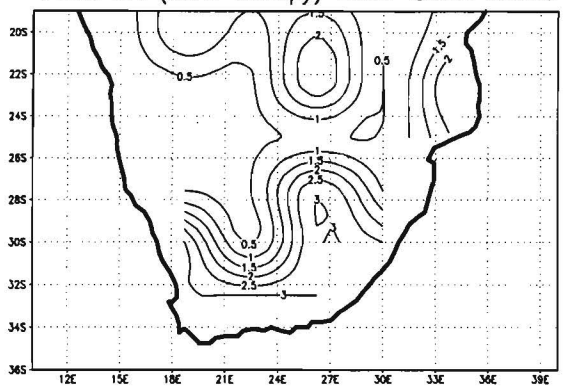

Anomaly (late – early 21st century): Ibissta

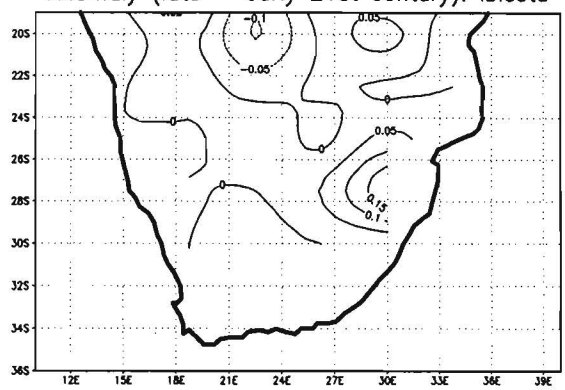

Winter LAI (lower canopy) 2000–2030: P1

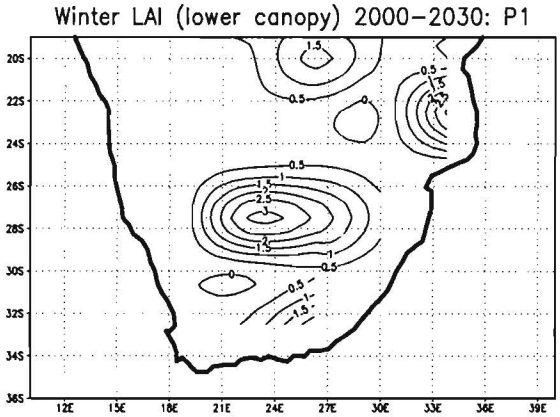

Anomaly (late – early 21st century): P1

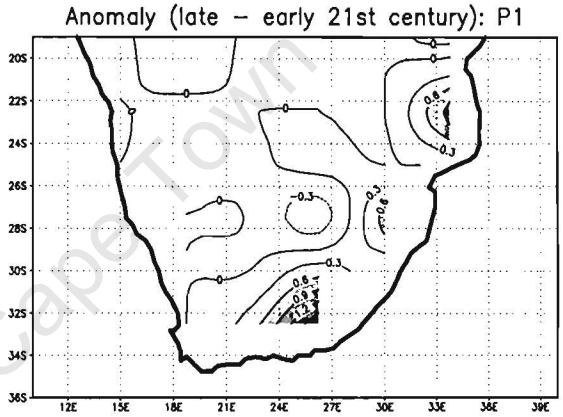

Winter LAI (lower canopy) 2000–2030: P2

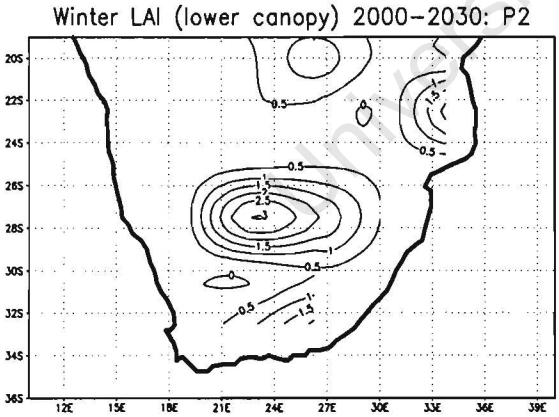

Anomaly (late – early 21st century): P2

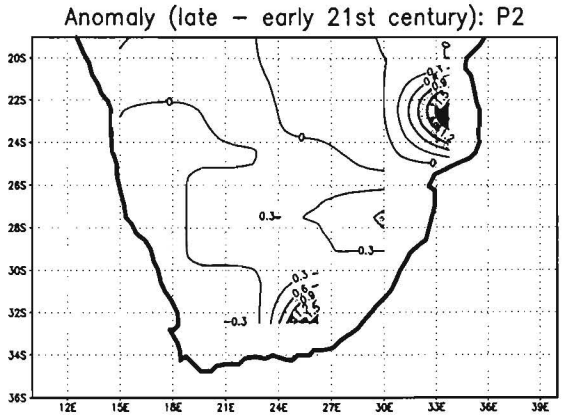

Winter LAI (lower canopy) 2000–2030: P3

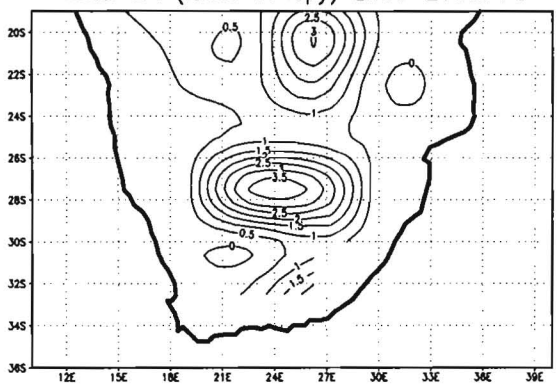

Anomaly (late – early 21st century): P3

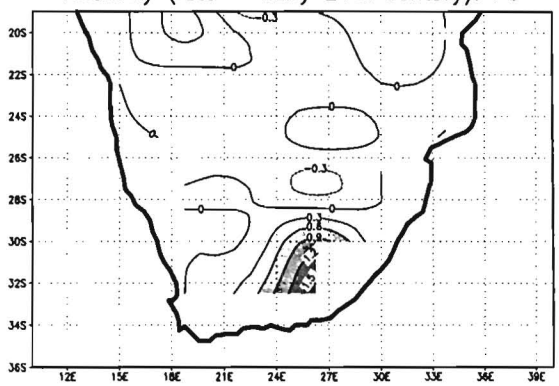

Winter LAI (lower canopy) 2000–2030: P4

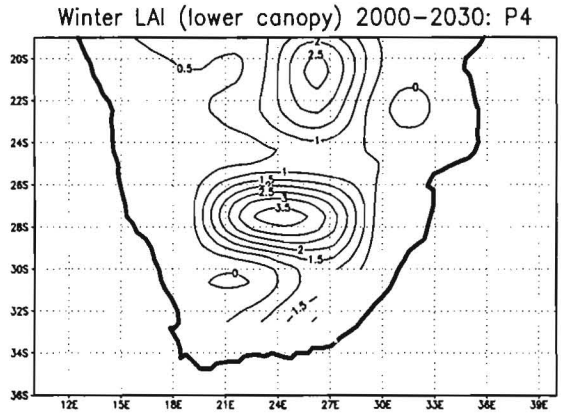

Anomaly (late – early 21st century): P4

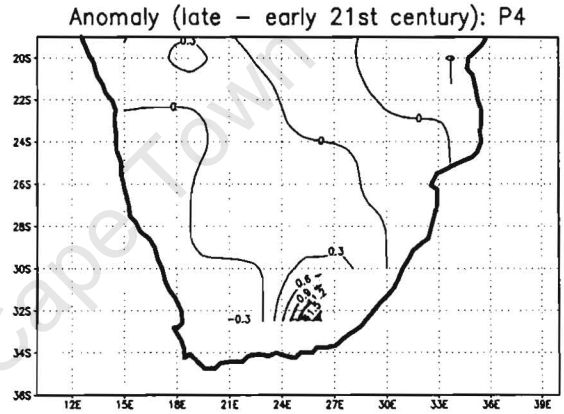

Winter LAI (lower canopy) 2000–2030: P5

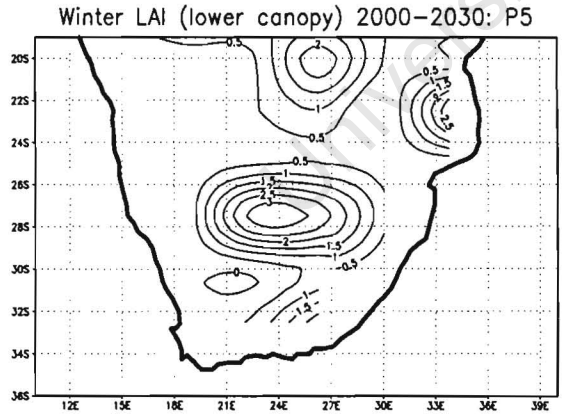

Anomaly (late – early 21st century): P5